Received: 21 March 2021 | Revised: 17 February 2022 | Accepted: 21 March 2022

DOI: 10.1002/ar.24949

SPECIAL ISSUE ARTICLE

The Anatomical Record | WILEY

Anatomy and relationships of the early diverging Crocodylomorphs *Junggarsuchus sloani* and *Dibothrosuchus elaphros*

Alexander A. Ruebenstahl[1,2] | **Michael D. Klein**[3] | **Hongyu Yi**[4,5] | **Xing Xu**[4,5] | **James M. Clark**[1]

[1]Department of Biological Sciences, George Washington University, Washington, District of Columbia, USA

[2]Department of Earth and Planetary Sciences, Yale University, New Haven, Connecticut, USA

[3]Tucson, Arizona, USA

[4]Key Laboratory for the Evolutionary Systematics of Vertebrates of the Chinese Academy of Sciences, Institute of Vertebrate Paleontology and Paleoanthropology, Beijing, China

[5]CAS Center of Excellence in Life and Paleoenvironment, Beijing, China

Correspondence
Alexander A. Ruebenstahl, Department of Earth and Planetary Sciences, Yale University, P.O. Box 208109, New Haven, CT 06520-8109, USA.
Email: alex.ruebenstahl@yale.edu

Funding information
Data Center of Management Science, National Natural Science Foundation of China - Peking University, Grant/Award Number: 41688103; National Science Foundation, Grant/Award Number: EAR 1636753

Abstract

The holotype of *Junggarsuchus sloani*, from the Shishugou Formation (early Late Jurassic) of Xinjiang, China, consists of a nearly complete skull and the anterior half of an articulated skeleton, including the pectoral girdles, nearly complete forelimbs, vertebral column, and ribs. Here, we describe its anatomy and compare it to other early diverging crocodylomorphs, based in part on CT scans of its skull and that of *Dibothrosuchus elaphros* from the Early Jurassic of China. *Junggarsuchus* shares many features with a cursorial assemblage of crocodylomorphs, informally known as "sphenosuchians," whose relationships are poorly understood. However, it also displays several derived crocodyliform features that are not found among most "sphenosuchians." Our phylogenetic analysis corroborates the hypothesis that *Junggarsuchus* is closer to Crocodyliformes, including living crocodylians, than are *Dibothrosuchus* and *Sphenosuchus*, but not as close to crocodyliforms as *Almadasuchus* and *Macelognathus*, and that the "Sphenosuchia" are a paraphyletic assemblage. *D. elaphros* and *Sphenosuchus acutus* are hypothesized to be more closely related to Crocodyliformes than are the remaining non-crocodyliform crocodylomorphs, which form several smaller groups but are largely unresolved.

KEYWORDS

Crocodylomorpha, CT scanning, Jurassic, phylogeny

1 | INTRODUCTION

The "Sphenosuchia" (Bonaparte, 1971, 1984) are archosaurs known from the Late Triassic to the Late Jurassic (Clark et al., 2001; Göhlich et al., 2005; Leardi et al., 2017) that fall within Crocodylomorpha (Hay, 1930) but outside Crocodyliformes. Crocodyliformes includes living crocodylian species and their extinct relatives that possess specializations that solidify the skull (Benton & Clark, 1988; Langston, 1973; Pol et al., 2013) and Crocodylomorpha is the most inclusive clade containing *Crocodylus niloticus* (Laurenti, 1768), but not *Rauisuchus tiradentes* (Huene, 1942), *Poposaurus gracilis* (Mehl, 1915), *Gracilisuchus stipanicicorum* (Romer, 1972),

Prestosuchus chiniquensis (Huene, 1942), or *Aetosaurus ferratus* (Fraas, 1877; Irmis et al., 2013). At least 13 valid monotypic genera are considered potential "sphenosuchians" (referred to as non-crocodyliform crocodylomorphs below): *Sphenosuchus acutus* (Haughton, 1915; Walker, 1990), *Saltoposuchus connectens* (Huene, 1921; Sereno & Wild, 1992), *Hallopus victor* (Marsh, 1877; Walker, 1970), *Terrestrisuchus gracilis* (Crush, 1984), *Dibothrosuchus elaphros* (Simmons, 1965; Wu & Chatterjee, 1993), *Hesperosuchus agilis* (Colbert, 1952), *Pseudhesperosuchus jachaleri* (Bonaparte, 1971), *Litargosuchus leptorhynchus* (Clark & Sues, 2002; *Kayentasuchus walkeri* (Clark & Sues, 2002), *Dromicosuchus grallator* (Sues et al., 2003), *Macelognathus vagans* (Göhlich et al., 2005; Marsh, 1884), *Almadasuchus figarii* (Pol et al., 2013) and *Junggarsuchus sloani* (Clark, Xu, Forster, & Eberth, 2004; Clark, Xu, Forster, & Wang, 2004). *Phyllodontosuchus lufengensis* (Harris et al., 2000), *Trialestes romeri* (Lecuona et al., 2016; Reig, 1963), *Carnufex carolinensis* (Zanno et al., 2015; Drymala & Zanno, 2016) and *Redondavenator quayensis* (Nesbitt et al., 2005) are known from incomplete or poorly preserved material and their affinities are not well understood but have been referred to the "sphenosuchians" in some studies, with the exception of *Carnufex carolinensis*. Another conflictive taxon is *Terrestrisuchus* which has been considered a junior synonym of *Saltoposuchus* (e.g., Benton & Clark, 1988), or as distinct taxa (e.g., Sereno & Wild, 1992); Allen (2003) considered *Terrestrisuchus* material to be juvenile individuals of *Saltoposuchus*, but Irmis et al. (2013) disagreed and consider them separate taxa. Nesbitt (2011) considered the specimen assigned to *Hesperosuchus* by Clark et al. (2001), CM 29894, to potentially belong to a different taxon due to its younger age within the Chinle Formation and the lack of autapomorphies shared by this specimen and the holotype of *Hesperosuchus agilis*, but Leardi et al. (2017) disputed some supposed differences between this specimen and the *H. agilis* holotype.

Many of the features shared by non-crocodyliform crocodylomorphs, like their long, gracile limbs positioned under their body, are related to an upright posture and terrestrial lifestyle, unlike living semi-aquatic crocodylians (Crush, 1984; Parrish, 1991; Sereno & Wild, 1992; Walker, 1970). However, there are few putative synapomorphies; thus, it is unclear whether or not these taxa comprise a monophyletic group. Analyses have shown the group either to be monophyletic (Clark et al., 2001; Sereno & Wild, 1992; Sues et al., 2003; Wu & Chatterjee, 1993) or paraphyletic, with some taxa being more closely related to Crocodyliformes (Benton & Clark, 1988; Clark & Sues, 2002; Clark, Xu, Forster, & Wang, 2004; Leardi et al., 2017; Nesbitt, 2011; Parrish, 1991; Pol et al., 2013; Zanno et al., 2015).

Early studies were not consistent with the use of their characters, however, and a critical review by Clark et al. (2001) revealed numerous problematic characters in earlier publications diminishing support for their results. A subsequent analysis (Clark, Xu, Forster, & Wang, 2004), including new characters and *J. sloani*, found in favor of a paraphyletic "Sphenosuchia" but with weak support. In an analysis without *Junggarsuchus*, Nesbitt (2011) also found a paraphyletic "Sphenosuchia," and more resolution among them, but with lesser taxonomic sampling. Results based on the Clark, Xu, Forster, and Wang (2004) data set, but with expanded taxon and character sampling (Leardi et al., 2017; Pol et al., 2013) have obtained similar results.

Here, the holotype specimen of *J. sloani*, IVPP 14010 (Figure 1), from the Middle-Upper Jurassic Shishugou Formation of China, is described in detail in comparison with other non-crocodyliform crocodylomorphs including detailed comparison to *D. elaphros*. The Shishugou Formation of Xinjiang (China) is a continuous series of sediments spanning the late Middle to early Late Jurassic (Clark et al., 2006; Eberth et al., 2001). The lower part of the formation has yielded a variety of turtles, brachyopoid amphibians, a mammaliaform, and theropod and sauropod dinosaurs; whereas the upper contains a more diverse fauna of dinosaurs and non-dinosaurian amniotes (Clark, Xu, Forster, & Eberth, 2004). An expedition in 2001 recovered the skull

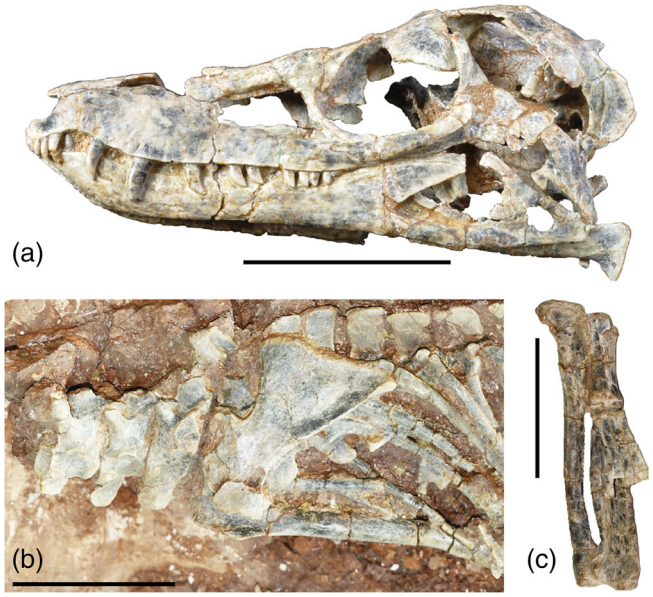

FIGURE 1 The holotype material of *Junggarsuchus sloani*: (a) the skull of *Junggarsuchus* in left lateral view; (b) the posterior cervical vertebrae and pectoral girdle of *Junggarsuchus* in left lateral view in the block; (c) the right forelimb of *Junggarsuchus* in right lateral view. Labels and details of these elements are shown in the following figures. Scale bar is equal to 5 cm.

and part of the postcranial skeleton of *J. sloani* as named by Clark, Xu, Forster, and Eberth (2004) and Clark, Xu, Forster, and Wang (2004), from the lower part of the Shishugou Formation. It was originally considered to be late Middle Jurassic (Clark, Xu, Forster, & Eberth, 2004; Clark, Xu, Forster, & Wang, 2004) based on the Gradstein et al. (2004) time scale, but later revisions (Gradstein et al., 2012) moved this boundary and indicate *Junggarsuchus* is earliest Late Jurassic (see Horizon and Locality below).

The holotype specimen consists of an exceptionally preserved skull and the anterior portion of the body, with a few disarticulated elements of the posterior portion of the skeleton that were recovered associated with the holotype (Figure 1). The holotype is the only significant specimen of *J. sloani* and was described briefly in a paper by Clark, Xu, Forster, & Wang (2004) which focused specifically on the features of the braincase and forelimbs. An initial detailed description of much of the known material of *J. sloani* was prepared by a Masters student working with Clark (Klein, 2007) but did not include CT scans. *J. sloani* has several features that reduce the morphological gap between more early diverging crocodylomorphs and crocodyliforms, including the contact of the ventral shaft of the quadrate to the otoccipital on the occipital surface of the braincase that is a key step in the beginning of the solidification of the skull (Clark, Xu, Forster, & Wang, 2004; Pol et al., 2013). We describe the external and internal anatomy of *Junggarsuchus* here using observations from CT data, including a detailed description of the palate, inner ear and braincase of *Junggarsuchus*. Previous detailed descriptions of sphenosuchian braincases have either lacked CT data and so were limited in some respects to breaks through which observations could be made (Walker, 1990; Wu & Chatterjee, 1993) or described incompletely preserved taxa (Leardi et al., 2020). *Junggarsuchus*, however, preserves nearly all aspects of the skull, and with the availability of CT data, it is one of the most completely known sphenosuchians to date.

D. elaphros is known from excellent material, including a nearly complete skull and much of the postcranial skeleton. *D. elaphros* is from the Zhangjiawa Member of the Lufeng Formation in Yunnan, China, which has been biostratigraphically dated as Early Jurassic, possibly Sinemurian (Fang et al., 2000; Luo & Wu, 1994). Several specimens are known, though the most complete is IVPP V 7907, comprising a complete skull, the anterior portion of the axial skeleton, the forelimbs and includes some elements of the hind limbs and pubis (Wu & Chatterjee, 1993). It was thoroughly described by Wu and Chatterjee (1993), but the skull has not previously been CT scanned.

Past analyses recover a similar pattern of relationships within Crocodylomorpha, in which *D. elaphros* and *J. sloani* are found to be closer to Crocodyliformes than are most other non-crocodyliform crocodylomorphs (Benton & Clark, 1988; Leardi et al., 2017; Pol et al., 2013; Wilberg, 2015), though not as close as *Macelognathus*, *Almadasuchus* and possibly *Kayentasuchus* (Wilberg, 2015). Although *Dibothrosuchus* and *Junggarsuchus* are two of the best represented members of this lineage of crocodylomorphs, there is limited comparison of these two, relatively closely related taxa, which this description improves upon.

The characters used in previous analyses are critically reviewed and reanalyzed, and the results support a paraphyletic Sphenosuchia. To better understand the evolution of important crocodylomorph characters and the relationships of *Junggarsuchus*, we have assembled the largest early diverging crocodylomorph character matrix currently in the literature, building on the most recent matrices of Leardi et al. (2017) and Wilberg (2015). Our sampling includes all currently described early diverging crocodylomorphs and 513 characters that cover important cranial and postcranial anatomy. We performed parsimony analyses with four different rooting taxa (*Gracilisuchus*, *Stagonolepis*, *Saurosuchus*, and *Postosuchus*) and weighting schemes (no implied weights, $k = 6, 12, 24$) to see how such variations might change tree topology and what this variation might tell us about how homoplastic character states affect some relationships. Taxa of particular interest to this analysis are those non-crocodyliform crocodylomorphs potentially closest to Crocodyliformes, including *Macelognathus* (Leardi et al., 2017), *Almadasuchus* (Pol et al., 2013), *Kayentasuchus* (Clark & Sues, 2002), and the marine thalattosuchians.

J. sloani, *Macelognathus vagans*, and *Almadasuchus figarii* are found to be the closest relatives of Crocodyliformes in most recent analyses, and species such as *Sphenosuchus acutus*, *D. elaphros*, *Terrestrisuchus gracilis*, and *Litargosuchus leptorhynchus* are usually found to have diverged earlier within Crocodylomorpha (Benton & Clark, 1988; Leardi et al., 2017; Pol et al., 2013; Wilberg, 2015). *Kayentasuchus walkeri*, a crocodylomorph from the Early Jurassic of Arizona (Clark & Sues, 2002), has been found in some analyses (e.g., Nesbitt, 2011) to be the sister taxon to Crocodyliformes, although *Junggarsuchus*, *Almadasuchus*, and *Macelognathus* were not included. This placement for *Kayentasuchus* as the sister taxon to Crocodyliformes was also found by later authors including Wilberg (2015), who included *Almadasuchus* and *Junggarsuchus*, and Zanno et al. (2015), who included *Junggarsuchus* though not *Almadasuchus* or *Macelognathus*. Although Wilberg's sampling included more crocodylomorph outgroup taxa, he noted that this position is not well supported, and two-character state changes would place *Junggarsuchus* and

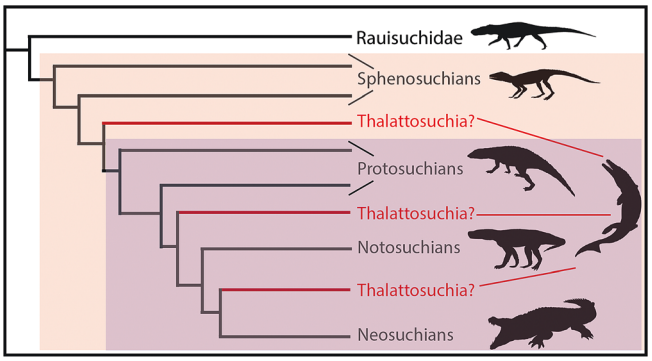

FIGURE 2 Generalized tree of crocodylomorph relationships. Thalattosuchia is placed in two positions within Crocodyliformes, and as the sister group to crocodyliforms. Sphenosuchians and protosuchians shown as paraphyletic groups. The three hypothesized placements of Thalattosuchia are in red. Crocodyliformes in purple and Crocodylomorpha in orange

Almadasuchus as sister to Crocodyliformes +- Thalattosuchia. We find *Kayentasuchus* in an earlier diverging position, a result that is consistent with the more recent results of some other researchers (Leardi et al., 2017) (see Discussion).

A further area of interest is the relationships of thalattosuchians, a group including the most highly specialized pelagic crocodylomorphs. Their relationships were considered to be obscured by homoplastic similarities with other marine crocodylomorphs (Clark, 1994; Sadleir & Makovicky, 2008), and they were placed either in their traditional position at the base of the Mesoeucrocodylia or grouped with other long-snouted taxa (Figure 2). However, Wilberg (2015) found many of the features related to a long snout to be homoplastic, and his analysis placed thalattosuchians as the sister-group of crocodyliforms, a position also discussed by Benton and Clark (1988).

2 | MATERIALS AND METHODS

The limb bones of *J. sloani* are described as if the animal was standing erect (Pol and Norell 2004). Hence, anterior = cranial and posterior = caudal. The terms "ventral" and "dorsal" are used in describing the digits but not the more proximal elements, assuming a digitigrades stance. The skull was separated from the rest of the skeleton and was transported to The George Washington University (Washington, DC, USA) for study and further prepared after the publication of Clark, Xu, Forster, and Wang (2004) and Clark, Xu, Forster, and Eberth (2004), and nearly all of the matrix was removed. Regarding the postcranial skeleton, only the left side of the skeleton has been prepared out of its plaster jacket, and the right side of the specimen has not been viewed except for the right forelimb (Figure 1a). The holotype skull was first CT scanned before extensive internal preparation on September 28, 2004 on a GE Lightspeed 16 CT scanner at Stony Brook University. The specimen was scanned at 140 kV and 160 mA with a slice spacing of 0.31 mm. Slices were reconstructed at a diameter of 96.0 mm using the GE BonePlus algorithm. The holotype skull was rescanned after nearly all of the matrix was removed in a Mi-CT 225 kV micro-computerized tomography scanner (developed by the Institute of High Energy Physics, Chinese Academy of Sciences) at the Key Laboratory of Vertebrate Evolution and Human Origins, IVPP. Slices were spaced at 0.0459 mm for a total of 3,402 slices along a 141.32-mm-long skull. We used Mimics software (Mimics Software, n.d.) (https://www.materialsise.com/en/medical/software/mimics) to segment and analyze the second CT scans of the skull. All nonphotograph illustrations of *Junggarsuchus* in this article are detailed 3D models of the masks reconstructed in Mimics and VG Studios. Additional analysis of the CT data, including the imaging of the lacrimal ducts, trigeminal nerve pathways and the generation of isosurface renders of incomplete elements was completed at Yale University, in the Bhullar Lab, using VG Studios Max Version 3.5 (VG Studio Max 3.5 (Volume Graphics), 2019).

The skull of *D. elaphros* (IVPP V7907) was CT scanned at the IVPP in Beijing using the same scanner. The rostrum and jaw were segmented in a single file, and the braincase was segmented separately, as the braincase was disarticulated from the rest of the skull. The non-photo illustrations of the skull of *Dibothrosuchus* used in our description were all also reconstructed from Mimics and VG Studio files. Slices for the rostrum were spaced at 0.19 mm for a total of 2,881 slices along a 164-mm-long skull. Slices for the braincase were spaced at 0.19 mm for a total of 1,481 slices along a 41-mm-long skull.

Characters: The characters used in previous analyses of early diverging crocodylomorphs have been critically reviewed and reanalyzed. The final character set of 513 characters is mostly a combination of characters from Wilberg (2015, 2017), from which 290 of the characters are taken from the former and 7 from the latter, and Leardi et al. (2017), from which we included 129 characters. An additional 69 characters for crocodyliforms were taken from a data set assembled by Tennant et al. (2016), and an additional 8 and 2 characters for thalattosuchians were taken from Young and Andrade (2009) and Young et al., 2012, respectively, (Supplementary information S1 is our revised list of characters, which notes the original matrix that each character was taken from in parentheses). One modified character (Char. 395) was included

from Clark (1994). For each data set, we looked at overlap between the characters and omitted repetitive, semantically dependent characters between the data sets (Supplementary information S1 includes a list of justifications for omissions). Additionally, some characters and scorings were edited in our assembly of this new dataset and a list of these changes can be found in our supplementary material S1. In addition to the 506 characters from previous authors, we included seven new characters that detail additional morphology of the pterygoid (Char. 283), the mandibular fenestra (Char. 321), the dentary (Char. 325), the angular (Char. 348), the prearticular (Chars. 351), the articular (Char. 356), and the dentition (Char. 395). This analysis included 41 ordered (additive) characters (indicated in a nexus file and .tnt file in Supplementary information S1).

Taxa: For most taxa, we used codings taken from existing matrices, including Wilberg (2015), Leardi et al. (2017), and Young and Andrade (2009). *J. sloani* (IVPP V14010) and *D. elaphros* (IVPP V7907) were studied in person and in CT segmentation, whereas *Hesperosuchus agilis* (AMNH 6758), *Kayentasuchus walkeri* (UCMP 131830), *Hallopus victor* (YPM 1914), *Nominosuchus matutinus* (IVPP V14392), *Protosuchus haughtoni* (BP-14746, BP/1/4770), an unnamed protosuchid (UCMP 97638/125871), *Zaraasuchus shepardi* (IGM 100/1321), *Shamosuchus djadochtaensis* (IGM 100/1195), *Gavialis gangeticus*, *Crocodylus niloticus*, and *Alligator mississippiensis* were all studied in person without CT data.

Our sampling of non-crocodyliform crocodylomorphs includes 16 species. Two crocodylomorphs of uncertain relationship, *Trialestes romeri* (Lecuona et al., 2016) and *Phyllodontosuchus lufengensis* (Harris et al., 2000), were included. Our sampling of outgroup taxa outside of non-crocodyliform crocodylomorphs includes *Dyoplax arenaceus* (Maisch et al., 2013), *Erpetosuchus granti* (Olsen et al., 2000), *Gracilisuchus stipanicicorum* (Butler et al., 2014; Lecuona et al., 2017; Romer, 1972), two additional gracilisuchids (*Yonghesuchus sangbiensis* (Butler et al., 2014) and *Turfanosuchus dabensis* (Butler et al., 2014; Wu & Russell, 2001), *Postosuchus kirkpatricki* (Chatterjee, 1985; Weinbaum, 2013), *Postosuchus alisonae* (Peyer et al., 2008), *Saurosuchus galilei* (Alcober, 2000; Sill, 1974), *Stagonolepis robertsoni* (Walker, 1961) and *Effigia okeeffeae* (Nesbitt, 2007). Our ingroup sampling was more limited, with 12 species of early diverging crocodyliforms, one early diverging mesoeucrocodylian, six thalattosuchians, two notosuchians, three tethysuchians, *Calsoyasuchus valliceps* (usually placed with goniopholidids; Tykoski et al., 2002, but recently placed with *Hsisosuchus* by Wilberg et al. (2019)), one paralligatorid, and three extant crocodylians: *Alligator mississippiensis*, *Crocodylus niloticus*, and *Gavialis gangeticus*. For the complete list of taxa, see Table 1 and for their scorings see (Supplementary Data S1- on Dryad, link included in "Data Availability" statement).

Rooting: This study uses four alternative rooting schemes which vary along with the sampling of outgroup taxa (Tables 2, 3, 5), as outgroup selection has been shown to have significant effects on the ingroup topology (Wilberg, 2015). Outgroups include *Gracilisuchus*, *Stagonolepis*, *Saurosuchus* and *Postosuchus*, representatives of groups found by Nesbitt (2011) to be close to crocodylomorphs, in the order found in his analysis. When the rooting taxon was changed, taxa that have been found outside the root were excluded. The rooting schemes were varied to examine the effect of outgroup selection on ingroup topology.

Outgroup taxa were selected that had been used in analyses of early diverging crocodylomorphs in past analyses (Clark, Xu, Forster, & Wang, 2004; Leardi et al., 2017; Wilberg, 2015; Wu & Chatterjee, 1993). Rooting strategy 1 uses *Gracilisuchus stipanicicorum*, a presumed relative of early crocodylomorphs in some analyses that is often used as the rooting taxa in phylogenetic analyses of crocodylomorphs (Nesbitt, 2011; Wilberg, 2015). When rooted on *Gracilisuchus*, two other gracilisuchids, two erpetosuchids, *Stagonolepis*, *Effigia*, *Saurosuchus*, and *Postosuchus alisonae* are also included in the outgroup. The two other gracilisuchids, *Yonghesuchus sangbiensis*, and *Turfanosuchus dabenensis*, are both from the Middle Triassic of China (Wu et al., 2001; Wu & Russell, 2001). However, due to their uncertain phylogenetic position and convergence with crocodylomorphs in their small, gracile forms (Nesbitt, 2011), three other rooting schemes were implemented with gracilisuchids excluded and rooted on other taxa. Rooting strategy 2 uses *Stagonolepis robertsoni*, which is a representative of the armored, Triassic aetosaurs, a group that have been consistently found as one of the most early diverging pseudosuchians (Nesbitt, 2011). *Effigia* was included in the outgroup as a representative of Poposauroidea due to the relative completeness of the specimen and its comprehensive description (Nesbitt, 2007), although it is very specialized. The remaining outgroup taxa were maintained with the *Stagonolepis* root (Nesbitt, 2011; Wilberg, 2015). This exclusion is maintained in all subsequent analyses. Rooting strategy 3 uses the early diverging loricatan *Saurosuchus galilei*, which has consistently been found closer to crocodylomorphs than gracilisuchids, erpetosuchids, and aetosaurs (Nesbitt, 2011). Aetosaurs and poposaurs were omitted from this round of analyses over concerns that the armored herbivorous and bipedal herbivorous pseudosuchians may be too specialized as a rooting taxon and affect character polarity. *Dyoplax* and *Erpetosuchus* (erpetosuchids) were also omitted in the analyses rooted on *Saurosuchus* and *Postosuchus*. Like gracilisuchids they are of uncertain phylogenetic position and all positions are outside

TABLE 1 List of taxa used in comparison for the text and in our phylogenetic analyses

Taxon	Source
Gracilisuchus stipanicorum	Romer (1972), Butler et al. (2014), and Lecuona et al. (2017)
Turfanosuchus dabensis	Young (1973), Wu and Russell (2001) and Butler et al. (2014)
Yonghesuchus sangbiensis	Butler et al. (2014)
Erpetosuchus granti	Olsen et al. (2000) and Newton (1894)
Dyoplax arenaceus	Maisch et al. (2013)
Stagonolepis robertsoni	Walker (1961) and Gow and Kitching (1988)
Effigia okeefeae	Nesbitt (2007)
Saurosuchus galeli	Sill (1974) and Alcober (2000)
Postosuchus alisonae	Peyer et al. (2008)
Postosuchus kirkpatricki	Chatterjee (1985) and Weinbaum (2013)
Carnufex carolinesis	Zanno et al. (2015) and Dtymala and Zanno (2016)
Phyllodontosuchus lufengensis	Harris et al. (2000)
Pseudhesperosuchus jachaleri	Bonaparte (1971)
Redondavenator quayensis	Nesbitt et al. (2005)
Trialestes romeri	Lecuona et al. (2016)
Terrestrisuchus gracilis	Crush (1984) and Allen (2003)
Hesperosuchus "*agilis*" (CM 29894)	Clark and Sues (2002)
Hesperosuchus agilis (Holotype)	AMNH FR 6758
Litargosuchus leptorhynchus	BP/1/5237; Clark and Sues (2002)
Dromicosuchus grallator	Sues et al. (2003)
Kayentasuchus walker	UCMP 131830; Clark and Sues (2002)
Sphenosuchus acutus	Walker (1990)
Dibothrosuchus elaphros	IVPP V 7907; Wu and Chatterjee (1993)
Hallopus victor	YPM 1914
Junggarsuchus sloani	IVPP V 14010
Macelognathus vagans	YPM VP 001415; Leardi et al. (2017)
Almadasuchus figarii	Pol et al. (2013) and Leardi et al. (2020)
Protosuchus richardsoni	AMNH 3024; UCMP 130860; MCZ 6727 limited CT data Clark (1986)
Protosuchus haughtoni	BP/1/4770; Gow (2000)
Gomphosuchus wellsi	UCMP-97638/125871
Orthosuchus stormbergi	Nash (1975)
Hemiprotosuchus leali	Bonaparte (1969)
Gobiosuchus kielanae	Osmólska et al. (1997)
Zosuchus davidsoni	IGM 100/1305; Pol and Norell (2004a)
Zaraasuchus shepardi	IGM 100/1321; Pol and Norell (2004b)
Nominosuchus matutinus	Storrs and Efimov (2000)
Fruitachampsa callisoni	Clark (2011)
Sichuanosuchus shuhanensis	Wu et al. (1997)
Shantungosuchus hangjiensis	Wu et al. (1994)
Hsisosuchus chungkingensis	Li et al. (1994)
Steneosaurus bollensis	Herrera et al. (2018)
Metriorhynchus superciliosus	Andrews (1913)
Cricosaurus araucanensis	Herrera et al. (2018)

TABLE 1 (Continued)

Taxon	Source
Geosaurus suevicus	Young and Andrade (2009)
Dakosaurus andiniensis	Pol and Gasparini (2009)
Pelagosaurus typus	Pierce and Benton (2006)
Simosuchus clarki	Kley et al. (2010)
Baurusuchus salgadoensis	Nascimento and Zaher (2010)
Goniopholis simus	De Andrade et al. (2011)
Calsoyasuchus valliceps	Tykoski et al. (2002)
Sarcosuchus imperator	Sereno et al. (2001)
Pholidosaurus purbeckensis	Mansel-Pleydell (1888) and Andrews (1913)
Dyrosaurus phosphaticus	Jouve (2005) and Jouve et al. (2006)
Shamosaurus djadochtaensis	IGM 100/1195; Turner (2015)
Gavialis gangetics	YPM HERR 010514
Crocodylus niloticus	YPM HERR 010521
Alligator mississippiensis	YPM HERR 16540; Dufeau and Witmer (2015)

Postosuchus + Crocodylomorpha (Nesbitt, 2011), including some positions well outside the node that unites even Gracilisuchidae with other close relatives of crocodylomorphs (Nesbitt, 2011). Rooting strategy 4 uses the rauisuchid *Postosuchus kirkpatricki*, which has consistently been recovered as either the sister to crocodylomorphs or very close and is commonly included as an outgroup of crocodylomorphs (Nesbitt, 2011). This scheme has the most limited outgroup sampling.

Parsimony analysis: For this project, 16 phylogenetic trees were constructed with parsimony analysis using 513 characters applied to 57 taxa with *Gracilisuchus* as the outgroup, 54 with *Stagonolepis* as the outgroup, 50 with *Saurosuchus* as the outgroup, and 48 with *Postosuchus* as the outgroup. TNT v1.5 (Goloboff & Catalano, 2016) was used to find the most parsimonious trees and the strict consensus. Forty-one multistate characters were treated as ordered. These 41 characters were originally treated as ordered in the matrices they were sampled from. Sixteen different analyses were run with characters ordered, four for each rooting scheme. Of these four analyses, one of the tests used equal weighting, the others used implied weights of $k = 12$, as simulation studies when the true tree was known outperformed others when homoplasy was more severely downweighted (Goloboff, 1993; Goloboff et al., 2017). The second and third set of implied weight analyses was carried out at the higher and lower k value ($k = 24$ and $k = 6$) to test the data sets sensitivity to decreased and increased downweighting of homoplastic characters. While ordering of characters is justified by the similarities among the states (Lipscomb, 1992), an additional 16 analyses were carried out with no ordered characters for comparison with other analyses that did not order the characters (e.g., Wu & Chatterjee, 1993). These analyses produce divergent results in which "Sphenosuchia" is found as a monophyletic clade even in equal weight analyses when Rooting Schemes 1 or 2 are used, though results when rooted on *Saurosuchus* and *Postosuchus* are similar to those found when 41 characters are ordered. Results of these analyses are discussed and the trees are figured in the supplementary data (Figures S10–S17).

For our equal weights analyses, minimal tree lengths were first found using new technologies searches. We set the search to look for the minimum tree length five times and set the initial addition sequences at 50. This search was carried out with drift, tree fusing, and sectorial search set at the default settings. Ratchet was also included in our new technologies search for all analyses with 100 total iterations. For our implied weight analysis, tree fusing, sectorial search, drift, and ratchet were maintained, but instead of finding the minimum tree length, we looked for the stabilized consensus two times, with a factor of 75, the default. For both equal weight and implied weight analyses, to ensure that all minimum tree lengths were discovered, all analyses were subjected to traditional search with tree bisection reconnection (TBR) branch swapping. Following the use of the TBR algorithm, a strict consensus was found for the set of trees retained from the analysis. For trees with equal weights, the consistency index and retention index were calculated for each set of most parsimonious trees (Table 2).

	Gracilisuchus	*Stagonoelpis*	*Saurosuchus*	*Postosuchus*
CI	0.315	0.328	0.358	0.368
RI	0.613	0.639	0.6984	0.7
Steps	1968	1888	1731	1,686
Max	4,133	4,133	4,133	4,133
Min	620	620	620	620

TABLE 2 CI, RI, and step for equal weight analyses

Note: Taxa in column heads are for rooting scheme.
Abbreviations: CI consistency index; RI retention index.

Synapomorphies: Synapomorphies were first mapped along trees using TNT. The synapomorphies were then checked against a tree built in Mesquite (Maddison & Maddison, 2005) from our data set to visualize the evolutionary history of the character and its ambiguous and unambiguous optimizations. Synapomorphies for the groups are presented in Table 3.

Node support: Support for the nodes was found using symmetric resampling (Goloboff et al., 2003), with a .33 change probability, the default. The results for the topologies were output as both absolute frequencies and frequency differences. Frequency differences tend to give slightly lower numbers but are considered more accurate as they compare the frequency of a given group versus the frequency of the next most likely group to be found. This tests the assumed group against possible contradictory groups (Goloboff et al., 2003). This resampling was run with 100 replicates and was set to collapse any node with a support number lower than 1. Trees were searched with a new technology search, which used sectorial searches, ratchet, tree fusing, and drift and inserted an additional 10 sequences as the starting point for each analysis prior to a new technology search. The minimum length was calculated only once.

2.1 | Institutional abbreviations

AMNH: American Museum of Natural History (Fossil Reptiles), New York, USA
BP: Evolutionary Studies Institute (formerly Bernard Price Institute for Palaeontological Research), University of the Witwatersrand, Johannesburg, REPUBLIC OF SOUTH AFRICA
CM: Carnegie Museum of Natural History, Pittsburg, PA USA
CUP: Fujen Catholic University of Peking (Beijing) collection in Field Museum of Natural History, Chicago IL USA
IGM: Institute of Geology, Mongolian Academy of Sciences, MONGOLIA
IVPP: Institute of Vertebrate Paleontology and Paleoanthropology, Chinese Academy of Sciences, Beijing, China
MCZ: Museum of Comparative Zoology, Harvard, Cambridge, MA USA
UCMP: University of California Museum of Paleontology, Berkeley, CA, USA

2.2 | Abbreviations

adpq: anterior dorsal process of the quadrate
adq: suture for dorsal head of the quadrate on the prootic
ahq: articular head of the quadrate
ajp: anterior process of the jugal
anf: antorbital fenestra
angb angular
antf: antorbital fossa
antr: anterior tympanic recess
aor: anterior orbital artery
aoto: suture for otoccipital on prootic
apf?: possible additional palatine fenestra
apf: anterior prootic foramen
apl: anterior process of the palatine
apt: anterior process of the pterygoid
ar: articular
as: suture of prootic on squamosal
aoto: region of the squamosal which articulates with the paraoccipital process of the otoccipital
aso: suture of prootic with supraoccipital
at: atlas
atc: atlas centrum
atf: anterior temporal foramen
atin: atlas intercentrum
atna: atlas neural arch
atns: atlas neural spine
atoa: anterior exit of the temporo-orbital artery
atr: atlas rib
ax: axis
bc: internal space of the braincase
bib: break for internarial bar
bo: basioccipital
boc: basioccipital condyle
borss: basioccipital recess sensu stricto
bot: basioccipital tubers

TABLE 3 Unambiguous synapomorphies for groups found in each analysis where the clade is recovered.

Group	Synapomorphies
'Sphenosuchia' monophyletic: 5/16	10(0)*, 15(0), 24(0), 35(0), 80(1), 110(1)*, 139(0), 152(3)*, 212(1)*, 222(1)*, 232(0), 234(1), 256(1)*, 283(0), 346(2), 357(1), 409(1), 412(1)*, 427(1), 431(1), 436(1), 455(1), 474(1)*,
Litargosuchus + *Terrestrisuchus*: 6/16	7(2)*, 12(0)*, 13(1)*, 82(1)*, 110(1)*, 142(0)*, 165(1), 170(1), 194(0)*, 325(1), 348(1)
Redondavenator + *Kayentasuchus*: 1/16	375(0), 385(0)
Sphenosuchus + *Hesperosuchus*: 1/16	147(1), 149(1), 155(1), 345(1)
Dibothrosuchus + *Sphenosuchus*: 3/16	51(2), 142(1), 147(1), 170(1)*, 268(1), 315(1), 368(0)
(*Dibothrosuchus* + *Sphenosuchus*) + (*Hallopus* + *Solidocrania*): 3/16	13(0), 26(0), 82(0), 157(1), 173(1), 192(1), 195(1), 205(1), 276(0), 305(1), 409(2)
Sphenosuchus + (*Dibothrosuchus* + *Solidocrania*): 6/16	13(0), 82(0), 192(1), 195(1), 205(1), 409(2)
Dibothrosuchus + *Solidocrania*: 13/16	7(1)*, 13(0)*, 82(0)*, 157(1), 158(1), 173(1), 191(1), 192(2)*, 195(1)*, 202(1), 305(1), 411(1)
Dibothrosuchus autapomorphies	10(1), 17(1)*, 24(2)*, 27(1)*, 51(2)*, 116(1), 137(1)*, 158(1)*, 188(0)*, 191(1)*, 256(2)*, 338(1)*, 468(0)*, 479(0)*, 499(1), 510(0)*
Junggarsuchus autapomorphies	9(1), 61(2), 67(0), 86(1)*, 93(1)*, 97(1), 98(1), 111(1)*, 128(1), 170(0)*, 188(0)*, 206(1), 224(1), 322(1), 337(1), 338(1)*, 339(1), 433(1), 434(1), 498(1), 500(4), 501(1)
Junggarsuchus + *Phyllodontosuchus*: 5/16	97(1), 98(1), 110(1)*, 111(1)*, 325(0)
Hallopus + Solidocrania: 8/16	427(0), 429(2), 452(1), 453(1)
'Solidocrania': 11/16 paraphyletic; 5/16 in monophyletic Sphenosuchia	11(1), 86(1), 139(1)*,140(1), 174(1), 175(2), 207(2), 236(2)*, 237(1), 270(1), 285(1), 296(0), 403(1), 422(1)
Hallopodidae: 3/16	452(2), 453(1), 454(0)*
Macelognathus + Almadasuchus: 3/16	206(0), 207(3), 465(0)
Hallopodidae + Crocodyliformes: 3/16	46(1), 47(0), 142(0), 171(1), 191*(1), 210(1), 232(1), 247(1), 249(1), 267(1), 357(0), 365(1)
Macelognathus + (*Almadasuchus* + *Crocodyliformes*): 8/16	75(1)*, 142(0)*, 210(1), 232(1), 249(1), 365(1)
Almadasuchus + Crocodyliformes: 8/16	35(2), 46(1), 47(0), 48(1), 171(1), 212(0), 220(1)*, 247(1), 267(1), 357(0), 456(0)*, 460(0)*
Crocodyliformes: 16/16	1(1)*, 19(0), 20(2), 26(2)*, 38(1)*, 44(1)*, 45(1)*, 49(1), 137(1)*, 157(0), 158(1)*, 164(1), 172(2), 173(0), 179(1)*, 181(1), 190(0)*, 194(0), 196(0), 206(1), 207(4), 208(1)*, 211(1)* 222(0), 223(1)*, 225(0)*, 234(0)*, 236(2)*, 242(1), 246(1), 259(0), 262(0)*, 263(1)*, 266(1), 271(1)*, 274(2)*, 277(1)*, 280(1)*, 282(0)*, 283(1), 284(1)*, 306(1)*, 321(0)*, 327(0)*, 336(1)*, 346(0)*, 350(1)*, 353(0)*, 368(1)*, 402(1)*, 408(1)*, 409(3), 416(1)*, 429(1)*, 432(0)*, 449(1)*, 450(1)*, 452(1)*, 453(0), 454(1)*, 455(0), 478(1)*, 491(1)*
Thalattosuchia + Crocodyliformes: 7/16	1(1)*, 2(1), 7(1), 13(0)*, 28(1)*, 30(1)*, 38(1), 44(1)*, 49(1), 58(2)*, 83(1)*, 116(1)*, 117(0)*, 124(1), 137(1)*, 147(1)*, 161(0)*, 172(2), 192(2), 195(1), 196(0), 210(1)*, 216(1), 225(0), 236(2)*, 237(1), 247(1), 259(0)*, 267(1), 271(1), 282(1), 284(1), 298(0)*, 299(1), 306(2), 361(1), 365(1)*, 408(2), 422(1), 446(1), 449(1), 450(1), 478(1), 491(1),
Hsisosuchus + Crocodyliformes: 7/16	1(1)*, 11(1)*, 15(0), 19(0), 45(1)*, 46(1), 47(0), 48(1), 86(1)*, 111(0)*, 171(1), 174(1), 175(2), 179(1), 181(1), 182(1)*, 191(1), 202(1), 207(4), 220(1), 223(1), 224(0)*, 246(1), 304(1)*, 352(1)*, 403(1), 411(0), 475(0), 479(0), 486(1)*, 490(1),
Protosuchia paraphyletic: 3/16	36(0), 50(0), 228(1), 348(1), 375(0), 385(0), 454(1)

(Continues)

TABLE 3 (Continued)

Group	Synapomorphies
Protosuchidae: 16/16	27(0)*, 36(0)*, 45(1), 67(3)*, 83(1)*, 85(0)*, 14,871)*, 174(0)*, 175(0)*, 182(0)*, 201(1)*, 209(1)*, 251(1), 274(3)*, 295(1)*, 350(0)*, 375(0)*, 385(0)*, 448(0)*, 466(0)*, 474(1)*, 508(1)*
Protosuchia monophyly: 13/16	3(0), 26(1), 67(2), 137(1), 206(1), 211(1), 262(0), 321(0), 353(0), 454(1), 486(1)
Mesoeucrocodylia (Protosuchians + Hsisosuchus): 3/16	11(2)*, 28(1), 86(0)*, 143(1)*, 170(0)*, 182(1)*, 214(1), 217(0)*, 274(2), 282(1), 305(0)*, 306(2)*, 325(2)*, 350(1)*, 416(0)*, 451(1)*, 452(0)*
Thalattosuchia: 16/16	10(1), 15(1)*, 19(1), 20(0)*, 21(1)*, 45(0)*, 46(0), 47(1), 48(0), 52(1), 66(1), 100(1), 134(1)*, 155(1)*, 158(2)*, 160(0)*, 164(1), 166(1)*, 168(0)*, 171(1)*, 174(0)*, 179(0)*, 180(0)*, 181(0)*, 184(1)*, 199(1), 207(1)*, 208(0)*, 209(0)*, 214(0)*, 220(0*), 235(0)*, 246(2)*, 248(2)*, 254(0)*, 255(0)*, 257(2)*, 258(2)*, 263(0)*, 275(1)*, 290(1)*, 304(0)*, 309(1), 327(1)*, 342(1)*, 344(1)*, 346(1)*, 348(0)*, 382(0)*, 382(0)*, 392(1)*, 402(0)*, 405(0)*, 407(1)*, 416(1)*, 424(0)*, 441(1)*, 444(0)*, 459(0)*, 465(1)*, 497(1)*, 513(1)*

Note: Number in parentheses is the character state. Ambiguous synapomorphies indicated by *.

bpt: basipterygoid process
bt: biceps tubercle
cc: crista cranii
ch: choana
ci: crista interfenestralis
cor: coronoid
corc: coracoid
cppro: crista prootica
cpt: capitate process
crn cranioquadrate canal
crt: opening for internal carotid artery
ct: centrum
ctn: chorda tympani nerve
d: dentary
dc: distal carpals
dect: dorsal process of ectopterygoid
dg: digit
dh: distal end of humerus
dia: diapophyses
dmq: dorsomedial process of quadrate on prootic
dmrap: dorsomedial process of retroarticular process
dpc: deltopectoral crest
dpf: descending process of the prefrontal
dq: dorsal head of the quadrate
dqf: dorsal quadratojugal
dr: distal end of radius
du: distal end of ulna
dvt: dorsal vestibule
ect: ectopterygoid
em: edentulous portion of the maxilla
excap: extracapsular buttress
f: frontal
fleu: foramen for the lateral eustachian tube
fmeu: median pharyngeal foramen
fpf: foramen in the prootic facial recess
fl: flocculus
fm: foramen magnum
fo: fenestra ovalis
fort: fenestra pseudorotundum
fr: frontal ridges
fro: fenestra rotunda
ftoa: fenestra for temporal orbital artery
gf glenoid fossa
h: humerus
hh: hooked head of humerus
ho: humerus oval depression on head
hri: heads of rib
hya: hyapophyses
hypf: hypophyseal fossa
ic: inner carotid
imkf: intrameckelian foramen
ir: intertympanic recess
itf: infratemporal fenestra
IV: cranial nerve 4
IX-XI: cranial nerves 9–11
j: jugal
jg: jugal ventral groove
l: lacrimal
lf: lacrimal fenestra
lg: lagena
llp: lateral lamina of the prootic
llpf: lateral lamina of the prootic foramen
lmd: lacrimal medial depression
lp: ligament pits
ls: laterosphenoid
m: maxilla

mbcf: medial braincase foramen
mc: metacarpals
mnf: mandibular fenestra
mpo: medial process of the postorbital
mpq: medial process of the quadrate
mft: metotic foramen
mnd a/v: mandibular artery or vein
mr: medial ridge of the humerus
n: nasal
na: neural arch
nf: nutrient foramina
nld: nasolacrimal duct
ns: neural spine
od: odontoid process
ol: olecranon process
op: opisthotic
or: orbit
oscc3: opening for the third semicircular canal
ost: osteoderms
oto: otoccipital
otor: otoccipital recess
otspc: otosphenoidal crest
p: parietal
pb: palpebral
pdq: posterodorsal process of the quadrate
pdt: pit for dentary tooth
pf: prefrontal
pfo: prefrontal overhang
pfap: prefrontal anterior process
pfpa: prefrontal palatine contact
pfr: prootic facial recess
pfrf: prootica facial recess foramen
ph: phalange
pi: pisiform
pl: palatine
plr: palatine rod
pm: premaxilla
po: postorbital
po2: postorbital alternate interpretation
poc: postorbital concavity
pocr: postcartoid recess
prcr: precarotid recess
pop: paroccipital process
poz: postzygapophysis
pp: postglenoid process of the coracoid
ppl: posterior process of the palatine
pqf: postquadrate foramen
prb: parabasisphenoid
prb/ls: parabasisphenoid-laterosphenoid suture
prl: proximal end of radiale
pro: prootic
prz: prezygapophysis
pt: pterygoid
ptf: posttemporal fenestra
ptp: pterygoid process
ptr: posterior tympanic recess
pul: proximal end of ulnare
q: quadrate
qf: quadrate fenestra
qj: quadratojugal
qp: pneumatic expanded region of the quadrate
qp1: dorsal pneumatic space of the quadrate
qp2: pneumatic space of the quadrate continuous with the quadrate foramen
qp3: ventromedially expanded pneumatic space of the quadrate
qrp: quadrate ramus of the pterygoid
r: radius.
rap: retroarticular process
rhomb: rhomboidal recess
ri: rib
rl: radiale
rmp: ridge for *M. pterygoideus ventralis*
r-q: right displaced quadrate
s: squamosal
s2: squamosal alternate interpretation
sa: surangular
sbng: subnarial gap
sbr: sub-basisphenoidal recess
sc scapula
scb: scapular blade
scca: anterior semicircular canal
sccp: posterior semicircular canal
sccl: lateral semicircular canal
scp: sagittal crest of the parietal
so: supraoccipital
sof: suborbital fenestra
sp: splenial
spo: supraorbital vein or artery
sqg: squamosal ventral groove
sqlc: squamosal lateral concavity
srf: surangular fenestra
stf: supratemporal fenestra
stfo: supratemporal fossa
sur/q: surangular/ quadrate
toa: temporo-orbital artery
toag: temporo-orbital artery groove
trh: tooth root hole
tri: trigeminal nerve exit
trir: trigeminal recess—this was the ventral fossa of the laterosphenoid?
trnf: elongate nutrient foramina for the mandibular branch of the trigeminal nerve
tpt: transverse process of the pterygoid
u: ulna
ul: ulnare

upr: unpreserved possible region of median pharyngeal foramen in *Junggarsuchus sloani*
v: vomer
v_2: maxillary path of the trigeminal nerve
v_3: mandibular path of the trigeminal nerve
vd displaced vomer
vg + cn: exit for cranial nerves and vagus nerve?
VII: exit for cranial nerve 7
vl: ventral process of lacrimal
vps: ventral process of the squamosal
XII: exit for cranial nerve 12

3 | SYSTEMATIC PALEONTOLOGY

Archosauria, Cope 1896
Pseudosuchia, Zittel 1887
Crocodylomorpha Hay, 1930 (*emend* Walker, 1970)

3.1 | *Dibothrosuchus* Simmons, 1965

Type species: *Dibothrosuchus elaphros* (Simmons, 1965), by original designation.

Comments: IVPP V7907 was originally described as a second species of *Dibothrosuchus*, *D. xingsuensis* (Wu, 1986), but it was synonymized with *D. elaphros* by Wu and Chatterjee (1993) and currently only the type species is recognized as valid in this genus.

3.2 | *Dibothrosuchus elaphros* Simmons, 1965

Holotype: CUP 2081, a partial skull and skeleton.
Referred specimens: IVPP V7907, a nearly complete skull and mandible and partial postcranial skeleton; Wu and Chatterjee (1993) referred three other, incomplete specimens (CUP 2106, 2084, and 2489) to this species.
Horizon and localities: The holotype and referred specimens were collected near Dawa village, about 10 km northeast of Lufeng, Yunnan (Wu & Chatterjee, 1993). They are from the Zhangjiawa Member of the Lufeng Formation (the Dark Red Beds of the Lower Lufeng Formation of Luo & Wu, 1994) following the terminology of Fang et al. (2000).
Revised diagnosis: Of the original character states in the diagnosis by Wu and Chatterjee (1993), the following remain valid: frontals with three parasagittal ridges converging at both ends; frontal–postorbital contact forming a crescentic ridge in dorsal view; and a transversely broad supratemporal fenestra, nearly 30% of the width of the skull table; pronounced oval depression on anterior surface of the humerus (may be present in *Junggarsuchus* but smaller). Wu and Chatterjee (1993) identified potential autapomorphies as uncertain due to the unknown conditions in other non-crocodyliform crocodylomorphs at the time and we find support for the following: the squamosal curves sharply medially anterior to the supratemporal fenestra; squamosal separated from quadratojugal by quadrate; elongate antorbital fenestra, over half the length of the obit, surrounded by a triangular antorbital fossa; ventral process of the postorbital covers the posteromedial surface of the jugal; a small mandibular fenestra, triangular in lateral view. The full sheathing of the basioccipital condyle by the otoccipital is not supported as an autapomorphy due to our uncertain reconstruction of that region in *Dibothrosuchus* and *Junggarsuchus*. The condition of the anterior temporal foramen is seen in *Junggarsuchus* and so rejected as an autapomorphy. The autapomorphies of the coracoid are also reported in other non-crocodyliform crocodylomorphs (Clark, Xu, Forster, & Wang, 2004). The trigeminal recess is also not supported as an autapomorphy and may be widely present in non-crocodyliform crocodylomorphs (Leardi et al., 2020). We also identified several other potential autapomorphies in *Dibothrosuchus* from our own analysis, including the lateral border of the orbit is medial to the lateral border of the supratemporal fenestra (Char. 10-1); the supratemporal fossae is sub-circular in dorsal view (Char. 17-1); the lateral temporal fenestra is over 50% the size of the orbit (Char. 24-2); the suborbital fenestra is over 50% the diameter of the orbit (Char. 27-1); the descending process of the prefrontal contacts the palatine, unlike other non-crocodyliform crocodylomorphs (Char. 116-1); the total anteroposterior length of lacrimal is equal or shorter than the anteroposterior length of the prefrontal (Char. 137-1); the postorbital bar of the postorbital is medial or posterior to jugal (Char. 158-1); a tapered and pointed distal end of the posterodorsal process of the squamosal (Char. 188-0); an anteriorly well-developed posterior shelf of the supratemporal fossa (Char. 191-1); a lack of a depression for the posterior tympanic recess (Char. 256-2); the basipterygoids are massively expanded ventrally and mediolaterally and are pneumatic (Char. 268-1); the posterior extension of the surangular pinched off anterior to the articular (Char. 338-1); a massively enlarged and pneumatic prootic and potentially ventrally closed prootic facial recess (facial antrum); the medial region of distal articular surface of the tibia extends further distally than the lateral region, forming a strongly oblique distal margin of the tibia (Char. 468-0); the anterolateral process of dorsal osteoderms is absent (Char. 479-0); all cervical neural spines are rod-like (Char. 499-1); a holocephalus rib head on the axis rib (Char. 510-0).

3.3 | Solidocrania, new taxon

Definition: The least inclusive clade including *Junggarsuchus sloani* Clark, Xu, Forster, & Wang, 2004), *Almadasuchus figarii* (Pol et al., 2013) and *Macelognathus vagans* (Marsh, 1884).
Etymology: Solidocrania is a combination of *solidum* (L., solid) and *kranion* (Gr., skull), in reference to the rigid skull of these taxa.
Diagnosis: Unambiguous synapomorphies supporting Solidocrania include: two large palpebrals (Char. 140-1); the squamosal contacts the posterodorsal surface of the quadrate enclosing the otic recess posteriorly (Char. 174-1); the quadrate, squamosal, and otoccipital enclose the cranioquadrate canal laterally (Char. 175-2); the primary head of the quadrate approaches the laterosphenoid (Char. 207-2); the otoccipital contacts the quadrate ventrolaterally (Char. 237-1); the parabasisphenoid is greatly expanded with pneumatic cavities (Char. 270-1); a developed anterior process of the ectopterygoid projecting along the medial surface of the jugal (Char. 296-0); the anterior edge of the scapular blade is larger than the posterior edge (Char. 403-1); the olecranon process of the ulna is very low (Char. 422-1). Ambiguous character states that may support group (found in Mesquite using parsimony): reduction in the size of the antorbital fenestra (Char. 11-1); the lacrimo–nasal contact is excluded by an anterior projection of the prefrontal meeting posterior projection of the maxilla (Char. 86-1); the presence of palpebral elements (Char. 139-1); the presence of an additional quadrate fenestra has been inferred as a synapomorphy of this group, and the loss of the additional fenestra in *Almadasuchus* and *Macelognathus* may be secondary losses (Char. 206-1); the otoccipitals contact ventral to the supraoccipital, which is reversed in *Almadasuchus* (Char. 236-2); and a pneumatized pterygoid (Char. 285-1).
Comments: The phylogeny of early diverging crocodylomorphs remains tentative, but the group including crocodyliforms and the taxa with a similarly reinforced skull is one that will likely be referenced repeatedly in the future. However, given the late appearance of the genera closest to Crocodyliformes, it is possible that they represent a group independent of crocodyliforms and the braincase characters are homoplastic, and the definition is phrased such that they would form a discrete group excluding crocodyliforms if that is the case.

3.4 | *Junggarsuchus* Clark, Xu, Forster, and Wang, 2004

Type Species: *Junggarsuchus sloani* (Clark, Xu, Forster, & Wang, 2004), by original designation.

3.5 | *Junggarsuchus sloani* Clark, Xu, Forster, and Wang, 2004

Holotype: IVPP14010, a nearly complete skull and mandible and the anterior part of the postcranial skeleton.
Horizon and locality: Upper part of lower Shishugou Formation, Wucaiwan, Altay Prefecture, Xinjiang, China. A tuff approximately 30 m stratigraphically above this specimen has been dated at 162.2 ± 0.2 million years (Choiniere et al., 2014), which places it younger than the 163.5 ± 4 mya estimated age of the Middle-Late Jurassic boundary (albeit with a large error; Gradstein et al., 2012). With an estimated sedimentation rate of ~4.6 cm/ka (Eberth et al., 2001), the fossil is estimated to be about 652,000 years older than the dated tuff, placing it at approximately 162.85 mya, still slightly younger than the boundary estimate.
Revised diagnosis: Autapomorphies of *J. sloani* found in all of our analyses include: Premaxilla, ventral edge is dorsal to the ventral edge of the maxilla (Char. 61-2); presence of prefrontal overhang (Char. 128-1); two quadrate fenestrae (Char. 206-1); the quadratojugal extends anteriorly forming part of the ventral edge of the infratemporal bar (Char. 224-1); the mandibular fenestra inclined anterodorsally (Char. 322-1); presence of a surangular foramen (Char. 337-1); dorsal edge of the surangular anterior to the glenoid fossa is arched dorsally (Char. 339-1); the first manus digit faces laterally (Char. 433-1); the first metacarpal is slender (Char. 434-1); well-developed hypapophyses present on cervical and anterior dorsal vertebrae (Char. 500-4); procoelous vertebral centra in the cervical vertebra (Char. 498-2) and dorsal vertebra (Char. 501-2). Depending on the relationships of *Junggarsuchus* relative to *Phyllodontosuchus*, the following may also be autapomorphies: a pit between premaxilla and maxilla for lower caniniforms not exposed laterally (Char. 67-0); the lateral edges of the nasals are oblique to one another (Char. 93-1); the jugal is arched dorsally (Char. 97-1); the ventral edge of jugal has a longitudinal concavity (Char. 98-1); the posterior process of the jugal is shorter than 50% of the anterior process (Char. 110-1); the jugal terminates just anterior to the posterior border of the infratemporal fenestra (Char. 111-1); the squamosal lacks a dorsal ridge along edge of the supratemporal fossa (Char. 170-0); the squamosal posterolateral process distal end is tapered and pointed (Char. 188-0); *M. pterygoideus ventralis* insertion extends well onto the angular (Char. 349-2). It is possible that additional fenestrations in the palate are present and the squamosal may make up the entire lateral border of the supratemporal fenestra (Char. 180-1). The presence of scleral ossicles is found as an autapomorphy (Char. 9-1), but the rarity of these structures could be due to a taphonomic bias against their preservation.

4 | DESCRIPTION OF *JUNGGARSUCHUS* AND COMPARISON WITH *DIBOTHROSUCHUS*

Nearly all of the matrix has been removed from the skull of *J. sloani* and the bone has been glued where it had separated along several large cracks. The largest of these is between the braincase and the rest of the skull, where the dorsal part of the braincase is now rotated 5 mm to the left and the ventral part was rotated anteriorly. The right posterolateral part of the skull and mandible were eroded before discovery. The quadratojugal, squamosal, postorbital, all but the anterior tip of the jugal, the paroccipital process lateral to the quadrate, much of the angular, most of the surangular except its most anterior end, and the posterior end of the splenial are missing or too fragmentary to identify. The right articular and a fragment of the angular and posterior dentary are preserved separately. The ventral portion of the right quadrate has been broken and separated from the rest of the bone and was preserved in the right orbit. The left ventrolateral part of the parabasisphenoid is missing, and both pterygoids are fragmentary. A large piece is missing from the dorsal part of the rostrum just anterior to the antorbital fenestra and another from the right laterosphenoid. The sclerotic ossicles were preserved in the right orbit and were removed in articulation, a portion of the hyoid skeleton and a portion of the right postorbital and palpebral were also removed along with numerous fragments. A fragment of a large tooth was collected on the surface. During preparation, part of the right palatine was broken off and mistakenly glued to the anterior palatal process of the pterygoid.

The postcranial skeleton was preserved largely in articulation and was prepared lying on its right side. The right side of the vertebrae and ribs and most of the right shoulder girdle are not exposed, but the incomplete right forelimb and the left, dorsal, and ventral surfaces of most vertebrae are visible. Nearly all of the elements of the left forelimb were preserved in articulation, and these were removed from the skeleton. Only three complete and four partial phalanges are preserved on the left side. The right ulna and radius are preserved with their proximal ends articulated with the humerus on the main block and the remainder in pieces separately. The disarticulated elements of the atlas were preserved with the skull, the axis and following two cervicals were removed from the block when the skull was separated, and a cervical and three posterior dorsal vertebrae were collected separately in the field. Fifteen cervical and dorsal vertebrae and nearly the entire rib cage is preserved in articulation. Osteoderms and gastralia are not preserved; an interclavicle, clavicles, and sternum are not evident, but the ventral midline of the skeleton has not been completely prepared. A distal caudal vertebra and a putative sacral rib were collected from the surface.

4.1 | Cranium

4.1.1 | Skull openings

The **antorbital fenestra** of *Junggarsuchus* (Figures 3a,b and 4a,b) is 26.9 mm long (Table 4), over a third of the length of the maxilla in lateral view, and triangular in shape, with corners anteriorly, posterodorsally, and posteroventrally. The maxilla borders the anterior, anterodorsal, and ventral sides of the fenestra. The ventral edge of the fenestra slopes posteroventrally relative to the ventral edge of the maxilla. The lacrimal borders the antorbital fenestra posteriorly and posterodorsally and as a consequence, the jugal is fully excluded from the border of the fenestra. The antorbital fenestra is smaller than the orbit in *Junggarsuchus*, which contrasts with the condition in *Dibothrosuchus* and *Sphenosuchus*, which have fenestrae nearly as large as their orbits. The fenestra is also taller and less elongate than in non-crocodyliform crocodylomorphs like *Terrestrisuchus*. The antorbital fossa is present as a dorsoventrally short lamina on the anterior, anterodorsal and anteroventral edges of the antorbital fenestra (Figure 3). The antorbital fenestra of *Junggarsuchus* is large (more than half the size of the large orbit), but not as large relative to the orbit as in other non-crocodyliform crocodylomorphs like *Dibothrosuchus* and *Sphenosuchus*. It is still large relative to the fenestra in *Protosuchus haughtoni* (BP/1/4770) and *Orthosuchus*, which have fenestrae less than 50% the length of their orbit (Brown, 1933; Nash, 1975).

The **orbit** of *Junggarsuchus* is circular and large (Figures 3a,b and 4a,b), at 37 mm long, it is over 130% the length of the 26-cm-long antorbital fenestra, and over one-fifth the length of the 14.3 cm skull. The orbit faces laterally and it is not exposed on the dorsal aspect of the skull, like *Dibothrosuchus* and other non-crocodyliform crocodylomorphs, but unlike living crocodylians, which have dorsally facing orbits (Jouve, 2009). Anteriorly, the orbit is bordered by the lacrimal, in which the posterior process contributes slightly to the medial wall of the orbit. The anterodorsal border of the orbit is formed by the prefrontal and the posterodorsal border is formed by the frontal and overlain by the palpebral. The posterior border of the orbit consists nearly entirely of postorbital. The jugal forms nearly all the ventral border of orbit, except the anterior most part. The posteroventral process of the lacrimal makes up this anteroventral border of the orbit.

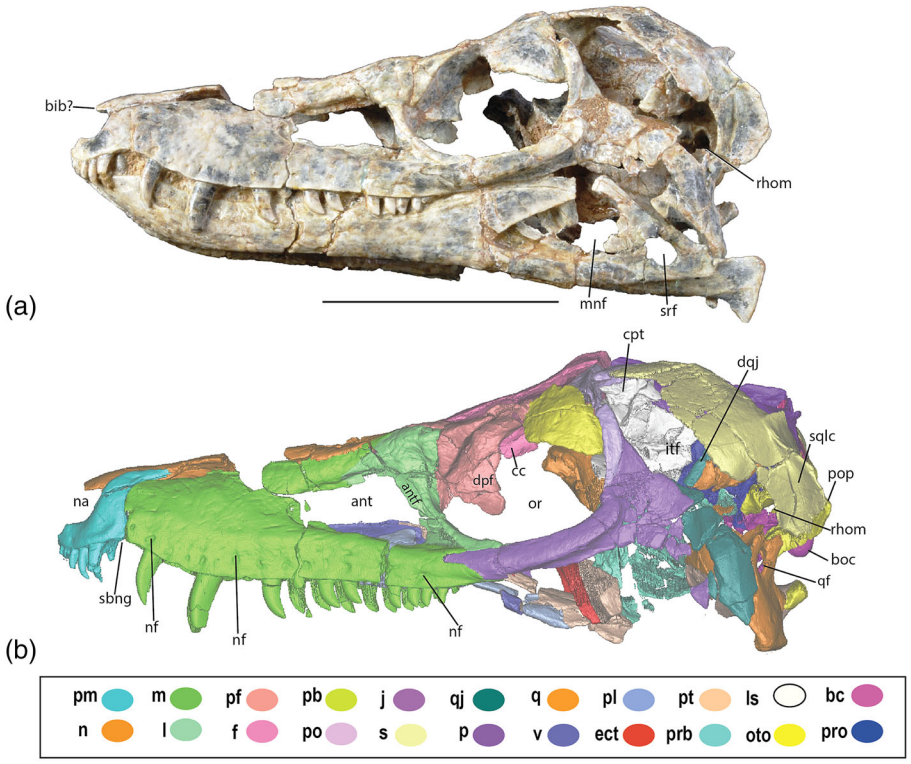

FIGURE 3 (a) Photograph and (b) CT reconstruction of the skull of *Junggarsuchus sloani* in left lateral view; scale bar is 5 cm (see list of anatomical abbreviations).

The orbit of *Dibothrosuchus* (Figures 5 and 10a) is smaller relative to the size of the skull than in *Junggarsuchus*, only roughly one-sixth the length of the skull, and smaller relative to other non-crocodyliform crocodylomorphs like *Sphenosuchus* (Walker, 1990), *Hesperosuchus agilis* (CM 29894) (Clark et al., 2001), *Terrestrisuchus* (Crush, 1984) and *Pseudhesperosuchus* (Bonaparte, 1969). In *Dibothrosuchus* and *Junggarsuchus*, the prefrontal contributes to the dorsal half of the anterior portion. In *Dibothrosuchus*, the prefrontal contributes more to the medial wall of the orbit and the jugal forms the posterior border of the orbit (Wu & Chatterjee, 1993) as opposed to the postorbital as in *Junggarsuchus*. The orbit of *Dibothrosuchus* lacks the prefrontal overhang seen in *Junggarsuchus*.

The **supratemporal fenestra** of *Junggarsuchus* is nearly one-fourth the length of the skull and is triangular (Figure 9a,b). The fenestra narrows anteriorly along with the skull table, like in *Almadasuchus*. In *Junggarsuchus*, the lateral and posterior borders of the supratemporal fenestra are formed by the parietal, whereas the squamosal contributes to the posterolateral corner and most of the lateral border. The frontal contributes slightly to the fossa but does not contribute to the fenestra. The anterior border of the supratemporal fenestra is comprised nearly entirely of the postorbital, if our primary interpretation of the postorbital is accurate (see below). Otherwise, this would imply that the squamosal borders the anterior and lateral edges and the postorbital is not involved at all, which is a condition unseen in other non-crocodyliform crocodylomorphs. The supratemporal fenestra narrows anteriorly similar to the condition observed in *Protosuchus haughtoni* (BP/1/4770) and *Protosuchus richardsoni* (Clark, 1986) and unlike the circular supratemporal fenestra in *Dibothrosuchus*.

In *Dibothrosuchus*, the supratemporal fenestra is smaller relative to the skull roof and oval with a similar axis (Figure 25d). Overall, the borders of the fenestra are largely similar, though the parietal contributes more to the posteromedial edge of the fenestra, the postorbital comprises the anterior border and the frontals contribute to the border anteriorly. In addition, *Dibothrosuchus*, unlike *Junggarsuchus*, has an anteroposteriorly elongate shelf-like supratemporal fossa that floors the posterior half of the fenestra. The prootic floors the posterior half of the fossa.

The **infratemporal fenestra** of *Junggarsuchus*, though incomplete, appears similar in shape to that of *Sphenosuchus* (Walker, 1990), as it is anteroposterior narrow and dorsoventrally tall (Figures 3a,b and 4a,b). The borders of the infratemporal fenestra in *Junggarsuchus* are not all clearly defined due to unclear sutures and incomplete jugal, quadratojugal, and postorbital. The postorbital appears to form the anterodorsal border of the fenestra. The posterodorsal border of the fenestra appears to be comprised of the squamosals. The quadratojugal forms the posterior border and some of the posterior ventral border of the fenestra. The ventral border and

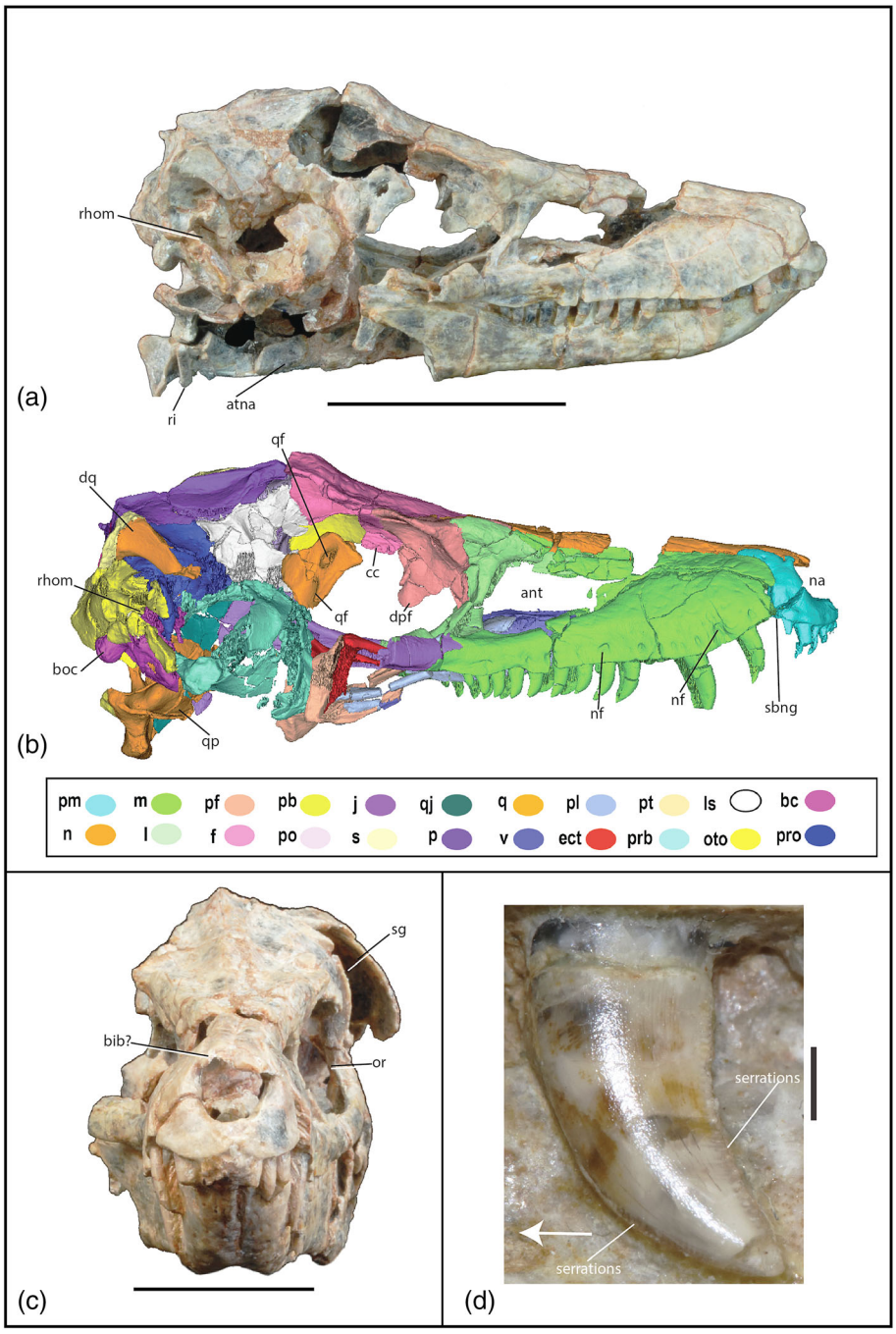

FIGURE 4 (a) Photograph of skull of *Junggarsuchus sloani* in right lateral view, and (b) CT reconstruction of skull in right lateral view; (c) skull in anterior view; (d) lateral view of fifth maxillary tooth. Scale bar is equal to 5 cm in (a), 1 cm in (c), and 2 mm in (d). Labels for maxilla neurovascular foramen indicate anterior and posterior extent of the foramina. Arrow indicates anterior direction.

anteroventral edge of the fenestra are formed by the jugal. Unlike in *Sphenosuchus*, *Protosuchus richardsoni* (AMNH 3024) and *Protosuchus haughtoni* (BP/1/4770), the jugal does extend posterior of the infratemporal fenestra.

The borders of the infratemporal fenestra of *Dibothrosuchus* are not well preserved, but the reconstruction by Wu and Chatterjee (1993) based on available material reconstructs the fenestra as longer that the orbit, unlike *Junggarsuchus*. The postorbital contributes to the entire anterior border of the fenestra and the anterior half of the dorsal border, unlike the condition in *Junggarsuchus*. Other differences include that the ventral border is comprised only of the jugal, whereas the quadratojugal only contributes to the posterior border. The ventral border of the infratemporal fenestra is flat, unlike the narrow, rounded ventral border seen in *Junggarsuchus* and *Protosuchus haughtoni* (BP/1/4770). Like *Junggarsuchus*, the posterior half of the dorsal border is comprised of the squamosal. We cannot comment further on the shape and size of this fenestra in *Dibothrosuchus* as we did not observe the holotype specimen (CUP 2081), which preserves more of this region than IVPP V7907 (Simmons, 1965).

TABLE 4 Table of measurements of the cranium and postcranium of *Junggarsuchus sloani* (IVPP 14010) in millimeter

Skull midline length	141.2
Orbit height/length	32.9/37.6
Antorbital fenestra height/length	13.9/26.9
Rostrum height at L lacrimal	31.5
Length supratemporal fenestra maximum length	32.3
Foramen magnum height/width	11.6/12
Palpebral length	15.4
Rostrum width/height at largest max tooth	24.5/26.5
Max depth of basisphenoid recess below braincase	24
Length mandibular fenestra height/length	13.9/25.9
Mandibular synthesis length	27.1
Length mandible total length	144.3
Length/height left retroarticular process	9.3/13.3
Max height of posterior mandible	23
Minimum height mandible just posterior to symphysis	11.9
Left scapula length along posterior edge (glenoid-dorsal rim)	51.8
Left scapula length along anterior edge (glenoid-anterior edge dorsal rim)	51.4
Left coracoid length (anteroproximal-posterior)	55.9
Left humerus length	105.9
Left humerus minimum shaft diameter	7.3
Left humeral deltopectoral crest length	22.9 (proximal end grades into articulation surface)
Left humerus width across distal condyles	17.8
Left radius length	94.9
Left radius minimum shaft diameter	4.9
Left ulna length	104.2
Left ulna minimum shaft diameter	4.9 (narrow region is crushed)
Left radiale length	36.2
Left ulnare length	26.7
Left metacarpal I length	20
Left metacarpal II length	24.4
Left metacarpal III length	28.3
Left metacarpal IV length	25.5
Left prox phalange length	10.9
Axis centrum length(w/o odontoid)	25
Odontoid process length	9.5
Odontoid process width	5
First articulated cervical: length centrum	18.5 (condyle length estimated)
Length/depth hypapophysis	7.2/4.1
Last articulated dorsal: centrum length	17.9
Length/height of neural spine	14.8/9.4

The **choanae** of *Junggarsuchus* are slit-like, six times as long as they are wide at the center and they narrow anteriorly and posteriorly. The maxilla borders the choanae anteriorly and anterolaterally; the vomer forms the entire medial border, and the palatines comprise the lateral and posterior edges of the choana (Figure 11c).

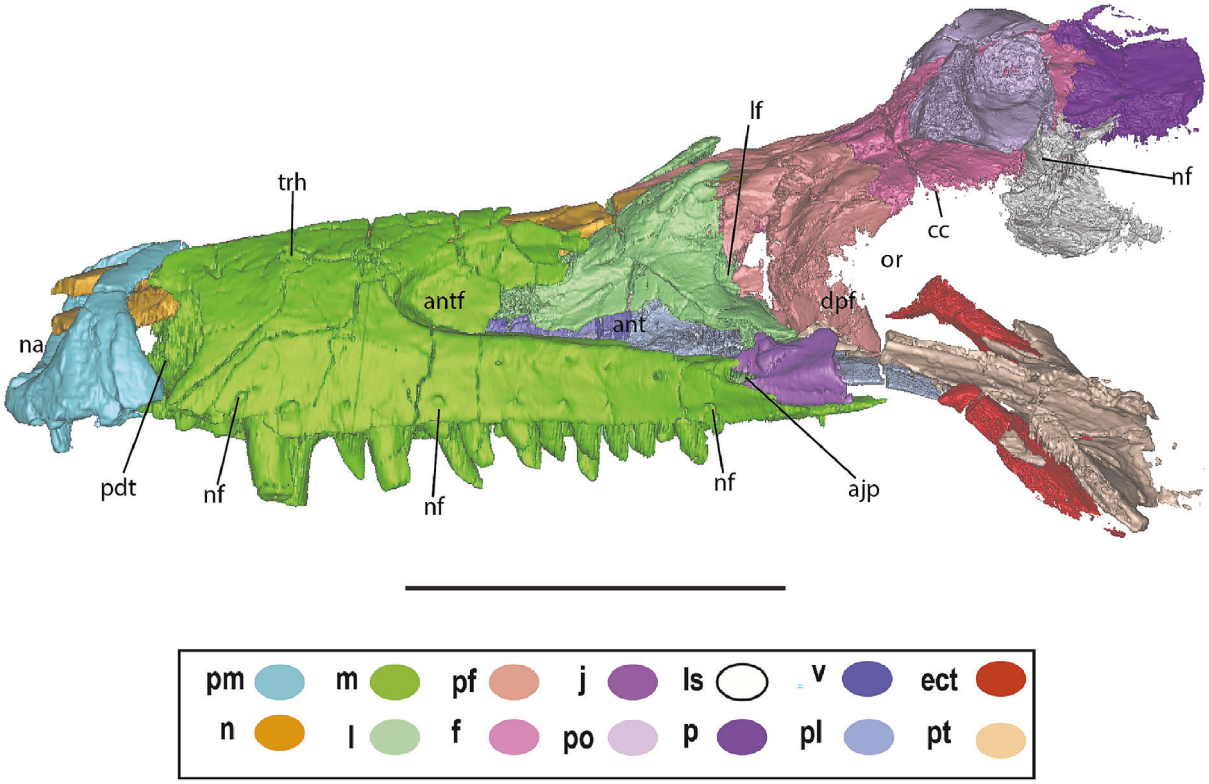

FIGURE 5 CT reconstruction of the rostrum of *Dibothrosuchus elaphros* in left lateral view; scale bar is 5 cm.

The borders of the choanae of *Dibothrosuchus* are formed by the same elements as seen in *Junggarsuchus*. The choanae themselves are slightly shorter and wider than in *Junggarsuchus*. The pterygoids are not involved with the choanae in *Junggarsuchus* unlike in crocodyliforms (Figure 11c).

The **suborbital fenestra** of *Junggarsuchus* is not clearly preserved as the incomplete palatine makes it difficult to determine the exact size of the fenestra. The anterior border of the fenestra is formed by the palatine exclusively (Figure 11a,c). A thin extension of the palatine encloses the anterior half of the lateral border of the fenestra. The anteromedial border is also comprised of the palatine. It is not clear how the pterygoid bordered the medial and posterior border of the suborbital fenestra. The posterolateral edge and part of the posterior edge are enclosed by the ectopterygoid. The fenestra appears to narrow posteriorly.

Dibothrosuchus has a large suborbital fenestra relative to the orbit, which is more oval than in other non-crocodyliform crocodylomorphs. The oval suborbital fenestrae are anteroposteriorly longer than they are mediolaterally wide, but the broken palatines do not allow us to give an exact comparison between the long and wide axes of the fenestra (Figure 11e). The borders of the fenestra are similar to those in *Junggarsuchus*. The pterygoid contributes more to the posterior border of the fenestra. The posterolateral process of the palatines is not preserved, so the extent of the palatines contribution to the lateral border is unclear. Wu and Chatterjee (1993) tentatively reconstructed the lateral process of the palatine as bordering the lateral edge of the fenestra, but we do not find evidence for this in the CT data.

4.1.2 | Bones of the cranium

Both of the **premaxillae** are nearly complete. There is a rugose region on the anterior end of the premaxilla that likely represents a break where the nasal process of premaxilla was located (Figures 3b, 4b,c, and 9b) and so the extent that the premaxilla contributed to the internarial bar is unknown. This region is similarly missing in *Dibothrosuchus* but has been preserved in *Dromicosuchus* (Sues et al., 2003), *Hesperosuchus* (CM 29894) (Clark et al., 2001) and *Sphenosuchus* (Walker, 1990) (Figures 3a and 9a). The anterior end of the right premaxilla has been pushed slightly toward the left, so that the narrow base of the broken internarial bar is a few millimeters left of the skull midline, and the facial portion of the left premaxilla has been displaced slightly medially where it contacts the maxilla. The premaxilla's contact with the maxilla is vertical and the entire posterior surface ventral to the posterodorsal process contacts the anterior surface

of the maxilla. In ventral view, the suture between the premaxilla and maxilla is straight. The preserved portion forms the ventral and posteroventral borders of the external nares, which faced anterolaterally (Figure 11c). The lateral surface posterior to the nares is approximately equal in length to the portion anterior to the posterior border of the nares when the posterodorsal processes are excluded from the total length. The shorter posterior process of the premaxilla is similar to some crocodyliforms, like *Fruitachampsa* (Clark, 2011) and *Dyrosaurus* (Jouve, 2005). Like other non-crocodyliform crocodylomorphs, the premaxilla bears a posterodorsal process that extends from the lateral surface between the anterior portions of the maxilla and nasal. The dorsal edge abuts the lateral edge of the nasal, which appears nearly flat in lateral view and the process extends posteriorly to above the level of the first preserved maxillary tooth. The dorsal edge of this process of the right premaxilla has a small indentation on its medial surface close to the narial border, but it is absent on the left side (Figure 9b). Assuming the internarial process was similar to other crocodylomorphs, the openings were narrow and elliptical in lateral view with the long axis running posterodorsally, which is also seen in *Dibothrosuchus*. The external surface of the lateral part immediately ventral to the narial opening has a shallow narial fossa, but a distinct border is lacking. There is only a very small subnarial gap (sensu Nesbitt, 2011) in the form of a slight ventral notch between the maxilla and premaxilla laterally where the fourth dentary tooth occludes (Figures 3b and 11a), unlike the far larger one seen in *Dibothrosuchus* and other non-crocodyliform crocodylomorphs such as *Sphenosuchus* (Walker, 1990), *Hesperosuchus* (CM 29894) (Clark et al., 2001), *Dromicosuchus* (Sues et al., 2003), and *Terrestrisuchus* (Crush, 1984) (Figure 10a) where the opening is large and constricted at its ventral edge. However, an internal pocket for enlarged dentary teeth is present, which is bordered anteriorly by the premaxilla and posteriorly by the maxilla notch (consistent with the subnarial foramen of Nesbitt, 2011), but is only visible in ventral view. The lack of a lateral notch is also seen in the non-crocodyliform crocodylomorph *Pseudhesperosuchus* (Bonaparte, 1969). The palatal portion of the premaxilla is short due to the anterior extent of the maxillary palatal process and does not meet medially, similar to other non-crocodyliform crocodylomorphs. A small, undivided incisive foramen is present on the midline where the maxilla and premaxilla meet opposite the posterior end of the narial opening. The ventrolateral edge of the premaxilla is gently convex ventrally, so that there is a gentle ventral concavity along the premaxillary symphysis and at the premaxilla–maxilla contact. Two faint circular impressions are preserved on the anterolateral surface of the premaxilla, dorsal to the third premaxillary tooth, which are interpreted as neurovascular foramina based on their small size and position dorsal to the toothrow.

The premaxilla of *Dibothrosuchus* is largely similar to that of *Junggarsuchus*; however, the two premaxillae of *Dibothrosuchus* are separate, likely due to postmortem deformation (Figures 5 and 10a). The premaxilla of *Dibothrosuchus* is taller, wider, and shorter than that of *Junggarsuchus* and the posterodorsal process of the premaxilla is shorter than that of *Junggarsuchus*, being less than half the length of the premaxilla anterior to the nares (Figures 5 and 10b). The nares face anterolaterally as in *Junggarsuchus*. On the anterior end of the premaxilla, anterior to the opening for the nares, there is a similar break to that of *Junggarsuchus*, which suggests the presence of the nasal process of the premaxilla though we cannot estimate its relative contribution to the internarial bar, a structure seen in other non-crocodyliform crocodylomorphs such as *Dromicosuchus* (Sues et al., 2003), *Hesperosuchus* (CM 29894) (Clark et al., 2001), and *Sphenosuchus* (Walker, 1990). The ventral edge of the premaxilla is in line with the ventral edge of the maxilla, unlike *Junggarsuchus*, in which the premaxilla's ventral edge is located dorsal to the majority of the maxilla's ventral edge. The palatal portion of the premaxilla is similarly short, but on the right premaxilla, a notch is present, medial to the fourth premaxillary tooth (Figure 11c); as it is not present in the left element, it is unclear whether this structure is asymmetrical or the result of post mortem deformation. Both elements also have a single small foramen on the anterior edge of the facial portion of the premaxilla, likely the same as that seen on *Junggarsuchus* (Figures 3a,b and 4a,b). *Dibothrosuchus* also possesses a slight depression on the facial portion of the premaxilla, but it is less concave than that in *Junggarsuchus*. Dorsal to the tooth row, the ventral most part of the lateral surface of the premaxilla has a slight ridge that trends along the entire length of the premaxilla and separates the tooth row from the rest of the lateral face. In *Dibothrosuchus*, this ridge is missing, and the bone dorsal to the tooth row is smooth. The greatest difference between the premaxilla of *Dibothrosuchus* and *Junggarsuchus* is the presence of the subnarial gap (Figure 3b), which occurs as a notch for the occlusion of the fourth dentary tooth. The notch between the premaxilla and maxilla in *Dibothrosuchus* is wide and ovate, nearly the length of the naris and more than half as wide (Figures 5 and 10a).

Each premaxilla of *Junggarsuchus* has five tooth positions, but the fifth tooth is preserved only on the right side. The anterior two right teeth were in the process of replacement as indicated by their small exposure relative to the teeth in the left premaxilla. Based on alveoli, which all occur as separate ventrally opening cavities, the

relative tooth sizes are 1 < 2 < 5 < 3 < 4. Only the posterior edge of the third, fourth, and fifth teeth is serrated. The anterior most two teeth are too poorly preserved to allow us to confidently describe any serrations. Serrations are similar in size to those of the maxillary teeth, each about 0.33 mm tall. The posterior third, fifth, and probably the fourth, teeth are slightly recurved, but are only slightly compressed labiolingually (Figures 3b, 4d, and 11b).

Dibothrosuchus has five teeth in its premaxilla, with relative sizes 1 < 2 < 5 < 3 < 4, just as observed in *Junggarsuchus*. None of the teeth are preserved in their entirety, and what teeth are observable lack serrations (Wu & Chatterjee, 1993). They have circular-ovate cross sections similar to *Junggarsuchus* teeth (Figures 5 and 11c).

Both **maxillae** are nearly complete, but both are missing a small portion just anterodorsal to the antorbital fenestra. The facial portion (Figures 3 and 4b) anterior to the antorbital fenestra is approximately 50% longer than it is tall in lateral view. Posteriorly, the maxilla divides into two processes that make up most of the dorsal and ventral borders of the antorbital fenestra. The posterodorsal process (=ascending process) meets the lacrimal approximately halfway along the dorsal edge of the antorbital fenestra; the suture between them is poorly preserved, but the lacrimal overlaps the maxilla laterally. The posterodorsal process is proportionally longer than those observed in other non-crocodyliform crocodylomorphs and appears to nearly totally separate the medial surface of the lacrimal from the lateral edge of the nasal. This posterodorsal process underlays the anterior edge of the lacrimal. The posterior process makes up the entire ventral border of the antorbital fenestra. The posteroventral process of the maxilla tapers gradually posteriorly, where the lacrimal broadly overlaps its posterior end. The tapered anterior end of the jugal inserts into the lateral surface of the posteroventral process of the maxilla to end dorsal to the last maxillary tooth and ventral to the center of the ventral edge of the lacrimal; the maxilla-jugal overlap extends for 10 mm. The premaxillary contact is extensive and nearly vertical anteriorly, and the anterior edge of the maxilla is slightly convex on the left side but not the right. The maxilla curves posterodorsally and is covered dorsally by the nasal along their straight contact in dorsal view. The ventral edge of the maxilla is gently convex at the positions of maxillary teeth three, four, and five and becomes straight posterior to the sixth tooth.

Anterior to the antorbital fenestra, the maxilla forms a very short fossa, preserved on the left side. On the dorsal edge of the fenestra, this fossa is dorsoventrally low forming a groove along the ventral edge of the maxilla's posterodorsal process. The fossa does not extend as far posteriorly or dorsally as that seen in *Dibothrosuchus*, *Dromicosuchus* (Sues et al., 2003), or *Hesperosuchus* (CM 29894) (Clark et al., 2001). Small ventrolaterally opening nutrient foramina pierce the ventrolateral surface of the maxilla dorsal to the tooth row, 12 on the right maxilla and 14 on the left (Figures 3a,b and 4b) and do not correlate one to one with the maxillary alveoli. The nutrient foramina are not evenly sized or space with the foramina more densely arranged dorsal to the third tooth. Along the medial surface of the posterodorsal process of the maxilla there is a groove, which continues onto the anteromedial surface of the lacrimal. We interpret this as for the maxillary branch of the trigeminal nerve (V2), as the passageway though the maxilla is dorsal to the alveoli, exhibits branching, and is in a similar position to the nerve observed in living crocodylians like *Alligator mississippiensis* (George & Holliday, 2013). The maxillary branch of the trigeminal nerve (V2) is preserved as a continuous passageway through the ventral body of the maxilla that extends the entire anteroposterior length of the bone. At least nine smaller ventral branches can be seen dorsal to the alveoli (Figure 6a,b). The spacing of these branches loosely follows the alveoli.

The two maxillae (Figure 5) of *Dibothrosuchus* are nearly complete and broadly similar to those of *Junggarsuchus*. Only the posterior most process that contacts the jugal is missing on the right maxilla. The maxillae are wider in articulation than those in *Junggarsuchus* and bow laterally posteriorly, though this lateral displacement is likely due to post mortem crushing (Figure 10). Unlike *Junggarsuchus*, the anterior end of the maxillae of *Dibothrosuchus* is concave in lateral view due to space for the enlarged fourth mandibular tooth that fits between the maxilla and premaxilla. The ventral edge of the maxilla is even more gently concave near the enlarged maxillary teeth than *Junggarsuchus*. The maxilla overlaps any lateral exposure of the nasal in latera view. The fossa also extends father posteriorly. Like *Junggarsuchus*, several ventrolaterally opening nutrient foramina pierce the ventrolateral surface of the maxilla. They are smaller and fewer than the ones present in *Junggarsuchus*, with eight to nine occurring dorsal to the tooth row. There also is an additional row of five or six small foramina on the dorsolateral surface of the posteroventral process of the maxilla immediately ventral to the ventral maxillary rim of the antorbital fenestra and dorsal to the posterior four neurovascular foramina (Figure 5). This row does not extend anterior to the anterior edge of the antorbital fenestra.

On the dorsal surface of both maxillae of *Dibothrosuchus*, there are two dorsal openings. The more anterior one (illustrated, but not described by Wu & Chatterjee, 1993), is located in line with the second maxillary tooth. The more posterior one is smaller and in line with the fourth maxillary

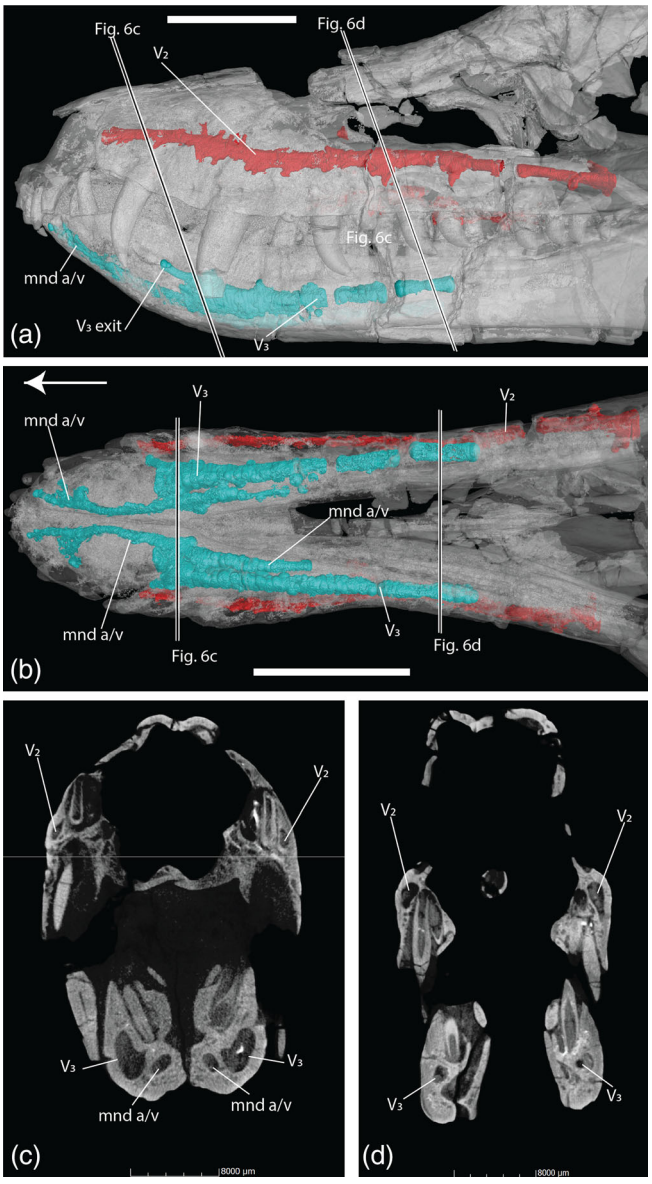

FIGURE 6 (a) The paths of the maxillary (red) and mandibular (blue) branches and associated vasculature of the trigeminal nerves in *Junggarsuchus sloani* in lateral view, figure made in VG studios; (b) the paths of the trigeminal nerves in ventral view; (c) cross sections of the maxilla and dentary in anterior CT view (slice 2,879); (d) cross section of the maxilla and dentary in CT view (slice 2,327). Black and white lines indicate where CT images in (c) and (d) were taken. Scale bar is equal 2 cm in (a)–(c) and 8 mm in (d) and (e). Arrow indicates anterior direction.

tooth. These openings are not seen in any other non-crocodyliform crocodylomorphs or crocodyliform. They appear to be due to postmortem crushing as they are associated with the roots of the tooth they correspond to (Figures 5 and 10). We interpret these as caused during deformation, as the dorsal surface of the skull was compressed, the roots of these teeth punctured the lateral wall of the maxilla, making weak spots.

The palatal process of the two maxillae in *Junggarsuchus* (Figure 11c) meets medially to form a bony palate. The bony palate begins anteriorly, between the premaxillae, and extends posteriorly up to the position of the fourth maxillary tooth. Anteriorly, the maxilla forms a pocket medial to the premaxillary contact into which the fourth dentary tooth inserted. This pocket opens dorsally, being visible from the narial opening. Posterior to this, the maxillary shelves of the palate become flatter in anteroposterior cross section and appear to thicken in CT scans, especially along the medial surface of the maxilla, where the two bones form a low midline ridge dorsally. The maxilla forms only the lateral and anterior borders of the choanae.

The palatal process of the maxilla of *Dibothrosuchus* (Figure 11e) is relatively wider than *Junggarsuchus*, though the partial separation is due to compression. The palatal shelf extends back to the position of the fifth maxillary tooth. A small medial extension of the palatal shelf forms the anterior and anterior most medial edges of the choanae. This process may be present in *Junggarsuchus*, but it is broken. However, there is a concavity on the ventral surface on the vomer that indicates its potential presence (Figure 11b).

We infer 14 tooth positions in each maxilla in *Junggarsuchus* (Figures 3b and 11b), the 14th is represented by an apparent tooth fragment in this position on the left side and alveolus on the right side. On both sides, the second and fourth teeth have been lost. The labial edge of the maxilla bulges laterally between the first and third teeth, indicating an alveolus, but the right maxillary edge extends inward at this position, possibly due to postmortem crushing. The third tooth is the largest and the alveolus for the fourth is smaller, whereas the first and fifth teeth are of similar size. The teeth gradually increased in size up to the third tooth, after which they decreased posteriorly. The third tooth is nearly twice as long as the fifth tooth, and the size of the alveoli and the ventral excursion of the maxilla in this region indicate that the second to fourth teeth were larger ones (the second tooth is nearly as anteroposteriorly long as the third and the fourth at least 25% longer based on the space of the alveoli) similar to the tooth positions in *Sphenosuchus* (Walker, 1990) and may have formed a functional unit separate from the posterior teeth. The fifth tooth is slightly smaller than the first tooth, and all teeth posterior to this become gradually smaller in size, until the last and smallest tooth is only 3 mm long. All of the teeth, except possibly the posterior one, are recurved, and the sixth and seventh are strongly recurved. The distal edge of each maxillary tooth is serrated in a similar manner

(Figure 4d). The mesial edge is also serrated on its distal half from the sixth tooth posteriorly, but the first and third teeth lack serrations mesially. A small, loose tooth is preserved on the lateral surface of the right dentary beneath the posterior end of the tooth row, similar in size to the 13th preserved maxillary tooth, and therefore it is possibly the 14th tooth.

Dibothrosuchus has positions for 15 maxillary teeth on both sides (Figures 5 and 11c). On the left side only alveoli 8, 10, and 15 are empty, and on the right side only alveoli 4, 14, and 15 are empty. The first two maxillary teeth are small, the second slightly larger than the first, but both are barely exposed laterally. The largest teeth and alveoli are the third and fourth teeth. Both the fourth alveolus and tooth are slightly larger, but neither the third or fourth tooth are preserved entirely, those seen are missing the apical ends of the crown. The fifth tooth is smaller than the third and fourth, but larger than the others. Relative to the height of the maxilla, the enlarged maxillary teeth (crowns at least 30% the height of the maxilla) are not as large as those of *Junggarsuchus*, which has enlarged maxillary tooth crowns at least 60% the total height of the maxilla. Like *Junggarsuchus*, the rest of the teeth decrease in size posterior to the 14th tooth. The maxillary teeth of *Dibothrosuchus* are recurved but slightly less recurved distally than those of *Junggarsuchus*. The seventh tooth is the most recurved. Like *Junggarsuchus*, the lanceolate hypertrophied maxillary teeth lack anterior serrations and from the sixth tooth posteriorly are serrated distally and mesially.

The **nasals** of *Junggarsuchus* are paired, long, narrow bones that make up the anterior half of the skull roof anterior to the orbit. They widen posteriorly in the lateral direction and reach their widest point at about 75% of their length, near their contact with the prefrontals, then narrow where it meets the frontal (though remain twice the width of the anterior part of the nasals) similar to *Sphenosuchus* (Walker, 1990), the crocodyliform *Orthosuchus* (Nash, 1975), and thalattosuchians like *Pelagosaurus* (Pierce & Benton, 2006) (Figure 9b). This differs from the condition in *Protosuchus richardsoni* (MCZ 6727, AMNH 3024, and UCMP 130860) (Clark, 1986) in which the nasals widen posteriorly to a transverse contact with the frontals. A large, central area where the nasal would have contacted the maxilla on both the right and left sides is missing, and the left nasal is also damaged anterior to this gap. Anterior to the prefrontal, their lateral edge bends ventrally, dividing the bone into dorsally and laterally facing parts. The dorsal part is slightly convex dorsally in the anterior half of the bone, resulting in a dorsal midline groove. Posteriorly, the nasals are nearly flat and rise medially to form a low midline ridge. The anterior ends of the nasals form a small part of the posterodorsal border of the external nares, which fit between both premaxillae. The nasal contacts the posterodorsal process of the premaxilla ventrolaterally and the nasal widens slightly anterior to this process. The nasal ends anteriorly in a broken base of the internarial process, which is broad and dorsoventrally flattened (Figures 3a, 5c, and 9a,e). The posterior end of the nasal does not feature a w-shaped suture with the frontals (Figure 9b). Two lateral posterior processes on the nasal extend between the prefrontal and frontal, where it overlies, the frontal and prefrontal partially. These posterior processes are similar to those in *Dibothrosuchus* and *Hesperosuchus* (CM 29894) (Clark et al., 2001), but the portions of the bone extending between the prefrontals and frontal are much shorter (about one-tenth the anteroposterior length of the prefrontal vs. one-third the length in *Dibothrosuchus*). Anterior to the prefrontal, the nasal has a short contact laterally with the anterodorsal process of the lacrimal. Unlike other non-crocodyliform crocodylomorphs, the lateral edge of the nasal does not contact the medial edge of the maxilla instead, the ventrolateral surfaces of the nasals contact the dorsal surface of the posterodorsal (=ascending) process of the maxilla. Posteriorly, the lateral edges of the nasals are largely excluded from contacting the medial edge of the lacrimal by the prefrontals. This is similar to the conditions seen in *Protosuchus haughtoni* (BP/1/4770) and *Orthosuchus* (Nash, 1975).

The paired nasals of *Dibothrosuchus* are more complete (Figure 10), with the exception of the anterior ends that extends between the premaxilla that would meet the internarial bar (Figure 10c). The nasals have been displaced ventrally, due to post mortem distortion. The nasal is largely similar to that of *Junggarsuchus*; it contacts the dorsal edge of the maxilla along its anterior third, and contacts the medial edges of the prefrontals posteriorly. There is also a short, 4-mm-long contact with the medial edge of the lacrimals posteriorly. Unlike the nasals of *Junggarsuchus*, the nasals of *Dibothrosuchus* do not widen posteriorly, and overall, are relatively wider than those of *Junggarsuchus*. The two bones are flatter, lacking the slight dorsal ridges present in other non-crocodyliform crocodylomorphs. The nasals also lack the lateral exposure seen in *Junggarsuchus* and possess a more distinct forked process of the posterior part of the nasals, which extend between the prefrontals and the frontals. These twinned posterior processes are separated by an anterior process of the frontals at the midline and are wider than those seen in *Junggarsuchus*.

The **lacrimal** of *Junggarsuchus* is in the shape of an inverted L with a long anterodorsal process and is approximately as long as it is high (Figures 3b and 9b). On the right side of the skull, the bone has been partially

crushed, and the left element is better preserved. Its ventral process is nearly vertical in lateral view, forming the posterior edge of the antorbital fenestra. The anterior edge of this process has a deep dorsoventral groove (Figures 3b and 7b) that becomes open laterally near the base, forming a narrow antorbital fossa. The posterior edge of this process curves posteroventrally, forming the anteroventral edge of the orbit, and is as long as the ventral process of the lacrimal at its midpoint. This elongate posteroventral process is longer than the process seen in *Dibothrosuchus*, which is only 50% of the length of the lacrimal's ventral process at its midpoint. The lacrimal has a very narrow exposure on the skull roof and contacts the prefrontal medially and posteriorly dorsal to the preorbital bar. The posterior contact with the prefrontal is short, and the prefrontal dorsally covers the posterior edge of the entire dorsal part of the lacrimal. The tapering anterodorsal process overlies the maxilla approximately at the midpoint of the antorbital fenestra, but this suture has been damaged on both sides of the skull. The dorsal part of the lacrimal has a rugose lateral surface, whereas the descending process has a smooth surface. Medially, within the skull, a large but shallow pocket is visible on the medial surface of the anterodorsal body of the lacrimal (Figure 7b). Based on its position well anterior to the orbit and the ventral lamina (=cristae cranii sensu Walker, 1990) of the frontal, we infer this as an excavation of the paranasal sinus; a similar pocket is present in *Dibothrosuchus*. The mediolateral wall of the lacrimal body is relatively thin and the anterior surface of the ventral process preserves a narrow dorsoventral groove that forms the posterior border of the antorbital fenestra, and we infer the lip of it to be the posterior limit of the antorbital sinus. There is an elongate, continuous space through the anterodorsal body of the lacrimal for the nasolacrimal duct, that is circular in cross section and nearly, but does not fully reach the anterior border of the antorbital fenestra. The anterior end of the duct opens medially into the skull at the end of the anterodorsal process of the lacrimal and the duct opens posteriorly into the orbit though an oval foramen, the lacrimal foramen (Figure 7d,e). This posterior exit into the orbit is set in a rhomboidal depression enclosed anteriorly by the lacrimal and posteriorly by the prefrontal (Figure 7a). The passageway is horizontal for much of its length. In lateral view, the passageway expands dorsally three-fourths of the way back, near the tallest point of antorbital fenestra. The passageway for the nasolacrimal duct then descends ventrally for the remainder of its length.

The lacrimal of *Dibothrosuchus* is similar to that of *Junggarsuchus* (Figures 5 and 7c). The anterodorsal process of the lacrimal is about the same length as the ventral process, which is proportionally longer than the process in *Junggarsuchus*, and forms the posterior half of the dorsal border of the antorbital fenestra. The lacrimal is longer than the prefrontal anteroposteriorly, which is similar to the relative length of the lacrimal to the prefrontal seen in *Protosuchus richardsoni* (AMNH 3027, UCMP 130860), *Protosuchus haughtoni* (BP/1/4770) (Gow, 2000) and other early diverging crocodyliforms like *Orthosuchus* (Nash, 1975), *Gobiosuchus* (Osmólska et al., 1997), and most Thalattosuchians, but not *Junggarsuchus* or *Sphenosuchus* (Walker, 1990). The groove that extends into the anterior antorbital fossa is shorter in *Dibothrosuchus*. The lacrimal appears to lack the posterior projection that overlays the anterior portion of the prefrontal, but the bone is crushed in this region on both sides, obscuring potential sutures. In *Dibothrosuchus*, the contact with the prefrontal extends ventrally for most of the lacrimal's ventral process, and the suture is vertical. As in *Junggarsuchus*, the lacrimal is thin walled and possesses an enlarged hollow space in the anterior body of the bone, relatively larger than that of *Junggarsuchus*. The posterolateral surface of the lacrimal, along the dorsoventral suture with the prefrontal, has a small opening for a lacrimal foramen that opens into the orbit, which is enclosed by the lacrimal laterally and the prefrontal medially (Figure 7c). In *Junggarsuchus*, the posterior exit of the nasolacrimal duct is set in a lateral depression between the lacrimal and prefrontal, whereas the actual posterior exit of the duct is fully enclosed in the lacrimal, contrasting with the condition in *Dibothrosuchus* (Figure 7a,b).

The rhomboidal **prefrontal** of *Junggarsuchus* overhangs the orbit anteriorly (Figures 3b, 8b, and 9b). Its mediolaterally broad ventral process extends into the anterodorsal region of the orbit, where its anteroposteriorly long and triangular lateral part borders the lacrimal posteriorly. This process forms the anterodorsal half of the orbit and medially it curves posteriorly to form a posterolaterally facing fossa. The body of the laterally expanded prefrontal makes up the anterior half of the orbit's dorsal border. The medial part of the descending process is mediolaterally thinner than the lateral part, its ventral edge is horizontal and its posterior edge is vertical (Figures 3b and 8b). Anterodorsally, the prefrontal narrows and fits between the lacrimal and the nasal. The contact with the frontal is approximately as long as the contact with the nasal. Posteriorly, as in *Dibothrosuchus*, the prefrontal does not appear to send a mediolaterally wide process to underlie the frontal, contrasting with the condition reported in *Sphenosuchus* (Walker, 1990) and *Hesperosuchus* (CM 29894) (Clark et al., 2001), though this is challenging to verify without CT data for these taxa. Its dorsal surface is shallowly concave posteriorly and becomes slightly convex in the area where it contacts the lacrimal. *Junggarsuchus* has a laterally expanded

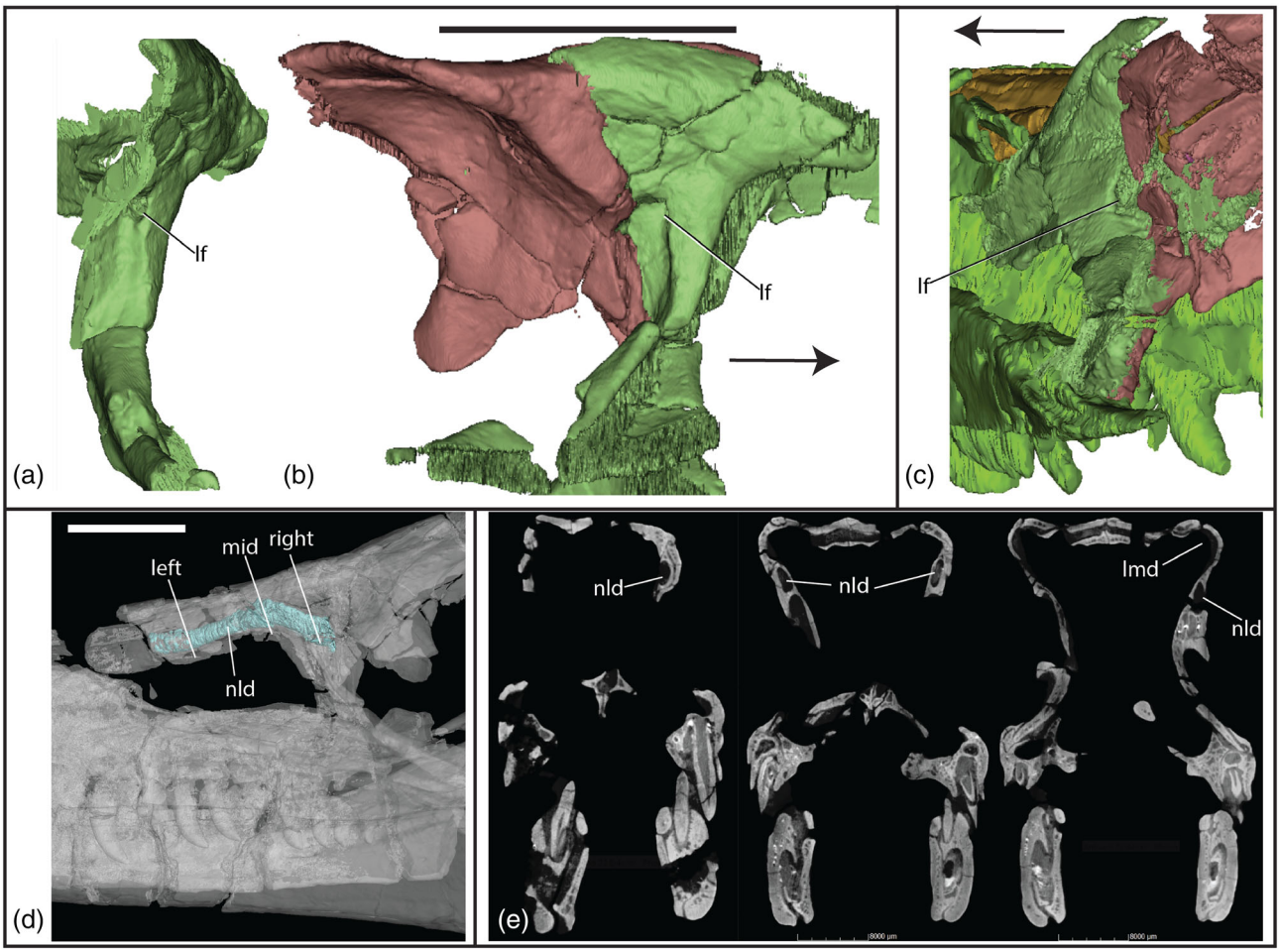

FIGURE 7 (a) The lacrimals of *Junggarsuchus sloani* in posterolateral view; (b) left lacrimal and prefrontal of *Junggarsuchus sloani* in lateral view showing rhomboidal depression for the lacrimal foramen; (c) the lacrimals of *Dibothrosuchus elaphros* in posterolateral view; (d) endocast of the nasolacrimal duct in lateral view; (e) nasolacrimal duct in cross section in CT view—anterior exit (left—slice 2,199), middle (slice 1,921), and posterior exit (right—slice 1,834). Black and white lines indicate where CT images in (e) were taken. Scale bars are equal to 2 cm in all figures except (e) where the scale bar equals 8 mm. Arrow indicates anterior direction.

prefrontal which forms a prefrontal overhang on the anterodorsal half of the orbit which is not observed in *Dibothrosuchus*, *Sphenosuchus* or other non-crocodyliform crocodylomorphs. The overhang is enlarged, twice the mediolateral width of the anterior process, and oblique, similar to the overhang seen in thalattosuchians such as *Pelagosaurus*, though not as enlarged as those overhangs in metriorhynchids like *Cricosaurus* ("*Geosaurus*") *araucanensis* (Young & Andrade, 2009), *Dakosaurus maximus* (Young et al., 2012) and *Metriorhynchus* (Andrews, 1913). The posterior face of the orbital fossa of the prefrontal has a small foramen that is directed posteriorly (Figure 8a, b). This foramen is preserved on both prefrontals and is likely an opening for the anterior path of the supraorbital vein or artery, because in extant crocodylians, the supraorbital vein passes through the frontals, exits the frontal and rests along the dorsomedial border of the orbit, then reenters the skull through the posterior surface of the prefrontal where it then continues into the nasal capsule (Porter et al., 2016). This foramen in the posterior face of the prefrontal is consistent with this interpretation, though the path of this vein through the frontal is not preserved and it is possible that the vein was resting on the exterior of the frontal in the orbit, then entering the skull and nasal capsule through the prefrontal. In living crocodilians, the supraorbital veins and arteries are closely associated with the ophthalmic branch of the trigeminal nerve, and this path of the trigeminal nerve is positioned medial to the prefrontal and does not enter the bone so it is unlikely that this foramen is for the ophthalmic branch of the trigeminal (Lessner & Holliday, 2020).

The prefrontal of *Dibothrosuchus* (Figures 5 and 10a) is largely similar to that seen in *Junggarsuchus* in being rhomboidal in dorsal view. More of the descending medial and posterior processes of the prefrontal are preserved in *Dibothrosuchus*. Like *Junggarsuchus* and other non-crocodyliform crocodylomorphs, the prefrontal of

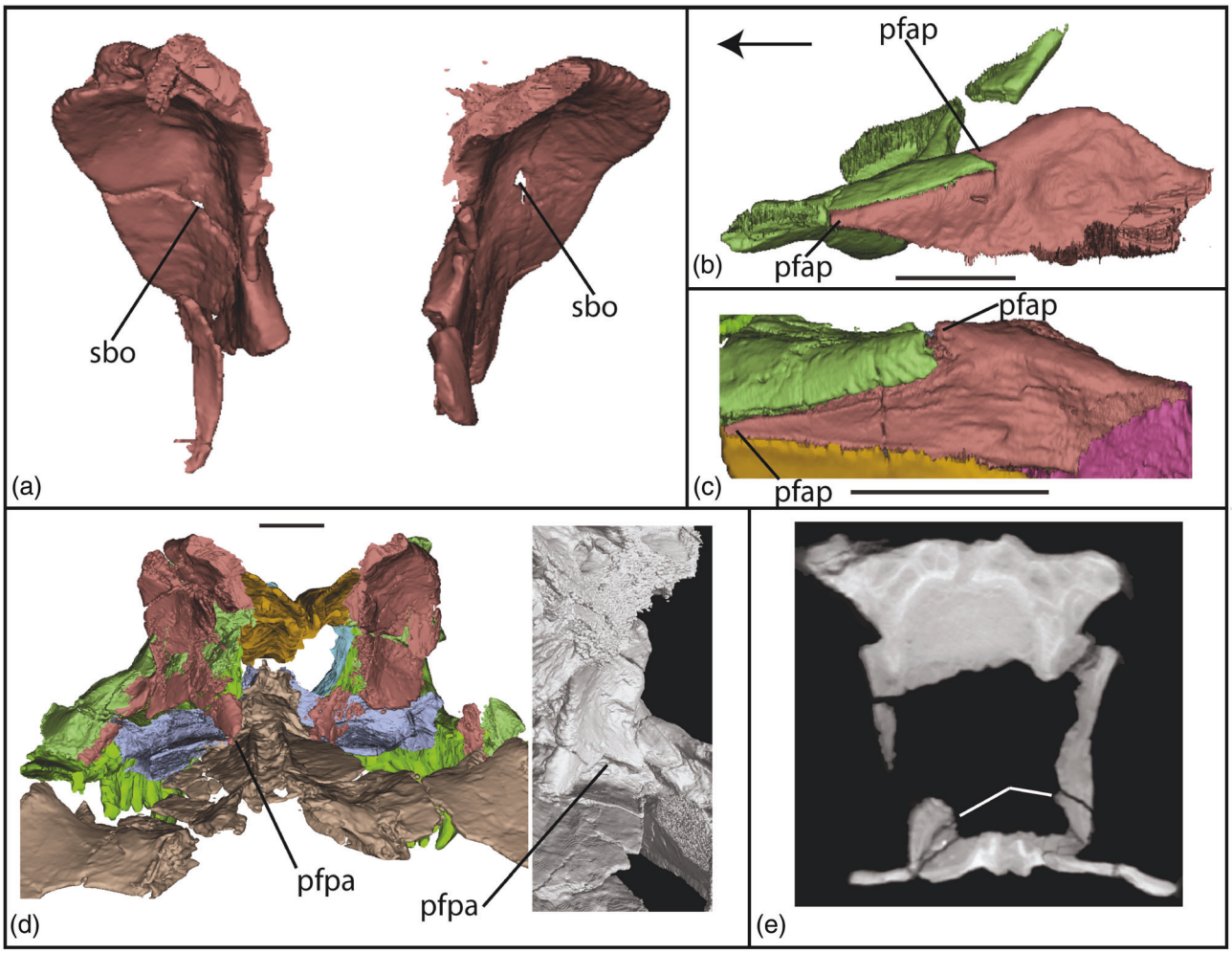

FIGURE 8 The prefrontals of *Junggarsuchus sloani* in (a) posterior and (b) dorsal views; prefrontals of *Dibothrosuchus elaphros* in (c) dorsal view, and (d) the prefrontals and palate in posterior view visualized in mimics (left) and as an isosurface render (right); (e) lack of prefrontal brace seen in CT data, indicated by white line (slice 1,541). Arrow indicates anterior direction; scale bars are 1 cm.

Dibothrosuchus features a concavity for the posterior process of the lacrimal along with forked anterior processes of the prefrontal; the additional lateral process is partially broken anteriorly (Figures 5 and 10a). The anterodorsal process of the prefrontal is longer and has a longer contact with the nasal than it does in *Junggarsuchus*. The posterior dorsal suture of the prefrontal with the frontal is not very clear, but it appears that not much of the prefrontal extends under the frontals. As in *Junggarsuchus*, the dorsal surface is concave medially and convex and ridge like laterally, though this may have been exaggerated by crushing. *Dibothrosuchus* lacks a prefrontal overhang.

The descending process of the prefrontal in *Dibothrosuchus* (Figure 5) extends farther ventrally and posteriorly than the process in *Junggarsuchus* and forms the entire anteromedial wall of the orbit. This is a greater contribution to the orbital wall than observed in any other non-crocodyliform crocodylomorphs, including *Sphenosuchus* (Walker, 1990). The medial contact of the prefrontals to form a "transverse-brace" reported by Wu and Chatterjee (1993) is not observed in the CT scans of the skull (Figure 7d,e). The ventral process of the prefrontals that contact the palatines do not appear to contact each other and, based on inferences from CT, data do not appear the medial surface of these ventral processes are broken (Figure 8c,d). The descending process contacts the palate at the point that the posterior edges of the palatine and meet lateral edges of the pterygoid. The contact between the prefrontal and palate is not observed in any other non-crocodyliform crocodylomorphs, but it is present in crocodyliforms including *Gobiosuchus* (Osmólska et al., 1997) and the more specialized thalattosuchians (*Cricosaurus* and *Metriorhynchus*) (Young & Andrade, 2009) and notosuchians and neosuchians. Despite the dorsoventrally tall ventral processes of the prefrontal, this contact may, however, be due

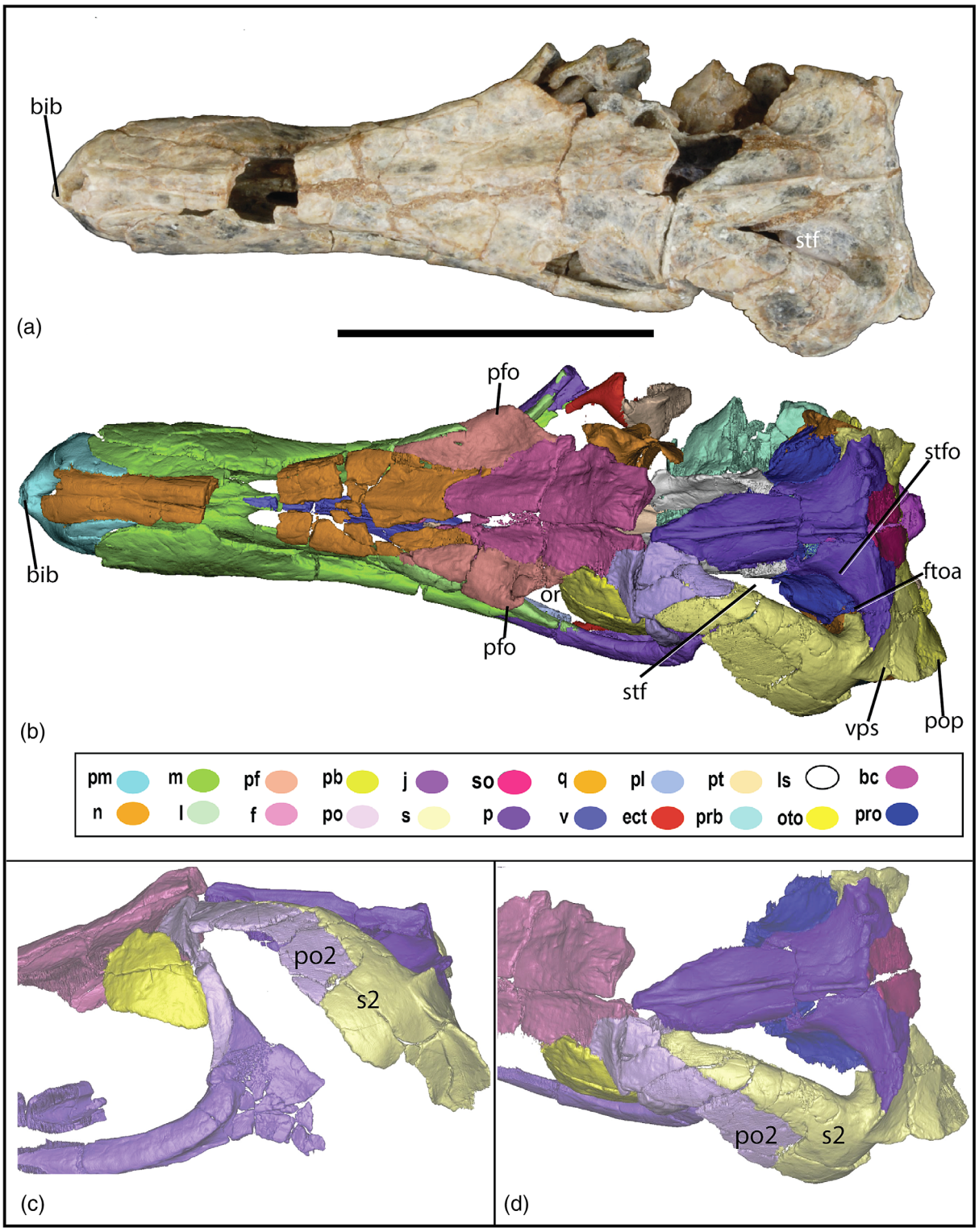

FIGURE 9 Photograph of the skull of (a), *Junggarsuchus sloani*; (b) CT reconstruction of the skull of *Junggarsuchus sloani* in dorsal view; (c) alternative interpretation of the postorbtial, frontal, squamosal contact in *Junggarsuchus sloani* in dorsal view; (d) alternative interpretations of squamosal–postorbital contact in *Junggarsuchus sloani* in left lateral view. Scale bar is equal to 5 cm.

to dorsoventral crushing of the skull. Unlike neosuchians, in which the ventral processes of the prefrontal's are expanded laterally and medially and widely contact the palatines, *Dibothrosuchus* lacks the ventral expansion of the ventral processes of the prefrontal which would not have provided the support it does in neosuchians.

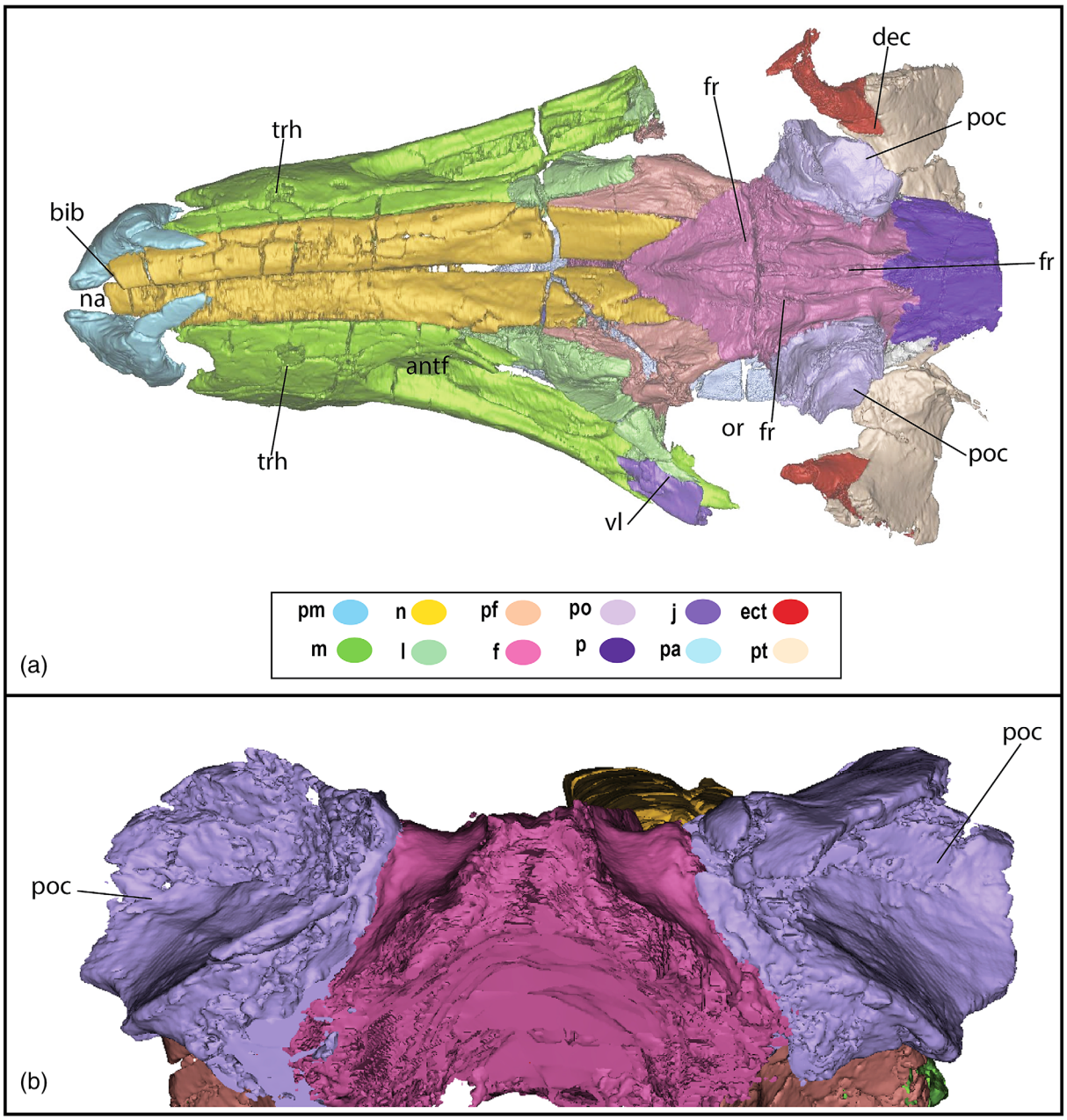

FIGURE 10 (a) The rostrum and orbital region of *Dibothrosuchus elaphros* in dorsal view; (b) postorbitals in posterior view; scale bars are equal to 1 cm.

In *Junggarsuchus*, the paired **frontals** form the skull roof medial to the orbits, posterior to the nasals and prefrontal, and anterior to the parietal and postorbital (Figures 3b and 9b). The frontal forms the posterodorsal margin of the orbit. The orbital margin is only preserved on the left side, where the palpebral covers it, and the frontal appears to be laterally concave. However, this concavity may be accentuated by the palpebral, which has been pressed unnaturally onto the surface of the frontal. Inside the orbit, the crista cranii (sensu Walker, 1990), forming the lateral margin of the olfactory tract, is mediolaterally thin but extends ventrally much further than in living crocodylians (Figures 3b and 4b). The crista is incomplete, but its anterior end is preserved on both sides where it contacts the medial surface of the descending process of the prefrontal. Posteriorly, a fragment of the left crista is preserved on the lateral surface of the braincase. A broad, low longitudinal ridge, similar to that of *Sphenosuchus* (Walker, 1990) and *Hesperosuchus* (CM 29894) (Clark et al., 2001), trends along the central region of the dorsal surface of the frontals the entire length. Anteriorly, the frontals form a blunt process at the midline that wedges between the posterolateral processes of the nasals. A thin, ventrally offset projection of

the frontals anterior to the frontal–nasal contact is overlain by the nasals on the midline.

Anterolaterally, the frontal contacts the posterior part of the prefrontal along a posterolaterally trending oblique suture. The frontals have a posterolaterally concave contact with the dorsal part of the postorbital in dorsal view. The posterior ends of the frontals are broken, corresponding to a large fracture in the specimen, the posterior end of the frontal does not extend as far laterally as in *Hesperosuchus* (CM 29894) (Clark et al., 2001), *Sphenosuchus* (Walker, 1990) and *Protosuchus richardsoni* (AMNH 3024, UCMP 130860, MCZ 6727) (Clark, 1986), giving the supratemporal fenestra its triangular rather than oval shape.

The paired frontals of *Dibothrosuchus* are similar in position to other non-crocodyliform crocodylomorphs (Figures 5 and 10a). However, the frontal lacks the deep lateral concavity seen in *Junggarsuchus*. The concavity is far shallower, which may be related to the lack of a palpebral. The cristae cranii of *Dibothrosuchus* are dorsoventrally shallower than observed in *Junggarsuchus*, though they may be broken. The frontal is also proportionally wider laterally, giving the supratemporal fenestra a more oval shape, but lacks the posterolateral processes seen in *Sphenosuchus* (Walker, 1990). The parasagittal ridges on the dorsal surface of the skull are dorsoventrally taller in *Dibothrosuchus* than they are in *Junggarsuchus*, which has lower dorsal ridges. The median ridge of the frontal is divided by a wide groove along the midline resulting in two midline ridges around the central ridge along the suture. These ridges converge anteriorly and posteriorly into a lanceolate shape (Wu & Chatterjee, 1993). Posteriorly, the parasagittal ridges are laterally separated from the postorbitals by another deep groove and ridge along the suture. This is a feature unique to *Dibothrosuchus* (Wu & Chatterjee, 1993). Anteriorly, the frontals narrow and have an anterolateral contact with the posteromedial edges of the nasals that is about 25% of the total length of the frontals. In *Dibothrosuchus*, this anterior narrowing is triangular, unlike the rounded anterior edge seen in *Junggarsuchus* (Figures 9b and 10a).

The left **palpebral** is observed only in *Junggarsuchus* and is preserved in contact with the frontal and postorbital bones at the dorsal margin of the left orbit, its lateral edge is displaced slightly ventromedially from its presumed sub-horizontal position (Figures 3b and 9b). It is ovoid in dorsal view, with an anteromedial–posterolateral long axis that divides the bone nearly symmetrically. It is dorsally convex and its surface is covered with a low, rugose sculpturing. Its posterior edge is preserved contacting the anterior edge of the postorbital and roughly reflects the latter's shape. This edge is only gently curved, less so than other edges. The posterolateral and anteromedial edges of the bones are acutely angled, roughly 72° (Figures 3b and 9b). The medial part of the bone, which overlies the frontal, has a small notch. In the only other non-crocodyliform crocodylomorphs for which a palpebral is known, *Hesperosuchus agilis* (CM 29894), it is more circular in shape, dorsoventrally thicker, and has very fine, extensive sculpturing.

The anterior process of the triradiate **jugal** in *Junggarsuchus* inserts into the posterior end of the maxilla, where the ventral process of the lacrimal borders it dorsally (Figures 3a,b and 4a,b). Posteriorly, the jugal widens mediolaterally, where it forms the ventral border of the orbit; this region is marked by a concave longitudinal depression along its entire ventrolateral surface. The bone then curves posterodorsally to form the posteroventral border of the orbit and the ventral half of the postorbital bar. Thus, its ventral edge is not flat, as in other non-crocodyliform crocodylomorphs like *Dibothrosuchus* and in many crocodyliforms like *Orthosuchus* (Nash, 1975), *Fruitachampsa* (Clark, 2011), *Gobiosuchus* (Osmólska et al., 1997), *Hsisosuchus* (Li et al., 1994), and neosuchians like *Crocodylus niloticus*. Instead, it is ventrally concave ventral to the postorbital bar, opposite the dorsal convexity of the surangular. The medial surface ventral to the orbit also possesses a longitudinal groove, bordered ventrally by a horizontal ridge along the ventral part of the bone (Figure 11c). The dorsal process of the jugal is covered by the descending process of the postorbital medial to the postorbital unlike other non-crocodyliform crocodylomorphs and most crocodyliforms, but as in thalattosuchians like *Cricosaurus* ("*Geosaurus*") *araucanensis* (Young & Andrade, 2009).

Posterior to the postorbital bar, the concavity on the ventrolateral surface of the jugal opens into a broad, thin, medially depressed lower temporal bar (Figure 3b). It is not clear which part of this region is formed by the jugal and which by the quadratojugal due to numerous breaks in the region of the lower temporal fenestra. The jugal most likely continues posterior to its contact with the postorbital (the jugal process contributing to the postorbital bar extends to about the midpoint of the ventral process of the postorbital), where there is a distinct suture, but this could also be the quadratojugal, as in some non-crocodyliform crocodylomorphs (Clark et al., 2001). The dorsal extent of the posterior process appears to nearly reach the posterior edge of the lateral temporal fenestra, whereas the posteroventral process extends further, possibly to the posterior end of the quadratojugal. The quadratojugal appears not to extend that far anteriorly, as discussed below, and the anterior half of the lower temporal bar is formed mostly by jugal. The posterior process of the jugal slopes posteroventrally posterior to the postorbital bar and is slightly shorter than the anterior process, unlike other non-crocodyliform crocodylomorphs

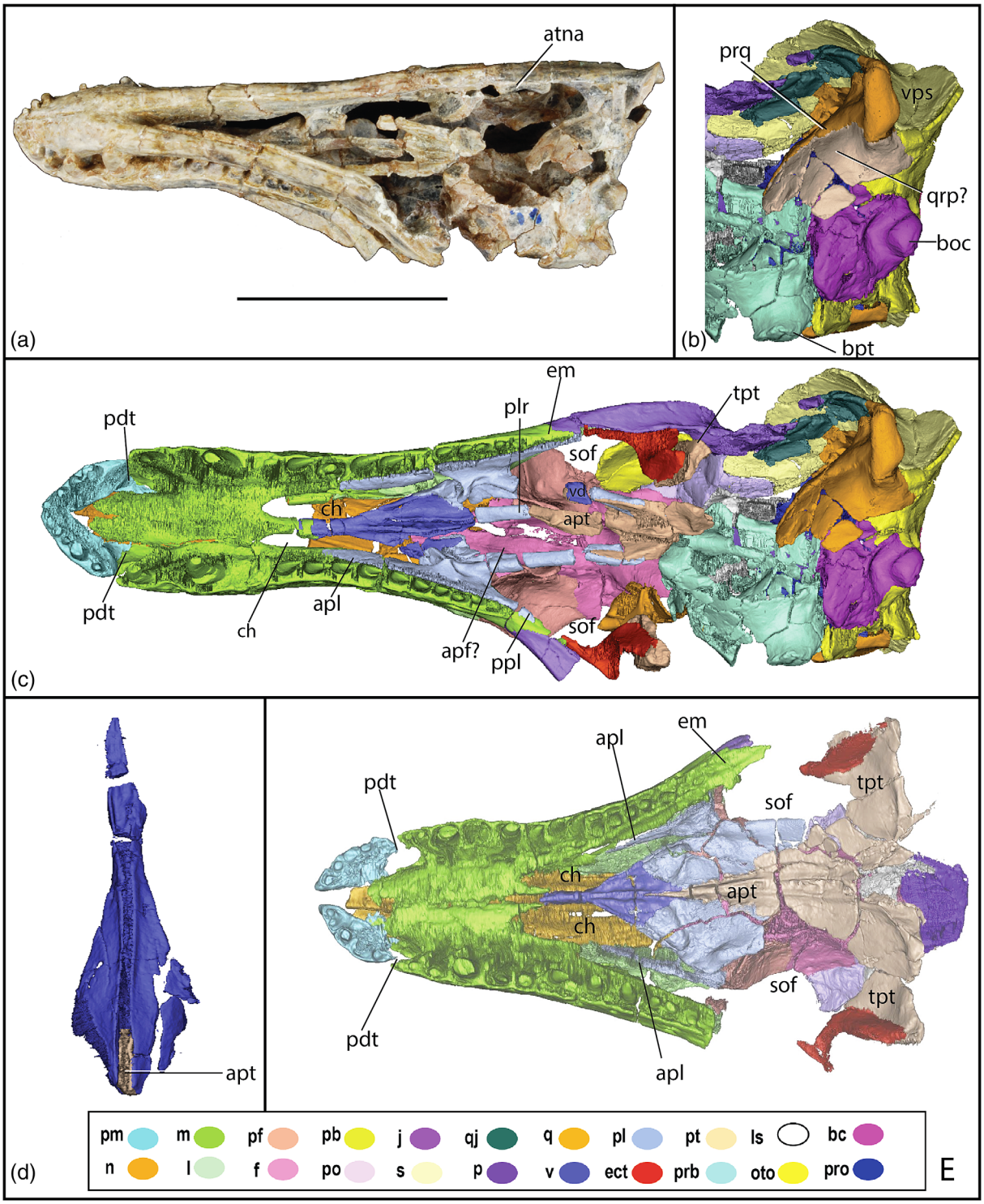

FIGURE 11 Photograph of the skull of (a) *Junggarsuchus sloani* in ventral view; (b) alternate CT reconstruction of the quadrate and pterygoid in *Junggarsuchus sloani* in ventral view; (c) CT reconstruction of the palate of *Junggarsuchus sloani* in ventral view; (d) vomer of *Junggarsuchus sloani* in dorsal view, anterior tip at the top of the image; (e) CT reconstruction of the rostrum and orbital region of *Dibothrosuchus elaphros*, in ventral view. Scale bar is equal to 5 cm in (a) and 1 cm in (e).

(Walker, 1990; Wu & Chatterjee, 1993). Posteroventral to the main body of the jugal and anterior to the quadratojugal an isolated broken oval section of bone is present which we reconstruct as jugal based on its position, which appears continuous with the rest of the jugal (Figure 3b). There is possibly an anteroposteriorly long contact between the jugal and quadratojugal, like the contact seen in early diverging crocodyliforms like

Protosuchus haughtoni (BP/1/4770) (Gow, 2000), *Protosuchus richarsoni* (AMNH 3024, UCMP 130860) (Clark, 1986), and *Zaraasuchus* (Pol and Norell 2004a) that reduces the size of the infratemporal fenestra. The lower temporal bar is dorsoventrally tall, nearly 50% of the height of the orbit, compared to *Sphenosuchus* (Walker, 1990) and is very thin mediolaterally.

Only the anterior end of the left jugal is known from *Dibothrosuchus* IVPP V 7907 (Figure 5b). The jugal is better known from CUP 2981 (Simmons, 1965), which allows for comparison to *Junggarsuchus*. The anterior tip of the jugal has two anterior processes, and the anterodorsal tip just barely participates in the posterior border of the antorbital fenestra (Figure 5). The jugal narrows in its dorsoventral height posteriorly, unlike *Junggarsuchus*. The posterior process of the jugal of *Dibothrosuchus* is straight, unlike *Junggarsuchus*, like most other early diverging crocodylomorphs and is not dorsally arched. The dorsal process of the jugal that contacts the postorbital bar lies lateral to the postorbital, as in most crocodyliforms like *Protosuchus richardsoni* (AMNH 3024) (Brown, 1933; Clark, 1986) and *Crocodylus niloticus*.

The **parietal** in *Junggarsuchus* lacks any trace of a midline suture, unlike in some non-crocodyliform crocodylomorphs such as *Litargosuchus* (Clark & Sues, 2002), *Hesperosuchus* (CM 29894) (Clark et al., 2001) and *Dromicosuchus* (Sues et al., 2003) (Figures 3b and 9b; Leardi et al., 2017). The parietal bears a sharp T-shaped crest in dorsal view that is comprised of an anteroposteriorly trending, mediolaterally narrow sagittal crest that trends along the entire midline length of the parietal and the nuchal (supraoccipital) crest that runs mediolaterally along the entire occipital portion of the skull roof. Anteriorly, the sagittal crest continues onto the posterior end of the frontals where it expands mediolaterally to twice the width of the crest at its posterior end, but the contact between the frontal and parietal is obscured by a large crack. In dorsal view, the crest along the posterior margin of the parietal is set at a 90° angle from the sagittal crest, as opposed to the V-shaped crest seen in almost all other non-crocodyliform crocodylomorphs except *Dibothrosuchus*, *Sphenosuchus* (Walker, 1990), and *Almadasuchus* (Clark, Xu, Forster, & Wang, 2004; Pol et al., 2013). The sagittal crest continues into a dorsal occipital (nuchal) crest laterally and curves anterolaterally at the posterolateral portion of the supratemporal fossa, and then continues onto the posterodorsal surface of the squamosal. The lateral edge of the body of the parietal is dorsolaterally convex and forms the medial and posteromedial border of the supratemporal fenestra. The parietal meets the squamosal in an anteromedially oblique suture approximately midway around the posterior edge of the fenestra. A small anterior opening to the anterior temporal foramen (Figure 9b) is situated between the parietal and squamosal, and the parietal forms the medial and dorsal edges of the foramen, whereas the prootic forms the ventral edge. The posterodorsal part of the supratemporal fenestra faces anterodorsally and forms only a short fossa rather than the much anteroposteriorly longer ones that often floors up to 50% of the supratemporal fenestra in early diverging crocodyliforms like *Orthosuchus* (Nash, 1975), ziphosuchians like *Baurusuchus salgadoensis* (Nascimento & Zaher, 2010), living crocodylians, *Dibothrosuchus*, *Almadasuchus*, and *Pelagosaurus* (Pierce & Benton, 2006). The parietal has a small process that fits onto the occipital surface and is rhomboidal in posterior view, overlaying the dorsal edge of the supraoccipital as in *Dibothosuchus* (Figure 12). The parietal also extends onto the occipital surface between the supraoccipital and squamosal and rests on the paroccipital process (Figure 13). It forms the dorsal border of the posttemporal fenestra, like in *Sphenosuchus* (Walker, 1990). The occipital portion of the parietal is triangular in occipital view, with a low, gently convex ventral end, and a broad dorsal base. The posterolateral process of the parietal extends dorsolaterally as a slender process over the squamosal to reach the posterodorsal corner of the supratemporal fossa and posterior skull roof. In *Dibothrosuchus* and crocodyliforms like *Protosuchus richardsoni* (MCZ 6727, AMNH 3024, and UCMP 130860), this posterolateral process is shorter and does not reach the posterolateral corner of the supratemporal fenestra. The dorsal roof of the braincase is formed by the parietals. Although the parietals contact with the frontals is not well preserved in *Junggarsuchus* due to a break, it appears that a small portion of the parietal projects between the posterior extension of the frontal and the laterosphenoid. This is similar to the condition seen in some thalattosuchians like *Steneosaurus bollensis*, *Pelagosaurus typus* (Pierce & Benton, 2006) and *Cricosaurus* ("*Geosaurus*") *araucanensis* (Young & Andrade, 2009), though the process is not elongate and does not participate in the supratemporal fossa.

The parietals of *Dibothrosuchus* (Figures 5, 10a, and 25a,d) have a lower sagittal crest than *Junggarsuchus* that is T-shaped in dorsal view, and features a visible midline suture anteriorly, though it is only visible due to a break in the sagittal crest. The parietals anterior contacts with the frontals are blunt and rectangular, though there is a slight anteromedial process that projects anteriorly. The lateral expansions of the occipital ridge do not extend as far laterally as those of *Junggarsuchus* and contribute to less than half of the medial posterior border of the supratemporal fenestra. The posttemporal fenestra is much larger in *Dibothrosuchus*, similar to *Sphenosuchus* (Walker, 1990) rather than *Junggarsuchus*. The parietal does not contribute to the edges of the anterior temporal foramen in *Dibothrosuchus*, where the medial and ventral

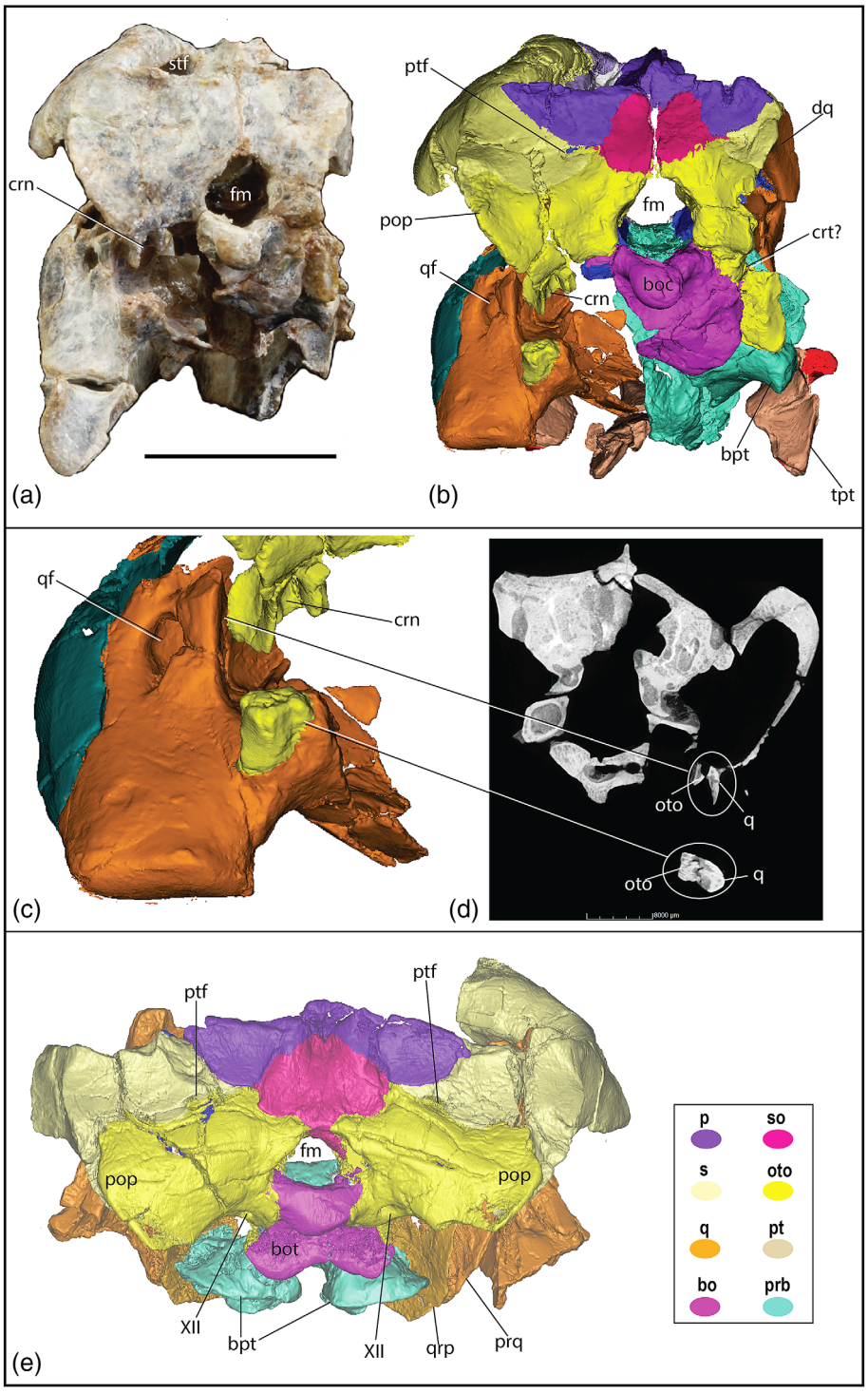

FIGURE 12 Occipital view of the skull of *Junggarsuchus sloani* in (a) a photograph and (b) CT reconstruction; (c) left quadrate otoccipital contacts; (d) CT cross section of quadrate occipital contact (slice 369); (e) CT reconstruction of the skull of *Dibothrosuchus elaphros* in occipital view. Scale bar is equal to 3 cm in (a) and 1 cm in (e).

edge are formed by the prootic and the dorsal edge by the squamosal (Figure 25b). The parietal and prootic contribute to a broader supratemporal fossa than seen in *Junggarsuchus*. The parietal of *Dibothrosuchus* is involved in the occipital portion of the skull, which has a medial rhomboidal projection into the supraoccipital and expanded rectangular processes that separate the squamosal and supraoccipital in occipital view. Unlike *Junggarsuchus*, the parietals of *Dibothrosuchus* do not contribute to the medial or dorsal edge of the fenestra. The parietals end dorsal to a thin process of the squamosal that forms the border of the posttemporal fenestra. *Dibothrosuchus* shares this parietal involvement in the posttemporal fenestra with other early diverging non-crocodyliform crocodylomorphs.

The ventral process of the **postorbital** in *Junggarsuchus* makes up the dorsal half of the postorbital bar and has a broad dorsal portion (Figure 3b). The

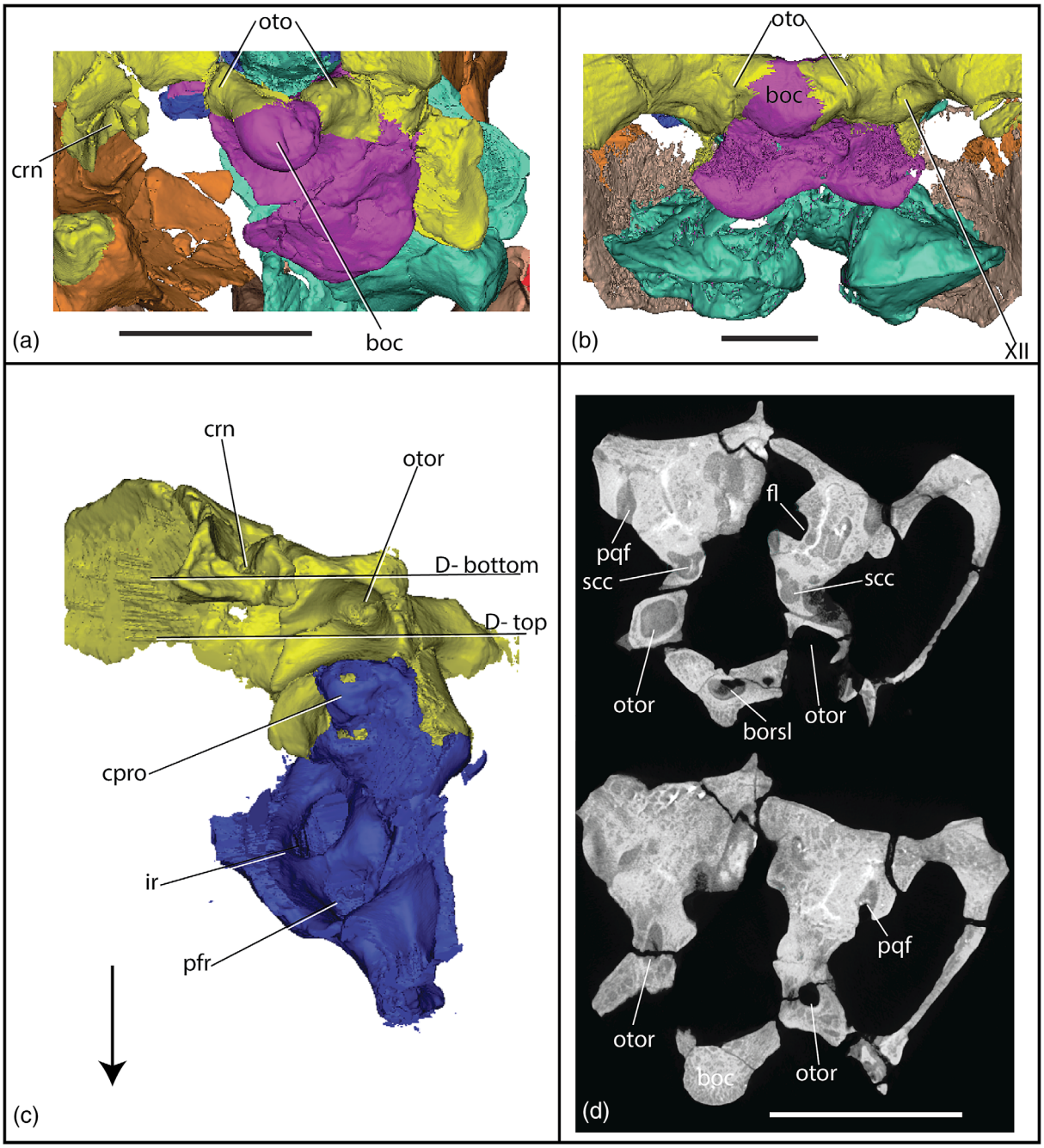

FIGURE 13 Alternative occipital views of CT reconstructions of the skull of (a) *Junggarsuchus sloani* and (b) *Dibothrosuchus elaphros* demonstrating alternative degrees of occipital contribution to the basioccipital condyle; (c) left occipital and prootic of *Junggarsuchus sloani* in ventral view; (d) ventral occipital in anteroposterior CT cross section in *Junggarsuchus sloani* (top slice anterior and bottom slice posterior). Horizontal white lines indicate position of CT slices. Scale bar is equal to 5 mm. Arrow indicates anterior direction.

ventral process of the postorbital overlies the dorsal process of the jugal anteriorly, making up the posterior border of the orbit as in other non-crocodyliform crocodylomorphs, but unlike the unusual condition of *Dibothrosuchus* in which the postorbital is posterior to the jugal and the jugal forms the posterior border of the orbit. However, the condition in *Dibothrosuchus* is similar to the condition seen in crocodyliforms such as *Protosuchus haughtoni* (BP/1/4770) (Gow, 2000), *Orthosuchus* (Nash, 1975), *Fruitachampsa* (Clark, 2011), and extant crocodylians. This descending process in *Junggarsuchus* extends medially as a broad sheet that meets the laterosphenoid (Figure 17c). A descending process along the lateral surface of the laterosphenoid is preserved on the left side, an unusual condition compared to other non-crocodyliform crocodylomorphs. Dorsally, the

suture between the postorbital and the frontal is semicircular in dorsal view, with the convex area directed anteriorly (Figure 9b). The frontal lies medial to the postorbital and the concave posterolateral edge of the frontal articulates with a convex medial edge of the postorbital. A narrow lateral expansion of the frontal borders the postorbital anteriorly. The posterior extent of the postorbital is difficult to determine due to several cracks in the region, and two possible interpretations exist though one would be unusual (Figure 9c,d). The first is that the postorbital has a relatively short posterior process and the squamosal extends far anteriorly. This process is directed posteromedially and is diamond shaped in dorsal view. Its medial edge is bordered by the parietal and potentially a thin portion of the frontal. The lateral edge of the process is sutured to the medial edge of the anterior process of the squamosal. The posterior process of the postorbital reaches the anterolateral edge of the supratemporal fenestra in this interpretation. The contribution to the anterior and lateral edge of the fenestra is short, and three-fourth of the lateral border is made up by the squamosal (Figure 9b).

The more unusual interpretation is that a longitudinal suture between the postorbital and squamosal in the anterior part of the supratemporal bar indicates that the postorbital forms the anterolateral part of the bar and does not border the supratemporal fossa (Figure 9c,d). This interpretation is not clarified by the CT data (broken elements make inferences uncertain), but some of the apparent sutures of the skull roof suggest it. Thus, rather than being medial to the squamosal, as in *Saltoposuchus* and *Dibothrosuchus*, or forming the anterior half of the bar as in *Hesperosuchus* (CM 29894) (Clark et al., 2001), it lies lateral to the squamosal as a long rectangular process, half the length of the squamosal and unlike the postorbital of any known non-crocodyliform crocodylomorph or early diverging crocodyliform like *Protosuchus richardsoni* (AMNH 3024 and UCMP 130860). The posterior extent of the postorbital of this interpretation is unclear, but it apparently ended about half way along the bar. Long posterodorsal processes of postorbital (reaching posterior to the midpoint of the supratemporal fenestra) are known in *Pseudhesperosuchus* (Bonaparte, 1971), *Hesperosuchus* (CM 29894) (Clark et al., 2001), *Sphenosuchus*, and *Almadasuchus* (Pol et al., 2013), but in these taxa, the postorbital is still involved in the lateral border of supratemporal fenestra. A long posterodorsal process has been reported in *Junggarsuchus* by other authors (Leardi et al., 2017) but only in this latter interpretation do we find the processes to be elongated. In the prior interpretation, which is more consistent with Clark, Xu, Forster, and Wang (2004), the posterodorsal process is shorter. The postorbital is strongly concave ventrally where it overhangs the lateral temporal fenestra, continuous with the concavity in the squamosal. In this case, the postorbital is fully excluded from the supratemporal fenestra. This interpretation is supported by the sutures observed on the specimen itself, but neither can be fully supported due to a lack of a clear suture in the CT data and multiple breaks in the region and so have not been scored for either in our matrix.

Only the dorsal portion of the postorbital is preserved in *Dibothrosuchus* (Figures 5 and 10a). The ventral portion of the postorbital bar is preserved on the holotype CUP 2081 (Simmons, 1965). The dorsal portion of the postorbital has a medial ridge that contacts the frontal along a smoothly concave contact. Lateral to this contact, the surface of the dorsal portion of the postorbital is slightly convex and then rises as a concave ridge, unlike the smooth dorsal portion of the postorbital in *Junggarsuchus* (Figure 10c). Both postorbitals are hollow and expanded laterally relative to *Junggarsuchus*, where the postorbitals are narrower and sheet like. The hollow nature of the postorbital in *Dibothrosuchus* is visible due to a posterolateral break in each element, which demonstrates a posterolateral concavity that is floored and roofed by lateral projections of the postorbital (Figure 10b). A broad medial expansion of the postorbital that contacts the laterosphenoid is not found in *Dibothrosuchus*. The postorbital process of the postorbital bar is posterior to the ascending process of the jugal, which is unlike the condition seen in other non-crocodyliform crocodylomorphs, but similar to *Protosuchus richardsoni* (AMNH 3024, MCZ 6727) and other crocodyliforms.

In *Junggarsuchus* the **squamosal** is a kidney-shaped bone in dorsal view that broadly overhangs the infratemporal fossa (Figures 3b, 9b, and 12b). It is broad posteriorly, more similar to *Saltoposuchus* (Sereno & Wild, 1992) than to the narrower squamosal of *Dibothrosuchus* and *Sphenosuchus*. It tapers anteriorly along the lateral edge of the supratemporal fenestra, reaching the anterior edge of the fenestra where it contacts the postorbital laterally. The exact contact between the squamosal and postorbital is unclear, so there are two interpretations of the anterior portion of the squamosal, which have been outlined in the discussion of the postorbital. The first possible condition, which is similar to the conditions seen in non-crocodyliform crocodylomorphs, is a laterally expanded squamosal. In this case, the squamosal still narrows anteriorly, but the postorbital contributes anterolaterally to the supratemporal fenestra and is not excluded from the border by the squamosal (Figure 9b). The anteromedial edge of the squamosal contacts the posterior projection of the postorbital. The alternative interpretation, with a long posterolateral process of the postorbital fully separated from the supratemporal

fenestra by a narrow anterior portion of the squamosal is unknown in other non-crocodyliform crocodylomorphs (Figure 9c,d). In this case, the squamosal would widen substantially posteriorly, contributing to the last third of the lateral temporal area overhang, and the anterior portion contacts a potential posterior process of the frontal anteromedially. The portion of the squamosal anterior to the occiput is ventrally concave. In this case, the squamosal comprises the entire lateral and anterior border of the supratemporal fenestra. This interpretation is supported by the sutures observed on the specimen itself, but neither can be fully supported due to a lack of a clear suture in the CT data. In both interpretations, the ventral surface of the anterior process of the squamosal is deeply concave and the bone of the anterior process is dorsoventrally thin due to this concavity. This concavity, which we will refer to as a ventral groove of the squamosal trends along the entire ventral surface of the anterior process and continues to the ventral expansion of the squamosal where the bone overhangs the lateral temporal fenestra (Figure 14a,b). An elongate ventral grooved or trough-like surface of the squamosal has also been reported in *Sphenosuchus* (Walker, 1990) and is present in *Dibothrosuchus* (Figures 14c,d and 25c) and possibly present in *Dromicosuchus* (Sues et al., 2003). However, we were unable to further identify this feature in most other non-crocodyliform crocodylomorphs from either a lack of description in the literature or incomplete preservation. This deep ventral groove is not seen in some non-crocodyliform crocodylomorphs, like *Almadasuchus* (Leardi et al., 2020), and in early diverging crocodyliforms like *Protosuchus haughtoni* (BP/1/4770) (Gow, 2000) or *Orthosuchus* (Nash, 1975), where the squamosal is shorter, broader and despite still overhanging the lateral temporal fenestra, lacks an extended lateral ventral process and associated ventral groove.

Unlike most other non-crocodyliform crocodylomorphs, the dorsal edge of the squamosal lacks a sharp ridge along the lateral edge of the supratemporal fossa (Figure 9b). This lack of a ridge along the dorsal surface of the squamosal is similar to the condition seen in early diverging crocodyliforms like *Orthosuchus* (Nash, 1975), *Protosuchus haughtoni* (BP/1/4770) (Gow, 2000), and *Fruitachampsa* (Clark, 2011), with the exception of thalattosuchians like *Pelagosaurus typus* (Pierce & Benton, 2006), *Cricosaurus* ("*Geosaurus*") *araucanensis* (Young & Andrade, 2009) and *Metriorhynchus superciliosus* (Andrews, 1913). The squamosal forms the dorsal and posterodorsal portion of the articulation surface for the dorsal head of the quadrate. As shown on the right side where the dorsal part of the squamosal is missing, the quadrate has a broad, short posterodorsal contact with the occipital portion of the squamosal (Figures 4b, 12b, and 17c). The contact continues anterolaterally along a thin anterolateral process of the quadrate, and the quadratojugal contacts an anteroposteriorly short ventral portion of the squamosal anterior to the quadrate. The quadrate articulation with the squamosal is more limited both mediolaterally and anteroposteriorly than in *Dibothrosuchus* (Figure 24b,c,e). The contact with the parietal within the supratemporal fossa is obscured by breakage and glue but appears to extend from the posterodorsolateral corner of the fossa ventromedially to end at the anterior temporal foramen, with the squamosal forming the entire dorsal and lateral edges of the foramen (Figure 9b). The occipital ridge on the parietal is continuous laterally with a much shorter ridge on the squamosal that extends anterolaterally and becomes dorsoventrally shorter laterally. Another ridge rises from just ventral to the lateral end of the occipital ridge and continues posteroventrally on the ventral process of the squamosal and onto the posterior edge of the expanded distal edge of the paroccipital process. This crest limits the triangular concavity of the ventral process of the squamosal.

The occipital portion of the squamosal is bordered medially by the parietal and ventrally by the paroccipital process of the otoccipital (Figure 12a,b). Medially on the occiput, the squamosal extends ventromedially ventral to the parietal, ending as a slender process which forms the lateral and much of the ventral edge to the posttemporal fenestra and nearly reaching the supraoccipital. The contact with the parietal is thus dorsomedial, unlike the strictly lateral contact in *Sphenosuchus*, and the occipital surface of the squamosal is triangular like *Dibothrosuchus* rather than squared as in *Sphenosuchus* (Walker, 1990) in posterior view. As in other non-crocodyliform crocodylomorphs, a ventral process of the squamosal extends along the anterior edge of the paroccipital process and terminates at the ventral edge of the latter process. The ventral process of the squamosal is slightly concave posterolaterally, similar to *Almadasuchus* (Leardi et al., 2020) and some longirostrine neosuchians like *Sarcosuchus imperator* (Sereno et al., 2001) but unlike early non-mesoeucrocodylian crocodyliforms like *Protosuchus richardsoni* (UCMP 130860 and AMNH 3024). The posterior contact of the squamosal with the dorsal head of the quadrate encloses the otic recess posteriorly, like *Almadasuchus* (Leardi et al., 2020; Pol et al., 2013), Crocodyliformes like *Nominosuchus* (Storrs & Efimov, 2000), *Zosuchus* (Osmólska et al., 1997), *Hsisosuchus* (Li et al., 1994) and later ziphosuchians and neosuchians, unlike other non-crocodyliform crocodylomorphs like *Dibothrosuchus* (Leardi et al., 2017, 2020) and thalattosuchians like *Cricosaurus* ("*Geosaurus*") *araucanensis* (Young & Andrade, 2009). A

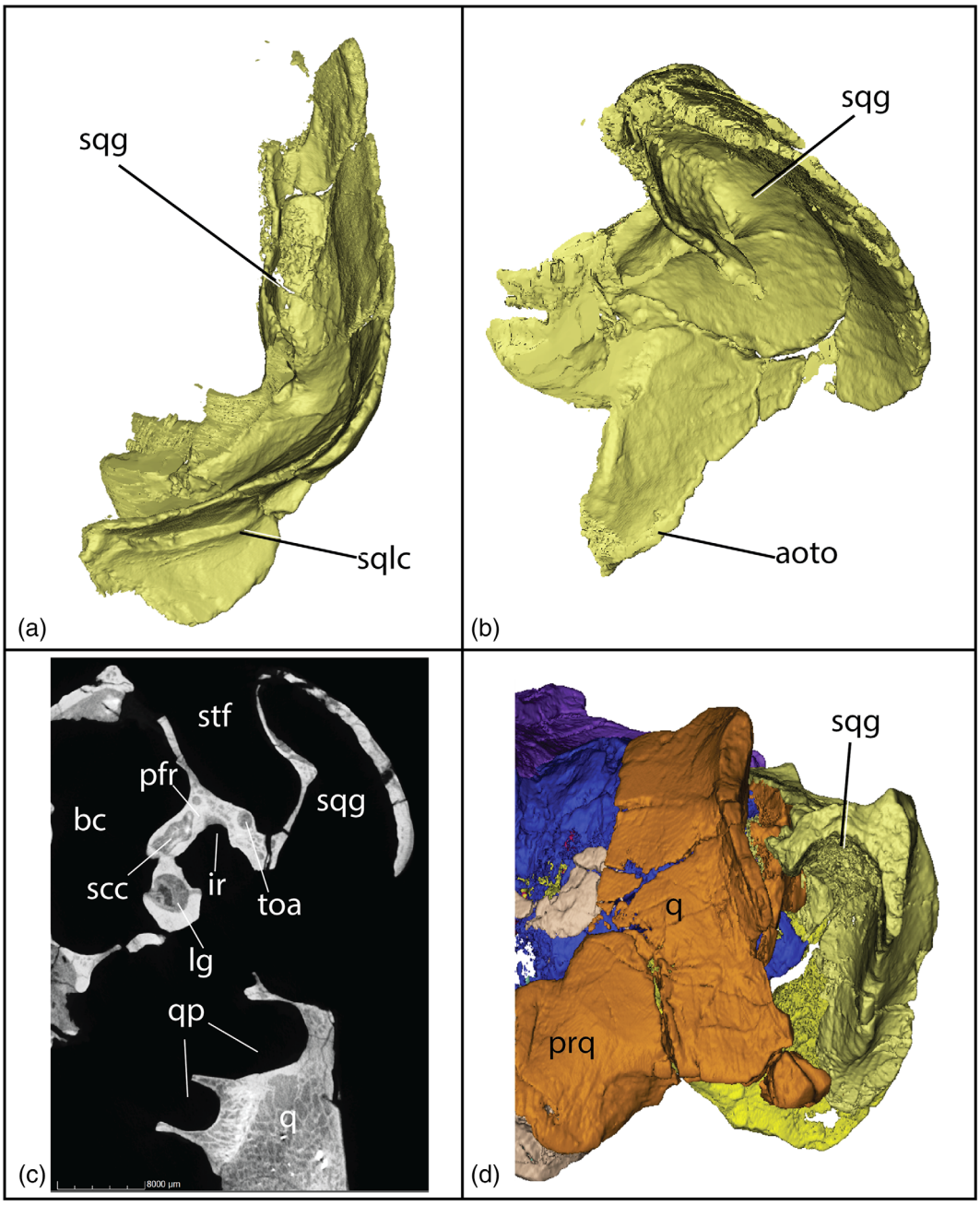

FIGURE 14 Left squamosal of *Junggarsuchus sloani* in (a) in ventral and (b) anteroventral view; (c) CT image of the left ventral squamosal groove in *Junggarsuchus sloani* in anteroposterior view; (d) CT reconstruction of *Dibothrosuchus elaphros* in anterior view

similar contact may be present in *Kayentasuchus*, in which the ventral process of the left squamosal, while broken, descends ventrally past the ventral edge of the paroccipital in occipital view (Clark & Sues, 2002), like *Almadasuchus*. Similar to *Almadasuchus*, a subtriangular concavity is located on the posteroventral process of the squamosal in lateral view, which contacts the paroccipital process (Leardi et al., 2020; Pol et al., 2013).

The right squamosal of *Dibothrosuchus* is well preserved (Figure 25a). The squamosal forms the entire lateral border, more than half the posterior border, and the anterolateral edge of the supratemporal fenestra. The anterior process of the squamosal curves medially, which gives the supratemporal fenestra a circular shape in dorsal view, unlike *Junggarsuchus*. Similar to *Junggarsuchus* and *Sphenosuchus*, the anterior process of the squamosal is ventrally concave along its entire length due to the lateral overhang of the squamosal, though the anterior overhang is broader and the ventral concavity shallower and wider than in *Junggarsuchus* (Figure 12a). The postorbital overlaps the anterior edge of the squamosal in a short triangular process in dorsal view, which is bordered on both

the lateral and medial edges by the squamosal. Beyond this contact, none of the postorbital squamosal contacts is preserved in either specimen (IVPP 7907 or CUP 2081) of *Dibothrosuchus* that preserve the skull roof.

Unlike *Junggarsuchus*, but similar to *Sphenosuchus* (Walker, 1990), there is a ridge along the lateral edge of the supratemporal fenestra along the dorsal surface of the squamosal in *Dibothrosuchus* (Figure 25d). As in other non-crocodyliform crocodylomorphs, the dorsal head of the quadrate contacts the ventral portion of the posteromedial surface of the squamosal, though the mediolateral and anteroventral contact is wider and longer than in *Junggarsuchus* (Figure 25a,e). In *Junggarsuchus*, the quadrate is involved in the lateral wall of the anterior temporal foramen, but in *Dibothrosuchus*, the prootic is more involved in the lateral wall posteriorly, though the quadrate is involved posteriorly. The occipital dorsal ridge in *Dibothrosuchus* is longer on the squamosal than the parietal and curves anteriorly. Like *Junggarsuchus*, there is also a posteroventral ridge that rises from the dorsal ridge. The squamosal descends anterior to the paraoccipital process. Part of this process is visible lateral to the paraoccipital process in posterior view (Figure 12e). A ventral extension of the squamosal is also present in *Junggarsuchus*, but it is more laterally expanded in *Dibothrosuchus*. The ventral portion of the squamosals exposed on the occiput does not contact the parietal laterally as in *Sphenosuchus* but sends a thin triangular medial projection of bone ventral to the ventral edge of the parietal and forms the entire dorsal border of the post-temporal fenestra. A shallow concavity is present on the ventrolateral surface of the descending process of the squamosal, in a similar location to where the deeper groove is present in the expanded posteroventral region of the squamosal of the *Junggarsuchus* and *Almadasuchus* (Pol et al., 2013). The occipital surface of the squamosal lateral to the process overlaying the fenestra is anteriorly concave, similar to *Junggarsuchus*. In *Dibothrosuchus*, the squamosal extends far posterior to the quadrate condyle in lateral view, which is a condition found in some non-crocodyliform crocodylomorphs like *Kayentasuchus* (Clark & Sues, 2002) as well as crocodyliforms like *Protosuchus haughtoni* (BP/1/4770) (Gow, 2000) and *Protosuchus richardsoni* (AMNH 3024). The quadrate condyle is in line with the posterior edge of the squamosals in *Junggarsuchus* in lateral view.

The left **quadrate** of *Junggarsuchus* is partially preserved—the central area connecting the proximal and distal ends is missing—but many of the details are visible dorsally and ventrally (Figures 3b and 11a). Moreover, the dorsal part of the right quadrate is preserved in articulation and the main body of the right quadrate has been displaced, but intact and connected to the posterodorsal part of the right orbit and rotated so that its dorsal end faces posteroventrally (Figure 17a,b). The anterodorsally concave anterior surface of the dorsal part of the quadrate is exposed in the posterior end of the supratemporal fenestra. The quadrate narrows dorsally in dorsal and lateral view, and at its contact with the squamosal it is mediolaterally narrow, just about half the width of the articular head of the quadrate. This contact is narrower than observed in *Dibothrosuchus* and *Sphenosuchus* (Walker, 1990) in which the quadrate is nearly as wide as the articular head of the quadrate and broad and plate-like in anterior view. Posteriorly, the quadrate head rests against the anterior surface of the occipital portion of the squamosal, but as in all crocodylomorphs, the dorsal process does not widely contact the otoccipital (Figure 17a–c). In lateral view, the articular head of the quadrate is gently convex posterodorsally. Medially, the dorsal head has a long, firm contact with the prootic (Figure 17a,b), and ventrally the dorsal head overlies the posterodorsal portion of the prootic in which the intertympanic recess (=mastoid antrum) is enclosed, similar to *Sphenosuchus* (Walker, 1990) and *Dibothrosuchus*. The anteroposteriorly elliptical postquadrate foramen (=superior tympanic recess of the quadrate sensu Walker, 1990) is enclosed between the dorsal head of the quadrate and the posterodorsal portion of the prootic posterior to the intertympanic recess, similar to *Dibothrosuchus* (Figures 16b and 17d). The quadrate extends lateral to the prootic to overhang the otic region slightly. On the right side, the quadrate approaches the laterosphenoid but does not contact it. Contact of the laterosphenoid and quadrate is known in *Almadasuchus* (Leardi et al., 2020), and in crocodyliforms including *Protosuchus haughtoni* (BP/1/4770) (Gow, 2000) (Figure 17b).

At least two fenestrae are present within the quadrate, partially preserved on both elements (Figures 12b and 15a,b). Both fenestrae pass though the posterior surface of the quadrate posteromedial to the pterygoid process to connect with an extensive middle ear cavity. A dorsoventrally oriented ovoid fenestra is preserved in both elements at about the same level as the suborbital ramus of the jugal, well dorsal to the mandibular articulation. There is no evidence for a siphonium that would have passed from the quadrate into the articular, as in living crocodylians. The ventral part of a second fenestra dorsal to the first is better preserved on the right element and is slightly more elongate than the ventral foramen (Figure 15a). This second fenestra is slightly offset medially from the first one and its long axis is oriented vertically. Like *Dibothrosuchus* and some other early diverging crocodylomorphs and most crocodyliforms and

unlike *Pseudhesperosuchus* (Clark et al., 2001) and potentially *Sphenosuchus* and *Hesperosuchus* (Leardi et al., 2020), on the ventromedial surface of the quadrate are three cavities similar to the multiple spaces observed in the quadrate of *Macelognathus* and *Almadasuchus* which are inferred to be pneumatic (Leardi et al., 2017, 2020). First is a small cavity dorsal to the lower, larger quadrate fenestra and exits through the smaller dorsal quadrate fenestra. This cavity along with the disarticulated remains of the right quadrate, which preserves at least two quadrate fenestrae, suggests that the entire body of the quadrate may have had similar cavities (Figure 15a–c). The second cavity is large, nearly the entire anteroposterior length of the quadrate, oval in lateral view, ventral to the first and exits through the larger and more completely preserved lower quadrate fenestra (Figure 15a–c). A third, more ventral, cavity is anteroposteriorly longer than the cavity dorsal to it and continues posterior to the articular ramus of the quadrate. This third cavity may be housed partially in the pterygoid, but the unclear contacts in this region make it uncertain. *Junggarsuchus* features numerous large fenestrae and spaces in the quadrate like those discussed above. The quadrates of living crocodylians are heavily pneumatized (Dufeau & Witmer, 2015; Kuzmin et al., 2021) and we interpret these foramina as pneumaticity in the body of the quadrate in *Junggarsuchus*. Similar fenestrae in *Almadasuchus* have been interpreted as spaces pneumatized by the infundibular diverticulum (sensu Dufeau & Witmer, 2015) as the fenestrae open internally into the quadrate and the quadrate is further filled with complex air cavities (Leardi et al., 2017; Leardi et al., 2020). This pneumaticity does not extend into the portion of the quadrate ventral to the lower quadrate fenestra like the pneumaticity does in *Almadasuchus* (Kuzmin et al., 2021), as the nonpneumatic internal spaces of the quadrate are divided into many small cavities by trabecular bone, visible in CT scans (Figure 15c). This is similar to the condition seen in the CT data of *Dibothrosuchus* in which the main body of the quadrate contains numerous small nonpneumatic spaces divided by trabecular bone but lacks large pneumatic cavities (Figure 15e). The quadrate is vertically oriented in articulation, and its anterior surface is shallowly concave. The contact with the quadratojugal occurs along the lateral edge and continues dorsally where it shares a short contact with the squamosal. Laterally, the contact narrows ventrally (Figure 12a). The quadrate condyles are low and are of similar length on the lateral and medial sides.

The ventromedial surface of the quadrate is complex, featuring the pneumatic cavities discussed above and is uniquely medially expanded relative to other non-crocodyliform crocodylomorphs. Due to several breaks on the expanded ventromedial surface of the bone, it is not clear if the quadrate ramus of the pterygoid contributes at all to this medial expansion (Figure 11b,c). An anteromedial process from the edge of the quadrate body is anteroventrolaterally convex. On the anterolateral surface of this projection, the ventral edge of the quadrate features a ventromedially directed convexity that trends along much of the quadrate's ventral surface and may represent the contact between these pterygoid processes of the quadrate and the quadrate ramus of the pterygoid (Figure 15f). If the pterygoid contributes to the expanded, pneumatic medial surface of the quadrate then this convex ridge is possibly where it overlies the pterygoid laterally (Figure 11b). If this ridge is the quadrate-pterygoid suture, then it continues anteriorly from this process, extending along the medial edge of a dorsal process of the quadrate that forms the lateral border of the ventral fenestra, but anterior to this process the suture and ridge are obscure. The 3 mm further dorsally, a short process extends posterodorsally from the quadrate, broken off after 2 mm. Its position is similar to that of the posteromedially projecting dorsomedial process of the quadrate, similar to the structure observed in *Macelognathus* (Leardi et al., 2017), which houses the cranioquadrate canal, and *Almadasuchus* (Figure 15a,b) (Leardi et al., 2020). This posterodorsal process suggests that this entire complex medial pneumatic surface belongs to the quadrate. A faint suture is present extending dorsally and slightly medially from the ventrolateral part of this process, but it is unclear whether the quadrate forms the dorsolateral part of this process or not. It seems more likely that it was formed by the ventrolateral process of the otoccipital, but the base of the process is broken and reglued, and whether it is continuous with the quadrate is unclear. Based upon our CT data, it appears to be a proper suture between the ventral portion of the otoccipital to the medial edge of the quadrate (Figure 12b,c). This contact is also seen in *Macelognathus*, *Almadasuchus* (Leardi et al., 2017, 2020) as well as crocodyliforms like *Protosuchus haughtoni* (BP/1/4770) (Gow, 2000) and other crocodyliforms but not in other non-crocodyliform crocodylomorphs. The condition of this contact is complicated by the uncertain shape of the contact between anteromedial surface of the quadrate and what may be the quadrate ramus of the pterygoid. The suture between the ramus for the quadrate and the pterygoid process of the quadrate are unfortunately not continuously clear even in CT data, with the suture appearing and disappearing (Figures 14c and 15c). If the posterior projecting process is the quadrate, an identification in part supported by the presence of a similar structure in *Macelognathus* and *Almadasuchus* (Leardi et al., 2017, 2020), which also contacts the otoccipital, then

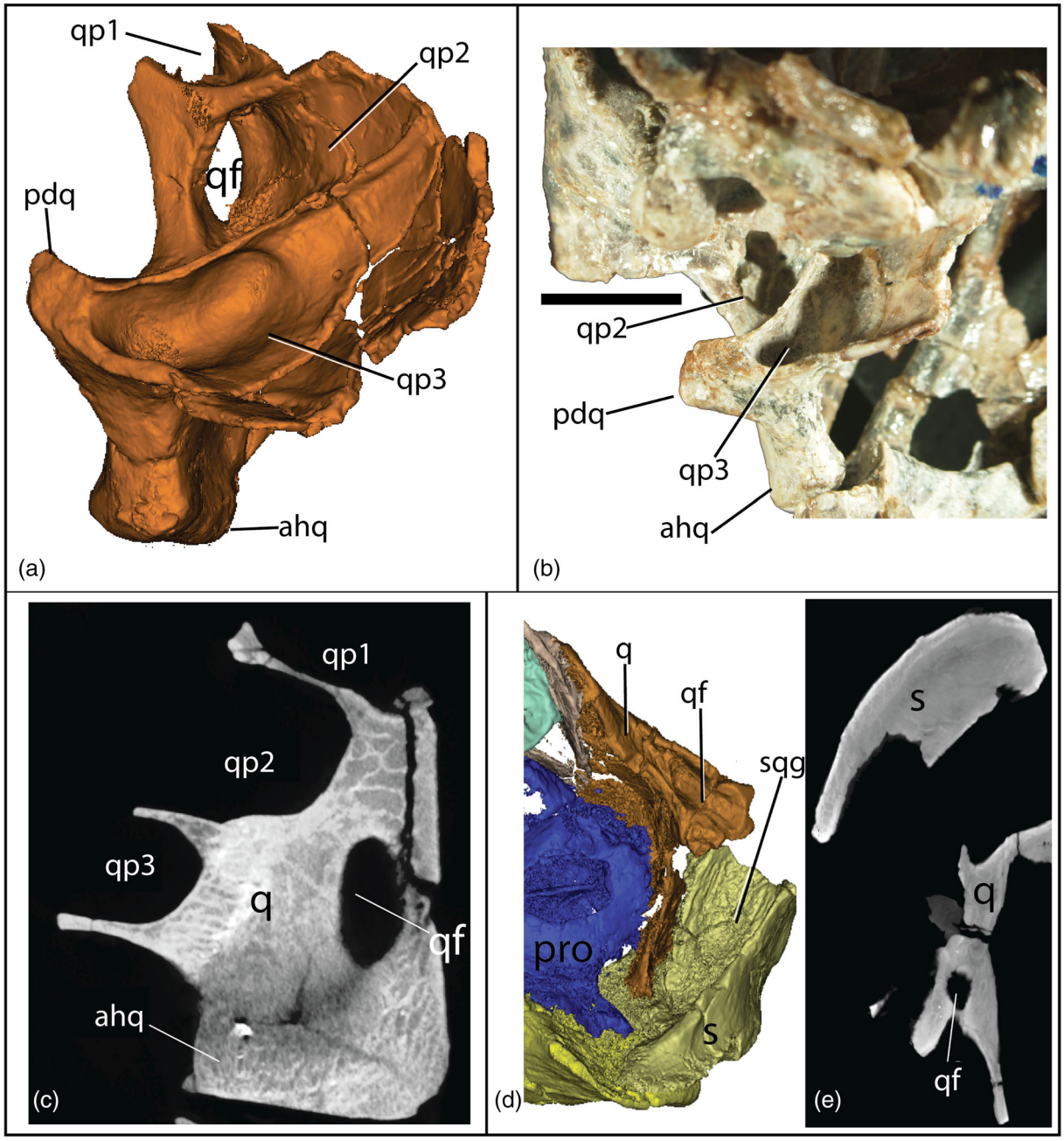

FIGURE 15 The pneumaticity of the quadrate of *Junggarsuchus sloani* and *Dibothrosuchus elaphros*, (a) the medial expanded pneumatic spaces of the quadrate in medial view; (b) photograph of the quadrate in medial view; (c) anteroposterior CT view of *Junggarsuchus sloani* quadrate; (d) CT reconstruction of the quadrate of *Dibothrosuchus elaphros* in ventral view; (e) CT cross section of *Dibothrosuchus* quadrate shaft in anteroposterior view

Junggarsuchus would possess a pneumatic medial expansion of the quadrate unlike that seen in any other crocodylomorph. However, if this process is comprised mostly of the pterygoid, then *Junggarsuchus* would possess a pneumatic pterygoid and a posteroventral projection of the pterygoid that extends beyond the articular ramus of the quadrate and contacts the ventral process of the otoccipital, a condition unlike any seen in crocodylomorphs. We reconstruct the quadrate as the element that formed the majority of this process. The quadrate contacted the broken piece of the otoccipital and that piece likely extended dorsally to contact the remainder of the otoccipital. A small portion of this contact can be seen in posterior view, where the portion of the otoccipital reconstructed as forming the dorsal border of the cranioquadrate canal contacts the medial shaft of the quadrate dorsally (Figures 12b and 13c,d). The dorsomedial portion of the quadrate contributes to the lateral

wall of the temporal-orbital fenestra, similar to *Dibothrosuchus* (Figure 10a). In *Junggarsuchus*, the cranioquadrate canal is enclosed dorsally by the otoccipital and likely ventrally by the otoccipital, similar to *Almadasuchus* (Leardi et al., 2020), lateral to the foramen magnum. The lateral position of the quadrate strongly suggests that the quadrate is not involved in the ventral opening we have identified for the cranioquadrate canal (Figures 12b and 13c,d).

Both quadrates of *Dibothrosuchus* are preserved, though the scans we have are missing the midsection and the articular heads of the quadrate have been crushed against the articulars (Figure 29e). The quadrate of *Dibothrosuchus* has a posteriorly projected ventral body and possesses an elongate dorsomedial process the overlays the ascending posterior process of the pterygoid, neither of which are seen in *Junggarsuchus* and *Sphenosuchus* (Walker, 1990) (Figure 25b,c,e). The dorsal process of the quadrate is also more anteroposteriorly expanded in *Dibothrosuchus* than *Junggarsuchus*, which lacks the "T" shape of the dorsal portion of the bone in lateral view. There is a short, anterodorsal process of the quadrate in *Dibothrosuchus* that is rectangular in anterior view. This process projects anterolaterally in dorsal view and contacts the medial rim of the squamosal that contributes to the supratemporal fenestra. The process curves slightly medially and is shorter than it is tall in anterior view. Anteriorly, this process contacts a long rectangular section of bone along the ventral edge of the anterior process of the squamosal, which is likely the anterodorsal process of the quadratojugal (Figure 25c,e). The quadrate does not contact the laterosphenoid at all, unlike in *Junggarsuchus*, where a narrow anterodorsal process approaches the laterosphenoid; however, the dorsal overhang of the intertympanic recess and cranial nerve V (trigeminal) are similar to *Junggarsuchus*. Ventrally, the pterygoid process is broad and overlaps the anteromedial surface of the quadrate ramus of the pterygoid.

The curvature of the quadrate shaft (in posterior view) that forms the posterior border of the external otic aperture (Montefeltro et al., 2016) lacks the marked medially concave surface in *Macelognathus* (Leardi et al., 2017) and is more similar to *Junggarsuchus*. *Dibothrosuchus* has only one quadrate fenestra unlike *Junggarsuchus* and early diverging crocodyliforms like *Protosuchus haughtoni* (BP/1/4770) (Gow, 2000) and *Orthosuchus* (Nash, 1975), which have two or more. The body of the quadrate is solid and not pneumatized as in crocodyliforms, *Junggarsuchus*, *Almadasuchus*, and *Macelognathus* (Leardi et al., 2020). The anterior concavity and crest on the ventral portion of the quadrate are not observed in other non-crocodyliform crocodylomorphs. There is no contact between the quadrate and exoccipital in *Dibothrosuchus* unlike *Junggarsuchus*, *Macelognathus*, *Almadasuchus*, and *Protosuchus haughtoni* (BP/1/4770) (Gow, 2000; Pol et al., 2013) (Figure 11e). The pterygoid process is similar in ventral view in both taxa, but the quadrate ramus of the pterygoid is not as medially expansive in *Dibothrosuchus* as in *Junggarsuchus*. *Dibothrosuchus* lacks the posterior medial contact with the pterygoid and posterior dorsal projection of the otoccipital or quadrate relative to the quadrate condyle seen in *Junggarsuchus*.

The **quadratojugal** in *Junggarsuchus* is poorly preserved on only the left side of the skull (Figures 3b, 11b, and 12b). Extensive breakage and the unusual shape of the quadratojugal and jugal—which limits comparison with other crocodylomorphs—do not allow definitive determination of their contact at the ventral border of the infratemporal fenestra. The contact with the quadrate may correspond to a vertical crack just lateral to the fenestra in the ventral part of the quadrate (Figure 12b). Assuming this to be the contact, the quadratojugal is a thin, anteroventromedially convex bone. Its ventral edge is obscured by fractures and may be underlain anteriorly by a portion of the jugal. The quadratojugal extends anterodorsally from the articular head of the quadrate, in which it does not participate. About one-third of the anteroposterior length along the infratemporal fenestra the quadratojugal curves dorsally, and the jugal articulated there. A large piece of bone anterior to a break may be part of the quadratojugal, as it has a depression anteroventrally on its lateral surface that articulates laterally with the jugal. However, this posterior lateral piece of bone appears continuous with the jugal and laterally overlaps the quadratojugal (Figures 3b and 4b). Dorsally, the quadratojugal continues along the anterior edge of the quadrate to reach the squamosal and forms most of the posterior border of the infratemporal fenestra, excluding the quadrate from the border. From our CT data, we were able to verify that this narrow dorsal process of bone, covering most of the lateral surface of the dorsal part of the quadrate on the left side, and meeting the squamosal is the quadratojugal. This contrasts with the lack of a dorsal continuation of the quadratojugal and the quadrate contributing to most of the posterior border of the infratemporal fenestra in most other non-crocodyliform crocodylomorphs including *Hesperosuchus* (CM 29894) (Clark et al., 2001), *Dromicosuchus* (Sues et al., 2003), *Macelognathus* (Leardi et al., 2017), *Almadasuchus* (Leardi et al., 2020) and, as interpreted by Clark et al. (2001), *Sphenosuchus* and *Pseudhesperosuchus*, but is similar to *Terrestrisuchus* (Crush, 1984), *Dibothrosuchus* (Wu & Chatterjee, 1993) and early diverging crocodyliforms such as *Protosuchus richardsoni* (UCMP 130860 and AMNH 3024).

Very little of the quadratojugal is preserved in *Dibothrosuchus* (IVPP V 7906). Two small rectangular pieces of bone on the lateral surfaces of the two dorsal

ascending process are observable in posterior view. A slightly larger portion of the right quadratojugal is preserved on the lateral surface of the descending process of the quadrate (Figures 12b and 29e). The largest portion of the element that is preserved in *Dibothrosuchus* is an elongate rectangular anterodorsal process of the quadratojugal positioned anterior to the anterodrosal process of the quadrate and ventral to the anterior process of the squamosal. This portion of bone extends as far anteriorly as the anterior rim of the preserved squamosal and is as tall as the anterodorsal process of the quadrate (Figure 25d). This condition of a dorsally tall quadratojugal that contacts the squamosal is similar to the condition seen in *Junggarsuchus*, *Terrestrisuchus* (Crush, 1984), and *Sphenosuchus* as interpreted by Walker (1990).

The **supraoccipital** of *Junggarsuchus* occupies the dorsomedial area of the occiput, from its ventral contact with the otoccipital dorsal to the foramen magnum to the dorsal edge of the occiput (Figure 12b). Except for the small exposure of the parietal along the midline extending into a midline notch in the supraoccipital, the supraoccipital is roughly a square plate on the occiput, of approximately equal height and width, although it widens on the left side toward the ventral edge in occipital view. This condition is similar to the condition in *Litargosuchus* (Clark & Sues, 2002), *Macelognathus*, *Almadasuchus*, and crocodyliforms like *Protosuchus haughtoni* (BP/1/4770) (Gow, 2000) where the supraoccipital is lateromedially wider than dorsoventrally tall (Leardi et al., 2017). Ventrolaterally, the supraoccipital is bounded by the otoccipital, which excludes it from the dorsal margin of the foramen magnum. This region is damaged and has been re-attached after separation of the left and right sides, but a dorsoventrally broad medial process of the otoccipital is preserved on the right-side ventral to the straight ventral edge of the supraoccipital. This process is broken on the left side, so that a dorsal extension of the foramen magnum is due to this break and the ventral dislocation of the left side of the braincase relative to the right. The supraoccipital is fully separated from the foramen magnum by the contact between the otoccipitals, which is the condition seen in crocodyliforms like *Orthosuchus* (Nash, 1975) and *Protosuchus haughtoni* (BP/1/4770) (Gow, 2000), though the process of the otoccipital separating the supraoccipital from the foramen magnum is dorsoventrally shorter in *Junggarsuchus*. The supraoccipital approaches the medial margin of the small posttemporal fenestra and very subtly contributes to the medial margin of the posttemporal fenestra (Figure 16e) similar to the condition in crocodyliforms such as *Orthosuchus* (Nash, 1975) and *Protosuchus haughtoni* (BP/1/4770) (Gow, 2000), in which the supraoccipital forms the medial and ventral edge of the fenestra. Based on our CT data, the intertympanic recess (sensu Dufeau & Witmer, 2015; Kuzmin et al., 2021) did not extend through the supraoccipital as it does in living crocodylians. In the anteromedial portion of the supraoccipital, the dorsomedially oriented space for the third semicircular canal is enclosed, where the bone contacts the prootic (Figure 22a).

The supraoccipital of *Dibothrosuchus* is more pentagonally shaped in occipital view than the squared bone in *Junggarsuchus* (Figure 12b). The parietal sends three ventral triangular extensions ventrally along the occipital surface of the supraoccipital, two on each side and a short one along the midline. The supraoccipital contacts the otoccipitals ventrally, and a ventral midline projection separates the otoccipitals and forms the dorsal border of the foramen magnum, which is similar to some other non-crocodyliform crocodylomorphs, like *Sphenosuchus* (Walker, 1990). The posterior surface of the supraoccipital is more concave than in *Junggarsuchus*. The ventrolateral process of the supraoccipital, that ventrally contacts the otoccipital, is anteriorly expanded anteromedially. In our CT data, the supraoccipital is not invaded by the intertympanic recesses as hypothesized by Wu and Chatterjee (1993:69).

The exoccipital is fused with the opisthotic to form an **otoccipital**, as in all crocodylomorphs and archosaurs where known (Clark, 1986) and forms the paroccipital process as well as part of the lateral wall of the braincase (Figures 3b, 9b, 12b, 13, 17, 21, and 24). The wing-shaped, dorsoventrally broad paroccipital process is fully preserved only on the left side of the skull. Its lateral end is dorsoventrally expanded and the anterior surface is concave, forming a broad dorsoventral groove along with the squamosal, which overlies it anteriorly. This unusual groove may have been the site of origin of the *M. depressor mandibulae*, as it aligns with the retroarticular process, although in living amniotes it does not arise from the lateral surface of the paroccipital process (Diogo, 2008). An alternative interpretation is that the groove may be related to the muscles of the ear flaps (Leardi et al., 2020). These structures present in living crocodyliforms have been identified based on the presence of a dorsal groove on the squamosal in both fossil crocodyliforms like *Protosuchus richardsoni* (AMNH 3024, UCMP 130860) as well as non-crocodyliform crocodylomorphs like *Kayentasuchus* (Clark & Sues, 2002). In *Almadasuchus*, the triangular concavity has been proposed as an origin for the *M. levator auriculae superior* (Montefeltro et al., 2016; Shute & Ballairs, 1955) though living crocodylians lack any distinct groove of scarring for this muscle of the ear flap (Leardi et al., 2020; Montefeltro et al., 2016). The groove between the otoccipital and squamosal is housed in the triangular concavity of the squamosal. However, *Junggarsuchus*, like

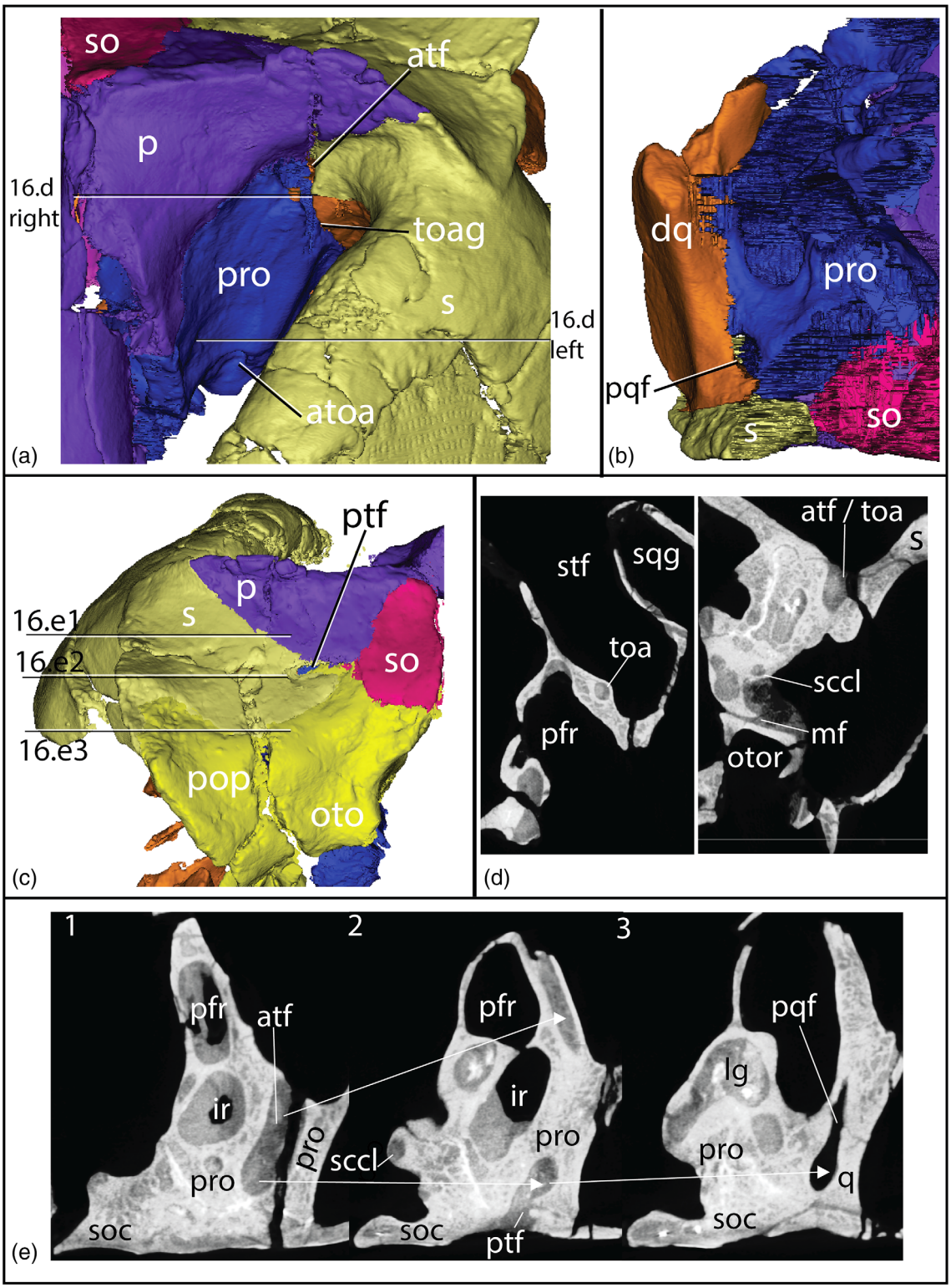

FIGURE 16 The temporo-orbital artery path of *Junggarsuchus sloani* (a) the left prootic in anterodorsal view; (b) right prootic in ventral view; (c) left occipital in posterior view; (d) CT images of the path of temporo-orbital artery in the prootic in anteroposterior view; (e) CT images of the connection of the post quadrate foramen and the posttemporal fenestra. Left image ventral to right image, white lines demonstrating continuation of passageway. Horizontal white/lack lines indicate where CT images are from.

Almadasuchus and unlike *Kayentasuchus*, lacks a dorsal groove or other indication of ear flap musculature. The ventral edge of the process is slightly concave, and a poorly preserved ventrolateral projection of the otoccipital is present ventral to the paroccipital process (Figures 11b, 14a b, and 17a). A small part of this projection is preserved near

the lateral end of the paroccipital process, where it preserves the dorsal and medial borders of a foramen that was identified as for the internal carotid artery by Clark et al. (2004) (Figure 12b,c). However, in living crocodylians, the inner carotid passes through the basioccipital and is placed medially (Dufeau & Witmer, 2015; Kuzmin et al., 2021) and so, given the foramen's lateral position and lack of involvement with the basioccipital we infer that the dorsal border of a foramen for the carotid foramen is not preserved. Instead, we interpret that this foramen is for the cranioquadrate canal (Figures 12b and 13a) as this foramen is positioned laterally and enclosed by the otoccipital in living crocodylians (Dufeau & Witmer, 2015; Kuzmin et al., 2021) and this position is more consistent with the foramen reported in *Junggarsuchus*. The otoccipital, squamosal, and quadrate meet lateral to this canal. Based upon the lateral position, lack of communication with the metotic foramen and posterior orientation we also conclude that this is not the posterior exit for the vagus nerve, as seen in *Almadasuchus* and other crocodyliforms like *Protosuchus richardsoni* (AMNH 3024,) and *Gobiosuchus* (Osmólska et al., 1997) where the exit for the nerve is smaller, more medially and ventrally oriented (Leardi et al., 2020). Another part of the otoccipital appears to be preserved on the right side of the occiput between the basioccipital and parabasisphenoid lateral to the basioccipital and dorsal to the parabasisphenoid (Figure 12b). Other pieces of this process were removed during preparation. The otoccipital may contact the ventral edge of the occipital portion of the parietal very mediolaterally narrow lateral to the posttemporal fenestra, separating the squamosal from the supraoccipital, and form part of the ventral edge of this mediolaterally ovoid foramen.

The contact between the otoccipital and basioccipital ventrolateral to the foramen magnum is obscured on the right side due to breakage, and on the left a suture or crack is evident ventrally on the lateral edge of the occipital condyle but not dorsally. If it is a suture, the otoccipital contributed a small anterior portion to the lateral surface of the condyle, but these contributions were limited, irregular and asymmetrical (Figure 13a). In CT scan images, these inferred sutures are difficult to interpret, however, and due to the irregularity, asymmetry and obliteration of a suture anteriorly were interpreted as cracks. In the majority of our figures, the occipital condyle is reconstructed as being nearly completely basioccipital (Figure 12b). The hypoglossal foramina are not evident lateral to the foramen magnum. On the right side, a smooth and flat laterally facing surface on the ventral part of the otoccipital lateral to the basioccipital is seen, forming the medial border of a passage through the otoccipital. This opening may be for the internal carotid artery as it is more medially positioned than the foramen interpreted as the opening of the cranioquadrate canal, but no comparable structure is seen on the more complete left side (Figure 12b). It appears similar to the foramen on the left side interpreted as for the cranioquadrate canal (Figure 12b), although the left opening lies slightly further laterally. The only other non-crocodyliform crocodylomorphs that the cranioquadrate canal is known in are *Macelognathus* and *Almadasuchus* (Leardi et al., 2020). In *Macelognathus*, the ventral position and contribution of the quadrate to the ventral border of the canal is similar to that seen in most crocodyliforms like *Gobiosuchus* and *Fruitachampsa* (with the exception of early forms like *Protosuchus* richardsoni (AMNH 3024, UCMP 130860) and *Orthosuchus*), but unlike the condition in *Almadasuchus*, where the canal is entirely enclosed by the otoccipital (Leardi et al., 2020). The condition in *Almadasuchus* is the most similar to that seen in *Junggarsuchus*. The ventral border of the cranioquadrate canal in *Junggarsuchus* is not preserved, but the medial edge of the quadrate shaft indicates that it would not have contributed to the border of the canal (Figure 12c) and the canal would have likely been fully bounded by the otoccipital, as in *Almadasuchus* (Leardi et al., 2020; Pol et al., 2013). There is a smooth surface on the medial surface of the fragment with the foramen on the left, which may indicate the presence of two foramina. No parabasisphenoid otoccipital suture is evident, though what may be the descending process of the right otoccipital may contact the parabasisphenoid.

The cranioquadrate canal (Figures 12b and 13a) is similar in position to *Almadasuchus*, though more ventrally directed; however, the latter is possibly due to breakage. The otoccipital, quadrate, and squamosal contacts lateral to the canal, are similar to *Almadasuchus* and crocodyliforms like *Protosuchus richardsoni* (UCMP 130860, AMNH 3024) and *Protosuchus haughtoni* (BP/1/4770) (Gow, 2000) and living crocodylians. However, due to breakage, whether this contact is broad is unclear. This contact is not seen in *Dibothrosuchus* or *Sphenosuchus* (Walker, 1990) or other early diverging crocodylomorphs. The ventrolateral contact of the otoccipital with the quadrate appears to be broad as in *Almadasuchus* (Leardi et al., 2020), but is incomplete. The posterior tympanic recess is a depression posterior to the fenestra ovalis located on the anterior surface of the paroccipital process and is angled sub-vertically as in *Almadasuchus* (Leardi et al., 2020) (Figures 17d, 21b, and 24). In *Dibothrosuchus* (Wu & Chatterjee, 1993), this recess is set in a deep depression at the same level of the intertympanic recess, which is similar to *Macelognathus* (Leardi et al., 2017) and *Protosuchus haughtoni* (BP/1/4770) (Gow, 2000). The subscapular buttress has a dorsally convex dorsal lip and medial to this is the dorsal lamina of the otic capsule. Posterior to this extracapsular buttress the

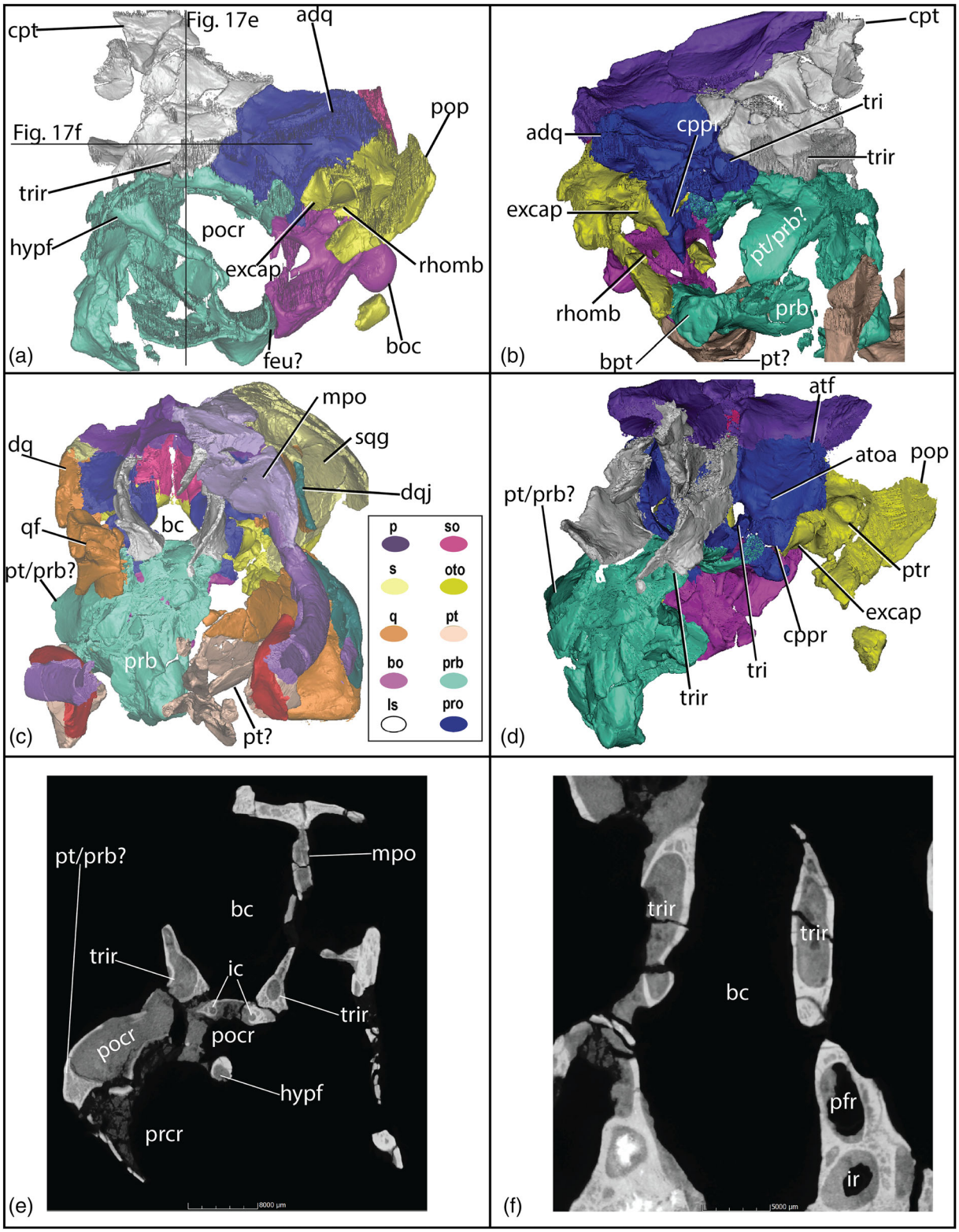

FIGURE 17 *Junggarsuchus sloani* braincase in (a) left lateral; (b) right lateral with alternative pterygoid reconstruction; (c) anterior view; (d) left anterolateral view; (e) CT images of the trigeminal recess of *Junggarsuchus* in anterior and (f) dorsal view

metotic foramen (Figures 17a, 20a, 21a,b, and 24) is visible. This general anatomy appears similar in *Dibothrosuchus*. The metotic foramen, for the vagus nerve and the opening for XI (accessory nerve) appear to be directed mediolaterally as in *Dibothrosuchus* and unlike crocodyliforms (Figures 17a, 20a, 21a and 24). Within the otic region, the fenestra

ovalis overlays the dorsoventrally narrow crista interfenestralis, which separates the ventral fenestra ovalis from the dorsal vestibule. This region of the opisthotic continues anterior to an enlarged region that contacts the prootic crista (Figures 17a, 21a,b, and 24). Due to the incomplete preservation of the medioventral portion of the otoccipital, the exit of the vagus nerve is not preserved.

The otoccipitals of *Dibothrosuchus* are well preserved on both sides of the skull. Dorsoventrally, the otoccipitals are shorter than in *Junggarsuchus* and terminate dorsal to the most ventral extension of the occipital condyle (Figure 12e). The medial borders of the foramen magnum are medially concave around the foramen magnum. Dorsally, the otoccipitals are separated by a ventral projection of the supraoccipital, unlike in *Junggarsuchus* and crocodyliforms like *Protosuchus haughtoni* (BP/1/4770) (Gow, 2000). Along the posterior midline of the edge of the occipital surface of the otoccipitals, there is a groove that trends from the lateral to the medial edge. The paroccipital processes are not as wing shaped as in *Junggarsuchus*, in which the dorsolateral edge curves dorsally, but instead have symmetrical dorsal and ventral edges, giving the paroccipital process a broad, spade-shaped lateral edge in occipital view. They are laterally concave, not convex as in *Junggarsuchus* and crocodyliforms. The ventral edge of the otoccipital contact with the basioccipital has a mediolaterally wider contact with the lateral edges of the condyle than in *Junggarsuchus*. In prior reconstructions (Wu & Chatterjee, 1993), the otoccipitals have been reported to form the dorsal portion of the occipital condyle and the posterior floor of the braincase. Our CT scans show that these portions of the otoccipital have unclear sutures with the basioccipital, and we reconstruct the otoccipital's contribution to the occipital condyle as less extensive than interpreted by Wu and Chatterjee (1993), though this interpretation is tentative due to the unclear nature of the sutures in our CT data. In our interpretation, the basioccipital forms most of the posterior floor of the braincase. The anteroventral process of the otoccipital on the occiput has two foramina, a smaller anterior one, and a slightly larger posterior one, both for branches of the hypoglossal nerve (XII) (Figure 12e). The dorsal contact of the otoccipital with the supraoccipital is almost straight in posterior view, except for the concave shape of this contact dorsal to the foramen magnum and the ventrolaterally curving contact of the otoccipitals with the squamosals in *Junggarsuchus*. Like *Junggarsuchus*, the posterior tympanic recess is bordered posteriorly by the otoccipital in *Dibothrosuchus*, but unlike *Junggarsuchus*, the posterior tympanic recess is bordered anteriorly by the prootic and set in a deep depression at the level of the mastoid antrum (Figure 25a,c). The exits for cranial nerve XII and the vagus nerve are ventrolateral and similar in position to *Sphenosuchus*, but not through a single opening as in *Almadasuchus* (Leardi et al., 2020; Pol et al., 2013; Walker, 1990) and crocodyliforms. The parabasisphenoid does not contact the otoccipital in *Dibothrosuchus* unlike in *Protosuchus haughtoni* (BP/1/4770) (Gow, 2000) and *Junggarsuchus*. Wu and Chatterjee (1993) describe the otic anatomy of *Dibothrosuchus* in detail and so this region is discussed in comparison with *Junggarsuchus* below. Besides the difference in the nature of the post tympanic recess, the overall anatomy of the otic region of the otoccipital is similar (Figures 25 and 26).

The otic region in *Junggarsuchus* is best exposed on the right side (Figures 17b, 21, and 24). The otoccipital forms the posterior portion of the otic region, and the horizontal crista interfenestralis is preserved extending anteriorly to separate the fenestra ovalis dorsally from the fenestra pseudorotundum ventrally, which is similar to that of *Dibothrosuchus* (Figures 17a,b, 21a, and 24). The prootic and otoccipital contact dorsal to the fenestra ovalis. The extracapsular process (sensu Kuzmin et al., 2021) (=subcapsular process of Clark, 1986) of the otoccipital projects anteroventrally as in *Dibothrosuchus* and the anterolateral surface preserves a slight otosphenoidal crest similar to *Almadasuchus* (Leardi et al., 2020) (Figure 21a,b). The extracapsular process continues ventrally and forms the posterior edge of the chamber housing the lagena, whereas an elongate descending lateral lamina of the prootic contributes to the anterior border (Figure 21a,c,e). On the left side, the ventral region of the element housing the lagena is perforated by a round fenestra, but this is not present on the right side of the skull. Posterior to and level with the extracapsular process the metotic foramen forms a narrow subvertical groove leading to the passage through the otoccipital similar to *Almadasuchus* (Leardi et al., 2020) and extant crocodylians (Kuzmin et al., 2021) (Figures 17a,b, 21a, 23, and 24), presumably for the vagus and accompanying posterior cranial nerves.

The metotic foramen is dorsoventrally narrow and in *Dibothrosuchus* this foramen is dorsoventrally taller and more rectangular (Figures 25a and 26a). Ventral to the extracapsular buttress, a large rhomboidal recess, a space for the enlargement of the pharyngotympanic canal (Kuzmin et al., 2021; Owen, 1850), is continuous with the basioccipital recess ventrally and the otoccipital recess dorsally (Figures 13c, 17a, 19c, 20a, and 21a). Both otoccipitals are incomplete ventrally and their broken ventral surfaces demonstrate that both possessed a recess, circular in ventral view, that narrowed dorsally through the dorsal part of the otoccipital dorsolateral to the basioccipital condyle (Figure 18a). These spaces are likely

the otoccipital pneumatic recess, sensu Dufeau and Witmer (2015), which is a pneumatic recess that invades the otoccipital and is continuous with the rhomboidal recess (for the rhomboidal sinus) in *Alligator mississippiensis* (Dufeau & Witmer, 2015; Kuzmin et al., 2021). The pneumatic spaces identified as the otoccipital recesses in *Junggarsuchus* differ from those in *Alligator mississippiensis* in that the recess is posterior to and separated from the intertympanic recess in *Junggarsuchus*, unlike the condition in *Alligator*, in which the otoccipital recess is directly continuous with the intertympanic recess (Kuzmin et al., 2021) (Figures 13c, 19c, and 20c,d). If this otoccipital space is the otoccipital recess then the rhomboidal sinus in *Junggarsuchus* is far more anterolaterally and dorsoventrally extensive than in *Almadasuchus*, as it continues dorsally and may communicate with the basioccipital recess ventrally as well, which the rhomboidal recess in *Almadasuchus* lacks (Leardi et al., 2020). The lack of clear osseous borders suggests a connection between the pharyngotympanic canal and median pharyngeal canals (=median eustachian canal) in the basioccipital recess (sensu lato) as is seen in crocodyliforms and some thalattosuchians like *Pelagosaurus typus* (Leardi et al., 2020).

The posteromedial contact of the otoccipital and basisphenoid surrounds a subcircular opening on the right side (Figure 20). This opening is not clearly present on the left side of the braincase, which may be due to postmortem crushing, but the border of the opening on the right side appears natural. This space is peculiar as it appears that the braincase communicates with the otoccipital recess and rhomboidal recess through this opening. It is unclear what passed through this opening as no comparably large opening is known in other crocodylomorphs in this position (Leardi et al., 2020; Walker, 1990; Wu & Chatterjee, 1993). The posterior position of this opening on the braincase suggests that it could have been an enlarged metotic foramen, an opening for the vagus nerve. However, this space is continuous with the rhomboidal recess and otoccipital recess, lacks a discrete lateral opening, and a narrow opening similar to that seen for the metotic foamen in *Almadasuchus* is present posterior to the opening for the rhomboidal recess in *Junggarsuchus* (Figure 19c). In extant crocodylians (Kuzmin et al., 2021) and extinct crocodylomorphs like *Almadasuchus*, *Macelognathus*, and *Dibothrosuchus*, the metotic foramen is posterior to the extrcapsular process and posteroventral to the fenestra pseudorotunda and laterally visible on the ear which is consistent with the narrow groove we identified as the metotic foramen in *Junggarsuchus* and not consistent with the enlarged medial foramen (Leardi et al., 2017, 2020; Wu & Chatterjee, 1993) (Figure 23). Due to the structure's asymmetry, lack of a similar feature in relatives and position, we are unable to confidently identify this structure.

In *Junggarsuchus*, the **basioccipital** is roughly circular in posterior view (Figure 12a,b), except at its dorsal margin where it becomes concave along the ventral margin of the foramen magnum and along its ventral margin where it is slightly arched dorsally along the midline. It extends anteriorly into the braincase where it forms the posterior part of its floor. Anterior to the foramen magnum, the dorsal surface of the basioccipital slopes slightly anteroventrally. Ventral to the occipital condyle, the posterior surface of the basioccipital is gently concave. The basioccipital diverticulum is extensively expanded ventrally in *Junggarsuchus* (Figures 17a, b, 18a, b, and 19a–c). Internal to this concavity, as exposed by a break on the left side, the basioccipital recess (sensu latu) occupies a large space, larger than in *Sphenosuchus* (Walker, 1990).

Junggarsuchus possesses a basioccipital with a large internal recess and like crocodyliforms lacks an external basioccipital recess ventrally like those seen in *Sphenosuchus* (Walker, 1990), *Dibothrosuchus* and *Almadasuchus* (Pol et al., 2013). *Junggarsuchus* may also possess a basioccipital recess that communicates with the middle ear cavity as in crocodyliforms as shown by the continuous connection between the rhomboidal recess and basioccipital recess (sensu stricto) (Dufeau & Witmer, 2015). *Junggarsuchus* possess a basioccipital recess (sensu stricto) but delimiting between the anterior sub-parabasisphenoid recess (median pharyngeal tube) (Dufeau & Witmer, 2015) and basioccipital recess (sensu stricto), as seen in *Sphenosuchus* (Walker, 1990) and *Almadasuchus* (Leardi et al., 2020), is complicated by a series of breaks. Two struts project ventrally into the anterior ventral open space of the basioccipital; the first projects posteroventrally (Figure 18a,d) immediately posterior to the anterior end of the parabasisphenoid and the second projects anteroventrally from the midpoint of the basioccipital's contribution to the floor of the braincase. There is no clear osseous anterior border of the basioccipital that would keep the recess from excavating the parabasisphenoid so we are tentatively naming this space the sub-basisphenoid recess (Figure 18a,b). Leardi et al. (2020) identified a complex posterior basioccipital recess (sensu stricto) in *Almadasuchus*, which possesses twin blind posterolateral excavations for the median pharyngeal canals, and noted the lack of external evidence of this recess in *Junggarsuchus* (Figure 19a). The posterior extent of the basioccipital recesses in *Junggarsuchus* excavates the ventral portion of the basioccipital posterior to the anteroventral strut and the dorsal body of the basioccipital as well, including the anterior half of the basioccipital condyle (Figure 19a). If this is the

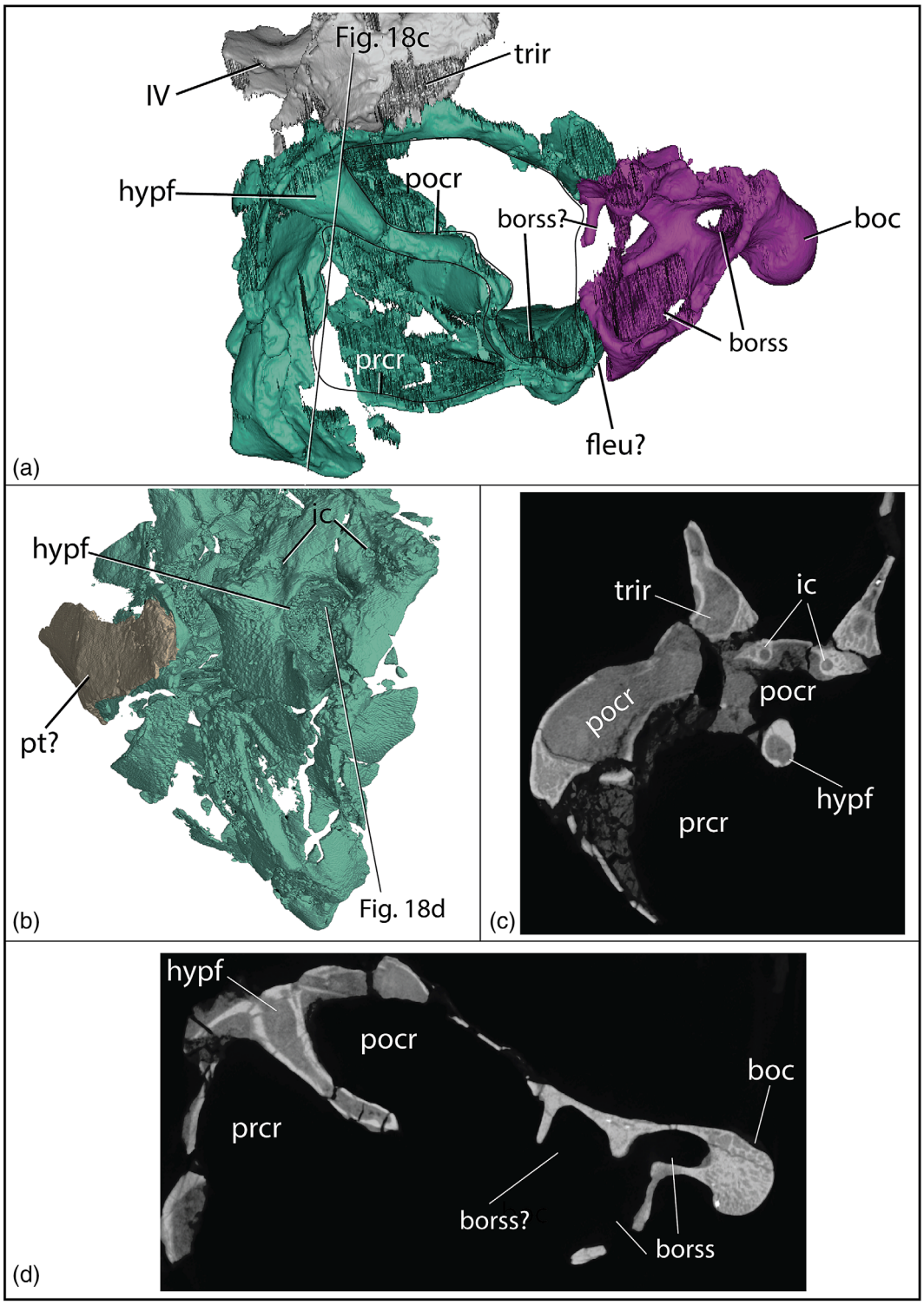

FIGURE 18 The spaces of the parabasisphenoid; (a) basioccipital spaces of *Junggarsuchus sloani* in left lateral view; (b) parabasisphenoid of *Junggarsuchus* in anterior view with alternative view; (c) CT images of the hypophyseal fossa and inner carotids in anterior view; (d) CT section of parabasisphenoid in lateral view—shows hypophyseal fossa

basioccipital recess (sensu stricto), it appears to differ from that seen in *Almadasuchus* in that it may communicate with the rhomboidal recess for the rhomboidal sinus (an expansion of the pharyngotympanic canal sensu Dufeau & Witmer, 2015; Leardi et al., 2020; Owen, 1850), a sinus that is separate in the Leardi et al. (2020) reconstruction of *Alamadasuchus*. *Junggarsuchus* seems to lack a ventral opening for the pharynx and features

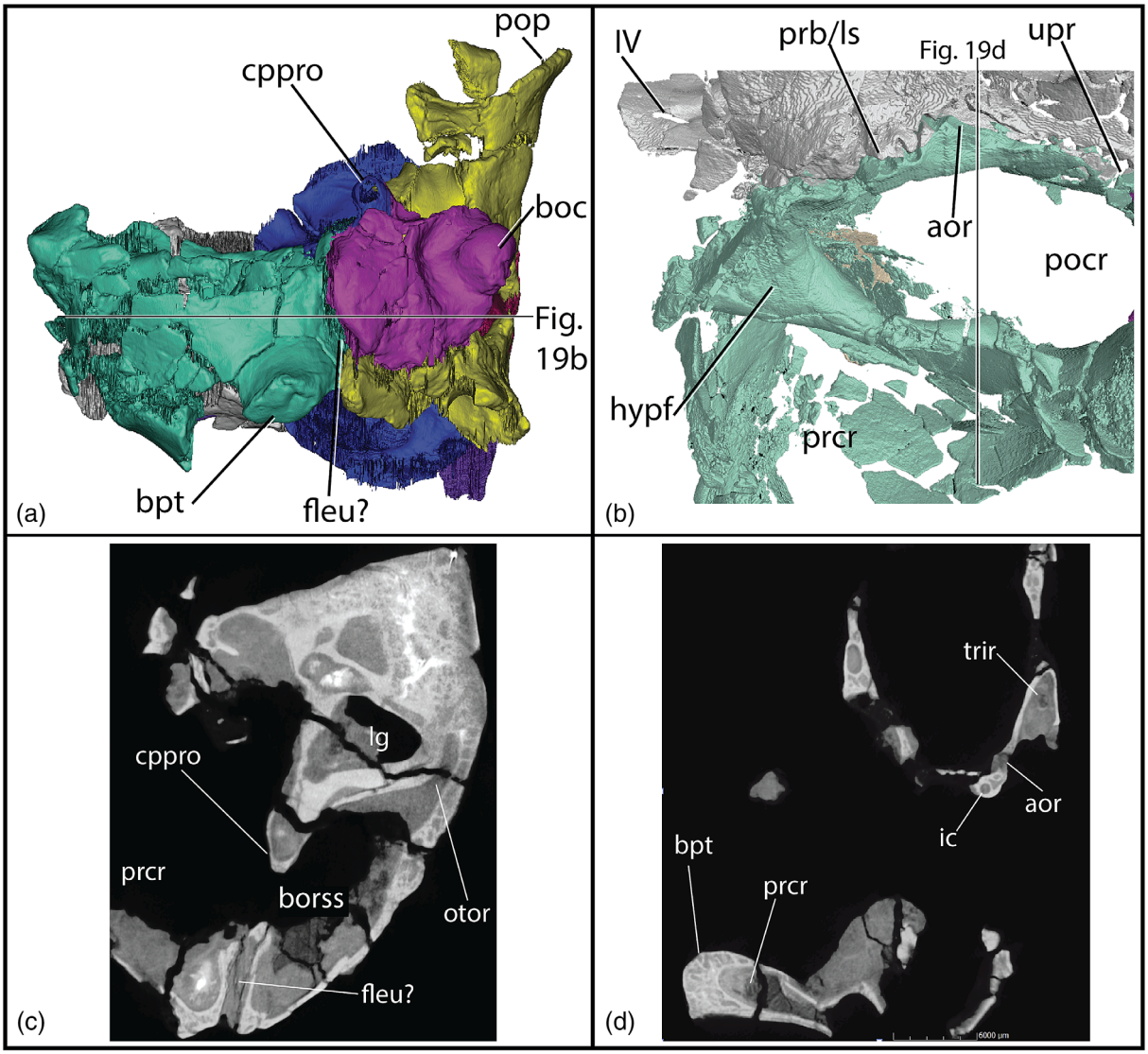

FIGURE 19 (a) The basicranium of *Junggarsuchus sloani* in ventral view; (b) possible eustachian groove of *Junggarsuchus sloani* in CT slice in lateral view; (c) left parabasisphenoid laterosphenoid contact in *Junggarsuchus sloani*; (e) contact in anterior CT view

communication between the basioccipital recesses (median pharyngeal canal) and pharyngotympanic canal, which are both conditions seen in crocodyliforms (Dufeau & Witmer, 2015; Leardi et al., 2020). This potential communication is preserved on the right side, where the basioccipital is more completely preserved, and in CT data, despite some breaks, it appears that the recess that excavates the basioccipital recess connects with the rhomboidal recess and even into the otoccipital pneumatic recess (Figures 13 and 20). A low anterodorsally ridge of bone is present between these two regions and could represent a broken surface for an osseous separation of these sinuses that was not preserved. However, the ventrolateral ridge of the basioccipital is continuous with the posterior continuation of the extracapsular process of the otoccipital, which suggests that these spaces connected in life (Figures 13, 19c, and 20a).

Dorsolaterally, the contact with the otoccipital is difficult to identify. However, it appears that the dorsolateral edge of the basioccipital contacts the medioventral surface of the posterior end of the otoccipital, which form the posterior lateral walls of the braincase. The posteroventral portion of the basioccipital differs from other non-crocodyliform crocodylomorphs like *Dibothrosuchus*, and *Almadasuchus* in that it is flat and lacks clear basioccipital tuberosities and pocketing (Figure 19a) (Leardi et al., 2020; Pol et al., 2013). Ventral to the basioccipital condyle, the element is shallowly concave before its ventral body expands slightly posteriorly. In occipital view, the ventral body of the basioccipital extends anterolaterally as a slightly rounded protuberance away from the mid line. The posteromedial side of the ventral body of the basioccipital is dorsally concave

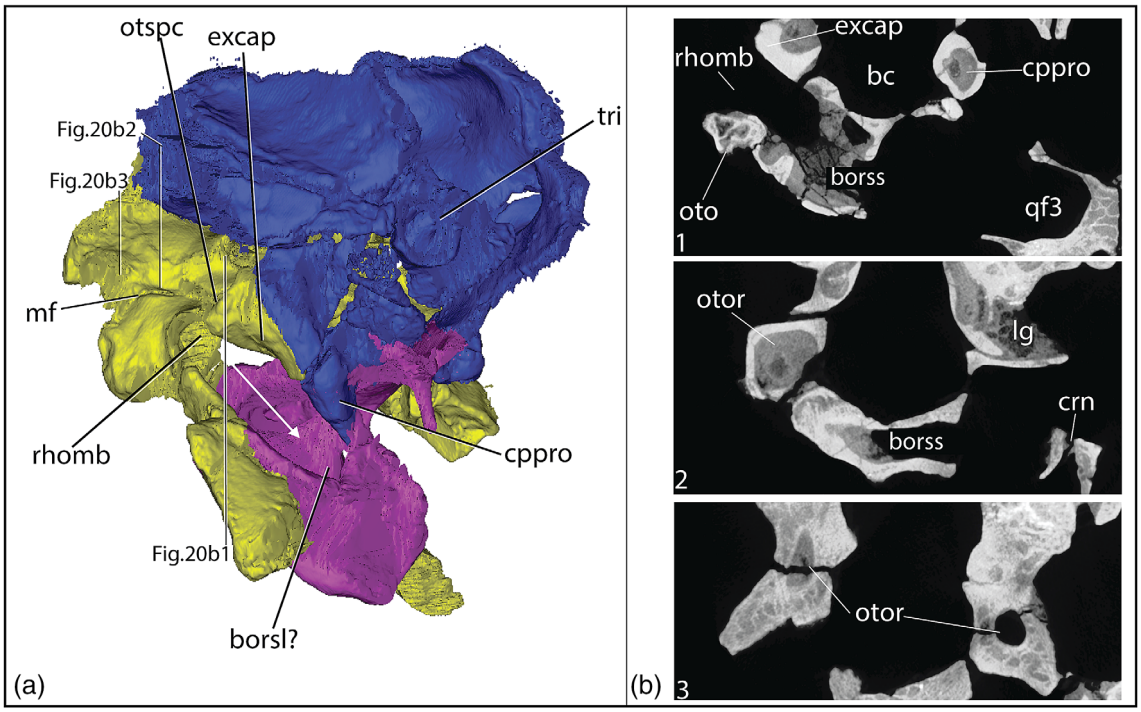

FIGURE 20 Communication between the rhomboidal recess and basioccipital recess. (a) Right posterior ear and basicranium of *Junggarsuchus sloani* in lateral view; (b) three anteroposterior sections of the skull in CT view showing the passageway of the rhomboidal sinus through the rhomboidal recess. The top image is anterior and the bottom image is posterior.

toward the occipital condyle and suggests that left side of the skull featured a similar slight anterolateral protuberance. Anteriorly and laterally, this ventral body articulates with the parabasisphenoid but does not extend laterally or ventrally past the basipterygoid processes. The center of the posteroventral surface of the right side of the basioccipital preserves a small hole that opens into the basioccipital recess. However, only the right posterior side is completely preserved and the edges of the opening are irregular and so we cannot verify if a similar structure was present on the left side and if this opening is simply a break (Figure 19a). Broken posterior surfaces of the basioccipital tuberosities are also known in theropod dinosaurs like *Velociraptor mongoliensis* and are believed to be broken depressions for the attachment of the M. rectus capitis anterior (Norell et al., 2004). It is possible the hole in *Junggarsuchus* represents a surface to which muscles attach. However, if real, this opening was not homologous to the basioccipital recess (sensu stricto) (a foramen for the pharynx) seen in *Almadasuchus* (Leardi et al., 2020) and *Dibothrosuchus* as such structures are not paired.

The orientation of the ventral part of the basioccipital depends on the correct orientation of the skull; when the ventral surface of the neurocranial cavity is horizontal, the basioccipital is nearly perpendicular to it and the sagittal crest of the parietal is oriented posteroventrally. On the ventral surface of the basioccipital, at the midline, there is an anterodorsally projecting lamina that contacted a dorsally concave posterior region of the parabasisphenoid (Figure 19). The basioccipital's ventral anterior contact with the parabasisphenoid is marked by a narrow mediolateral concavity that trends along the entire contact to the point at which the ventral process of the otoccipital contacts the basioccipital and parabasisphenoid. Part of this contact is filled with matrix but CT data show (Figure 19b) that the basioccipital and parabasisphenoid are not in contact (Figure 19c,d). It is likely that the parabasisphenoid has been slightly displaced anteriorly. This is supported by the step-like contact between the basioccipital and basisphenoid (Figure 19c).

A possible alternative interpretation is that the pharyngotympanic canal (=lateral eustachian opening) may exit where the basioccipital meets the otoccipital and basisphenoid ventrolaterally, forming a mediolaterally elongate slit. If this is not an artifact then this posteroventrally open slit would enclose the pharyngotympanic canal between the parabasisphenoid and the basioccipital (Figure 19a,b) and exit posterior to the basipterygoid process (Figure 19a). If not an artifact of postmortem crushing, *Junggarsuchus* would be the only non-crocodyliform crocodylomorph to possess openings for the pharyngotympanic canal between the basioccipital and parabasisphenoid, a feature believed to

be a derived feature of Crocodyliformes (Kuzmin et al., 2021). This interpretation is supported by the communication of the pharyngotympanic canal and basioccipital recesses, the crocodyliform condition. The pharyngotympanic canal in crocodyliforms continues from the rhomboidal recess, through the basioccipital recess ventrally and then exits further ventrally between the basioccipital and parabasisphenoid (Kuzmin et al., 2021; Porter et al., 2016). However, due to the uncertain nature of the preservation and possible role of deformation, we did not score the pharyngotympanic canal enclosed by the parabasisphenoid and basioccipital as present (Char. 266).

Wu and Chatterjee (1993) report that *Dibothrosuchus* has posterolateral exits for the pharyngotympanic canal between the basioccipital, parabasisphenoid, and otoccipital that communicated with the rhomboidal recess but not the basioccipital recess (Wu & Chatterjee, 1993), similar to *Almadasuchus* (Leardi et al., 2020). This external opening is evident in the 3D objects generated by our CT data (Figure 26) but due to the resolution of parts of the scan of *Dibothrosuchus* we cannot confirm the internal connection of these spaces as reported by Wu and Chatterjee (1993). This lateral exit dorsal to the parabasisphenoid cannot be identified in *Junggarsuchus* due to a series of breaks in the region. The more posterior position of the rhomboidal recess and lack of communication between the rhomboidal recess and basioccipital recesses in *Dibothrosuchus* relative to *Junggarsuchus* suggests a different condition than that seen in *Dibothrosuchus*.

The basioccipital of *Dibothrosuchus* is similar to the basioccipital found in *Sphenosuchus*. Unlike *Junggarsuchus*, there are more obvious basioccipital tuberosities present ventral to the occipital condyle and two ventrally opening foramina of the basioccipital recess (Figure 25a,c). These foramina are oval and separated along the midline. They are located in a ventral concavity and the foramina are fully enclosed by the basioccipitals. The anterior portion of the basioccipital's vertical surface is overlain by two posterior projections of the parabasisphenoid. Lateral to the occipital condyle, the otoccipitals limit the lateral extent of the basioccipital relative to *Junggarsuchus*. The dorsal concavity of the foramen magnum in *Dibothrosuchus* is also less pronounced than it is in *Junggarsuchus*. *Dibothrosuchus* possesses the basioccipital recesses present in most other non-crocodyliform crocodylomorphs, including *Macelognathus* (Leardi et al., 2017), *Junggarsuchus*, and crocodyliforms like *Protosuchus haughtoni* (BP/1/4770) (Gow, 2000).

A small anteroventrally oriented foramen is present ventral to the extracapsular process of the otoccipital. It is enclosed posteroventral by the basioccipital, ventrally by the basisphenoid and anterodorsally by the otoccipital (Figures 25a and 26). Wu and Chatterjee (1993) describe this opening as continuous with the rhomboidal recess and as the exit for the pharyngotympanic canal. This exit, dorsal to the main open space for the basioccipital recess (sensu stricto), demonstrates that the rhomboidal recess and pharyngotympanic canal did not communicate with the basioccipital recess as in *Junggarsuchus*. In this case, the canal is not enclosed between the basioccipital and parabasisphenoid as it is in crocodyliforms. Due to the nature of the CT scans for this region, we were unable to determine whether this foramen is continuous with the rhomboidal recess, though its position does lend support to this hypothesis (Figure 26a).

The **parabasisphenoid** in *Junggarsuchus* is expanded ventrally compared with other non-crocodyliform crocodylomorphs (Figures 11b and 17d), similar to some early diverging crocodyliforms such as *Protosuchus haughtoni* (BP/1/4770) (Gow, 2000) and to the therizinosaurid theropod *Erlikosaurus* (Lautenschlager et al., 2014). It is therefore visible on the anterovental part of the occipital surface, where the basioccipital overlies it posteromedially. The body of the parabasisphenoid houses a large cavity, similar in size to the neurocranial cavity (Figures 17a,e and 18a). This enlarged open space is not comparable to the pneumaticity observed in the parabasisphenoids of living crocodylians (Dufeau & Witmer, 2015), but the dorsoventrally tall open internal spaces of this bone are interpreted as pneumatic due to the extensive pneumatization of the basicranium by the paratympanic sinuses in *Alligator mississippiensis* (Dufeau & Witmer, 2015). The ventral midline portion of the parabasisphenoid was separated from the skull, and showed that the ventral surface of the parabasisphenoid is convex ventrally. A robust posterolateral process from the ventral surface of the parabasisphenoid just anterior to its contact with the otoccipital on the right side is has been interpreted as the basipterygoid process, although it is in an unusually posterior position and laterally directed relative to the ventrally projected basipterygoid processes of *Dibothrosuchus* (Figures 11b, 17d, and 19a). The process possesses an internal recess and a broad, flat, circular surface that faces laterally and only slightly ventrally. Medial to it, the parabasisphenoid is dorsoventrally tall. The parabasisphenoid is not preserved at its midline contact with the basioccipital. No clear ventral opening for the pharyngotympanic canals is observable between the parabasisphenoid and basioccipital. A potential exit for these canals has been identified as a mediolaterally elongate ventral groove opening posterior to the basipterygoid process (Figure 19), but this groove may be caused by the displacement of the basioccipital relative to the parabasisphenoid. In this case, the pharyngotympanic canal of *Junggarsuchus* does not pass between the two elements of the basicranium, which is similar to the

condition seen in other non-crocodyliform crocodylomorphs (Leardi et al., 2017; Leardi et al., 2020; Walker, 1990; Wu & Chatterjee, 1993). However, *Junggarsuchus* demonstrates a communication between the basioccipital recess (sensu stricto) and rhomboidal recess for the pharyngotympanic canal similar to crocodyliforms (Kuzmin et al., 2021; Leardi et al., 2020), though three discrete exits cannot be identified. Additionally, the lateral exit for the pharyngotympanic canal reported in *Dibothrosuchus* (Wu & Chatterjee, 1993) cannot be verified in *Junggarsuchus*. The lateral region of this recess is preserved, and it is separated from the basioccipital recess (sensu stricto) posteriorly and from the larger pneumatic cavity anteriorly, but may have been connected along the midline. The ventral surface of the parabasisphenoid medial to the basipterygoid process is very slightly concave ventrally, lateral to the midline expansion. The parabasisphenoid contacts the otoccipital posteriorly along the ventromedial edge of the otoccipital's ventral process though a suture is not evident (Figure 17b). On the right side, the anterior extent of the parabasisphenoid and its relationship with the pterygoid is unclear. Post mortem crushing has fragmented the anterior portion of the parabasisphenoid and potential overlap from the posterior process of the pterygoid onto the parabasisphenoid is unclear. Elements in this region of the skull have also likely been shifted during fossilization as the quadrate ramus of the pterygoid or the expanded pterygoid process of the quadrate (Figure 15a,b) appears nearly in level with the ventral portion of the parabasisphenoid. If the medial expansion of the pterygoid process continues to ascend dorsally and medially, and if complete, it may contact the parabasisphenoid. Anteriorly, at the contact between the laterosphenoid and parabasisphenoid, there is an opening, which we interpret as the opening for the orbital artery seen in *Almadasuchus* (Leardi et al., 2020) (Figure 19b–e).

The large pneumatic cavity within the parabasisphenoid is exposed by a lateral break. The anterior lateral portion of the parabasisphenoid pneumatic cavity may communicate with an expanded trigeminal recess of the laterosphenoid (discussed below). In ventral view, part of this enlarged parabasisphenoid would be covered broadly by the quadrate ramus of the pterygoid if the latter were complete. Anteriorly, the recess is very deep, but it is unclear which parts of the anterior wall are formed by the parabasisphenoid and which by the pterygoid. The parabasisphenoid forms more than half of the neurocranial floor anteriorly, and the hypophyseal fossa is poorly preserved at its anterior end. Lateral to the large dorsal midline opening of the hypophyseal fossa, there are two small foramina in the dorsal surface of the portion of the parabasisphenoid that forms the anterior portion of the bottom of the braincase. These two opening continue through the body of the parabasisphenoid, but are unfortunately lost with cracking of the posterior portion of the bone. These foramina are interpreted as the exits of the internal carotid arteries, which exit through a medial opening on the otoccipital identified earlier (Figure 18c,d). The internal carotid exits are not the same as the feature identified as such by Wu and Chatterjee (1993) in *Dibothrosuchus*, which were later identified as the post carotid recess by Leardi et al. (2020). The parabasisphenoid of *Junggarsuchus* possesses a distinct hypophyseal fossa and pre- and postcarotid recesses. The paired foramina in *Junggarsuchus* are lateral to the anterior opening of the hypophyseal fossa, not dorsal as with the postcarotid recess (Figure 18b) (Leardi et al., 2020). As the hypophyseal fossa descends the paths for the inner carotid arteries remain separate from the postcarotid recess and continue as well separated, thin, circular canals for most of the length of the parabasisphenoid, until they are lost (Figure 18b–d). This differs from the condition of the postcarotid recess in *Dibothrosuchus* and *Almadasuchus*, which are relatively enlarged, closely associated and sometimes continuous pneumatic structures, with an irregular shape (Figures 25 and 26) (Leardi et al., 2020).

A delicate strut traverses the pneumatic space within the parabasisphenoid along the midline, extending posteroventrally, ventral to the hypophyseal fossa and dividing the space into dorsal and ventral parts. The strut is circular in cross section and narrows posteroventrally as the anterior portion is twice the diameter of the strut from the midpoint (Figure 18c,d). A thin lamina of bone extends from the right lateral side of this strut to completely divide the parabasisphenoid recesses. This region is not preserved on the left side and the lamina on the right side, despite being fragmented, appears continuous (Figures 17a, and 18a,b). Using the descriptions of Walker (1990) and Leardi et al. (2020), we identify the ventral recess as the precarotid recess and the dorsal recess as the postcarotid recess. The precarotid recess occupies the anterior and ventral regions of the parabasisphenoid and narrows dorsoventrally posteriorly. There is no parabasisphenoid rostrum present and so no parabasisphenoid rostrum recess is present. The precarotid recess also excavates the basipterygoid process (Figure 18a). The postcarotid recess excavates the entire posterior region of the parabasisphenoid as well as the near majority of the mid and posterior dorsolateral region of the parabasisphenoid. Due to the lack of a clear osseus separation between the pneumatic spaces of the parabasisphenoid and basioccipital, it cannot be stated what of the postcarotid recess is actually invaded by the sub-

basisphenoidal recess. The postcarotid recess appears continuous with the basioccipital recess (sensu lato) (Figure 18a). This differs from the condition seen in *Almadasuchus* in which the basioccipital recess (sensu stricto) is continuous with the ventral precarotid recess (Leardi et al., 2020) but appears similar to the condition illustrated in *Sphenosuchus* (Walker, 1990, figure 28). Our CT data demonstrate that the circular central strut from which the lateral lamina extends is hollow (Figure 18d). The hollow strut opens anterodorsally on the parabasisphenoid between the exits for the inner carotids and houses the hypophyseal fossa, which is expanded anteriorly.

The parabasisphenoid of *Dibothrosuchus* (Figure 25a–c) is not as dorsoventrally tall as *Junggarsuchus*, and despite an anteroposterior long but dorsoventrally short recessed space, lacks the extensive pneumaticity seen in *Junggarsuchus*. As in *Junggarsuchus*, the basioccipital overlays the parabasisphenoid anteriorly, but the two posterolateral processes of the parabasisphenoid seen here are not observed in *Junggarsuchus*. The parabasisphenoid is enlarged lateromedially relative to the basioccipital, though not as much as it is in *Junggarsuchus* and *Protosuchus haughtoni* (BP/1/4770), in which the expansion is more in the dorsoventral direction. The basipterygoid processes of *Dibothrosuchus* are radically different from the posterior, laterally directed knobs seen in *Junggarsuchus*. The basipterygoid processes are enlarged, bulbous and pyramidal and extend substantially ventrally (Figure 25a–c). These two processes are invaded by several large open spaces visible in our CT data and anteriorly overlain by the quadrate ramus of the pterygoid. The quadrate ramus does not seem to contact the basipterygoid processes in *Junggarsuchus*.

The anterior break in the parabasisphenoid reveals passageways for the postcarotid recess on the anterodorsal surface, dorsal to the openings for the hypophyseal fossa (Leardi et al., 2020) which had previously been interpreted as the internal carotid arteries (Wu & Chatterjee, 1993) (Figure 25b). Like *Junggarsuchus* and *Almadasuchus*, *Dibothrosuchus* possesses an anteroposteriorly elongate hypophyseal fossa bordered dorsally by a postcarotid recess and ventrally by a pneumatized precarotid recess (Figure 25b,d). It is unclear whether the postcarotid recess or precarotid recess is continuous with the basioccipital recesses (sensu stricto) in *Dibothrosuchus*. The parabasisphenoid–otoccipital suture is absent in *Dibothrosuchus*, though the otoccipital ventrally approaches the posterior extent of the parabasisphenoid. This suture is possibly present in *Junggarsuchus* on the posterior surface of the braincase. Whereas the parabasisphenoid itself is expanded dorsoventrally and mediolaterally in *Junggarsuchus*, the parabasisphenoid recess in *Dibothrosuchus* appears more anteroventrally expanded than it is in *Junggarsuchus*, though this region is incomplete.

The posterodorsal surface of the parabasisphenoid contributes to the ventral border of two elongate, oval openings, which can be seen in ventrolateral view (Figures 25a and 26a,b). The anterior most of these two openings is dorsoventrally taller than the other and the laterosphenoid may contribute in part to its dorsal border. This opening is identified by Wu and Chatterjee (1993) as the anterior tympanic recess but based on redescription of this region from Leardi et al. (2020), this could be one of two features enclosed between the laterosphenoid and parabasisphenoid. The first is a lateral opening of the postcarotid recess. The alternative is that this is the anterior exit of the orbital artery seen in *Almadasuchus*, possibly *Junggarsuchus* and in living crocodylians, as it is bordered by the same elements and in a similar position (Leardi et al., 2020). A similar opening may be present in *Junggarsuchus* but are not known in *Sphenosuchus* (Walker, 1990) or *Macelognathus* (Leardi et al., 2017). Posterior to this opening, just anterior to the lateral lamina of the prootic, there is a dorsoventrally shorter oval opening between the parabasisphenoid and prootic. Wu and Chatterjee (1993) refer to this as the anterolateral branch of the median eustachian tube (Figures 25a and 26). Such an opening is not observed in *Junggarsuchus* in which the relevant region is largely broken.

The **prootic** of *Junggarsuchus* is visible within the supratemporal fossa between the parietal and quadrate (Figures 9b, 16, and 17a,b). It faces anterodorsally and has a gently concave dorsal surface. Posterodorsally, it forms the ventral, ventrolateral and medial edges of the anterior temporal foramen. The canal for this vasculature is lateral to the dorsal most extent of the braincase sinuses lateral to the inner ear and endosseous labyrinth. The anterior opening of the temporal canal is the anterior temporal foramen, and the temporo-orbital artery exits ventrally through the ear via the postquadrate fenestra and posteriorly via the posttemporal fenestra (Figures 12b, 16, and 17). The prootic facial recess is the most dorsally expanded of the recesses of the braincase. The prootic extends anteriorly to meet the laterosphenoid midway in the supratemporal fenestra, bordering the trigeminal opening posteriorly and dorsally. The trigeminal opening is directed anterolaterally, and the prootic forms most of the dorsal, ventral and posterior border (Figures 16 and 17a–c,e). Ventral to the dorsal head of the quadrate, it encloses the opening of the intertympanic recess extending dorsomedially and borders a small postquadrate foramen. The intertympanic recess is anteroposteriorly long and more oval than the recesses in *Almadasuchus*, though not as enlarged as in *Dibothrosuchus*. The prootic facial recess is anterior to and enlarged and oval

relative to the intertympanic recess and opens ventrally. The left prootic facial recess preserves a small circular opening in its dorsomedial surface that would enter the braincase, but an opening is not preserved in the right prootic facial recess (Figures 21c and 24). The development of the prootic facial recess and the intertympanic recesses are asymmetric. The right complex has a single dorsoventral lamina of bone separating the two recesses, whereas the left two recesses have a short perforation in the lamina dividing the two recesses and dividing the lamina in a dorsal and ventral region (Figures 21e and 24). The exit for cranial nerve VII is preserved through the anteroventral surface of the prootic, on the anterodorsal part of the lateral lamina of the prootic (=the prootic-parabasisphenoid flange of Walker, 1990), in a similar position to the exit for CN VII in *Almadasuchus*, *Macelognathus*, and *Protosuchus richardsoni* (Gow, 2000; Leardi et al., 2017, 2020) (Figures 21c and 24). The lateral lamina of the prootic is dorsoventrally tall, extending vertically ventral to the anterior end of the otic recess. The lamina descends ventrally to contact the parabasisphenoid and the anterior portion of the basioccipital and does not contact the laterosphenoid. The lateral lamina of the prootic is contacted posteriorly by the extracapsular process and together encloses a hollow space for the lagena (Figures 21a and 22–24). A foramen appears to open between the ventral surface of the lateral lamina of the prootic and the ventral surface of the extracapsular process (Figures 17d, 21d, and 24). The function of this ventral opening is unclear as it is unlikely the lagena would continue through it. Such an opening is not observed on the right side either because it is obscured or not present. This asymmetry suggests that this is not a natural opening and may be a broken surface. The prootic forms the anterior and dorsal border of the fenestra ovalis, which is separated from the ventral fenestra pseudorotunda by the crista interfenestralis (Figures 17a, 21a, and 22–24).

The endosseous labyrinths are preserved on the medial surface of both prootics (Figure 22a). They are medial to the dorsally expanded extent of the open space in the prootic facial recess and the openings are partially exposed on the lateral side of the prootic (Figures 21 and 24). The anterior semicircular canal is visible on the medial surface of the posterior prootic and anteromedial to the supraoccipital around a deep medial depression around which the canal curves (Figure 22a). The posterior semicircular canal is visible exposed on a depressed posteromedial surface of the otoccipital anterior to the supraoccipital. A concavity on the medial surface of the prootic medial to the prootic facial recess houses the floccular recess (Figure 22a,b) and is similar to the condition observed in *Almadasuchus* (Leardi et al., 2020). An anteroposteriorly elongate, rectangular lobe-like floccular recess projects laterally through the anterior semicircular canal and ends medial to the lateral extent of the lateral semicircular canal (Figures 13d and 22c,d). Well-developed, posteromedially projecting, floccular recesses are known in other crocodylomorphs like *Almadasuchus* (Leardi et al., 2020) but are not present in extant crocodylians (Kuzmin et al., 2021). We have segmented the endocasts of the spaces in the inner ear including all three semicircular canals (Figure 22c). Our reconstruction agrees with that published by Schwab et al. (2020).

These canals are clear in CT sections and the entire length of canals can be followed (Figure 22b,c). The anterior semicircular canal is steeply inclined posterodorsomedially and is as dorsoventrally tall as the lagena. The anterior half of the semicircular canal is enclosed in the posterodorsal region of the prootic and posteriorly by the anterior body of the supraoccipital (Figure 22b,c). The posterior edge of the posterior semicircular canal is comparably steep and nearly as tall as the anterior canal (Figure 22b). The posterior semicircular canal passes through the posterior portion of the supraoccipital and the dorsal portion of the otoccipital and merges with the anterior semicircular canal posterior to the midpoint of the lateral semicircular canal. The lateral semicircular canal does not extend laterally past the ventral origins of the anterior and posterior semicircular canals. The lateral semicircular canal is positioned just dorsomedially to the fenestra ovalis and extends from the ventral body of the prootic posteriorly through the anterior otoccipital. Whereas the length and orientation of the lagena in *Junggarsuchus* are similar to extant crocodylians, the semicircular canals of *Junggarsuchus* differ. The anterior and posterior semicircular canals are more steeply inclined and taller relative to the height of the endosseous labyrinth than those seen in *Alligator mississippiensis*, *Crocodylus novaeguineae*, *Tomistima schlegelii*, and *Gavialis gangeticus* and the lateral semicircular canals do not project as far laterally in *Junggarsuchus* as they do in extant crocodylians (Kuzmin et al., 2021). The orientation and height of the anterior canal in *Osteolaemus tetraspis* are similar to that seen in *Junggarsuchus*, but the posterior semicircular canal is much shorter and the body of the endosseous labyrinth is greatly expanded (Kuzmin et al., 2021). The nature of the semicircular canals in *Dibothrosuchus* cannot be described due to the condition of the scan.

Both of the prootics in *Junggarsuchus* preserve the path of the temporo-orbital artery through the body of the prootic (Figure 16). On the medial half of the prootic's anterior surface, there is a small foramen. This foramen continues as a circular canal and moves laterally and proceeds posteriorly. This canal continues through the body of the prootic, slightly posteromedially from the midpoint of the prootic until it opens dorsally so that the

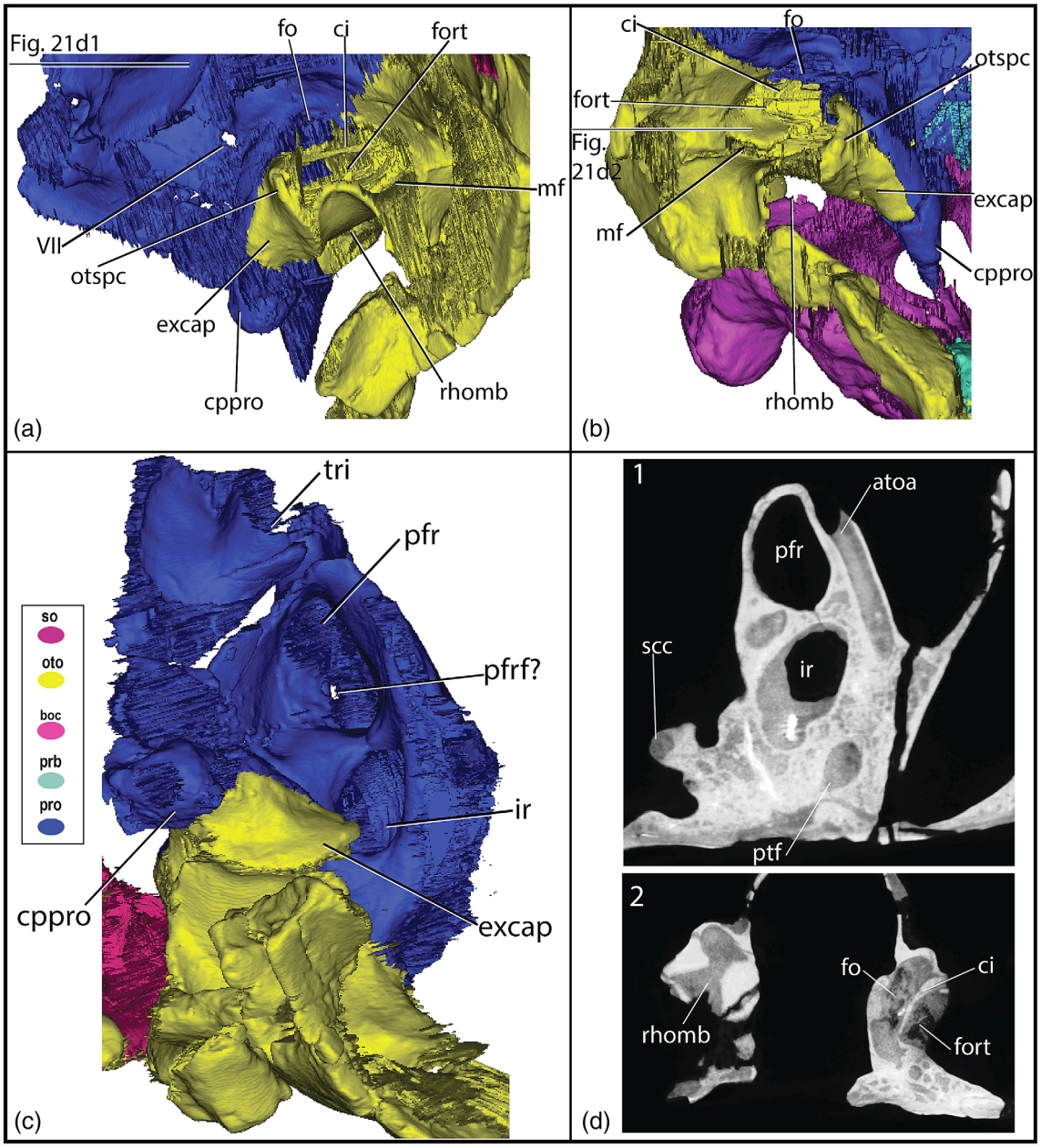

FIGURE 21 Ear region of *Junggarsuchus*. (a) Ear region in left lateral view; (b) right lateral view; (c) left prootic in ventral view; (d) series of dorso-ventral cross section from CT file of the right prootic, top image dorsal to bottom

artery would not have been fully enclosed along the lateral posterdorsal region of the prootic. The canal then continues through the anterior temporal foramen between the quadrate and prootic (with a ventral branch exiting through the postquadrate fenestra) until it exits posteriorly through the posttemporal fenestra, between the parietal, squamosal, and otoccipital. This enclosed temporoorbital artery canal differs from the condition observed in extant crocodylians, where the anterior portion of the temporo-orbital artery is not enclosed and instead rests along the ventromedial edge of the lateral rim of the supratemporal fossa before descending anteroventrally (Kuzmin et al., 2021; Porter et al., 2016). Birds are also known to have enclosed temporo-orbital artery canals, though they are not directly comparable to *Junggarsuchus*, in which the canals are partially enclosed and follow a different route through the bone (Sedlmayr, 2002).

The dorsoventrally expanded prootic of *Dibothrosuchus*, with large internal recessed spaces, is unique among non-crocodyliform crocodylomorphs. The prootic is bulbous and dorsally convex and contributes to 50% of the anteroposterior length of the supratemporal fossa (Figure 25b,d). The condition of the prootic is

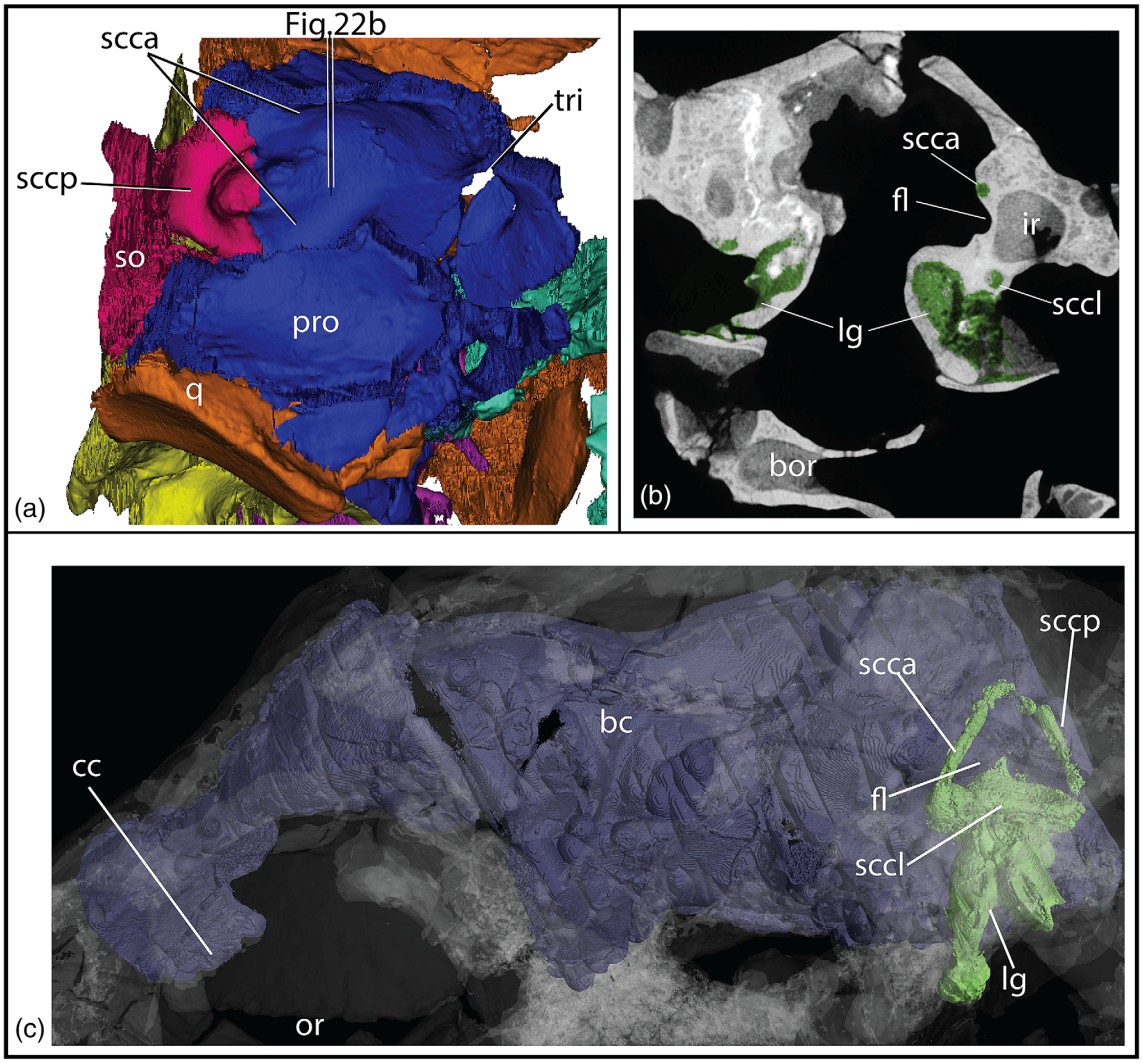

FIGURE 22 The prootic, otoccipital and supraoccipital of *Junggarsuchus sloani*; (a) in dorsomedial view; (b) reconstruction of the left semicircular canals and braincase of *Junggarsuchus sloani* in lateral view; (c) cross section of the semicircular canals in anterior view

dissimilar to any living crocodiylian, but in *Alligator mississippiensis*, the basicranium and prootics are invaded by diverticulae of the paratympanic sinus (Dufeau & Witmer, 2015) and so we interpret this dorsal expansion of the prootic as a pneumatic feature. The prootic is far more pneumatic than observed in other crocodylomorphs and the pneumatic spaces are divided into three regions by thin sheets of bone that expand dorsolaterally from the front of the expanded region to the midsection and posterior region. The prootic forms the ventral border of the foramen for the temporo-orbital artery, as seen in other crocodylomorphs (Walker, 1990). The exit of cranial nerve VII and the fenestra ovalis is exposed on the lateral surface of the prootic (Figures 25a and 26). The prootic encloses the postquadrate foramen posteriorly (Figure 16c) and medially, which is larger in *Dibothrosuchus* than the oval recess in *Junggarsuchus*. The anterior most enlarged aspect of the prootic is interpreted here as corresponding to the opening for the prootic facial recess. On the right side, an opening appears present, though this may be due to the incomplete nature of the prootic. On the left side, this enlarged region is floored for by a thin sheet of bone, though a narrow slit oriented lateromedially bisects this region of the bone (Figures 25a,c and 26). The intertympanic recess is about the same length and width as the posterior tympanic recess and is mediolaterally wider than the prootic facial recess and is far wider mediolaterally than the openings in *Junggarsuchus*. The intertympanic recess in *Dibothrosuchus* is divided along the midline by a thin sheet of bone like *Almadasuchus* (Leardi et al., 2020), but unlike *Junggarsuchus*. The posterior tympanic recess is anteriorly bounded by the prootic but posteriorly bounded by the otoccipital. The depression for this recess is similar to *Macelognathus* and *Protosuchus haughtoni* (BP/1/4770), in that it deeply penetrates the otoccipital

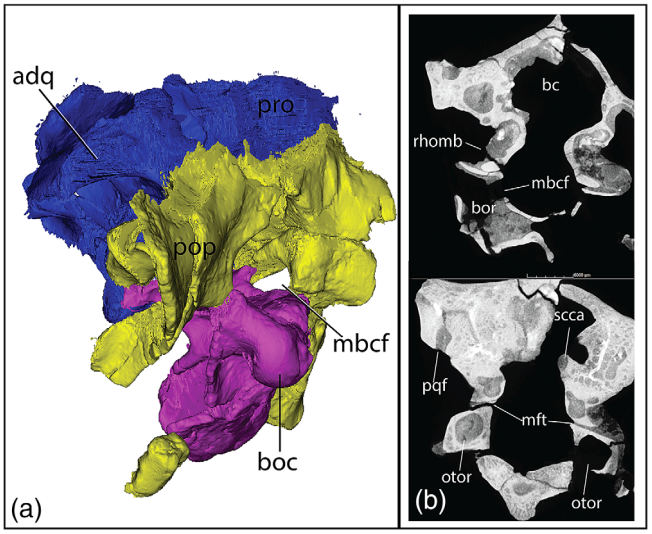

FIGURE 23 (a) The occiput of *Junggarsuchus sloani* in posteromedial view; (b) CT cross section of posterior braincase anterior image the top, showing the metotic foramen and the bottom image showing the medial braincase opening.

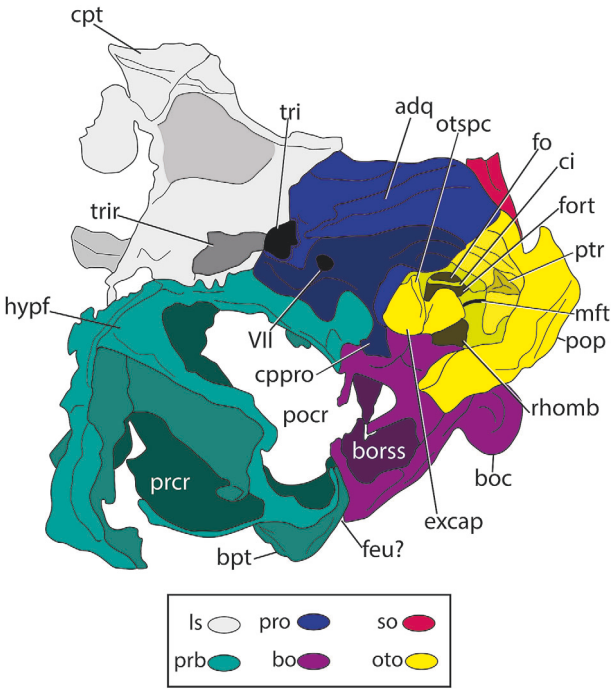

FIGURE 24 A line drawing of the braincase of *Junggarsuchus sloani* in left lateral view, detailing the anatomy of the inner ear, cranial nerves, and paratympanic sinuses.

and prootic, unlike the condition in *Junggarsuchus*, *Almadasuchus* (Leardi et al., 2020) and other non-crocodyliform crocodylomorphs. The prootic is anteroposteriorly longer than in *Junggarsuchus* and has a robust lateral lamina of the prootic, a ventrally descending pillar of the prootic that contacts the lateral surface of the laterosphenoid and posterodorsal edge of the parabasisphenoid similar to that found in *Junggarsuchus* (Figures 25a,c and 26). The endocranial pneumaticity in *Junggarsuchus* is extensive laterally and ventrally, though diverticulae do not extend dorsal to the braincase as in Crocodyliformes. In contrast, *Dibothrosuchus* has highly pneumatized prootics, the dorsal edge of which nearly reaches the level of the dorsal edge of the parietal. This dorsal reach of pneumatic space is unknown in other non-crocodyliform crocodylomorphs. *Dibothrosuchus* lacks pneumatic diverticulae in the parietal and quadrate. These dorsally expanded diverticulae are known in crocodyliforms (Dufeau & Witmer, 2015).

The **laterosphenoid** of *Junggarsuchus* is incompletely preserved ventral to the parietal and frontal within the supratemporal fenestra (Figures 9b and 17a,b). The right element is more complete but is fragmented. As preserved, it is a largely flat, vertical bone that makes up the anterolateral sidewall of the braincase. Few features are evident, other than a round, undivided trigeminal opening posteriorly and the capitate process anterodorsolaterally, visible within the orbit. A ribbon of bone extends anteroventrally from the anterior end of the laterosphenoid on the left side lateral to the **hypophyseal fossa** (Figures 17a–c and 18a,b), extending farther ventrally than is usual for this bone. There is a small anteriorly directed opening on the posteroventral process of the bone, similar to those seen in *Macelognathus* (Leardi et al., 2017). On the right side, the anterior process of the laterosphenoid has a ventrolaterally directed foramen, interpreted as the exit for cranial nerve IV (Figure 19b). We do not find evidence of an epipterygoid (Holliday & Witmer, 2009). The laterosphenoids may meet anteroventrally, but due the missing anterior region, we cannot confidently identify any medial contact between the laterosphenoids. The lack of the anterior portion of the laterosphenoid also does not allow for inference of the anterior extent of the dural envelope chamber. In *Junggarsuchus*, the laterosphenoid extends anterior to the postorbital frontal suture, farther anterior than seen in *Dibothrosuchus*, though the rest of the braincase is relatively shorter. The laterosphenoid and prootic meet in a posteroventrally trending contact on the braincases lateral surface. The trigeminal foramen is enclosed between these two bones and is directed anterolaterally. Around the trigeminal foramen is a recessed space divided between the prootic and laterosphenoid that is likely the trigeminal recess reported in *Dibothrosuchus* and *Almadasuchus* (Figure 17a,b) (Leardi et al., 2020). Similar to the condition in *Almadasuchus* and unlike the condition in other non-crocodyliform crocodylomorphs such as *Dibothrosuchus* (Leardi et al., 2020), the trigeminal recess of *Junggarsuchus* extends anteriorly and

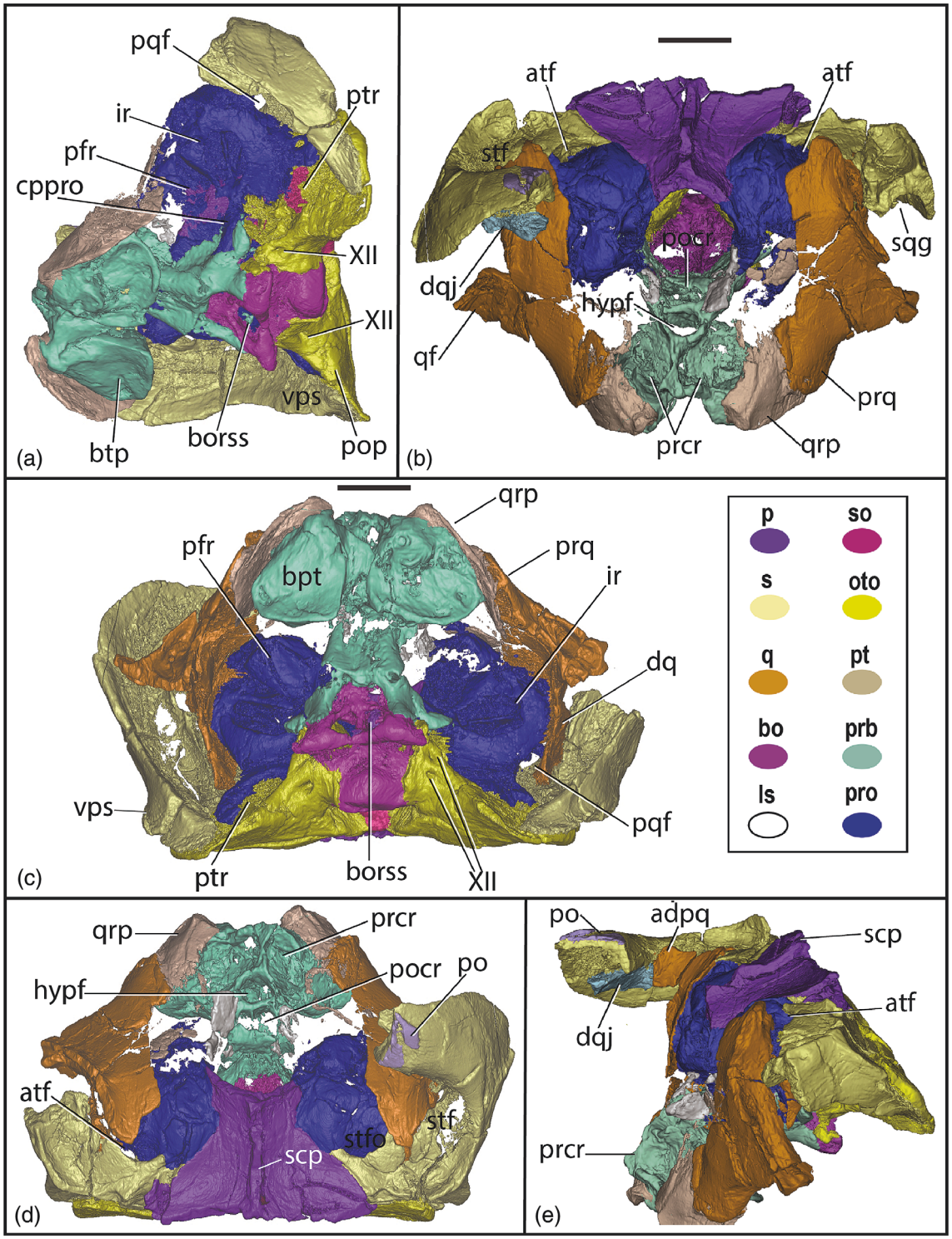

FIGURE 25 *Dibothrosuchus elaphros* braincase and ear region in (a) left ventrolateral view; (b) anterior view; (c) ventral view; (d) dorsal view; (e) braincase and skull roof in left lateral view; scale bar is 1 cm in (e).

ventrally as an elongate ventrally open fossa. This recess excavates a ventrally open fossa that reaches the mid height of the laterosphenoid and runs for over two-third the bones length, positioned anterior to the trigeminal foramen (Figure 17a,b,f). The ventral fossa of the trigeminal recess may be the dorsal border of a space that continues into the body of the parabasisphenoid, though fractures indicate the dorsal region of the parabasisphenoid in this region is broken (Figure 17f,g). At one point along the laterosphenoid–parabasisphenoid

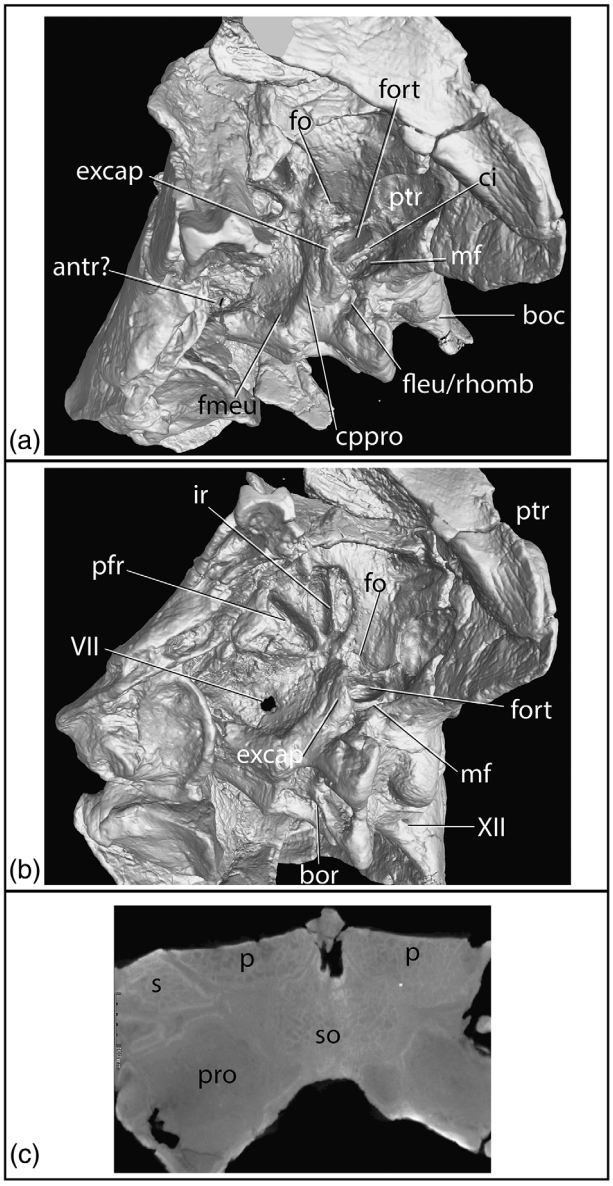

FIGURE 26 *Dibothrosuchus elaphros* braincase and ear as an isosurface render in VG studio with higher density sampling in (a) left lateroventral and (b) left ventrolateral view; (c) anteroposterior CT cross section of the supraoccipital demonstrating lack of communication

contact, there is an interdigitated suture anterior to a small ovate foramen which we identify as the anterior exit for the orbital artery, based on the position of the anterior exit for this artery in *Alligator mississippiensis* (Porter et al., 2016) (Figure 19f). A similar foramen between the laterosphenoid and parabasisphenoid has been reported in *Almadasuchus* (Leardi et al., 2020).

The laterosphenoids of *Dibothrosuchus* are better preserved in the specimen than is observed in the CT scans due to the low contrast of the posterior section of the rostral scan. The laterosphenoids are long and extends anterodorsally, though in CT scans, the posterior walls of the laterosphenoids are poorly preserved. The laterosphenoid is better preserved anteriorly and the capitate process projects dorsally and contacts the postorbital (Figures 5 and 10b). The laterosphenoids meet ventrally and forms the anterior portion of the ventral surface of the braincase, which is not preserved in *Junggarsuchus*. The long laterosphenoid in *Dibothrosuchus* meets the postorbital at the postorbital-frontal suture. The laterosphenoid is also longer posteriorly, where the descending process of the prootic contacts the posterior end of the laterosphenoid. The anterior border of the trigeminal nerve foramina is circular, as in *Junggarsuchus*, but different from the bilobate opening of *Sphenosuchus* (Walker, 1990). Unlike *Junggarsuchus* and other non-crocodyliform crocodylomorphs, Wu and Chatterjee (1993) describe the exit for the trigeminal in *Dibothrosuchus* as enclosed by the laterosphenoid. Unfortunately, the resolution of our CT data for the braincase does not allow us to confidently identify the bone comprising the posterior border of the foramen. The trigeminal recess consists of the most dorsal opening in the laterosphenoid and is larger and complex. The anterior end bifurcates in a T-shape and the dorsal cavity opens into the pharyngotympanic cavity. The trigeminal recess has been considered an autapomorphy of *Dibothrosuchus* but is also present in *Almadasuchus*, *Kayentasuchus*, *Maceloganthus*, and *Junggarsuchus* (Clark & Sues, 2002; Leardi et al., 2017, 2020).

The paired **vomers** of *Junggarsuchus* extend along the midline from the palatal shelves of the maxilla, anterior to the pterygoids (Figures 3b and 11b,d). The vomers divide the elongate choanae, and the vomers are rod-like in cross section between the anterior half of the choanae. The anterior portion of the vomer sits on the dorsal side of the posterior extent of the palatal portion of the maxilla. The vomer expands posteriorly into a rhomboid shelf in dorsal view and contacts the anteromedial edges of the palatines. The expanded portion of the vomer is separated along the midline by a tall ventral septum. There are deep anteroposteriorly elongate grooves along the ventral surface of the expanded processes of the vomers lateral to the midline septum. This central bony wall is ventrally taller than the septum seen in *Dibothrosuchus*. The dorsal side of the expanded region of the vomer is a smooth surface that slopes gently ventrolaterally. The dorsal midline of the vomer's posterior half is marked by a deep groove that trends nearly the entire length of the bone in which the anterior processes of the pterygoids would have articulated (Figure 11d). The vomers rise slightly around the lateral margins of this canal. The same structure is seen in *Dibothrosuchus* and houses a narrow anterior process of the pterygoids. It is likely that

a similar process of the pterygoid existed in *Junggarsuchus* but was not preserved. A part of the vomer rod has accidentally been placed by preparators as part of the palatine rods (Figure 11c), but as it is a paired element, and contains paired pterygoids within them, these elements are not part of the right palatine.

The vomers of *Dibothrosuchus* are similarly paired, rod-like bones that divide the choana and expand to contact the medial edges of the palatines (Figure 11e). In *Dibothrosuchus*, the vomer is not as well preserved and is missing the anterior portion dorsal to the palatal shelves of the maxilla. However, the contact with the pterygoid is preserved. The pterygoid extends as a thin anterior process in the dorsal groove between the two vomers, as seen in *Junggarsuchus*. Relative to the width of the palate and skull, the mediolaterally expanded region of the vomer of *Dibothrosuchus* is only half the anteroposteriorly length of the vomer and smaller than that of *Junggarsuchus* where the mediolaterally expanded region comprises over 60% of the element's length. The ventral septum along the midline is also far less ventrally expanded than the one in *Junggarsuchus*, and the depressions on the ventral surface of the vomer of *Dibothrosuchus* are faint. The portion that separates the choana is taller and less rod like than that of *Junggarsuchus*.

The dorsal surface of the **palatine** of *Junggarsuchus* is visible through the antorbital fenestra, indicating that it may have been displaced dorsally (Figures 3b and 4b). The medial part of its dorsal surface is convex and smooth and, as in *Sphenosuchus* (Walker, 1990), there are no apparent depressions or pockets in the dorsal surface. If present, any midline contact between the palatines is not preserved, although they come close to contacting each other. In ventral view, the palatine is triangular, expanding posterolaterally, where it borders the ventral edge of the expanded portion of the vomer (Figure 11a,c). The body of the palatine is ventrally concave, forming, with the vomer, a longitudinal depression roofing a broad passage medial to the posterior end of the choana. The depression is divided along the midline by a longitudinal septum formed at least partly by the vomers. The septum is separated from the palatine by a longitudinal crack or suture, suggesting it is formed mainly by an anterior projection of pterygoid that projects into a groove on the dorsal surface of the vomer. Laterally, the palatine narrows as it reaches the maxilla. The anterior edge of the palatine is expanded ventrally where it forms the posterior end of the choana, separating the choana from the depression. This expansion forms the anterior edge of a pocket on the ventral surface of the palatine that is continuous anteromedially with the depression. This pocket corresponds in position to a small opening on the palatine of *Dibothrosuchus* (Wu & Chatterjee, 1993, figure 2b) and *Sphenosuchus* (Walker, 1990, figures 3a and 10b). Anterior to the posterior end of the choana, the palatine descends ventrally to separate the choana and the medial depression. The medial section of the left posterior bar of the palatine has been mistakenly moved into the space between the two palatine bars, where it contacts the anterior process of the pterygoid (Figure 11a,c).

Posteriorly, the palatine is damaged, and its contacts with the pterygoid are unclear. A strut is preserved on each side extending posteriorly from the maxillary contact to the preserved portions of the pterygoid. A fragment of bone medial to the level of the ectopterygoid on the right side may be the posterior end of the palatine. As preserved, the palatine is separated from most of the pterygoid to form an elongate fenestra paralleling the suborbital fenestra, but this unusual feature may be due to damage to the palatine. However, some parts of the palatine have finished surfaces, and this additional medial fenestra may be real (Figure 11c). The palatine forms the medial and anterior borders of the suborbital fenestra, but its precise contribution to the medial edge is not clear. The contact with the pterygoid near the midline is also obscured, and the pterygoid may contribute to the midline septum. Laterally, the palatine extends posteriorly along the lateral border of the suborbital fenestra to the fenestra's midpoint and extends dorsally to contact the jugal and lacrimal where they contact. An elongate, slender, anterior maxillary process of the palatine extends along the medial surface of the maxilla, to opposite the sixth maxillary tooth.

The palatines of *Dibothrosuchus* are more completely preserved and less dorsally arched than those in *Junggarsuchus* (Figure 11e). A thin portion of bone overlaps the dorsolateral surface of the vomer, but the dorsal contact of the palatines is not preserved. Like in *Junggarsuchus*, the ventral surface of the anteromedial surface of the palatine has a concavity posterior to the choana, though it is shallower than the depression seen in *Junggarsuchus*. Anteriorly, the lateral surface of the palatines extends a long way along the medial surface of the maxilla to the ninth maxillary tooth. The extent of the lateral posterior process cannot be determined as the posterior most portion of this process is broken. The palatines are separated ventrally by an anterior projection of the pterygoid. The palatines narrow posteriorly on either side of the posteriorly expanding pterygoid. No additional palatal fenestrae are preserved medial to the sub orbital fenestra, though laterally the palatines have a concavity on the medial border of the suborbital fenestra. This is similar to the rod-shaped posterior process of the palatines seen in *Junggarsuchus* and suggests that existing medial border of the suborbital fenestra in *Junggarsuchus*

is accurate, but that what has been interpreted as an additional palatal fenestra may actually be covered by a thin sheet of the palatine that extended from the lateral edge of the anterior process of the pterygoid to the preserved ridge like processes of the palatines. The palatines form the medial and the posterior portions of the medial and lateral borders of the choana.

The **pterygoid** is poorly preserved in *Junggarsuchus*, though its remains suggest that it may have had an unusually broad, long quadrate ramus compared to other non-crocodyliform crocodylomorphs. Although we have reconstructed the medially expanded pneumatic complex lateral to the parabasisphenoid as mostly the quadrate, a series of breaks in the anterior part or possible sutures suggest that the quadrate ramus of the pterygoid may contribute to some part of this complex. In this interpretation, the posterior part extends posteriorly to just dorsal to the quadrate's mandibular condyles, where it is firmly attached to the quadrate, like in crocodyliforms, and to the ventrolateral end of the otoccipital which is a condition unique to *Junggarsuchus* among crocodylomorphs (Figures 11e and 15f). This piece of bone posterior to the medial edge of the quadrate condyle is not the pterygoid or quadrate but a dorsolateral fragment of the otoccipital (Figure 12b). This portion of the ramus or medially expanded quadrate forms part of the lateral edge of the cavity of the parabasisphenoid, which is thin and anteroventrolaterally complex. The articular surface for the basipterygoid process is not preserved, though a small thin fragment of bone is preserved on the anterolateral surface of the right side of the parabasisphenoid in right anterolateral view (Figures 17d and 18b, c). This rectangular posteroventrally oriented piece of bone likely represents an expanded region of the pterygoid that articulates with the parabasisphenoid and may have been part of a mediolaterally expansive quadrate ramus of the pterygoid similar to that observed in *Dibothrosuchus* (Figure 24b). This inference is supported as this bone fragment overlaps the anterolateral surface of the parabasisphenoid and is positioned posterior to the preserved pterygoids transverse process's articulation with the ectopterygoids. Unfortunately, distortion has obscured further interpretations as cracks and sutures become difficult to distinguish. This preserved fragment of the anterior part of the quadrate ramus of the pterygoid indicates that this portion was also dorsoventrally broad, and contributed to the anterolateral wall of the parabasisphenoid pneumatic space. The transverse flanges of the pterygoids are both preserved separate from the main body of the pterygoid, adhering to the mandible laterally and with the posterior edge of the ectopterygoid, and are rectangular and lack any large recessed spaces internally. The flange is oriented sub-vertically as preserved, and is inclined slightly anteroventrally, less than 20°. Posteriorly on the palatal midline, the pterygoids are poorly preserved, and the quadrate ramus of the pterygoid ventrally form a gently concave plate (Figure 11c). They continue anteriorly along the midline as a long, slender process, and the smooth lateral surface of this process supports the interpretation that the fenestra lateral to them is not an artifact. However, the bone is thin here and may have been broken, and if not, this would be the only non-crocodyliform crocodylomorph known to have this accessory palatal fenestra. The midline process rises anteriorly where it meets the palatine, and is dorsal in position to the rod formed by the pterygoid and palatine laterally. The ventral surface of this midline anterior process has a small ventrally directed notch. The anterior extent of the pterygoid is unclear, but it may contribute to the midline septum between the palatine bodies, although there is a gap between the posterior end of the septum and the midline process of the pterygoid. Anterolaterally, the pterygoid extends along a rod-like structure formed with the palatine, but its extent is limited to the posterior one-fourth of the palatine rods. Posterior to the concave midline portion, two pieces of the pterygoid are preserved ventrolateral to the portion discussed above (Figure 6a). The portion on the right side is more completely preserved and is ventrally and anteriorly convex.

The pterygoid is more completely preserved in *Dibothrosuchus* than it is in *Junggarsuchus* (Figure 11e). The pterygoid expands posteriorly, from a narrow anterior process that begins in the posterior groove in the vomers, widens gradually between the palatines, then widens laterally into the transverse flanges of the pterygoid. The lateral edges of the pterygoid articulate with the ectopterygoids. No evidence for an additional medial fenestra in the palate is preserved. Along the anterodorsal midline surface of the pterygoid, there is a shallow groove that expands posteriorly, and the ridges curve laterally along the transverse flange. The quadrate ramus ascends along the posteromedial edge of the quadrate, with which it forms a joint and contacts the anterior end of the parabasisphenoid, overlapping part of the basipterygoid process (Figure 11e). It approaches the prootic dorsally. The ascending process of the pterygoid is dorsoventrally taller than in other non-crocodyliform crocodylomorphs such as *Sphenosuchus* (Wu & Chatterjee, 1993).

The pterygoid of *Dibothrosuchus* differs from the pterygoid of *Junggarsuchus*. It features broader pterygoid transverse flanges and a dorsally tall quadrate ramus of the pterygoid. The ramus does not extend as far posteriorly as may occur in *Junggarsuchus* and lacks the pneumatic medial expansion of what may be the pterygoid, or more likely the quadrate, seen in *Junggarsuchus* (Figure 15). The posterior projections of the pterygoid

between the parabasisphenoid and quadrate are also seen in *Sphenosuchus* (Walker, 1990) and some thalattosuchians like *Pelagosaurus*.

The small **ectopterygoid** of *Junggarsuchus* is completely preserved on both sides.

It contacts the jugal along the longitudinal ridge on the medial surface of the jugal ventral to the orbit (Figure 11c). The anterior process is long and expanded, similar to the anterior processes of *Protosuchus haughtoni* (BP/1/4770) (Gow, 2000) and other early crocodyliforms such as *Gobiosuchus* (Osmólska et al., 1997) and *Fruitachampsa* (Clark, 2011). In dorsal view, the lateral portion of the ectopterygoid is triangular, with a lateral base, and the base extends further anteriorly than posteriorly. The ectopterygoid narrows medially and twists to face posteromedially as it proceeds ventrally to the posterior surface of the transverse flange of the pterygoid. The medial portion is also triangular in ventral view. The ectopterygoid covers the dorsal third of the posterior surface of the pterygoid flange and sends a short process onto the lateral surface of the flange.

The ectopterygoids of *Dibothrosuchus* are relatively larger than those of *Junggarsuchus*, though only the right one is more completely preserved (Figures 10b and 11c). The posterior portion of the ectopterygoid contacts the lateral third of the ventral edge of the transverse flange of the pterygoid. Like *Junggarsuchus*, the anterior process that contacts the medial edge of the jugal is longer than the posterior process, but in *Dibothrosuchus*, the anterior processes are reduced in size relative to the posterior portion of the ectopterygoid. The angle of contact between the ectopterygoid and pterygoid in *Dibothrosuchus* is less steep, at 35° (Wu & Chatterjee, 1993) than the near vertical contact between the ectopterygoid and pterygoid flange of *Junggarsuchus*. Whereas the anterior end arches dorsally similar to *Sphenosuchus* and *Junggarsuchus*, the posterior end's contact with the pterygoid demonstrates a condition not seen in other non-crocodyliform crocodylomorphs; a dorsal process of the ectopterygoid overlays a brief portion of the pterygoid laterally, and the main, elongate posterior process of the ectopterygoid underlays the same transverse process. In *Junggarsuchus*, the contact does not underlie the pterygoid in the same way.

Portions of seven thin **scleral ossicles** were preserved within the right orbit and later removed. These ossicles are small, squared bones, which partially overlap one another, mentioned briefly by Nesbitt et al. (2013). They appear to be from the ventral part of the series, and they curve anterodorsally, originally extending from the back of the orbit to the ventrolateral edge of the descending process of the prefrontal.

No scleral ossicles are known from *Dibothrosuchus*.

4.1.3 | Mandible

In *Junggarsuchus*, the **dentary** is a long, relatively mediolaterally thick, bone that makes up the anterior two-thirds of the mandibular ramus (Figure 27a–c). Nearly all of its medial surface is overlain by the splenial. Posteriorly, it extends approximately to the midpoint of the orbit when in articulation, where it splits dorsally and ventrally forming parts of the borders of the mandibular fenestra. The posterodorsal process tapers as it contributes to the anterodorsal border of the mandibular fenestra and underlies the anterodorsal process of the surangular on an anteroventrally sloping lateral suture, eventually ending at the posterior margin of the mandibular fenestra, as indicated by a fragment of dentary adhering to the surangular in this region (Figure 27a). This posterodorsal process is three times the length of the posteroventral process. The posteroventral process is broken but appears to be very short and contributes little to the ventral border of the mandibular fenestra. Anteriorly, the dentaries meet at the symphysis that extends medial to the fifth dentary tooth, opposite the third maxillary tooth. The symphyseal region faces anteroventrally and is not as flattened as in *Macelognathus*. Small nutrient foramina are present on the lateral surface of the anterior half of the dentary but not the posterior half, about midway on its lateral surface. The ventral surface of the anterior portion of the mandible is moderately pitted. In the anterior fourth of both dentaries, two elongate pathways are preserved trending through the ventral body of portion the dentaries (Figure 6c,d). The dorsoventrally taller passageway is circular in cross section and located lateral to the other passageway on both dentaries (Figure 6c,d). These passageways are connected with each other at their midpoint. Along their dorsal edge, there are openings for possible additional branches. This passageway extends anteriorly from the anterior end of the Meckelian groove, ventral to the 10th dentary tooth, to the third dentary tooth where it exits from an elongate nutrient foramen laterally and opens medially into the alveoli for the fifth dentary tooth (Figure 6c). Living crocodylians, like *Alligator mississippiensis*, possess a passageway of similar diameter and lateral position that is for the mandibular branch of the trigeminal nerve (George & Holliday, 2013). Based upon the similar diameter, position and branching, we interpret this continuous space as the mandibular branch (V3) of the trigeminal nerve (Figure 6a,b). The narrower pathway is also circular in cross section and extends from a nutrient foramen at the anterior tip of the dentary to posterior to the position of the eighth dentary tooth at which the canal opens into the Meckelian groove (Figures 6a–d and 27a). This is a narrower passageway and medial to the third branch of

the trigeminal nerve of which it also extends anterior to. In living crocodylians, like *Alligator mississippiensis*, a similar space is for the pathway for the mandibular vein or artery (Porter et al., 2016). Based on the medial position, narrow diameter and close association with the space we assign to branch V3 of the trigeminal nerve, we infer that the mandibular vein and/or artery occupies this space in *Junggarsuchus*.

Most of the dentary teeth of *Junggarsuchus* are not exposed, but CT scans show 17 teeth in each dentary (Figure 27a,b). The teeth become dorsoventrally taller from the first dentary tooth to the fourth. The fourth dentary tooth projects into a pocket between the premaxilla and maxilla. The dentary is only slightly expanded ventral to the fourth tooth. The teeth posterior to the fourth tooth are half or less the height of the fourth tooth or less. Dentary teeth 5 through 13 are similar in size and teeth 14–17 are smaller than these. The anterior dentary teeth opposite the premaxillary teeth are conical and the dentary teeth opposite the maxillary teeth are recurved and labiolingually compressed. The anterior dentary teeth, exposed between the third and fifth right maxillary teeth, are serrated distally but not mesially, and the serrations are similar in size (one-third of a mm tall) to those on the maxillary teeth (Figure 4d). The dentary teeth are not enlarged ventral to the enlarged maxillary teeth, and the teeth exposed anteriorly on the right side are similar in size to the teeth in the middle of the maxillary tooth row. The posterior four dentary teeth (14–17) differ slightly in morphology from the anterior teeth; they are constricted at the base, with concavities on the mesial and distal edges of the tooth root (Figure 27e). These posterior dentary teeth are less recurved than the anterior ones. *Junggarsuchus* has serrations on the mesial and distal edges of both posterior maxillary and dentary teeth.

The dentary of *Dibothrosuchus* is nearly fully preserved, though it has been dorsoventrally crushed which has separated the dentaries at the symphysis (Figure 29a–c). The dentary symphysis extends to the fourth dentary tooth and is shorter than in *Junggarsuchus*. The dentary of *Dibothrosuchus* is slightly narrower and longer than *Junggarsuchus* in dorsal view. The posterodorsal and posteroventral processes of the dentary are not well preserved, but like *Junggarsuchus*, the posterodorsal process appears slightly longer, but the extent that it borders the mandibular fenestra is unclear, though the posterodorsal end is overlain by part of the anterodorsal process of the surangular. The ridge along the posterodorsal process, ventral to the surangular, is longer and more concave than *Junggarsuchus*. Like *Junggarsuchus*, the anteroventral portion of the bone is pitted and the lateral anterior dentaries have several foramina. Both pitting and foramina continue farther posteriorly and ventrally in *Dibothrosuchus*, reaching up to the 13th dentary tooth.

Each dentary of *Dibothrosuchus* has 16 teeth (Figure 29a,b). Like *Junggarsuchus*, the teeth increase in size posteriorly from the first to the fourth tooth, though the second tooth is nearly as tall as the fourth. The 5th to 14th teeth are half the height of the anterior dentary teeth and become less recurved farther posteriorly. Alveoli for two to three more teeth posterior to the teeth preserved are observed, but the teeth are not preserved. The constriction below the root of the posterior dentary teeth is not present in any anterior preserved teeth. Serrations are difficult to determine from CT data, though previous analysis have shown that the enlarged fourth tooth had distal serrations (Wu & Chatterjee, 1993).

In *Junggarsuchus*, the **splenial** lies medial to the dentary and makes up the medial surface of the mandible anterior to the mandibular fenestra (Figures 27c and 28a, b) and anterior border of the internal mandibular fenestra. It does not reach the mandibular symphysis anteriorly, ending about 2 mm posterior to it. Its anterior edge is forked, forming an opening for the mandibular portion of the V3 nerve, as seen in living crocodylians like *Alligator mississippiensis* (George & Holliday, 2013) (Figure 28a). Similar structures are known in *Dibothrosuchus* and *Sphenosuchus* (Walker, 1990). The suture between the splenial and the dentary is clearly visible along the ventral surface of the mandible, and the splenial forms the medial one-third of the ventral surface (Figure 27c). The medial surface of the splenial is flat and smooth. Posteroventrally, the splenial's contact with the angular is not well preserved, but the splenial apparently extended posteriorly to about midway beneath the mandibular fenestra. Posteriorly, the ventral extent of the splenial forks, for what may be the anterior opening of the inframeckelian fenestra (Figure 28a). Ventral to this there is an additional fork where the posterodorsal and posteroventral processes articulate with the angular. This fenestra is also reconstructed in *Dibothrosuchus* (Wu & Chatterjee, 1993) and *Sphenosuchus* (Walker, 1990).

Both splenials of *Dibothrosuchus* are preserved (Figure 28c,f), contributing to the anterior border of the internal mandibular fenestra, contacting the medial surface of the dentary and are widely similar in their ventral suture to the dentary and anterior extent to *Junggarsuchus*. Like *Junggarsuchus*, the splenial contributes to the medial wall of the mandibular fenestra. Though incomplete, it appears that posteriorly the splenial forks into a posterodorsal process and the longer posteroventral process, which contacts the medial edge of the angular more extensively than it does in *Junggarsuchus*. The posterior extent of the splenial has been reconstructed to have formed the anterior border

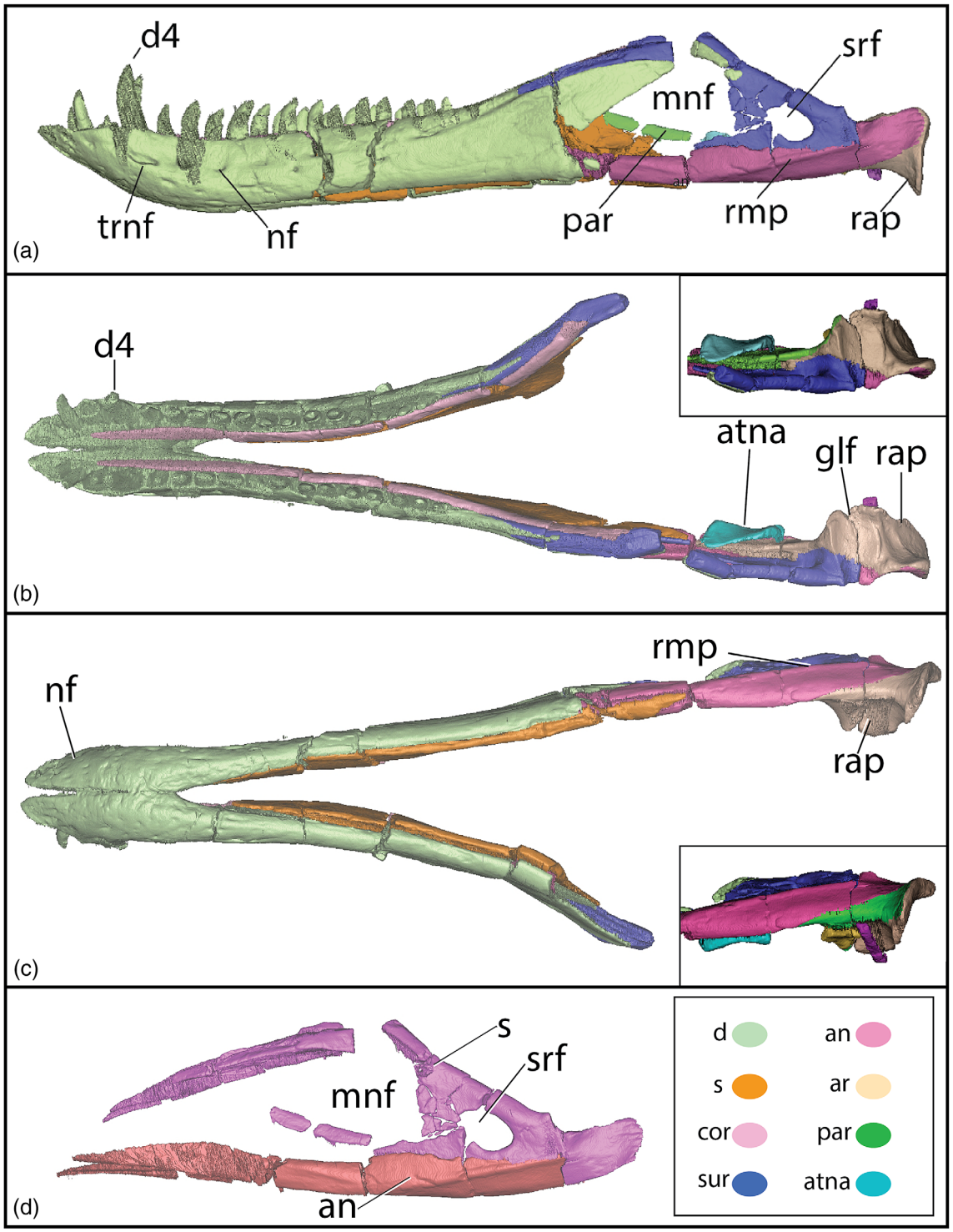

FIGURE 27 Mandible of *Junggarsuchus sloani* in (a) left lateral; (b) dorsal; (c) ventral view; (d) alternative interpretations of surangular in left lateral view; (e) and alternative surangular in left medial view; scale bar is equal to 1 cm.

for the inframeckelian fenestra, similar to that reconstructed in *Sphenosuchus* (Walker, 1990), in which the splenial forms the anterior borders and the prearticular forms the posterior border (Figure 29f). We support this interpretation based on our CT data. No anterior fork is preserved (Wu & Chatterjee, 1993).

The **coronoid** of *Junggarsuchus* is an elongate, but dorsoventrally low, bone that lies medial to the dorsal portion of the alveoli and dorsal to the splenial and is 70% of the mandible's length (Figures 27b and 28a,b). The coronoid extends from the second dentary tooth to the midpoint of the anterior dorsal process of the

surangular. It widens dorsoventrally around its midpoint, and posterior to this, it constricts faintly and then expands slightly, at the end of the dentary. The coronoid arches dorsally along with the dorsal process of the dentary. Laterally, it contacts the anterodorsal portion of the dentary anteriorly and the anterodorsal process of the surangular on its medial surface. The ventral edge of the coronoid contacts the splenial from the sixth dentary tooth to the end of the posterior bone. The posterior end of the left coronoid contacts a broken fragment of the splenial ventrally. A similar dorsoventrally tall plate of bone is not observed in the same posteriorly concave shape on the right side, so it is unlikely this is a ventral extension of the coronoid.

The coronoid of *Dibothrosuchus* was originally reported as a short crescentic bone (Wu & Chatterjee, 1993), but CT scans demonstrate the coronoid is a long, blade-shaped bone in medial view. In overall shape, the coronoids are similar to those of *Junggarsuchus*, though they are dorsoventrally shorter relative to the dentary (Figure 28c). In our review of coronoids in non-crocodyliform crocodylomorphs, we found that this condition is present beyond *Dibothrosuchus* and *Junggarsuchus*, appearing to be widespread among non-crocodyliform crocodylomorphs. In addition to *Dibothrosuchus* and *Junggarsuchus*, *Dromicosuchus* (Sues et al., 2003) and *Sphenosuchus* (Walker, 1990) are reported as having elongate coronoids and we report the presence of an elongate coronoid in the holotype of *Kayentasuchus walkeri* for the first time. In other non-crocodyliform crocodylomorphs the mandible is either not preserved, like *Macelognathus* and *Almadasuchus*, or the coronoids are not visible as in *Litargosuchus*, *Hesperosuchus* (AMNH FR 6758, CM 29894) (Clark et al., 2001) and *Pseudhesperosuchus* (Bonaparte, 1971). Only in *Terrestrisuchus* are the coronoids apparently genuinely short crescentic elements (Crush, 1984) as seen in early diverging crocodyliforms like *Protosuchus haughtoni* (BP/1/4770) (Gow, 2000) and *Orthosuchus* (Nash, 1975), though this identification could change as it is based on descriptions in the literature rather than firsthand observation. Elongate coronoids are also present in thalattosuchians like *Pelagosaurus typus*, *Cricosaurus* ("*Geosaurus*") *araucanensis* and *Dakosaurus andiniensis* (Pierce & Benton, 2006; Young & Andrade, 2009), but the morphology of the coronoids in thalattosuchians differs from that observed in non-crocodyliform crocodylomorphs as the coronoids do not often extend along the entire length of the dentary (often less than one-third the length of the dentary) and are more posteriorly positioned on the mandible (Young et al., 2012; Young & Andrade, 2009), though there are some exceptions in which the coronoids are slightly over one-third the length of the dentary (Sachs et al., 2019). Anteriorly, the coronoid contacts the splenial ventrally and the laterally contacts the medial side of the dentary, medial to the alveoli. The posterior portion of the coronoid contacts the anterodorsal process of the surangular. The coronoids do not arch dorsally, but bow out laterally, likely due to postmortem crushing. Much of the bone is obscured by crushing, which has moved the midsection deep to the splenial.

In *Junggarsuchus*, the **angular** is nearly fully preserved on the left side and only the anterior most portion is preserved on the right side (Figure 27a,c). In lateral view, it extends anteriorly to meet the dentary near the anterior end of the mandibular fenestra and proceeds anteriorly between the dentary and splenial to the 17th dentary tooth. The angular contacts the splenial medially, ventral to the mandibular fenestra. The dorsal surface of the angular is only slightly concave ventral to the mandibular fenestra. The posterior half of the angular does not expand dorsally and makes a longitudinal dorsal contact with the surangular at the level of the ventral edge of the mandibular fenestra. A distinct longitudinal ridge near the dorsal edge of its lateral surface begins anteriorly, ventral to the posterior end of the mandibular fenestra, and ends posteriorly ventral to the quadrate articulation. A similar ridge is seen in living crocodylians, like *Alligator mississippiensis*, in a similar position and serves as the insertion area for the *M. pterygoideus ventralis* (Holliday et al., 2013). We therefore interpret this marked dorsal edge in *Junggarsuchus* as the insertion area for the *M. pterygoideus ventralis* muscle (Clark, Xu, Forster, & Wang, 2004) (Figure 27a). This surface is seen in extinct mesoeucrocodylian crocodyliforms, like *Simosuchus* and *Shamosuchus*, but not in non-crocodyliform crocodylomorphs or most early crocodyliforms. The angular continues posteriorly to the end of the mandible, forming the dorsal part of the lateral surface of the retroarticular process, and contributes to the lateral edge of the glenoid fossa, a condition rarely seen in crocodylomorphs. Some crocodyliforms like *Protosuchus richardsoni* (UCMP 130860; AMNH 3024) have this posterior dorsoventral expansion of the angular. This posterior contribution may be in part from the surangular, but the sutures between the surangular and angular posteriorly are unclear due to a break in the articular. If it is part of the surangular then the angular does not reach the end of the mandible and terminates in a dorsoventrally tall posterior process, with a small medial extension on the medial portion of the bones lateral surface (Figure 27d). Medially, the angular is covered by the splenial and posteriorly by the prearticular (Figure 28a). The angular tapers in medial view on the ventral surface. Any contact with the prearticular is difficult to interpret.

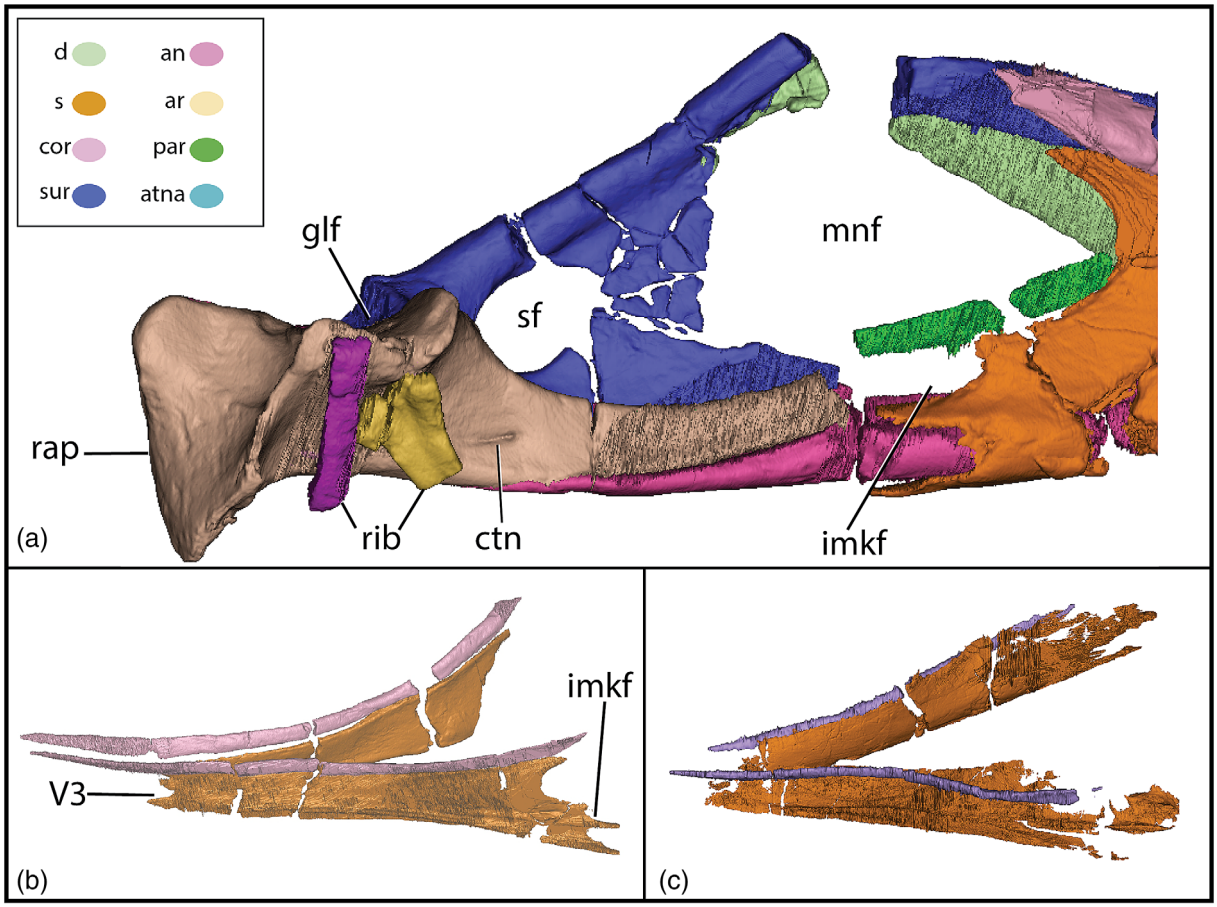

FIGURE 28 (a) Left mandible of *Junggarsuchus sloani* in posteromedial view; (b) coronoids and splenial of *Junggarsuchus sloani* in left dorsolateral view; (c) coronoids and splenials of *Dibothrosuchus elaphros* in left dorsolateral view; scale bar is equal to 1 cm.

Both angulars are nearly completely preserved in *Dibothrosuchus* (Figure 29a,c,d) and are longer and dorsoventrally shorter than in *Junggarsuchus*. The angular contacts the prearticular on the ventromedial contact. Unlike *Junggarsuchus*, the angular does not extend to the end of the mandible. Instead, it narrows into a short projection that arches slightly dorsally on the lateral surface of the surangular, which has a substantial ventral process. The angular also lacks the distinct ridge for the insertion of the *pterygoideus* muscles seen in *Junggarsuchus*. The angular forms the ventral border of the mandibular fenestra, but the exact size and shape of the fenestra are unclear due to the fragmentary nature of the posterior mandible. Wu and Chatterjee (1993) reconstructed the fenestra as a small circular fenestra, but the CT scans do not preserve the surangular and angular completely, which limits confident reconstruction of the size and shape of the mandibular fenestra.

The anterior process of the **surangular** laterally overlies the dentary dorsal to the mandibular fenestra (Figure 27a,b). On the lateral surface, the dentary separates the surangular from the dorsal edge of the fenestra, but the surangular forms the dorsal roof of the mandibular fenestra. Its anterior tip is narrow and gradually widens posteriorly dorsally to the fenestra. The main body of the remaining bone has a flat dorsal surface that faces posterodorsally. The surangular forms the entire posterior edge of the mandibular fenestra and at least the posterior most ventral border. The surangular likely contributed to the dorsal border of the inner mandibular fenestra, though this region is incompletely preserved. Of particular interest is a small fenestra near the posterior end of the surangular (Figures 3a, 4a, and 27a). The anterior edge of this opening is broken but otherwise the edges are smooth, and it is a natural feature. An enlarged surangular foramen does not appear in any other crocodylomorph, and they are completely absent in other non-crocodyliform crocodylomorphs like *Dibothrosuchus* and *Sphenosuchus* (Walker, 1990), but one is present in some theropod dinosaurs, specifically the Tyrannosauridae and Dromaeosauridae (Osborn & Brown, 1906; Ostrom, 1969). The posterior, ventral suture of the surangular to the angular is unclear. The surangular may end anterior to the potential dorsal projection of the angular onto the lateral surface of

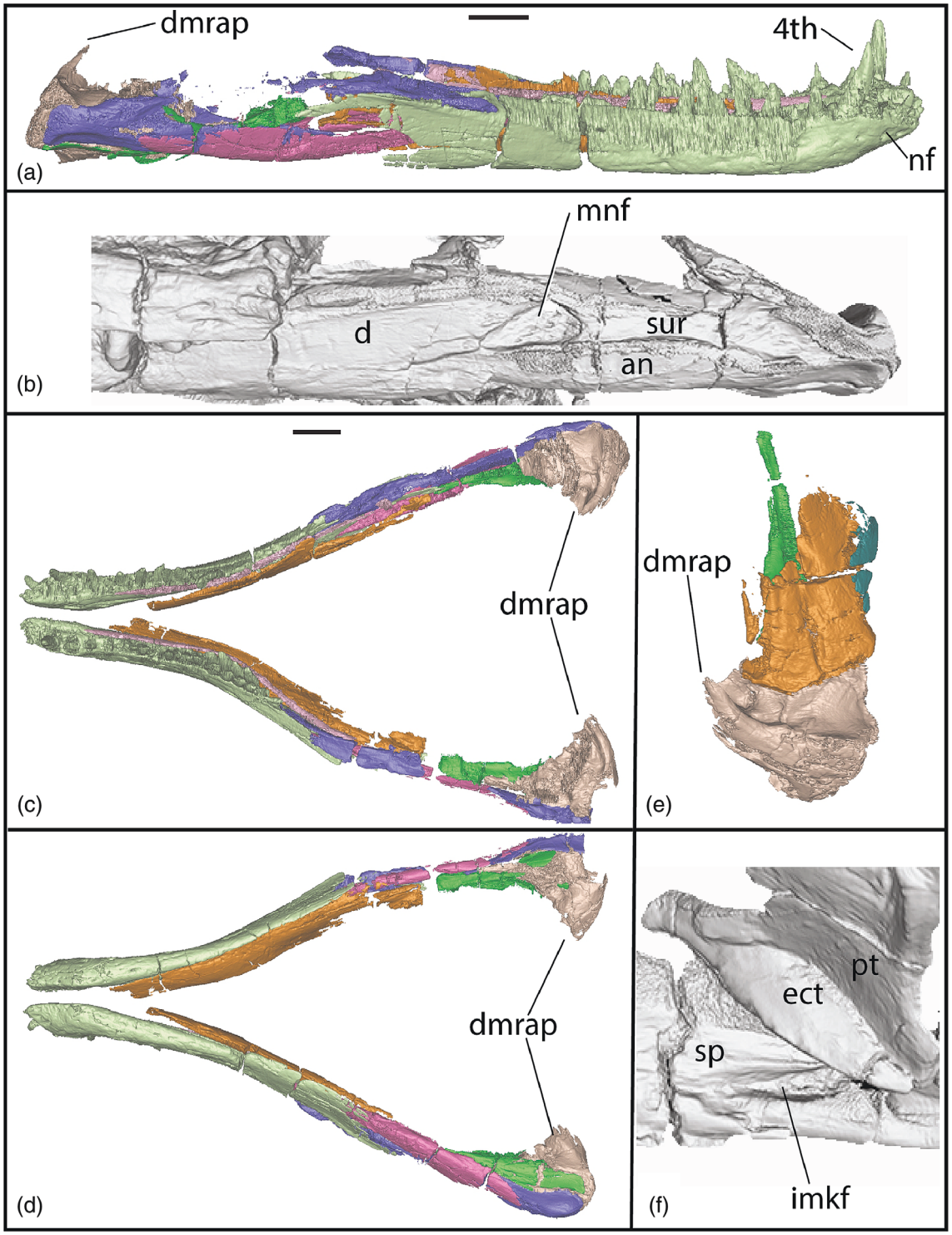

FIGURE 29 Mandible of *Dibothrosuchus* in (a) left lateral; (b) left lateral with isosurface render in VG studio to show external mandibular fenestra; (c) dorsal; (d) ventral view; (e) quadrate distal end (orange) contact with articular in dorsal view; (f) left posterior mandible in medial view; scale bar is equal to 1 cm.

the articular (Figure 27a). However, if the surangular forms this lateral cover of the articular and contributes to the lateral edge of the articular fossa, the angular ends with a dorsoventrally tall posterior edge (Figure 27d). If the latter is the case, this is similar to the condition of the surangular in *Dibothrosuchus* and *Sphenosuchus* (Figure 29d,e). CT scans suggest that the latter is more accurate, with an anteroposteriorly elongated surangular posteriorly. Unfortunately, even in CT scans, the suture interpreted here is not fully evident.

Both surangulars of *Dibothrosuchus* are preserved, and they contribute to the posterodorsal border of the external mandibular fenestra and the dorsal border of the internal mandibular fenestra. (Figures 3a and 29f). They are long narrow bones, lacking the dorsal arch seen in *Junggarsuchus*. Wu and Chatterjee (1993) report the mandibular fenestra as a short oval fenestra, which is dorsoventrally shorter than in *Junggarsuchus*. This is evident in observations of the specimen but not as clear in the CT data in which much of the midsection of the surangular is lost. Separate isosurface renders of the skull demonstrate this small opening as reported by Wu and Chatterjee (1993) (Figure 29b). The anterior process of the surangular, overlaying the posterior process of the dentary is broader than in *Junggarsuchus*. The posterior portion of the surangular differs from *Junggarsuchus*; *Dibothrosuchus* has a surangular that is dorsoventrally as tall as the mandible. The surangular extends ventrally along the medial surface of the angular and forms the ventral and posterior border of the medial surface of the mandibular fenestra, unlike in *Junggarsuchus*. The surangular covers the entire lateral surface of the articular and also expands slightly laterally as a ridge on the posterior end of the mandible. Ventral to this posterior ridge, the laterally expanded surface of the surangular is concave. The lateral posterior cover of the articular is longer in lateral view in *Dibothrosuchus* than any other non-crocodyliform crocodylomorphs, but is similar to *Sphenosuchus*. *Dibothrosuchus*, like all other non-crocodyliform crocodylomorphs except *Junggarsuchus*, lacks an enlarged surangular fenestra.

In *Junggarsuchus*, the **articular** is preserved on the left side as an anteroposteriorly short bone (one-seventh mandibular length in ventral view) that expands in its dorsoventral height posteriorly (Figure 27c). The element is visible in ventral, medial, dorsal, and lateral view. The quadrate articulation is anteroposteriorly short as in most crocodylomorphs including *Dibothrosuchus*. The articular is dorsoventrally taller on the medial portion of the anterior edge of the articulation surface than on the posterior edge. The articular covers the medial surface of the angular and the posterodorsal part of the surangular, but a displaced rib and neural spine cover the articular medially. Midway, along the ventral portion of the medial surface of the articular, there is a small groove that appears to open in a foramen, which may be for the chorda tympani nerve (Goodrich, 1915).

The condition of the retroarticular process in *Junggarsuchus*, preserved well on both sides, is unusual among early diverging crocodylomorphs (Figure 27b,c). Whereas in other non-crocodyliform crocodylomorphs, there is often a dorsomedial projection, as in *Dibothrosuchus*, or a posterior one, like in *Pseudhesperosuchus* (Bonaparte, 1971), the process in *Junggarsuchus* is ventrally directed. The retroarticular process has concave dorsal and posterior surfaces, for the insertion of the *M. depressor mandibulae*. This concavity gradually opens up posteroventrally. All of this surface is composed of the articular. The posterior edge is rimmed laterally by a vertical lip that extends outward from the main body of the articular. We interpret this as the posterior border of the insertion area for the *M. pterygoideus* based on the similar anatomy of the articular for this muscle in *Alligator mississippiensis* (Holliday et al., 2013). A triangular, lateral exposure of the articular anterior to this lip forms part of this insertion area ventral to the angular. The medial edge of the articular also forms a lip along the dorsomedial edge of the retroarticular process.

At the anteromedial end of the mandibular fenestra, an acute process inserts into the splenial and borders the ventral edge of the splenial; this process belongs to a **prearticular** if one is present covering the medial surface of the articular and it appears to contribute to the posterior borders of the inframeckelian fenestra (Figure 28a). CT scans suggest this narrow anterior process that runs along the dorsal side of the angular might be part of the articular, but identification of the prearticular remains indeterminate, even with CT scans. A very thin sheet of bone projects along the ventral end of the articular and appears continuous with the projection of bone dorsal to the angular which is interpreted as prearticular (Figure 28a). If this is the prearticular, the contact with the articular and angular is very similar to that in *Dibothrosuchus*, where the massive posterior part of the prearticular braces the articular and contributes to the articular fossa and the base of the articular (Figure 28e). It also appears to form the ventral border of an internal mandibular fenestra, though the incomplete preservation in this area makes it unclear (Figure 28e). Prearticulars, while absent in neosuchians, some notosuchians and early diverging crocodyliforms like *Gobiosuchus* (Osmólska et al., 1997), are known from most non-crocodyliform crocodylomorphs (with the exception of *Pseudhesperosuchus*) where the posterior portion of the mandible is preserved including *Hesperosuchus* (CM 29894) (Clark et al., 2001), *Dromicosuchus* (Sues et al., 2003), *Terrestrisuchus* (Crush, 1984), *Litargosuchus* (Clark & Sues, 2002), *Sphenosuchus* (Walker, 1990), and *Dibothrosuchus* as well as in early diverging crocodyliforms like *Protosuchus haughtoni* (BP/1/4770) (Gow, 2000), *Orthosuchus* Nash (1975) and thalattosuchians like *Pelagosaurus* (Pierce & Benton, 2006). In thalattosuchians like *Cricosaurus* ("*Geosaurus*") *araucanensis* (Young & Andrade, 2009); however, the prearticulars are short, triangular elements that do not reach the posterior edge of the mandibular fenestra (Andrews, 1913). Due to the widespread distribution of this bone, it is likely that the element medial to the articular is

the prearticular in *Junggarsuchus*. The issue is that it is difficult to identify any dorsal suture with the articular and so the prearticular is only hypothetically reconstructed in Figure 28a, as it may be fused with the articular. A thin rectangular wall of bone is located medial to the anterior process of the articular where the prearticular would have articulated. It is possible that this thin wall of bone may be part of the prearticular, but further investigation suggests this is a displaced neural spine of the atlas (Figure 28a) as the prearticulars of *Sphenosuchus* (Walker, 1990) and *Dibothrosuchus* are medially continuous with the angulars and in *Junggarsuchus* this element projects medially from the angular and possesses a substantial ventral groove along its entire length, suggesting it is an element foreign to the mandible.

The retroarticular process of the articular in *Dibothrosuchus* expands dorsomedially, unlike *Junggarsuchus* (Figure 29a,c,d,e). Like *Junggarsuchus*, there is an anterior process of the articular that extends toward the posterior end of the splenial. This may be a portion of the prearticular, the exact suture is not fully apparent due to some crushing. The ventral exposure of the articular is limited to the posterior end of the mandible, with much of the bone covered by the prearticular, surangular, and angular. Whether this condition is present in *Junggarsuchus* is unclear due to the uncertainty of the extent of the prearticular. No medial groove is preserved in *Dibothrosuchus*, though the foramen aerum is present on the dorsal surface of the posteromedial portion of the articular, unlike in *Junggarsuchus*. The articular fossa of *Dibothrosuchus* is mediolaterally wide and shorter dorsoventrally than in *Junggarsuchus*. The medial walls of the glenoid fossa are also lower in *Dibothrosuchus* than *Junggarsuchus*.

Both prearticulars of *Dibothrosuchus* are preserved, and the right prearticular is better preserved (Figure 29c, d,f). The bone extends anteriorly along the dorsal groove of the angular. The lateral and dorsal surface of the prearticular contact the anteriomedial surface of the articular. The prearticular contacts the ventral edge of the angular anteriorly and the surangular posteriorly and reaches the posterior end of the articular. The bone is thin and there may be more exposed on the left and right sides along the medial surface of the articular, but the sutures are not clear in our CT data. Overall, the contacts and general morphology of the prearticular are similar to the prearticulars of other non-crocodyliform crocodylomorphs, including *Sphenosuchus*. The prearticulars of *Sphenosuchus*, *Dibothrosuchus*, and *Dromicosuchus* are some of the better preserved and articulated prearticulars in non-crocodyliform crocodylomorphs and demonstrate a consistent morphology, where the prearticular is a long element on the medial face of the posterior mandible. In *Dibothrosuchus* and other non-crocodyliform crocodylomorphs, the prearticular forms the ventral and posterior border of the internal mandibular fenestra, contacting the splenial anteriorly, the angular on its anterolateral face, the surangular on its posterolateral face and the articular posteriorly (Sues et al., 2003; Walker, 1990; Wu & Chatterjee, 1993). The anterior process of the prearticular forks and forms the posterior border of the inframeckelian foramen (Figure 29f) and a similar foramen is also reported in *Sphenosuchus* (Walker, 1990).

4.1.4 | Pectoral girdle and forelimb

The **scapula** of *Junggarsuchus* is completely preserved on both sides of the skeleton but is only exposed on the left side. It is similar in overall shape to the scapula of other non-crocodyliform crocodylomorphs but is slightly broader and more triangular in lateral view, becoming more anteroventrally broad dorsally and is twice the anteroposterior length of the scapula near its contact with the coracoid (Figure 30a). The dorsal portion is much wider anteroposteriorly than the ventral portion, and is slightly constricted at its mid-height. The glenoid at the anteroventral edge of *Junggarsuchus* has no lateral component, unlike in living crocodylians like *Alligator mississippiensis*. It is directed ventrally and slightly posteriorly, if the scapula-coracoid articulation was horizontally oriented. This condition is seen in other non-crocodyliform crocodylomorphs like *Dromicosuchus* (Sues et al., 2003), *Dibothrosuchus* (Wu & Chatterjee, 1993), *Hesperosuchus* (CM 29894) (Clark et al., 2001), and *Terrestrisuchus* (Crush, 1984). This results in an unusual area for articulation with the humerus, leaving little space between the edge of the scapula and the coracoid (Figure 30b,c). In posterolateral view, the glenoid fossa comprises a circular concavity that accommodated the rounded head of the humerus.

The anterior edge of the proximal portion of the scapula is anteriorly convex in its ventral part, forming a rounded surface. In *Junggarsuchus*, the anterior edge of the scapula is more strongly concave than the posterior edge in lateral view (Figure 30a–c). This condition may also be present in *Dibothrosuchus* (Figure 30d), though the anterior edge of the scapula is broken (Wu & Chatterjee, 1993). In *Sphenosuchus*, the anterior and posterior edges of the scapular blades are both concave at their mid-height and the bone is anteroposteriorly narrower relative to *Junggarsuchus* (Walker, 1990). The anterior edge of the scapular blade of *Junggarsuchus* becomes anteriorly concave, continuing to the dorsal edge of the scapula. The most anterodorsal area of the

scapula is anteriorly convex, whereas the dorsal margin of the scapula is slightly concave. The dorsal edge is gently sinuous in lateral view, with a broad depression in the middle and an extended posterodorsal corner. The posterior margin does not curve, but there is a long, narrow ridge along the posterodorsal half of the margin. We interpret this as the anterior edge of the insertion area of the large *M. serratus ventralis thoracis* based on the insertion of this muscle observed in *Alligator mississippiensis* (Meers, 2003). The lateral surface of the scapular blade is mostly flat and smooth, with a low but distinct ridge near to and paralleling its anterior edge. We hypothesize that this would have served for the attachment of the *M. deltoideus scapularis*, or possibly the *M. deltoideus clavicularis*, based upon the insertions of the forelimb musculature observed in *Alligator mississippiensis* (Meers, 2003). The surface of the bone is also raised immediately dorsal and slightly posterior to the glenoid fossa, where the *M. coracobrachialis brevis dorsalis* would have attached to the scapula in *Alligator mississippiensis* (Meers, 2003). A raised area in the posterodorsal part of the lateral surface may be due to deformation from the underlying vertebra.

Both **coracoids** of *Junggarsuchus* are preserved in articulation with the scapula; the left element is completely exposed whereas the right is not (Figure 30b, c). The coracoid is nearly the same anteroposterior length as the scapula, as seen in other early diverging crocodylomorphs like *Sphenosuchus*, *Dibothrosuchus*, and early diverging crocodyliforms like *Protosuchus richardsoni* (AMNH 3024) and *Orthosuchus* (Nash, 1975). The left scapula and coracoid have been slightly disarticulated so that the coracoid is bent ventromedially and shifted slightly posterior relative to the scapula (Figure 30a–c). The anterior edge of the glenoid fossa of the coracoid is displaced to lie beneath the posterior edge of the fossa on the scapula. The coracoid features a smooth rod-like postglenoid process that extends posteroventrally, as in *Dibothrosuchus* (Figure 30d), which lacks the ventral groove found in *Sphenosuchus* (Walker, 1990), *Terrestrisuchus* (Crush, 1984), and earlier crocodylomorphs and pseudosuchians (Nesbitt, 2011). The elongate, posteromedial, postglenoid process is as long as the scapular blade and body of the coracoid in lateral view, about 5 cm long in lateral view, similar to *Dibothrosuchus* and *Sphenosuchus* and unlike the posteromedially tapering rod-like processes in *Terrestrisuchus* and *Dromicosuchus* (Crush, 1984; Sues et al., 2003). The postglenoid process extends to the posterior margin of the second dorsal vertebrae as preserved specimen. The process lacks any indication of the articulation with the sternum and a biceps tubercle, such as are present in *Dibothrosuchus* (Wu & Chatterjee, 1993) and *Sphenosuchus* (Walker, 1990), so the extent of the articulation between the coracoid and sternum, if present, cannot be determined. The coracoid portion of the glenoid fossa is nearly perpendicular to the scapular portion, and faces posteriorly and somewhat dorsally, similar to *Protosuchus richardsoni* (AMNH 3024). However, the orientation of the glenoid fossa of the coracoid remains more sub-horizontal than in early diverging crocodyliforms like *Protosuchus richardsoni* (AMNH 3024) and *Orthosuchus* and more like other crocodylomorphs, like *Dibothrosuchus* and *Sphenosuchus*, and earlier pseudosuchians like *Postosuchus kirkpatricki*. Anteriorly, the coracoid is relatively mediolaterally thick and square shaped in anterior view.

An interclavicle is not evident, but the ventral midline of the skeleton has not been completely prepared.

Both **humeri** of *Junggarsuchus* are preserved (Figure 31a,b). The right element remains in articulation with the shoulder girdle, but much of the rest of the forelimb was lost to erosion. Nearly all of the elements of the left forelimb have been preserved in articulation and removed from the skeleton. The left humeral shaft shows a slight concavity medially at mid-shaft and laterally near the distal end, but some of this may be due to distortion. The humeral shaft is gently but distinctly curved, with the shaft distal to the deltopectoral crest forming an anteriorly concave arc. This curvature is similar to that of *Sphenosuchus* (Walker, 1990) and more pronounced than that of *Dibothrosuchus*, *Hesperosuchus* (CM 29894) (Clark et al., 2001), and *Terrestrisuchus* (Crush, 1984). The proximal articular surface projects posteriorly perpendicular to the rest of the articulating surface and forms an expanded and hooked semi-spherical head similar to that seen in crocodylomorphs and closely related pseudosuchians (Nesbitt, 2011). The proximal articular surface of the bone is proportionally large when compared to other non-crocodyliform crocodylomorphs. This expansion extends onto the posterior surface of the proximal articulation. A small depression lies laterally opposite the head on the left humerus, but this may have been caused by postmortem crushing, as its presence on the right side was undetectable. The remaining articulating surface is mediolaterally broad and slightly concave anteriorly, and the medial tuberosity is slightly narrower than the part lateral to it, and tapers medially. A thin ridge descends from the medial edge of the articulation, gradually declining into the shaft distally about one-fourth of the dorsoventral height of the bone. Laterally, the proximal articular surface is continuous with the dorsal surface of the deltopectoral crest and there is no separation, as in some crocodylomorphs (Nesbitt, 2011). The deltopectoral crest does not project as far from the shaft as in *Sphenosuchus*, and is similar in proportional size to

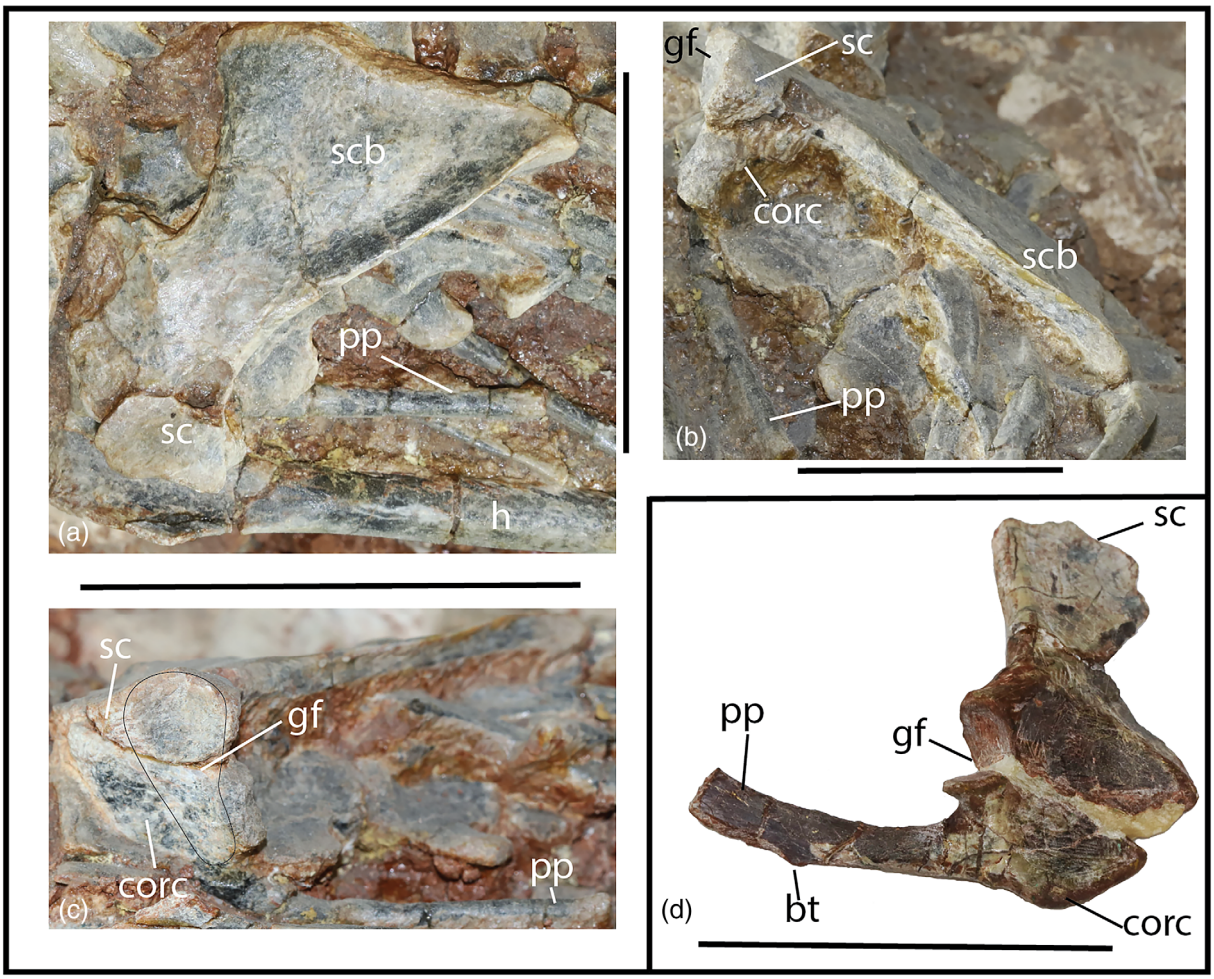

FIGURE 30 Close up of the left scapula and coracoid of *Junggarsuchus sloani* in (a) lateral view; (b) scapula and coracoid in posterolateral view; (c) ventral view of the glenoid fossa and coracoid body; (d) right scapula and coracoid of *Dibothrosuchus elaphros* in right ventrolateral view. Scale bar is equal to 5 cm.

Dibothrosuchus, *Hesperosuchus* (CM 29894) (Clark et al., 2001), and *Terrestrisuchus* (Crush, 1984) but extends further distally than in the latter. The anterolateral edge of the deltopectoral crest is straight for three quarters of its length beginning on the proximal humeral end. The flat portion has a rough surface similar to that of the proximal articulating surface and continuous with it. Together, the deltopectoral crest and the medial ridge enclose a fairly deep depression on the proximal end of the humerus on the anterior side (Figure 31b).

The distal end of the humerus is approximately the same width as the proximal end, which is seen in other non-crocodyliform crocodylomorphs like *Dibothrosuchus* (Figure 31e) and *Sphenosuchus*. The lateral and medial condyles are similar in size and separated by a shallow intercondylar groove posteriorly; the anterior surface is not exposed. The lateral condyle is slightly narrower and deeper than the medial condyle and forms a sharper ridge lateral to the intercondylar groove. However, the disparity in size is not as much as in *Dibothrosuchus* (Figure 31e) (Wu & Chatterjee, 1993, figure 12), *Terrestrisuchus* (Crush, 1984, figure 7), and *Sphenosuchus* (Walker, 1990, figure 43).

The left and right **ulnae** are complete, the left element is preserved intact with the rest of the forelimb (Figure 31a,b). The right ulna and radius are preserved in pieces, except for the proximal ends articulated with the humerus on the main block. The left ulna is nearly 10 mm longer than the radius, and only a small part of this disparity (2 mm) is due to the olecranon process on the ulna with the remaining difference is the length. The proximal end of the ulna is subtriangular in lateral view, similar to that of *Dibothrosuchus* but with a more concave posterior edge (Figure 31e). The olecranon process is low, broad and gently convex in lateral view. It is proportionally lower than in *Dibothrosuchus*, *Terrestrisuchus*, and *Hesperosuchus* (AMNH FR 6758and CM 29894), and less distinct than in the latter two taxa (Crush, 1984; Clark et al., 2001). A low ridge continues medially from the

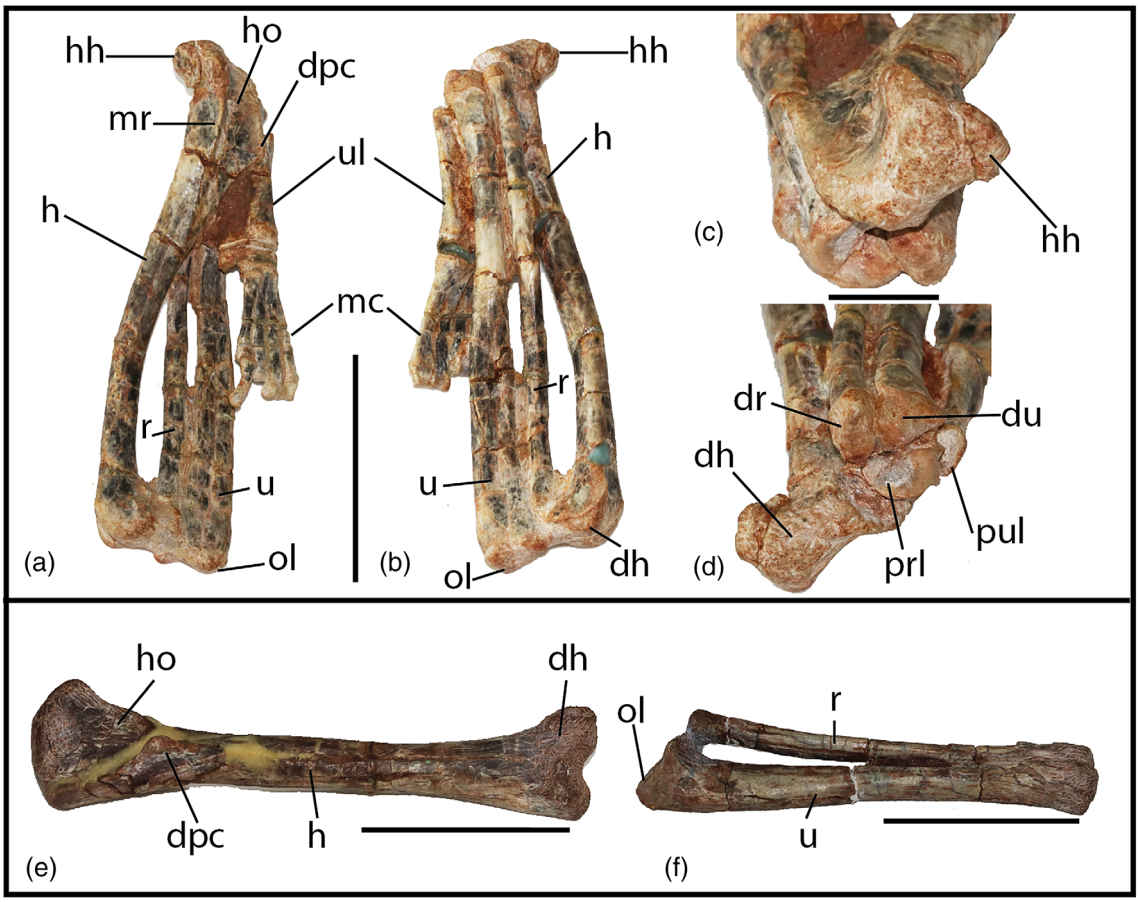

FIGURE 31 The left forelimb of *Junggarsuchus sloani* showing the elements as preserved in (a) antero-medial and (b) posterolateral view; (c) proximal head of the humerus and (d) articular ends of ulna and radius; (e) the right humerus; (f) radius and ulna of *Dibothrosuchus elaphros* in right lateral view. Scale bar is equal to 5 cm in (a), (b), (e), and (f); 1 cm in (c) and (d).

olecranon process along the anterior edge but does not reach the medial edge. Medially, the proximal articular surface is flat anteriorly and has a small but pronounced process posteromedially. The shaft of the ulna is widest at the proximal end, where it has been anteroposteriorly crushed on the left element; it becomes thinner and more circular in cross section distally, and the distal end is only slightly thicker dorsoventrally than the shaft. The distal end of the ulna has an anterior expansion that is found in nearly all Crocodyliformes, with the exception of thalattosuchians (Andrews, 1913; Young & Andrade, 2009). As preserved, the radius and ulna have only a short contact proximally, and a more extensive contact near the distal end, where they meet for the distal third of the bone's length. As in *Dibothrosuchus*, the distal end of the ulna's medial facet for articulation is not confluent with the distal articulation for the ulnare (Figure 31d). This contact occurs along a flat medial surface of the distal ulna, seen best on the right element. This surface may also have contacted the lateral edge of the radiale. The ulna ends in a rounded process that may have contacted a pisiform, as in *Dibothrosuchus* and *Terrestrisuchus* (Crush, 1984), but one is not preserved. The articulation surface extends laterally from this process, tapering in anteroposterior width and in distal length. The posterior surface of the ulna's distal end forms a broad groove on the right element, but the left element appears to be flatter in this region, although it is largely unexposed.

The **radius** is a cylindrical bone about half the diameter of the ulna (Figure 31a). Unlike most other non-crocodyliform crocodylomorphs, with the exception of *Hesperosuchus* (CM 29894 and AMNH FR 6758) (Clark et al., 2001), the radius is shorter than the humerus, similar to the condition in *Protosuchus richardsoni* (AMNH 3024) (Brown, 1933). The proximal end of the radius is preserved on the left side ending ventral to the ulna's proximal articulating surface, due presumably to distal dislocation. The proximal end is expanded anteroposteriorly, but the proximal surface is not exposed. A faint ridge is present trending along the anterior edge of the proximal end of the bone. The distal end is expanded anteroposteriorly but is only slightly wider than the shaft.

Its lateral surface is flat and abuts against the medial surface of the ulna.

The radiale and ulnare of *Junggarsuchus* are preserved only on the left side. They are elongate, as in most crocodylomorphs, although to a greater degree than most (Bonaparte, 1971; Clark, 1986; Clark & Sues, 2002; Clark et al., 2001; Crush, 1984; Gow, 2000; Lecuona et al., 2016; Pol et al., 2013; Sues et al., 2003; Walker, 1990; Wu & Chatterjee, 1993). The **radiale** is more than a third of the length of the radius (Figures 31 and 32a), unlike other non-crocodyliform crocodylomorphs or crocodyliforms, like *Dibothrosuchus* (Figure 32c), *Almadasuchus* (Pol et al., 2013) and *Protosuchus richardsoni* (AMNH 3024), which have an elongated radiale, but not to the degree seen in *Junggarsuchus*. The convex distal end of the radius articulated with a concavity on the proximal end of the radiale in a concavo–convex joint. The articulation surface on the radiale is semicircular, with a flat posterior edge, and the curved edges are raised, whereas the flat one is not. In anterior view, the proximal end of the radiale is hatchet-shaped, with a broad proximolateral process. This expanded area has two longitudinal ridges on its medial surface descending from the proximal end, with a surface similar to that of the articulation. The anterior ridge is about half the length of the posterior ridge. The ulna would have articulated with the medial surface along these ridges, but it is unclear what surfaces were in contact. The proximal end of the ulnare contacts the radiale at the base of this lateral process. The dorsal surface of the radiale is smooth and slightly convex; it increases gradually in breadth to the distal end. The distal end abuts a medial distal carpal, but it is not exposed. The distal end of the radiale is convex, at least anteriorly, but the more posterior part of this surface is not exposed. The distal end of the radiale also has a lateral contact with the broad distal end of the ulnare.

The **ulnare** in *Junggarsuchus* is shorter and narrower than the radiale in anterior view, but with a much broader distal end (Figure 32b). Its proximal surface is concave, and there is no pisiform preserved proximal to it, unlike the condition observed in *Dibothrosuchus* (Figure 32c) and *Terrestrisuchus* (Crush, 1984) where a pisiform element is present. The anterior edge of the proximal surface forms an anterior buttress to the articulation of the ulna or pisiform. The proximal end of the ulnare is slightly more than half the mediolateral width of the distal end of the ulna. The shaft is thin and straight. The dorsal surface of the shaft is rounded, whereas the ventral side appears to be flatter, although it is mostly covered by matrix. The distal end of the ulnare flares distally to become twice as broad as the proximal end and is flattened anteroposteriorly. Relative to the proximal end it is twisted about 45°, so the anterior surface faces anteromedially.

At least two distal carpals are present (Figure 32a,b) and another may be present articulated with the proximal end of the I metacarpal, but the contact is unclear and may be an artifact of preparation (contra Clark, Xu, Forster, & Wang, 2004; figure 3d; figure 33a). The lateral distal carpal is flattened and articulates broadly with the distal end of the ulnare and the proximal ends of metacarpals II–III. It is unclear whether this carpal is a fusion of carpals III and IV, as was hypothesized by Wu and Chatterjee (1993) in *Dibothrosuchus* (Figures 32c and 33a). The medial distal carpal is proximodistally thin, mediolaterally long and articulates with metacarpals I and II and extends about 4 mm beyond the lateral edge of metacarpal one (Figure 33a). A space between the radiale and the proximal ends of metacarpals IV–V suggests the presence of a medial distal carpal, but it is not exposed. A thin, mediolaterally rod-like, portion of bone articulated to the proximal end of metacarpal I and II may be an additional distal carpal, but appears continuous with metacarpal II and is likely the mediolaterally expanded proximal head of this elements.

Four **metacarpals** are present, and the lack of articulation surfaces medially on the medial element and

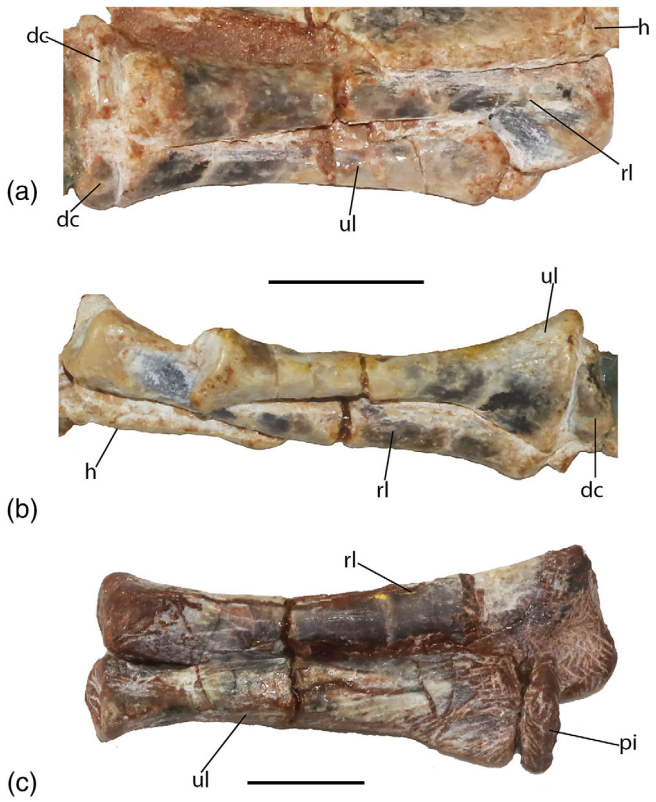

FIGURE 32 (a) Close up of the left carpals of *Junggarsuchus sloani* in dorsolateral view; (b) and in ventromedial view showing the distal end of the ulnare; (c) close up of right carpals in *Dibothrosuchus elaphros* in ventral view. Scale bar is equal to 1 cm.

laterally on the lateral element suggest that another one was not present. Contrary to Clark, Xu, Forster, and Wang (2004), digit I is interpreted here as reduced relative to the other digits of the manus, based on the observations that metacarpal I is displaced distally, shorter than the other metacarpals, has a narrow proximal head that does not articulate with the proximal ends of the other metacarpals and lacks distal condyles, and digit V absent, as in *Dibothrosuchus* (Figure 33b). The third metacarpal is the longest, the second and fourth are slightly shorter and approximately the same length (Table 4) (Figure 33a). The first metacarpal does not reach as far proximally or distally as the other metacarpals, is about half the breadth and width of metacarpal II, and adheres to the shaft of metacarpal II over its entire length. The proximal end of metacarpal II is twice the mediolateral width of the proximal end of metacarpal I (Figure 33a). The metacarpals of digits II–IV are similar in mediolateral breadth, but metacarpal IV is slightly thicker than the other two. Metacarpals II–IV are preserved compacted together, similar to the preservation of *Saltoposuchus* (Sereno & Wild, 1992), *Terrestrisuchus* (Nesbitt, 2011), *Hesperosuchus* (CM 29894) (Clark et al., 2001), and *Dibothrosuchus* (Clark et al., 2001; Leardi et al., 2017; Char 120). The proximal ends of metacarpals II–III are mediolaterally flattened and wide, but that of metacarpal IV is convex laterally. The distal ends of metacarpals II-IV have two anteroventrally developed condyles, the medial condyle is slightly larger than the lateral on metacarpal III and the lateral condyle slightly larger than the medial on metacarpal II. The distal surface of metacarpal I is simple, lacking distinct condyles.

Three entire phalanges, the proximal part of two more, and the distal part of two others are preserved. A phalanx preserved with the manus is attached near the end of the first metacarpal. It is a proximal phalanx, and is too large to be from digit I so may be from digit II. Its proximal end is gently concave, is about four times as long as wide, and distally it has a single convex condyle with only a very gentle indentation where the intercondylar groove usually lies. Distinct ligament pits indent the lateral and medial surfaces, and the condyle is slightly flared ventrolaterally, so that the ventral part of the condyle is wider than the dorsal part. The fourth digit retains its natural articulation with the proximal end of a phalanx. The proximal end of the phalanx has a very short extensor process on its ventral surface, which fits into the intercondylar groove of metacarpal IV. The proximal end, preserved separately, is similar to the phalanx articulated near II, and one of the distal pieces probably belongs with it as it is very similar to the articulated phalanx. The distal piece differs from the articulated phalanx in having an intercondylar groove, although

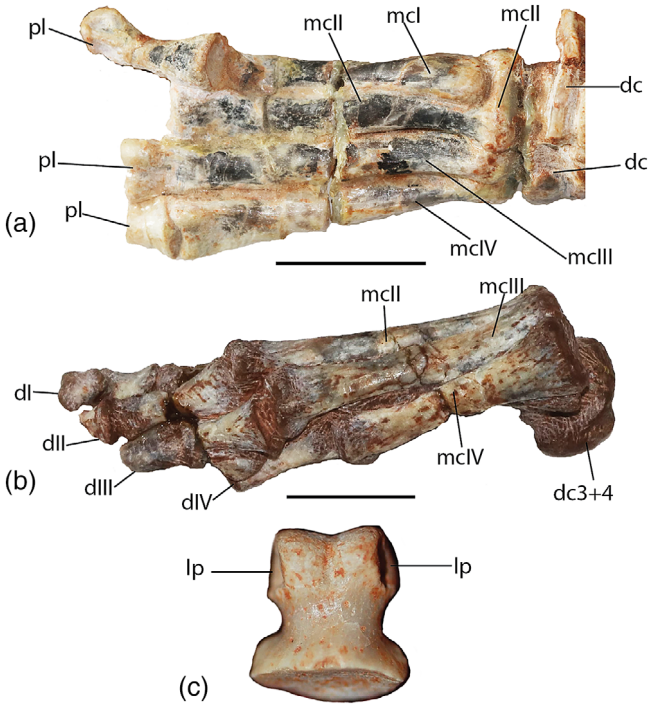

FIGURE 33 (a) The left Manus of *Junggarsuchus sloani* with the metacarpals labeled in dorsal view; (b) the right Manus of *Dibothrosuchus elaphros* in dorsolateral view; (c) isolated Manus phalanx in dorsal view. Note the phalanx (pI) still attached to metacarpal I in *Junggarsuchus sloani*. Scale bars are equal to 1 cm.

it is very broad and shallow. A small isolated complete phalanx is about two-third as long as the articulated phalanx, and its distal end is not flared ventrolaterally. The other distal phalanx has a broad, shallow intercondylar groove but no ligament pits, is not flared ventrolaterally, and expands medially and laterally more than does the articulated phalanx. The phalanges that can be observed appear mostly similar to those present in *Dibothrosuchus* in overall form. No unguals are preserved in *Junggarsuchus*, unlike *Dibothrosuchus*.

An isolated phalanx is similar to phalanx IV-2 of *Dibothrosuchus* (which is not as figured by Wu & Chatterjee, 1993, figure 13f). It is about as long as its proximal end is wide. Its proximal end is greatly expanded, about twice as broad as at mid-shaft, and flat proximally. It narrows distally, and two distal condyles are dorsoventrally tall, rounded and confluent. The condyles are slightly beveled and face slightly medially and laterally. Shallow ligament pits are present.

4.1.5 | Axial skeleton

The disarticulated intercentrum and neural arch of the **atlas** of *Junggarsuchus* were preserved adjacent to the

medial surface of the left angular and surangular (Figures 28a and 34c). The intercentrum is flattened dorsoventrally and dorsally concave. It is concave anteriorly where it contacted the occipital condyle. Anterolaterally, the atlas centrum projects anteriorly to form a flange on either side of the anterior concavity where the neural arch would have articulated dorsally.

The right half of the atlas neural arch is preserved and exposed adjacent to the mandible (Figures 3c, 15b, 28a, and 34c). The prezygapophysis projects laterally from the flat anterior surface of the neural arch and do not have a long posterior component. There is a notch immediately medioventral to the prezygapophysis that separates it from the ventral process. This process would have made up part of the articulation with the odontoid process as well as the intercentrum, which is preserved (33b). Posterodorsally, a subtriangular, flat surface would have articulated with the axial postzygapophysis. Two disarticulated atlas ribs are preserved. The rib has two articular heads, the anterior articular head is short and squared whereas the posterior articular head is anteroposteriorly long and rounded posteriorly. The posteroventral process of the rib is short and triangular in lateral view (Figure 34b). The atlas of *Dibothrosuchus* is largely similar to what is preserved of *Junggarsuchus*.

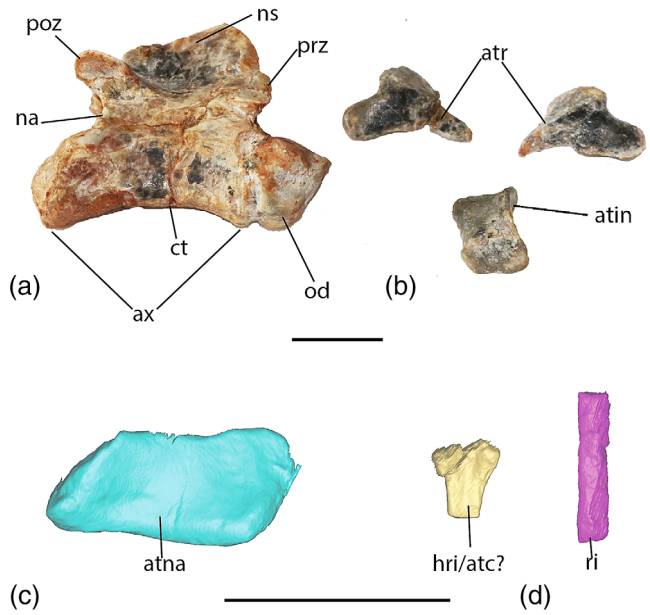

FIGURE 34 Atlas and axis elements of *Junggarsuchus sloani*: (a) the axis in right lateral view; (b) atlas ribs and intercentrum in lateral views; and (c) the neural spine of the atlas separated digitally from the left mandible of *Junggarsuchus sloani*, in right lateral view; (d) possible cervical rib head and cervical or axis rib shaft separated from the left mandible in medial? views. Scale bars are equal to 1 cm.

The **axis** is preserved disarticulated from the rest of the vertebral column (Figure 34a). Anteriorly, the odontoid process is semicircular in anterior view, with a flat dorsal surface and a rounded ventral surface. The diapophysis and parapophysis are represented by two small, round projections from the ventrolateral surface of the process. They are almost adjacent and are only separated by a slight concavity on the ventral surface of the centrum. Three low projections are present on the dorsal part of the odontoid process: an anteromedial one and a lateral one on either side. These would have inserted at the junction of the atlas centrum and neural arch. The centrum body is both narrower and anteroposteriorly longer (Table 4) than the other cervical vertebrae and it is strongly concave ventrally. The posterior end of the axis centrum has a concave dorsal surface and slopes posteroventrally. It has a convex condyle posteriorly. The neural arch is smooth, due to the lack of rib articulations. Anteriorly, there are two very small pre-zygapophyses, similar to the pre-zygapophyses seen in *Dibothrosuchus* (Figure 35b) and *Sphenosuchus*. The postzygapophyses are larger and more horizontally oriented. The neural spine appears to have been mostly broken off, leaving only a low ridge that slopes downward toward the posterior end. The axis does not feature a hypophysis ventrally. Two elements preserved on the posterior medial face of the left mandible may represent the broken and disarticulated shaft and head of an axis or another cervical rib (Figure 33d).

The **post-axial vertebrae** of *Junggarsuchus* are procoelous, unlike the amphicoelous or amphiplatyan vertebrae of all other non-crocodyliform crocodylomorphs like *Dibothrosuchus*, *Terrestrisuchus*, and *Sphenosuchus* and most crocodyliforms with the exception of *Fruitachampsa* (Clark, 2011) and eusuchians. Four postaxial **cervical vertebrae** are still articulated with the skeleton (Figure 35a) and another one was collected separately. The centrum and neural spines of the anterior most cervicals are both taller than those of the dorsals, and the centra and neural spines of the more posterior cervical vertebrae become progressively smaller until they grade smoothly into the dorsal vertebrae. The neural spines are broken off on most of the vertebrae but when present they are equal in height to the entire centrum and neural arch complex. They are flattened mediolaterally and taller than they are anteroposteriorly long, resembling the vertebrae of living crocodiles, although the neural spines of *Junggarsuchus* do not become rod-like in posterior cervical vertebrae as in the latter and *Dibothrosuchus* (Clark, 1994). The prezygapophyses are pronounced and almost completely vertically oriented, with angles of close to 90°. These interlock with the vertebrae anterior to them across a flat contact. The lateral surfaces of the vertebrae

are depressed compared to the anterior and posterior ends, particularly between the parapophyses and diapophyses. On the three exposed cervicals, the parapophysis is situated anteroventrally on the lateral side of the centrum and faces laterally, the diapophysis is nearly in the center of the lateral surface, at the level of the neurocentral suture, and face ventrolaterally. The parapophysis of the posteriormost cervical vertebra, despite being similar in shape, is positioned more dorsally on the centrum than those on the more anterior cervical vertebra, at about the centrum mid-height as opposed to the bottom of the centrum. Similarly, the diapophyses on this last vertebra move dorsally and are positioned on the neural arch (Figure 35a).

Hypapophyses, mediolaterally narrow and dorsoventrally tall processes projecting ventrally from the ventral surface of the centrum, are present on the ventral surface of at least the four most posterior cervical vertebrae

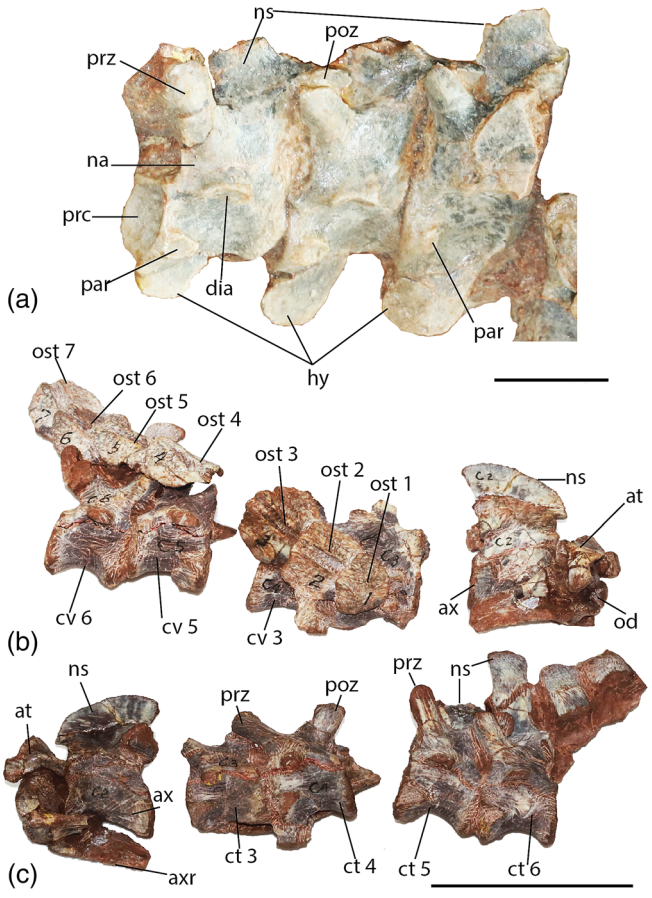

FIGURE 35 (a) The posterior three cervical vertebrae of *Junggarsuchus sloani*. Note the parapophysis on the complex neural arch and the hypophyses present on the ventral surface of each centrum; (b) the full cervical series of *Dibothrosuchus elaphros* with articulated osteoderms in right lateral view; and (c) left ventrolateral view. Cervical vertebrae numbered on specimen. Scale bars are equal to 1 cm.

(Figure 35a). These are also present on extant crocodylians but are absent in other non-crocodyliform crocodylomorphs and early diverging Crocodyliformes. The hypapophysis on the anterior-most of the articulated cervical vertebra is restricted to the anterior end of the centrum. On the following three vertebrae the hypapophysis becomes more anteroposteriorly elongated compared to living crocodylians.

The posterior articular surface of the centrum is hemispherical peripherally, but a central depression occupies more than half the diameter of the condyle. The depression on the anterior end of the centrum is smoothly concave, lacking any expansion corresponding to the depression in the condyle.

All nine cervical vertebrae are preserved in *Dibothrosuchus*, including the neural arches and most of the neural spines (Figure 35b). The cervicals are similar to *Junggarsuchus* in size, shape and in the form of the neural spine. The cervical zygapophyses are sub-vertical, as in *Junggarsuchus*. In general anatomy the cervical vertebra are similar, but *Dibothrosuchus* lacks hypapophyses on the cervical and dorsal vertebrae.

Eleven **dorsal vertebrae** remain in articulation and four more are separated from the skeleton in *Junggarsuchus* (Figure 36). The parapophyses and diapophyses are concave except for the parapophyses on the anterolateral edge of the vertebral centrum. The parapophyses and diapophyses of the dorsal vertebrae are more inline than they are in the posterior cervical vertebrae. The parapophyses are laterally expanded ridges at the base of the neural arch that are more dorsally positioned than in the posterior cervical vertebra and close to the body of the centrum. The parapophyses do not change their position much along the preserved dorsal series. The diapophyses are positioned more dorsally on the neural arch (though still more in line with the parapophyses than in the cervical vertebra) than the parapophyses. The diapophyses are rounded and, like the parapophyses, do not change position along the preserved dorsal series. On their lateral surface, the postzygodiapophyseal laminae of the neural arches, a lamina that connects the postzygapophyses with the diapophyses, are a low ridge located posterodorsally, which makes up part of the diapophysis. A short and transverse process is present, but it is only exposed on the last articulated vertebra where it is inclined posterodorsally. The relationship of the parapophysis and diapophysis to the transverse process is unclear, as the distal end of the process is broken on the last vertebra. In the preserved dorsal vertebrae, the prezygapophyses are less vertically oriented than those of the cervical vertebrae, with angles closer to 65°. They are also shorter in anteroposterior length. The neural spines are slightly taller than half the

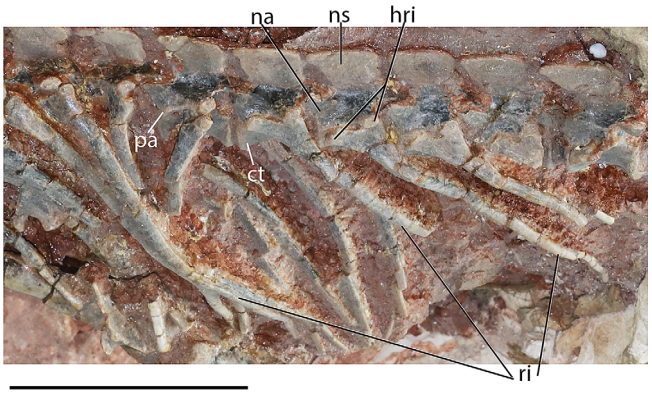

FIGURE 36 Close up view of the dorsal vertebrae of *Junggarsuchus*. Note the simple centrum and neural arch and the anteroposteriorly broad neural spines. The double-headed ribs retain their natural contact with the parapophyses and diapophyses. Scale bar is equal to 5 cm.

height of the centra, and their anteroposterior length is nearly equal to that of the centra. Their height is consistent throughout the entire dorsal section of the vertebral column, and the dorsal edge is horizontal throughout. The posterior edge of the neural spines of the most anterior dorsal vertebrae has a short posterior projection dorsally, while more posterior dorsal vertebrae develop a short anterior projection on the dorsal part of the anterior edge of the neural spine. The transition from cervical to dorsal vertebrae is hidden by the scapula, so the dorsal progression of the parapophysis on more posterior vertebrae is not visible. The four most anterior dorsal vertebrae have dorsoventrally tall hypapophyses projecting from the ventral surface of the dorsal centrum, which curve posteroventrally, unlike those of the cervicals. The anterior depression and posterior condyle on the centra are similar in shape to those on the cervicals.

The first three and last three dorsal vertebrae are known from *Dibothrosuchus*. The cervico-dorsals are amphicoelous, which is standard for non-crocodyliform crocodylomorphs and pseudosuchians other than *Junggarsuchus*. The anterior three dorsal vertebrae are similar in form to those in *Junggarsuchus*. The parapophyses migrate dorsally posterior to become confluent with the diapophysis at the 13th dorsal vertebrae. The neural arch is as tall as it is long, and the angle of the pre-zygapophyses appears similar to that seen in *Junggarsuchus*. The neural spine is preserved on the first dorsal vertebrae and is narrower and slightly taller than those in *Junggarsuchus*. They also lack the posterior and anterior projections seen in *Junggarsuchus*.

The **ribs** are preserved only on dorsal vertebrae, except for one cervical rib partially exposed to the right of the second preserved cervical on the main block (Figure 36). Many dorsal ribs have been preserved undistorted and articulated, but they are badly fractured at many points along the bone. The shaft of the cervical rib is straight with a short anterior process and a long posterior process, about the length of the centrum of the subsequent cervical. The cervical ribs are double-headed, as indicated by the parapophyses and diapophyses of the vertebrae. The preserved dorsal ribs are all double-headed, mediolaterally narrow and distally become nearly cylindrical. Dorsally, the ribs are flattened dorsoventrally, and distally they become thinner and curve medially. Particularly well-preserved examples, such as the ribs on dorsal vertebrae two to five, show an anterior longitudinal depression in the proximal third to half of the rib. The anterior dorsal ribs have likely been displaced and are propped up on their heads, sitting perpendicular to the vertebrae and not preserving the natural contact. The more posterior dorsal ribs lie flat on their heads against the ridges on the lateral surfaces of the vertebrae, with the parapophyses placed more dorsally on the centrum and the tuberculum meeting the diapophysis anteroventral to the postzygapophysis. The diapophysis is further posterior when compared with the cervical vertebrae. Although they are partially flattened, the ribs of *Junggarsuchus* have only a small horizontal component dorsally, as in other non-crocodyliform crocodylomorphs (Crush, 1984; Walker, 1990) but unlike in extant crocodylians. This would have made the animal's body dorsoventrally taller, unlike the mediolaterally wide bodies of modern crocodylians. The condition in *Junggarsuchus* is inferred from the sharp curvature of the proximal ends of the ribs in which the rib is directed ventrally, almost immediately lateral, to the head.

Two dorsal ribs are known from *Dibothrosuchus*, unfortunately the proximal ends of the ribs are not preserved. The bodies of the ribs appear similar to the dorsal ribs of other non-crocodyliform crocodylomorphs (Wu & Chatterjee, 1993). The sacral vertebrae are all preserved in *Dibothrosuchus*, but not in *Junggarsuchus*, though a disarticulated sacral rib is known from the latter.

A single disarticulated **caudal vertebra** is known from *Junggarsuchus*. It is a small, elongate centrum, three times as long as it is wide. It is likely from the mid to posterior section of the tail. The caudals preserved in *Dibothrosuchus* are from the more anterior series of the caudal and cannot be directly compared to the disarticulated caudal.

Though **osteoderms** are well known in crocodyliforms and in some other non-crocodyliform crocodylomorphs, like *Dibothrosuchus* (Figure 35b), *Dromicosuchus*, and *Hesperosuchus* (CM 29894), no osteoderms are preserved in *Junggarsuchus*. *Junggarsuchus* seems to be one of the only non-crocodyliform crocodylomorphs known from relatively

complete, articulated material that lacks osteoderms. In *Dibothrosuchus* (Wu & Chatterjee, 1993) the first eight osteoderms are preserved along the neural arches of the cervical vertebrae and are similar to other known non-crocodyliform crocodylomorph osteoderms, like in *Dromicosuchus* and *Hesperosuchus* (CM 29894) (Clark et al., 2001), arranged in a single, longitudinal pair of rows. The anterior most osteoderm is an unpaired, semielliptical osteoderm that is smaller than those posterior osteoderms to which it articulates. All the posterior paired osteoderms are semicircular, flat and are ornamented with grooves and ridges. These paired osteoderms all have a furrow that trend along their midline and that is bordered by a dorsally directed parasagittal crest. These paired osteoderms overlap the straight anterior edge of the osteoderms behind them (Figure 35b).

5 | PHYLOGENETIC RESULTS

From our analyses, we produced 16 strict consensus trees (Figures 37–40 and Figures S1–S9) using the various rooting schemes, ordered characters, and implied and equal weights as in our methods. The four equal weights analyses resulted in four strict consensus trees, with steps ranging from 1,968 to 1,686. The full set of CI, RI, and relevant information on our trees can be found in Table 2. Our results generally agree with the results of Clark, Xu, Forster, and Wang (2004), Nesbitt, 2011, Pol et al. (2013), Wilberg (2015), and Leardi et al. (2017) who found a paraphyletic "Sphenosuchia." All of our equal weight analyses produced partial polytomies along a paraphyletic "Sphenosuchia." Our implied weight analyses (k = 6, 12, and 24) show greater resolution among non-crocodyliform crocodylomorphs, though the support given at many of these nodes, with the exception of nodes subtending *Junggarsuchus*, *Almadasuchus*, M*acelognathus*, *Dibothrosuchus* and *Sphenosuchus*, are very low (support of 17 to 10) and nodes with support under 10 were collapsed. However, in all implied weight analyses rooted on *Gracilisuchus* and two rooted on *Stagonolepis* (exception of k = 6), "Sphenosuchia" is found as a weakly supported monophyletic clade outside of Crocodyliformes (Figure 37 and Figure S3). In 11 of the 16 analyses, we find *Junggarsuchus* as the sister taxon to (*Macelognathus* + [*Almadasuchus* + Crocodyliformes]), with the weakest support being a score of 11 in an implied weight (k = 24) analysis with *Postosuchus* as the outgroup (Figures 38–40 and Figures S1–S2 and S4–S9). The strongest support for Solidocrania is a score of 59 and found using implied weights (k = 6) with *Saurosuchus* as the outgroup and when Hallopodidae (*Hallopus* + *Macelognathus* + *Almadasuchus*) is recovered (Figure S2) (see Supplementary Document S1 for a more detailed discussion of the node supports and character states supporting recovered clades) (Table 5).

We found relatively strong support (Table 5) for *Macelognathus* and *Almadasuchus* as closer to Crocodyliformes, as in the analyses of Leardi et al. (2017) and Pol et al. (2013). Within the paraphyletic, "Sphenosuchia" *Almadasuchus* is always found as the sister taxon to Crocodyliforms (Figures 39 and 40) and in this topology *Macelognathus* is sister to *Almadasuchus* +- *Junggarsuchus*. Only three of four analyses which used the implied weights k = 6 found support for a monophyletic Hallopodidae sister to Crocodyliformes, but even when this clade is recovered it is still sister to Crocodyliformes and more closely related to Crocodyliformes than *Junggarsuchus*. *Hallopus* was found grouped with *Macelognathus* and *Almadasuchus* by Leardi et al. (2017), but we find this taxon outside Solidocrania, as its sister taxon, when this group is not recovered (Figure 38). It is united to *Junggarsuchus*, *Macelognathus*, *Almadasuchus*, and Crocodyliformes by features of its postcranial anatomy (Table 3), but the lack of cranial material likely limits the confidence to where we can assign this taxon among these non-crocodyliform crocodylomorphs. As Hallopodidae is only found in implied weight analyses with a k constant of 6 (homoplasy is more severely downweighted), it is possible that the paraphyletic topology of Hallopodidae that we recover in most of our analyses is supported by several homoplastic characters or at least requires several reversals.

Some of the non-crocodyliform crocodylomorphs are found in consistent positions. *Dibothrosuchus* is found as the sister to *Hallopus* + Solidocrania in the majority of our analyses (Figures 37, 39, and 40) (Tables 3 and 5). This earlier diverging position relative to *Junggarsuchus* is consistent with prior analyses (Clark, Xu, Forster, & Wang, 2004; Leardi et al., 2017; Pol et al., 2013; Wilberg, 2015). In 6 of our 16 analyses, we find *Sphenosuchus* as the sister taxon to (*Dibothrosuchus* + [*Hallopus* + Solidocrania]), which is similarly consistent with prior analyses (Clark, Xu, Forster, & Wang, 2004; Leardi et al., 2017; Pol et al., 2013; Wilberg, 2015). When implied weights (k = 6) were used we recovered *Dibothrosuchus* + *Sphenosuchus*, which in turn formed a sister clade to *Hallopus* + Solidocrania (Figure 38), though this result is less frequent and does not use the implied weighting value suggested by Goloboff (k = 12) (Goloboff et al., 2017).

Relationships among the other non-crocodyliform crocodylomorph were not as consistent or as well supported as those reported above. *Pseudhesperosuchus*, *Redondavenator*, *Dromicosuchus*, *Hesperosuchus*, *Trialestes*, and *Kayentasuchus* are often found in a basal polytomy or with interrelationships with node support

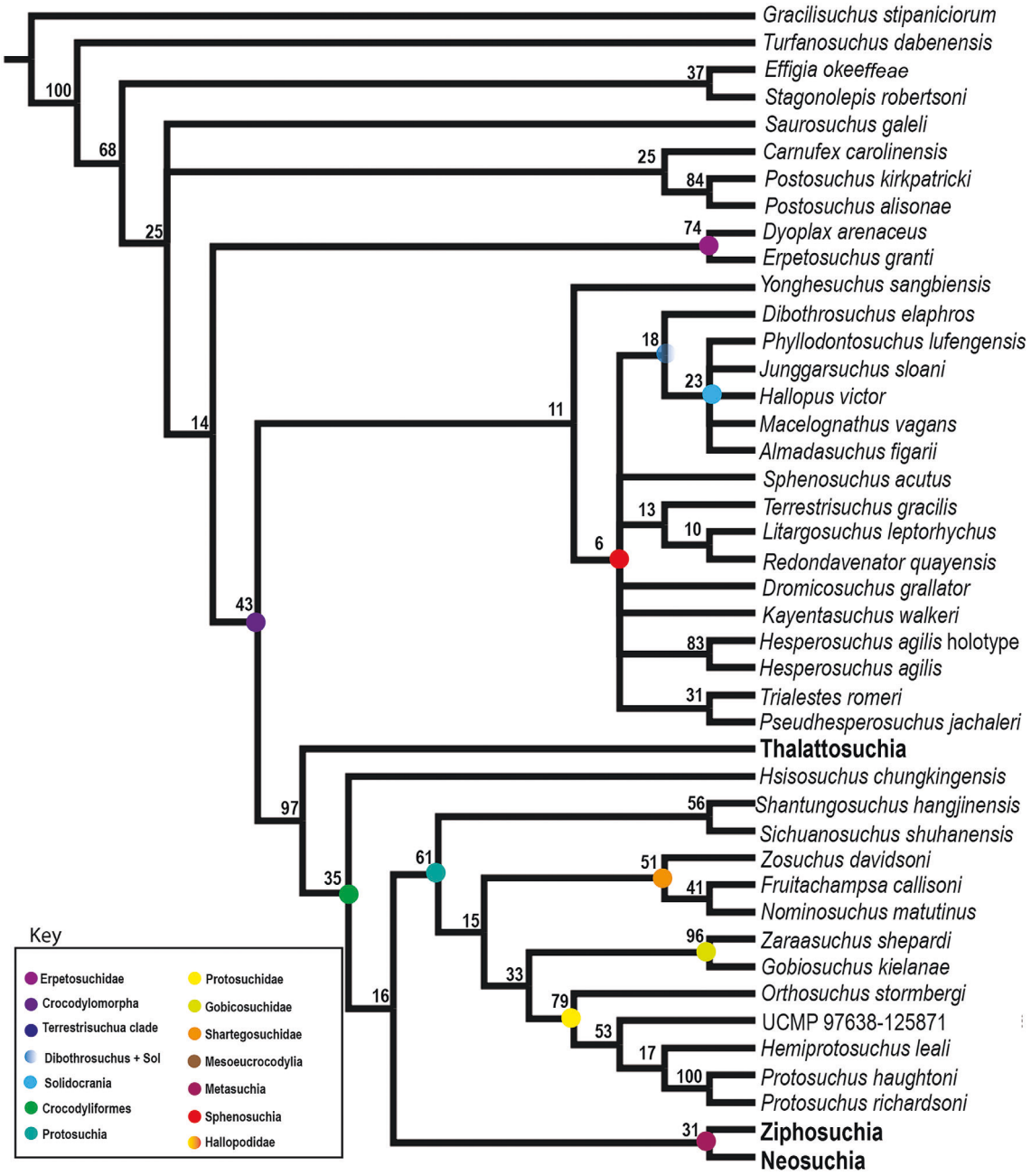

FIGURE 37 Consensus tree of four most parsimonious trees found with an implied weights ($k = 12$, 24 or 6) analysis rooted with *Gracilisuchus stipanicicorum*. Scores given on nodes. Score supports under 10 are collapsed into polytomies. Tree topology with $k = 6$, 12, and 24 was identical.

under 10. *Hesperosuchus*, *Trialestes*, *Redondavenator*, and *Pseudhesperosuchus* have all separately been recovered as the most basally branching non-crocodyliform crocodylomorph previously referred to "Sphenosuchia" (Figures 38, 39, and 40) (See Supplementary document S1 for more details). *Carnufex*, however, is commonly found as the most basally branching crocodylomorph (Figures 38 and 40) and when it is not found here it is recovered as sister to *Postosuchus* or in a polytomy at the base of Crocodylomorpha (Figure 39).

While it appears that even though "Sphenosuchia" may not be a monophyletic group of crocodylomorphs, there may be smaller clades within it, like Hallopodidae and *Sphenosuchus* + *Dibothrosuchus*, a result recovered in previous analyses (Clark & Sues, 2002). Another group that finds some support in our analysis is *Terrestrisuchus* + *Litargosuchus*, which often falls in the early diverging non-crocodyliform crocodylomorph polytomy (Figure 39; y Figures S1, S2, S5, S7, S8 and Supplementary Document S1). The group of *Terrestrisuchus*

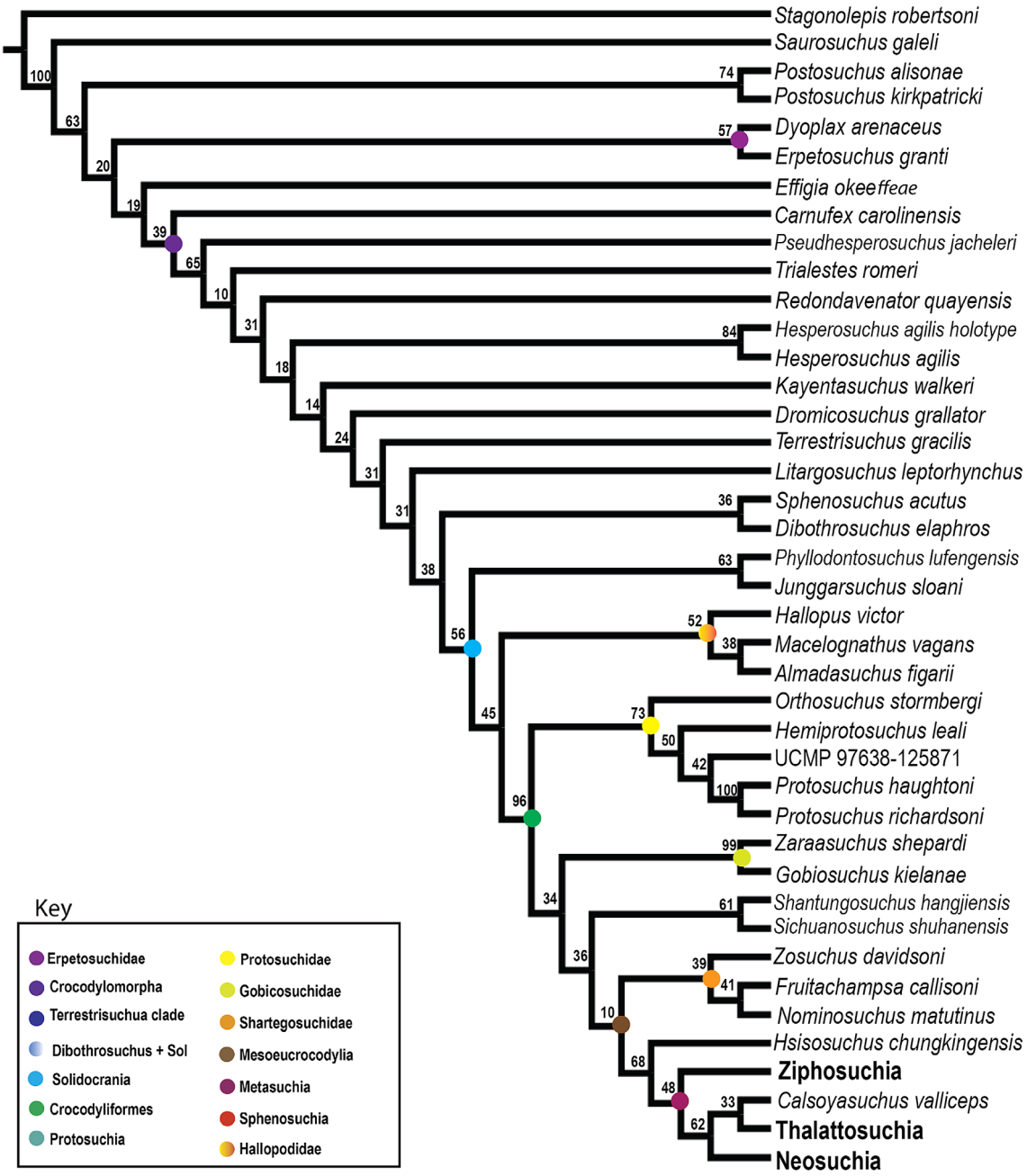

FIGURE 38 Strict consensus of two most parsimonious trees generated by implied weight analysis ($k = 6$) TNT and FigTree. Rooted with *Stagonolepis robertsoni*. Scores given on nodes. Score supports under 10 are collapsed into polytomies.

and *Litargosuchus* is notable because these are often referred to as the more "gracile" forms and may be assigned similar states due simply to size (Clark et al., 2001). The support for this group is low and based on only a few synapomorphies (Tables 3 and 5).

In all implied weight analysis where $k = 6$, with the exception of the analysis rooted on *Gracilisuchus*, *Phyllodontosuchus lufengensis* was found as the sister taxon to *J. sloani* with relatively high support (65) (Figure 38; Figures S4, S6, and S9) (Table 5). It should be noted that the extent of comparison possible with *Phyllodontosuchus* is limited by the weathering of its holotype skull which obscures many sutures. One unusual relationship that we found in our implied weight analysis ($k = 6$), with *Postosuchus* as the outgroup, was that *Redondavenator* and *Kayentasuchus* formed a clade (with a support of 36) (Figure S9). We find *Kayentasuchus* within the polytomy at the base of Crocodylomorpha in the majority of our analyses and cannot provide any further clarification on its position relative to other non-crocodyliform crocodylomorphs. This position is in contrast with Nesbitt (2011) and Zanno et al. (2015), who found it as sister to

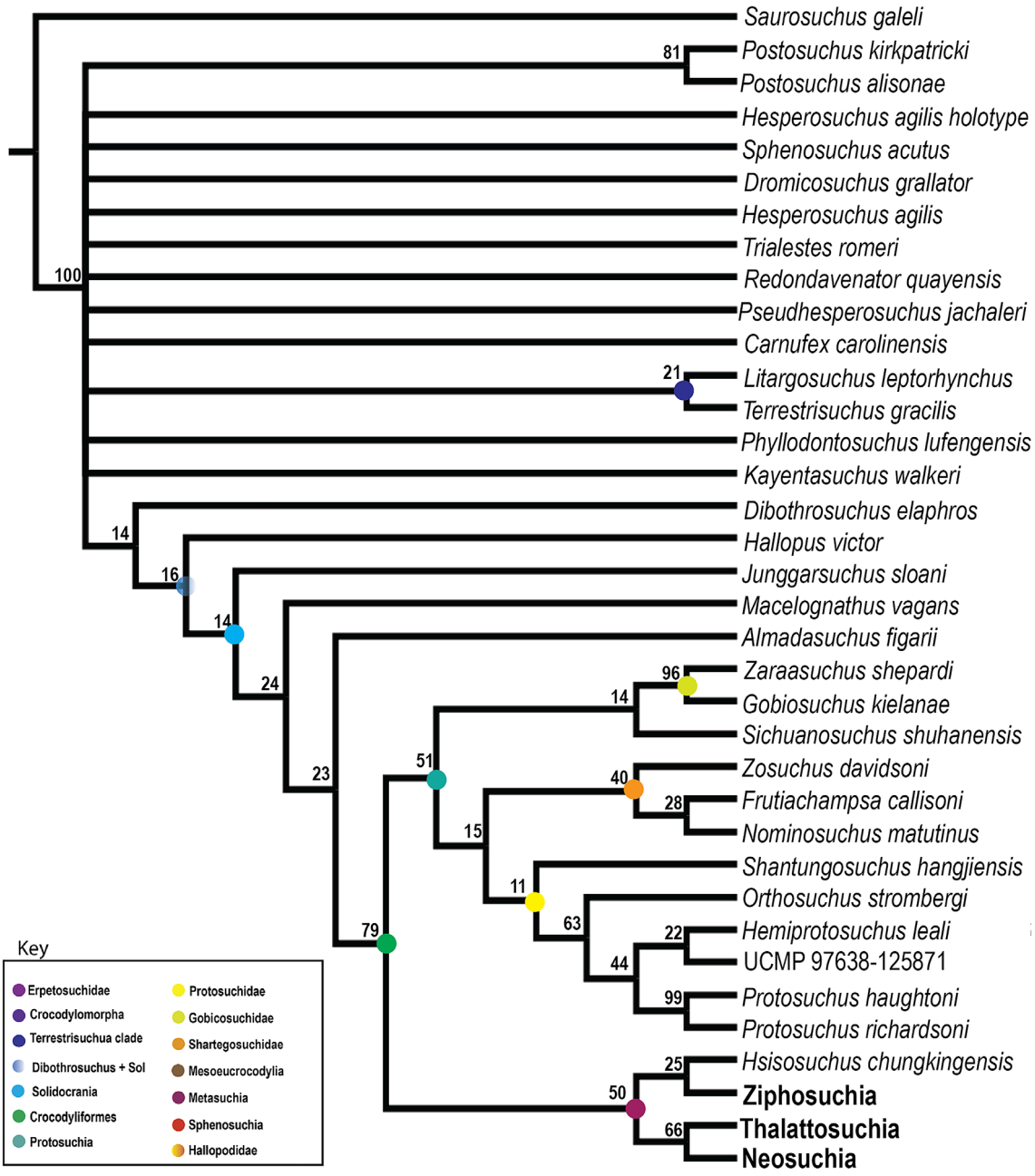

FIGURE 39 Strict consensus of 42 most parsimonious trees of 1731 steps with CI = 0.358 and RI = 0.684 generated by an equal weight analysis in TNT and FigTree, rooted with *Saurosuchus gallei*. Scores given on nodes, score supports under 10 are collapsed into polytomies.

Crocodyliformes, but the more basal position was also found by Leardi et al. (2017).

While all of our equal weight analyses and the majority of our implied weight analyses recovered a paraphyletic "Sphenosuchia," five of our analyses recovered a weakly supported (support of 10–11) monophyletic Sphenosuchia. When Sphenosuchia is found to be monophyletic, Protosuchia is found to be monophyletic and thalattosuchians are recovered as sister to Crocodyliformes (Figure 37; Figure S3), a topology that has been reported in past analyses (Wilberg, 2015). Within the monophyletic Sphenosuchia, we recover Solidocrania with (Figure 37; Figure S3). When recovered in the monophyletic Sphenosuchia, Solidocrania consists of a polytomy of *Junggarsuchus*, *Phyllodontosuchus*, *Hallopus*, *Macelognathus*, and *Almadasuchus*. In all of the recovered topologies of this nature, *Dibothrosuchus* is found as the sister taxon to Solidocrania and when rooted on *Stagonolepis*, *Sphenosuchus* is found as the sister taxon to *Dibothrosuchus* + Solidocrania.

All of our analyses recover a well-supported Crocodyliformes, though the support changes with the

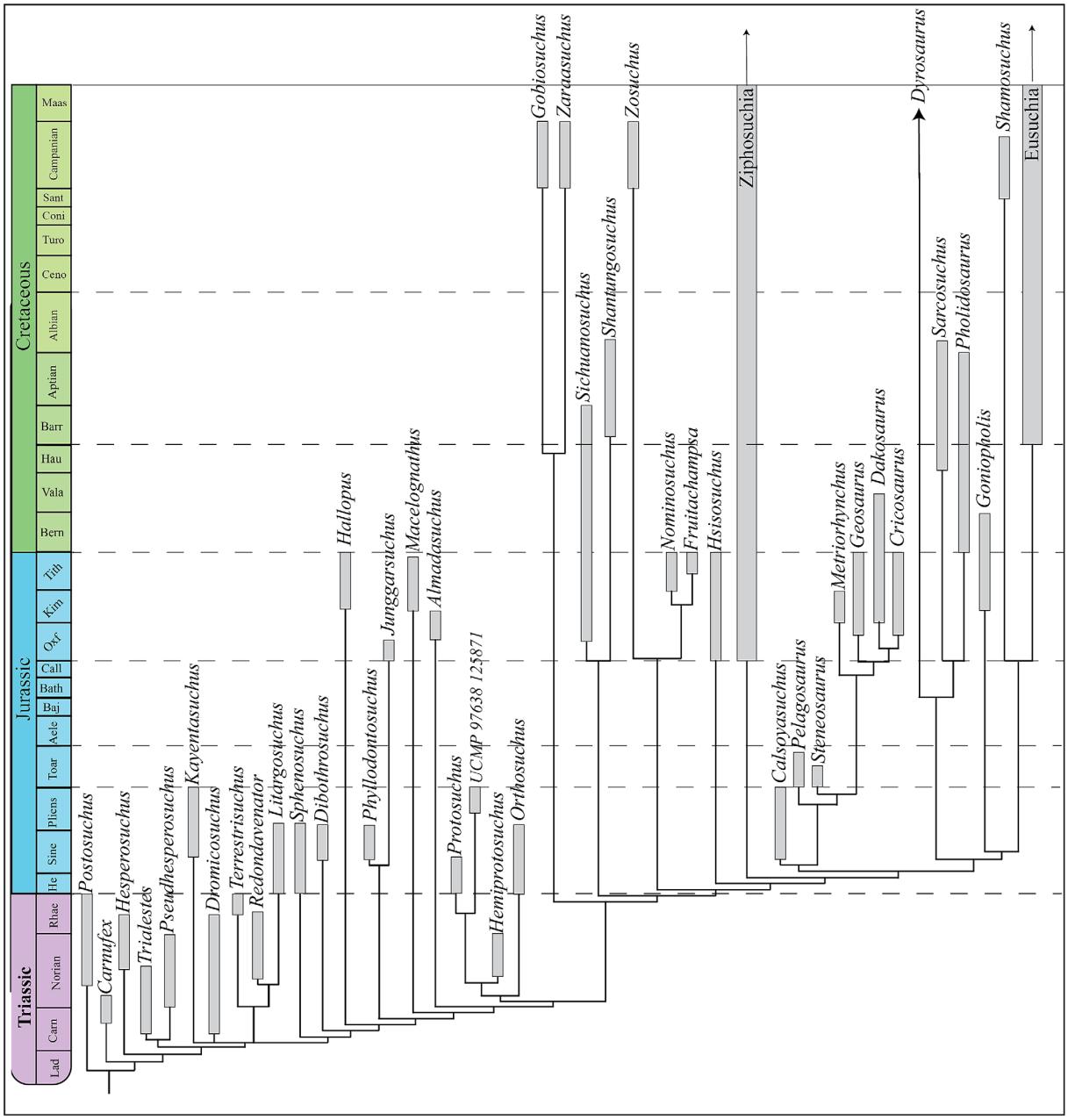

FIGURE 40 A time calibrated tree based on the consensus trees of two trees found in an implied weight ($k = 12$) analysis rooted with *Postosuchus kirkpatricki*. Thicker lines indicate groups above the genus level.

monophyly of Protosuchia. We found Protosuchia as a paraphyletic assemblage in only a minority of our analyses (Figures 38 and 40; Figure S4). The support for Crocodyliformes is stronger when Protosuchia is found as a paraphyletic clade (Figures 38 and 40) (Table 5). The support found via resampling for a monophyletic "Protosuchia" is low (Table 5) (Figures 37 and 39), but it is found in more of our analyses, similar to the results found by Wilberg, 2015, where a monophyletic "Protosuchia" is often found with a non-crocodyliform Thalattosuchia. We recovered this paraphyletic "Protosuchia" with implied weights only, suggesting that the monophyletic Protosuchia depends on homoplastic characters. Within the paraphyletic topology, Protosuchidae is found as the most early diverging clade of crocodyliforms (Figures 38 and 40). Despite these different results there are some consistent relationships found within these early diverging crocodyliforms, including (*Orthosuchus* + *Protosuchus*), a strongly supported Gobiosuchidae and a weakly supported Shartegosuchidae (Figures 38 and 40) (Table 5). We find Thalattosuchia within Crocodyliformes and as sister to neosuchians in all of our equal weight analyses and several of our implied weight analyses with well-supported

TABLE 5 Groups found in analyses

	Grac equal: Of 8	Grac $k = 6,1$ 2,24: Of 4	Stag equal: Of 8	Stag $k = 12$, 24: Of 4	Stag $k = 6$: Of 2	Saur equal: Of 42	Saur $=-k = 12$ of 2	Saur $k = 24$: Of 2	Saur $k = 6$: Of 2	Post equal: Of 6	Post $k = 12$: Of 2	Post k = 24: Of 2	Post $k = 6$: Of 2
Erpetouchus + Dyoplax	71	74	51	NA	57	NA	NA	NA	NA	NA	NA	NA	NA
Sphenosuchia − monophyletic	NA	6	NA	10	NA	NA	NA	NA	NA	NA	NA	NA	NA
Litargosuchus + Terrestrisuchus	40	NA	31	NA	NA	21	NA	26	NA	35	NA	39	NA
Sphenosuchus + Hesperosuchus	NA	NA	NA	NA	NA	NA	19	NA	NA	NA	NA	NA	NA
Dibothrosuchus + Sphenosuchus	NA	NA	NA	NA	36	NA	NA	NA	40	NA	NA	NA	42
(Dib + Sphen) + Sol	NA	NA	NA	NA	38	NA	NA	NA	41	NA	NA	NA	48
Sphenosuchus + (Dibothrosuchus + Solidocrania)	9	9	12	NA	NA	NA	NA	9	NA	10	37	13	NA
Dibothrosuchus + (Hallopus + Solidocrania)	9	18	17	14	NA	14	23	15	NA	19	29	15	NA
Hallopus + Solidocrania	17	NA	21	NA	NA	16	53	21	NA	18	48	20	NA
Junggarsuchus + Phyllodontosuchus	NA	NA	NA	NA	63	NA	49	NA	69	NA	47	NA	63
Solidocrania	16	23*	13	17*	56	14	22	17	59	14	21	11	56
Macelognathus + (Almadasuchus + Crocodyliformes)	25	NA	23	NA	NA	24	28	35	NA	22	28	28	NA
Almadasuchus + Crocodyliformes	25	NA	23	NA	NA	23	27	35	NA	22	27	28	NA
Hallopodidae (Hallopus + [Macelognathus + Almadasuchus])	NA	NA	NA	NA	52	NA	NA	NA	55	NA	NA	NA	54
Macelognathus + Almadasuchus	NA	NA	NA	NA	38	NA	NA	NA	35	NA	NA	NA	38
Hallopodidae + Crocodyliformes	NA	NA	NA	NA	45	NA	NA	NA	49	NA	NA	NA	42
Crocodyliformes	90	35	79	23	96	79	96	99	28	79	90	92	37
Thalattosuchians + Crocodyliformes	NA	97	NA	98	NA	NA	NA	NA	97	NA	NA	NA	91
Protosuchia-monophyletic	48	61	54	53	NA	51	NA	55	48	54	NA	63	53
Protosuchidae	70	77	72	74	73	63	69	70	68	70	81	80	78

Note: NA indicates absence. When group is recovered, node support is given in parenthesis (xx). Implied weights given as $k = (x)$ followed by number of trees givens "of x". x* indicates the value of Solidocrania found in a monophyletic Sphenosuchia.

values (Table 5). This position implies several reversals in the braincase to more plesiomorphic conditions such as dorsally exposed prootics and a quadrate that does not contact the laterosphenoid. The synapomorphies for this group, include elements of the quadrate, braincase, mandible, skull roof, ulna and osteoderms (Table 3). When implied weights are used, mostly when $k = 12$ or 6, Thalattosuchia is found as the sister group to the odd grouping of *Hsisosuchus* + Crocodyliformes and Protosuchia is also monophyletic. This is an unusual position for *Hsisosuchus*, which is considered a mesoeucrocodylian (Li et al., 1994; Sereno et al., 2001; Wilberg et al., 2019), and this position for Thalattosuchia is also found with a monophyletic Protosuchia, a clade not recognized in analyses by Pol et al. (2004) and Wilberg (2015). The use of implied weights, $k = 12$, appears to break up *Goniopholis* and *Calsoyasuchus* (making the latter sister to Thalattosuchia), which suggests homoplastic character states support this monophyletic group.

Thalattosuchians, a clade of predatory marine crocodyliforms, have been found in various analyses as either the sister group to Crocodyliformes, a clade nested in Mesoeucrocodylia, in a longirostrine clade sister to tethysuchians and as sister clade to Neosuchia (Wilberg, 2015). In all of our equal weight analyses, implied weight analyses ($k = 12$ and 24) rooted on *Saurosuchus* and *Postsuchus* and implied weight analysis ($k = 6$) rooted on *Stagonolepis* we found Thalattosuchia forms the sister group to Neosuchia (Figures 38–40; Figures S1, S2, S4, S5, S7, S8). The support for this position ranges from scores of 53 to 66, with the highest support found in the *Stagonolepis* rooted equal weight analysis. This position is supported by nine unambiguous synapomorphies with several more depending on alternative topologies. This includes characters for the squamosal, quadrate, quadratojugal, skull roof, dentary, lateral temporal fenestra, ulna and osteoderms which alongside higher node support does suggest that this placement is not dependent on convergent "longirostrine" characters (Table 3). This position supports a single origin for the palatine secondary palate (with variation among "protosuchians") but also requires multiple reversals of character states, like the lack of contact between the laterosphenoid and quadrate and dorsal exposure of the prootic.

In all implied weight analyses rooted on *Gracilisuchus*, $k = 12$, 24 analyses rooted on *Stagonolepis* and $k = 6$ implied weight analyses rooted on *Saurosuchus* and *Postosuchus* Thalattosuchia is recovered as the sister group to *Hsisosuchus* + Crocodyliformes, with high support (91–98). This topology is recovered in analyses that find both monophyletic and paraphyletic "Sphenosuchia" (Figure 37; Figures S3, S6, and S9; Table 5). When Thalattosuchia is recovered in this position *Hsisosuchus* is found as the sister group to Crocodyliformes, an unusual position for a taxon considered to be closer to mesoeucrocodylian Crocodyliformes (Li et al., 1994; Sereno et al., 2001; Wilberg et al., 2019). *Hsisosuchus* is found as sister to Metasuchia in all other analyses we performed (9/16). When Thalattosuchia is placed outside Crocodyliformes, Protosuchia is recovered as a monophyletic clade which is similar to the results of Wilberg (2015) and Leardi et al. (2017) in which Thalattosuchia were found outside Crocodyliformes. The synapomorphies supporting this relationship can be found in Table 3. In general, this position is supported by parsimonious explanations of the evolution of features of skull sculpturing, the premaxilla, prefrontals, postorbitals, posttemporal fenestra, parietals, quadrate, quadratojugal, otoccipitals, braincase, basipterygoid processes, ectopterygoid, tooth crown serrations, the olecranon process of the ulna, the ischium, pubis and potentially osteoderms. This position requires several reversals in the evolution of the secondary palate including the position of the choanae and palatines, the evolution of the supratemporal fossa, quadrate orientation, pneumaticity of the basicranium, the retroarticular process and the glenoid surface of the coracoid.

In implied weights analyses ($k = 12$), rooted on *Saurosuchus* and *Postosuchus* and $k = 6$ rooted on *Stagonolepis*, the long snouted mesoeucrocodylian *Calsoyasuchus* was found as the sister taxon to Thalattosuchia (Figures 38 and 40; Figure S4). This node is not as well supported as the node that supports Neosuchia + Thalattosuchia (values range from 18 to 33) (Table 5) and is supported by two unambiguous synapomorphies of the jugal and postorbital (Table 3). In all other analyses, *Calsoyasuchus* is found as the sister taxa to *Goniopholis* (Figures 37 and 39; Figures S1, S2, S3, and S5–S9), which is consistent with earlier analyses (De Andrade et al., 2011; Wilberg et al., 2019). This position is better supported with scores ranging from 49 to 58 (Table 5). This clade is supported by four unambiguous synapomorphies (Table 3).

In equally weighted analyses and implied weights analyses ($k = 12$) rooted on either *Saurosuchus* or *Postosuchus*, *Hsisosuchus chungkingensis* is found as the sister taxon to *Simosuchus* + *Baurusuchus* (Figure 39; Figures S5, S7, S8). Support for this node ranges from 20 to 29 (Table 5) and is supported 6 unambiguous synapomorphies (Table 3). In all other analyses, *Hsisosuchus* is found as a mesoucrocodylian and the sister taxa to Metasuchia (Figures 37, 38, and 40; Figures S1–S4, S6, S9). Support for this node is higher, ranging from 67 to 77, and is consistent with earlier analyses (Bronzati et al., 2012).

An additional set of analyses was performed (the identical four rooting schemes with equal and implied weights) with all characters treated as unordered. While the implied weight results are largely similar, generally analyses using equal weights with nonadditive characters produced divergent results. The trees rooted on *Gracilisuchus*, using implied weights, are very similar to those found with ordered characters. Sphenosuchia is found as a monophyletic sister group (support of 13) to Thalattosuchia, (*Hsisosuchus* + Crocodyliformes) is found with low support, and the gracilisuchid *Yonghesuchus* is the sister taxon to this monophyletic Sphenosuchia (support of 23) (Figures S3, S10, and S11). This would make *Yonghesuchus* a crocodylomorph, which is divergent from the original gracilisuchid assignment. In the equal weight analyses, *Yonghesuchus* is found as sister to *Dibothrosuchus* and is found as the sister group to a polytomy of *Hallopus*, *Phyllodontosuchus*, *Junggarsuchus*, *Macelognathus* and *Almadasuchus* (Figure S10). In the implied weight analyses that did not use ordered characters rooted on *Gracilisuchus* and *Stagonolepis* (with a monophyletic Sphenosuchia), *Kayentasuchus* is also found as a member of Solidocrania, sister to *Phyllodontosuchus* (Figures S11, S13, S14). This relationship is weakly supported (support of 7) by the following character states: the presence of a thin, but not narrow posterior edge of the supratemporal fenestra; (Char. 20-1); the medial margins of the supratemporal fenestra separated by a flat plate (Char. 194-0); the anterior maxillary teeth are similar in size to the posterior maxillary teeth (Char.375-0). Further up the tree Thalattosuchia is found as the sister clade to Crocodyliformes (with high support of 94), which has been found in previous analyses (Clark, 1994; Leardi et al., 2017; Wilberg, 2015). *Hsisosuchus* is found to be the most basal crocodyliform, outside a monophyletic (support of 53) "Protosuchia" + Metasuchia (support of 16). Relationships among "protosuchians" remain similar (e.g., the composition of gobiosuchids, shartegosuchids and protosuchids) when the clade is found to be monophyletic (Figure 37, Figure S3) when rooted on *Gracilisuchus* and *Stagonolepis* but paraphyletic when rooted on *Saurosuchus* and *Postosuchus*. The relationship of *Hsisosuchus*, protosuchians and metasuchians is highly unusual and poorly supported. These relationships are also found when character weights are treated as equal, which differs from the results of the analysis with ordered characters, where "Sphenosuchia" is paraphyletic.

The results above are largely similar to those found when the un-ordered implied weights analysis is rooted on *Stagonolepis*, with the exception of analyses when $k = 6$, where in the un-ordered analysis, the topology is largely similar to those found when rooted on *Gracilisuchus* and does not recover a paraphyletic "Sphenosuchia" or "Protosuchia," which are recovered in the ordered character analysis (Figures S12 and S13). Similar to the result rooted on *Gracilisuchus*, the equal weight analyses diverge in similar ways. The un-ordered analyses rooted on *Saurosuchus* fail to recover a paraphyletic "Sphenosuchia" and Solidocrania, and relationships between non-crocodyliform crocodylomorphs are poorly resolved. In equal weight analyses rooted on *Saurosuchus* a paraphyletic "Protosuchia" is recovered with a monophyletic Sphenosuchia (Figure S14). When implied weights were used non-crocodyliform crocodylomorphs are found in a massive polytomy outside Crocodyliformes (Figures S15). Un-ordered analyses rooted on *Postosuchus* are largely congruent with analyses carried out with ordered characters in which "Sphenosuchia" is paraphyletic, Solidocrania is recovered as including crocodyliforms and Thalattosuchia is nested within mesoeucrocodylians (Figures S16 and S17).

6 | DISCUSSION

6.1 | *Junggarsuchus* and the evolution of the crocodyliform skull

The features that unite *Junggarsuchus* with Crocodyliformes are largely related to the reorganization of the skull, specifically strengthening it for more powerful bite force (Clark, Xu, Forster, & Wang, 2004). When compared to the conditions in *Dibothrosuchus*, they demonstrate a gradual shift from the earlier diverging crocodylomorphs like *Dibothrosuchus* to crocodylomorphs closer to Crocodyliformes, like *Almadasuchus*. Whereas the quadrate is free ventrally in other non-crocodyliform crocodylomorphs, in *Junggarsuchus*, the otoccipital contacts the ventral part of the quadrate (Char. 237-1), as in early diverging Crocodyliformes and *Almadasuchus*. The broad contact of the quadrate, squamosal, and otoccipital lateral to the cranioquadrate canal helps form a larger more solid occiput (Char. 175-2). The posterior exit of the cranioquadrate canal appears to be completely enclosed by the otoccipital similar to the condition seen in *Almadasuchus*, but differing from the condition seen in crocodyliforms (in which the exit for the canal is enclosed between the quadrate and otoccipital) (Leardi et al., 2020). Char. 270-1 is related to this; the expansion of the parabasisphenoid moves the otoccipital laterally. Although the parabasisphenoid is expanded and filled with airspaces in *Sphenosuchus* and *Dibothrosuchus*, it is even larger in *Junggarsuchus* as in early diverging Crocodyliformes such as *Protosuchus*. This caused the

occipital exposure of the bone to increase in size, forming yet another buttress to the skull along the medial surface of the quadrate. *Junggarsuchus*, as well as *Almadasuchus* and Crocodyliformes, possess a contact between the posterdorsal surface of the quadrate and the squamosal that closes the otic recess posteriorly and further contributes to reduction of kinesis in the skull and the solidification of the occiput (Char. 174-1) (Pol et al., 2013). The reduction of the size of the antorbital fenestra in the rostrum may also be related to the solidification of the skull and reduction of cranial kinesis (Witmer, 1997). Within early diverging crocodyliforms, as the secondary palate becomes anteroposteriorly elongate and involves the pterygoids, the antorbital fenestra becomes reduced, limiting the open space in the skull. The anterior process of the ectopterygoid projecting along the surface of the jugal can also be interpreted as a step toward the solidification of the palate (Char. 296–0), which is not seen in *Dibothrosuchus*.

In *Junggarsuchus*, as well as Crocodyliformes, the otoccipitals make contact directly ventral to the supraoccipital, forming the dorsal margin of the foramen magnum (Char. 236-2). In all of these taxa, the occipital region of the parietal is reduced, becoming narrow between the squamosal and supraoccipital. With the otoccipitals closing in the mid-occipital region of the skull, these preclude the participation of the other bones in that area, namely the parietal and the supraoccipital. In other non-crocodyliform crocodylomorphs, the supraoccipital alone borders the foramen magnum. Moreover, other species like *Sphenosuchus* and *Dibothrosuchus* also have a relatively wider occipital contribution from the parietal, which contacts the supraoccipital on a vertical median suture. We also observe that the quadrate approaches, but does not contact, the laterosphenoid in *Junggarsuchus*, another important feature in the restriction of cranial kinesis in non-crocodyliform crocodylomorphs.

Not all of the morphological shifts from more early diverging non-crocodyliform crocodylomorphs to Solidocrania are obviously involved in the increased bracing of the skull though, such as the presence of additional quadrate fenestrae, the near exclusion of the nasal's contact with the lacrimals and the presence of two large palpebrals.

6.2 | Pneumaticity in the quadrate and braincase of *Junggarsuchus*

The pneumatic features of the quadrate (and possibly the pterygoid) and braincase of *Junggarsuchus* may be related to the strengthening of the skull. First, the pneumatized quadrate (or pterygoid) expanded the body of the bone and may have acted similar to the expanded parabasisphenoid, helping to form an additional medial buttress to the quadrate shafts (Char. 285-1). However, this explanation is complicated as the function of the extensive paratympanic pneumatization in crocodilians is not currently understood. We cannot conclude any inference on the role of braincase pneumaticity in *Junggarsuchus* based upon conflicting explanations and the possible non-adaptive nature of cranial sinuses. Some early explanations for skull pneumatization have been proposed including shock absorption (Buhler, 1986; Verheyen, 1953) or that it is a strategy to maximize the strength of an element while reducing weight and material that contribute to it (Buhler, 1986). However, Witmer (1997) showed these explanations lacked demonstrable evidence and in turn proposed that at least the initial development of pneumatic spaces in the skull are nonadaptive and instead the cranial pneumaticity is driven by the invasive nature of the cranial sinuses, and the bone around them is deposited in a way to maintain structural integrity. The role of skull pneumatization in shock absorption is further called into question by the work of Dufeau (2011), who demonstrated that an increase in jaw adductor muscle volume in extant crocodilians appears to lead to reduced anterior braincase pneumatization. *Junggarsuchus* has extensive pneumaticity in its braincase but also a lateral ridge on the angular for the insertion of the *M. pterygoideus* that is similar to that seen in extant neosuchians, suggesting the pneumaticity has an unrelated function or is possibly non-adaptive. Due to the uncertain borders of the pneumatic medial expansion that we describe as in the quadrate (but are possibly in the pterygoid), it is difficult to confidently compare the condition of the pterygoid process of the quadrate to the condition seen in *Dibothrosuchus* or *Sphenosuchus* where the anterior process of the pterygoid is not firmly sutured to the pterygoid. If this pneumatic medial complex is not the quadrate, but the pterygoid it may help to further strengthen the palate and the braincase relative to the quadrate.

Junggarsuchus appears to demonstrate a derived condition for the path of the pharyngotympanic canal relative to other non-crocodyliform crocodylomorphs, even those found to be closer related to crocodyliforms like *Almadasuchus* (Leardi et al., 2020). *Junggarsuchus* features a rhomboidal recess that appears to communicate with the basioccipital recess, which suggests that the pathway of the pharyngotympanic canal is more similar to that seen in crocodyliforms (Kuzmin et al., 2021) than non-crocodyliform crocodylomorphs like *Dibothrosuchus* (Wu & Chatterjee, 1993) and *Almadasuchus* (Leardi et al., 2020). No lateral exit for the pharyngotympanic

canal, like that seen in *Dibothrosuchus*, is reported in *Junggarsuchus*. However, the inference of this derived condition is complicated by the uncertain nature of the exit of the pharyngotympanic canal. While the canal seems to enter the basioccipital recess and meets the median pharyngotympanic canal, an exit between the basioccipital and parabasisphenoid as seen in crocodyliforms is not obvious (Kuzmin et al., 2021; Porter et al., 2016). A ventral slit between the basioccipital and parabasisphenoid has been tentatively identified as a possible exit, but we cannot confidently state that this space is not due to deformation.

6.3 | Unique cranial features of *Junggarsuchus* among non-crocodyliform crocodylomorphs

Although the skull of *Junggarsuchus* had begun to resemble the strongly reinforced skull of living crocodylians, as indicated by the features uniting it to Crocodyliformes in our phylogenetic analyses, it has a number of interesting autapomorphies not seen in any other non-crocodyliform crocodylomorphs or pseudosuchian outgroups. In the skull, some of these features seem to be related to further strengthening the skull and possibly increasing bite force. The area for the insertion of the *M. pterygoideus ventralis* on the lateral surface of the angular present in *Junggarsuchus* is not seen in other non-crocodyliform crocodylomorphs and is seen in later crocodyliforms, like *Alligator mississippiensis*, though the condition in *Almadasuchus* and *Macelognathus* is not known. This expanded area indicates an increased area for the adductor muscles of the jaw, likely related to an increase in jaw strength. The jugal is dorsoventrally tall and arched below the infratemporal fenestra, likely due to the arching of the dorsal surface of the surangular (Char. 339-1), which may be related to the action of jaw muscles, like the *M. adductor mandibulae externus superficialis* which inserts on the dorsal surface of the surangular in extant crocodylians (Holliday et al., 2013). This may be related to an increase in bite strength as it is one of the jaw adductor muscles in living crocodylians (Holliday et al., 2013). The mandibular fenestra is also increased in anteroposterior length compared to other non-crocodyliform crocodylomorphs such as *Dibothrosuchus* (Figure 30) and may have allowed for more muscle insertion on the mandible like the *M. intermandibularis* and *M. adductor mandibulae posterior* (Holliday et al., 2013). However, the function of other autapomorphies is less clear, including an unusual possible additional palatine fenestration and a laterally closed opening for the caniniform tooth of the dentary, the presence of a prefrontal overhang, the lack of a squamosal ridge on the dorsal surface of the supratemporal fossa, additional quadrate fenestra, a theropod-like surangular foramen and a dorsally enclosed canal for the temporo-orbital artery running the anteroposterior length of the prootic.

6.4 | Evidence for cursoriality in the postcranial skeleton and inner ear of *Junggarsuchus*

The postcranial autapomorphies may be related to its increased cursoriality relative to other non-crocodyliform crocodylomorphs (Clark, Xu, Forster, & Wang, 2004). The first of these autapomorphies is the anterior edge of the scapular blade is larger than the posterior, which may provide more room for the attachment of arm retractor muscles. The outer digits are reduced, similar to cursorial mammals (Hildebrand & Goslow, 2001). The radius is also slightly longer than the humerus, and the olecranon process of the ulna is very low. The glenoid surface of the coracoid is extended on a posterovertical plane as in some other non-crocodyliform crocodylomorphs like *Dibothrosuchus* and *Dromicosuchus* (Sues et al., 2003). This is interpreted as an adaptation that moved the arms under the body and allowed for a more cursorial lifestyle (Clark, Xu, Forster & Wang, 2004). Further characters include the absence of osteoderms (Char. 477-1), that the first manus digit flexes toward digit II, facing laterally as opposed to ventrally as in other crocodylomorphs (Char. 433-1), and the first metacarpal is more slender than the second metacarpal (Char. 434-1). The lack of osteoderms may have allowed a greater range of movement while the reduced digits are indicative of animals that are highly cursorial (Coombs, 1975). Other features that are related to this form of locomotion are a ventrally or posteroventrally facing glenoid fossa; the large, perpendicularly facing humeral head, allowing the humerus to be held in a nearly vertical position; and the flattened distal end of the ulna, which forms a straight joint along with two flattened distal carpals that place the wrist in line with the rest of the forelimb (Clark, Xu, Forster, & Wang, 2004). Vertical zygapophyses may also be indicative of higher degrees of sagittal bending (Boszczyk et al., 2001) and reduced lateral undulation (Sumida, 1997), as opposed to modern crocodylians, whose locomotion has a larger horizontal element. The procoelous vertebrae and hypapophyses on the cervical and anterior dorsal vertebrae are less obvious in their possible role, though such structures are known

to serve as the attachment point for the *longus colli* muscles in snakes (Gasc, 1981).

The endosseous labyrinth of the inner ear of *Junggarsuchus* provides further evidence for a terrestrial, active lifestyle. The labyrinth, especially the anterior semicircular canal, is dorsoventrally tall and narrow, unlike the low, broad semicircular canals of semiaquatic and marine crocodylomorphs. These tall, narrow canals are believed to be related to head and gaze stabilization, which would need to be more developed in terrestrial, running forms, but less so in forms that can orient their entire body suspended in water (Schwab et al., 2020). While this provides evidence of a terrestrial lifestyle, the semicircular canals of *Junggarsuchus*, a crocodylomorph which appears to have several cursorial adaptations, do not differ in their morphology from other terrestrial, presumably less cursorial crocodylomorphs like *Protosuchus*. This suggests that while the semicircular canals may be informative of general mode of life, they cannot be used to infer a more cursorial lifestyle in crocodylomorphs.

Like *Almadasuchus*, but unlike extant crocodylians (Leardi et al., 2020), *Junggarsuchus* possesses a distinct floccular recess. A floccular recess and elongate anterior semicircular canal have been hypothesized to indicate the presence of a mechanism mediated by the vestibulo-ocular and vestibulochollic reflexes for stabilization of the head, eye and neck (Sookias et al., 2020; Witmer et al., 2008). Such features for stabilizing the movement of the head and eyes are hypothesized to be related to active hunting and navigating complex environments (Bronzati et al., 2017; Dudley & Yanoviak, 2011; Vasilopoulou-Kampitsi et al., 2019). This anatomy is consistent with our reconstruction of *Junggarsuchus* as an active terrestrial predator. This anatomy of the anterior semicircular canal and floccular recess, while absent in living crocodylians, is known not only in other crocodylomorphs but more distantly related archosauriforms like *Euparkeria* (Sookias et al., 2020). This is consistent with the hypothesis that crocodylomorphs were ancestrally active terrestrial predators (Leardi et al., 2020), inheriting this anatomy and lifestyle from more ancient archosauriform ancestors and that this anatomy was lost as the clade evolved to semiaquatic and marine niches (Schwab et al., 2020).

6.5 | Ghost lineages of Jurassic Solidocranians

Although *Junggarsuchus*, *Macelognathus*, and *Almadasuchus* show the gradual acquisition to traits in the skull related to the bracing of the braincase, the age of these three taxa is substantially younger than the oldest Crocodyliformes and results in long ghost lineages for the non-crocodyliform crocodylomorphs closest to Crocodyliformes. These three taxa are all from the Late Jurassic, *Junggarsuchus* and *Almadasuchus* from the Oxfordian (Eberth et al., 2001; Leardi et al., 2017; Pol et al., 2013), whereas the oldest crocodyliforms are known from the Late Triassic, no younger than 213 mya (Kent et al., 2014; Martínez et al., 2019). As these taxa form the immediate outgroups of crocodyliforms, this creates a nearly 50-million-year long ghost lineage in *Junggarsuchus* and similarly long ones in *Hallopus*, *Macelognathus*, and *Almadasuchus*, depending on the precise phylogeny. This suggests that these changes in morphology evolved in the Late Triassic, and that *Junggarsuchus* and the three other genera are late surviving members of the organisms in which these traits arose. The discovery of Late Triassic forms similar to *Junggarsuchus* and these genera would help to support this idea (Figure 40).

6.6 | Features in *Dibothrosuchus* related to the evolution of the Crocodyliform cranium

Dibothrosuchus is not the most early diverging non-crocodyliform crocodylomorph and in many of our analyses is found as sister to *Hallopus* + Solidocrania, a relationship reported in some previous analyses (Clark, Xu, Forster, & Wang, 2004; Leardi et al., 2017; Wilberg, 2015). In addition to the unique traits it possesses, such as its massively expanded prootic, *Dibothrosuchus* also demonstrates several important traits in the transition from even more early diverging non-crocodyliform crocodylomorphs to Solidocrania, which may be related to the strengthening of the skull such as the absence of an inter-parietal suture, a well-developed flooring of the supratemporal fossa, and a straight occipital portion of the parietals. *Dibothrosuchus* also has the quadrate fenestra bounded solely by the quadrate which may also help provide integrity to the structural quadrate. Some of these features are also found in *Sphenosuchus* (Walker, 1990) and we found limited support in resampling for nodes and in synapomorphies for both *Dibothrosuchus* +- *Sphenosuchus* (Figure 38; Figures S6 and S9) (Tables 3 and 5) a relationship found in some earlier analyses (Clark et al., 2001; Wilberg, 2015) and alternatively (*Sphenosuchus* + [*Dibothrosuchus* + Solidocrania]) (Figure 40, Figures S1, S2, S5, S7, S8) which has also been reported in some previous phylogenetic analyses (Clark, Xu, Forster, & Wang, 2004; Leardi et al., 2017). An interesting autapomorphy of *Dibothrosuchus* that may be involved in the solidification of the skull is the bracing of the palate by the descending process of the prefrontal (Char. 116-1), though this feature is absent in *Junggarsuchus*.

6.7 | Survey of the coronoid in non-crocodyliform crocodylomorphs

Elongate coronoids medial to the dentary are found widely in non-crocodyliform crocodylomorphs. Long, blade-like coronoids in non-crocodyliform crocodylomorph have been reported in *Sphenosuchus* (Walker, 1990) and *Dromicosuchus* (Sues et al., 2003). An elongate coronoid dorsal to the splenial is a trait that occurs widely across non-crocodyliform crocodylomorphs, present also in *Junggarsuchus*, *Kayentasuchus* and *Dibothrosuchus* based on our personal observations but previously unreported. Elongate coronoids are not present in crocodyliforms except thalattosuchians, in which they reach from the posterior end of the dentary tot at least the caudal most alveoli of the dentary, though are not as long as those seen in most non-crocodyliform crocodylomorphs, where the coronoid reached the third or fourth dentary tooth (Young & Andrade, 2009). An elongate bone similar to the coronoids described here has been reported in sauropodomorphs, basal theropods, tyrannosaurids, abelisaurids and dromaeosaurs (Hurum & Currie, 2000; Sampson & Witmer, 2007). It is referred to as a "supradentary" in tyrannosaurids (Sampson & Witmer, 2007), but this identification is likely inaccurate (Walker, 1990). The functional result of the elongation of this bone is poorly understood, though it has been suggested that it plays a role in reinforcing the mandible (Hurum & Currie, 2000).

6.8 | Terrestrisuchus and Litargosuchus

Some of our analyses recovered a clade in the early diverging members of non-crocodyliform crocodylomorphs comprised of *Terrestrisuchus*, which would include its possible junior synonym, *Saltoposuchus* (Benton & Clark, 1988) and *Litargosuchus* (Figure 39). In addition to the synapomorphies found (Table 3, Supplementary Document S1) these two taxa share digitigrade forelimbs, with long, slender metacarpals are considered to be shared among these taxa, whereas other taxa have somewhat stouter digits that may have contacted the ground differently when walking (Sereno & Wild, 1992). However, this digitigrade condition with slender metacarpals has been observed in other non-crocodyliform crocodylomorphs where a manus was found articulated (when articulated the manus was compressed) as in *Saltoposuchus*, *Hesperosuchus*, *Terrestrisuchus* (Crush, 1984), *Hallopus* (Walker, 1970), *Dibothrosuchus* (Wu & Chatterjee, 1993), and *Junggarsuchus*. Overall, their skeletons are all in the lower range of sizes for "sphenosuchians", yet *Junggarsuchus* is also small, with a skull length of 141 mm and humerus to metacarpal length of 29 cm, compared to some of the larger taxa like *Hesperosuchus* (CM 29894) which has a skull length of 195 mm and a humerus to metacarpal forelimb height of 30.8 cm tall (Clark et al., 2001), so the similarity between these gracile taxa may not simply be the result of allometric differences, as proposed by some authors (Clark et al., 2001).

6.9 | The relationships of *Kayentasuchus*

The position of *Kayentasuchus* was not clarified despite several more identified derived traits, like a trigeminal recess, and a posteriorly closed otic recess. Additionally, an intertympanic recess in the lateral surface of the prootic is present in *Kayentasuchus*, though this character state may be a feature shared by early diverging crocodylomorphs. The posterior section of the skull of *Kayentasuchus* is not completely preserved, and as many key elements in the evolution of the crocodylomorph skull are located in the braincase, *Kayentasuchus* is missing critical information that would be essential in better resolving its relationships (Clark & Sues, 2002). However, one of the characters that supported Nesbitt (2011) placement of *Kayentasuchus* as sister to crocodyliforms, the posterior process of the maxilla (Nesbitt's character 2), is problematic. Leardi et al. (2017) found that the character states were poorly defined, and that taxa with similar morphologies of the posterior process of the maxilla were scored for different character states. This character was omitted by Leardi et al. (2017) and *Kayentasuchus* was found in an earlier diverging position. The prootic is obscured in *Terrestrisuchus* which makes determining the condition in early diverging crocodylomorphs difficult (Leardi et al., 2020) and the intertympanic recess is known in other early diverging crocodylomorphs like *Hesperosuchus* though the condition of this recess is unclear (Clark et al., 2001). Not enough of the rest of the anatomy is known to clarify this taxon's relationships beyond the basal polytomy of non-crocodyliform crocodylomorphs.

6.10 | Impact of weighting and outgroup selection on the relationships of non-crocodyliform crocodylomorphs

Despite the numerous rooting schemes, in all analyses we consistently find the grouping of Solidocrania, where the clade is defined as (*Junggarsuchus* (*Macelognathus* [*Almadasuchus* + Crocodyliformes])), (*Junggarsuchus* (Hallopodidae+Crocodyliformes) or a polytomy when Sphenosuchia is monophyletic, the prior two which are

similar to the relationships reported in previous analyses (Clark, Xu, Forster, & Wang, 2004; Leardi et al., 2017; Wilberg, 2015) (Figures 37–40 and all supplementary figures). The major effects of changes to the outgroup sampling were on the monophyly of "Sphenosuchia," which was found as monophyletic in implied weight analyses rooted on *Gracilisuchus* and *Stagonolepis* (Figure 37 and Figure S3). Several differences in our analyses came from changing weighting schemes. In all of our equal weight analyses we find non-crocodyliform crocodylomorphs as a paraphyletic assemblage with Solidocrania that contains Crocodyliformes, *Phyllodontosuchus* is found in the early diverging non-crocodyliform crocodylomorph polytomy (Figure 39), *Calsoyasuchus* is sister to *Goniopholis*, *Hsisosuchus* is sister to Ziphosuchia and *Litargosuchus* and *Terrestrisuchus* are sister taxa. This variation in the above relationships indicates that the latter relationships are supported by homoplastic characters. Variations in the k value of the implied weight analyses demonstrate that decreasing the k constant had some noteworthy effects on tree topology. Relationships between major groups recovered when $k = 12$ or 24 are largely the same. However, when homoplasy is most down weighted, where $k = 6$, results differ from other implied weight analyses (Table 5). With $k = 6$, we recover a monophyletic Hallopodidae, break up Protosuchia and find *Phyllodontosuchus* sister to *Junggarsuchus*.

When ordered characters are treated as nonadditive and analyses are rooted on *Gracilisuchus*, *Stagonolepis* or *Saurosuchus* (regardless of equal or implied weight) results are very different from those above, including Thalattosuchia as sister to crocodyliforms, protosuchians recovered as a monophyletic clade, *Hsisosuchus* as the most early diverging crocodyliform, and a monophyletic Sphenosuchia. These divergent results may be due to the use of non-ordered characters. In the analyses with ordered characters, those ordered characters are likely helping to give structure to the tree and break up "Sphenosuchia" but when states are nonadditive these transformative characters can be used to construct trees differently. However, when rooted on *Postosuchus*, using non-additive characters, we found the relationships of most of the paraphyletic sphenosuchians identical to those analyses using ordered characters, including the position of *Junggarsuchus* and the "hallopodids," though non-mesoucrocodylian crocodyliformes ("Protosuchians") are recovered as a monophyletic group. This result suggests that it may be the use of *Gracilisuchus* as the rooting taxa that generates these radically different results. A review of our characters demonstrates that several derived character states that are shared between gracilisuchids, some non-crocodyliform crocodylomorphs and crocodyliformes that are not seen in in those non-crocodyliform crocodylomorphs closer to crocodyliformes and the other outgroup taxon. These characters include an external nares subequal in length and width (Char. 7); a rounded antorbital fenestra (Char. 13); a supratemporal fenestra smaller than the orbit (Char. 15); a wide cranial table (Char. 45); large aligned neurovascular foramina on the lateral surface of the maxilla (Char. 80); the jugal is excluded from the antorbital fenestra (Char. 96); the jugal exceeds the posterior border of the infratemporal fenestra (Char. 111); v-shaped occipital margin of the parietal (Char. 195); a narrow occipital margin of the parietal (Char. 196); quadratojugal extends to contact the postorbital (Char. 222); five premaxillary teeth (Char. 368); lack of a postzygodiapophyseal laminae on the vertebra (Char. 492). These characters, when unordered, affect character polarity and so generate a crocodylomorph polytomy and pull *Hsisosuchus* and thalattosuchians down out of crocodyliformes.

The purpose of this comparative phylogenetic analysis is not to recommend a single weighting or rooting scheme, but to demonstrate how variations in these factors can demonstrate which relationships are more consistently found and those that are more likely to be affected by homoplasy, as discussed earlier. We find largely consistent support for a paraphyletic "Sphenosuchia" and Solidocrania in both the paraphyletic and monophyletic "Sphenosuchia." The time calibrated tree (Figure 40) was constructed from our analysis rooted on *Postosuchus kirkpatricki* that used implied weights of $k = 12$ and 41 ordered characters. In this analysis, we find "Sphenosuchia" is paraphyletic as are "Protosuchians." *Dibothrosuchus* is found sister to Solidocrania and Hallopodidae is broken up and *Almadasuchus* is the sister taxa to Crocodyliformes. Thalattosuchians are recovered as Crocodyliformes. Rooting taxa on *Gracilisuchus* should be the preferred scheme as it is the scheme in which the most taxa are included; however, this scheme generates highly irregular results, where *Hsisosuchus* is found as the sister taxon to all of Crocodyliformes, when implied weights are used (Figure 37 and Supplementary Figures S2, S7–S10). While we recommend future researchers try several rooting schemes for their analyses, *Postosuchus* is the outgroup taxon that has been most consistently recovered as the sister to crocodylomorphs (Nesbitt, 2011) and produces well supported clades that are consistent with those found by other researchers (Clark, Xu, Forster, & Wang, 2004; Leardi et al., 2017; Wilberg, 2015; Wu & Chatterjee, 1993). We also recommend using both implied and equal weighting to investigate the influence of homoplasy on a dataset, but an implied weighting scheme of $k = 12$ is supported as simulation studies when the true tree was known outperformed others when homoplasy was more

severely downweighted with this k value (Goloboff, 1993; Goloboff et al., 2017). We also recommend maintaining the 41 ordered characters. Ordering of characters is justified by the similarities among the states (Lipscomb, 1992) but in the specific context of this matrix, the unordered characters often produce highly irregular trees with a collection of relationships that are not supported by any other crocodylomorph analyses (Leardi et al., 2017, Wilberg, 2015), in which *Hsisosuchus* is sister to Crocodyliformes, Thalattosuchia is outside Crocodyliformes, "Sphenosuchia" and "Protosuchia" are monophyletic (Table 2, Figures S2–S17, Supplementary Document S1).

7 | CONCLUSIONS

We find that Solidocrania is supported by a number of cranial synapomorphies related to the strengthening of the skull on the way to the crocodyliform condition. *Junggarsuchus* exhibits derived traits shared by *Almadasuchus*, *Macelognathus* and Crocodyliformes as well as autapomorphies similarly related to the skull and also related to a cursorial lifestyle. The features of the skull demonstrate the transition of the skull from more early diverging non-crocodyliform crocodylomorphs to that of Crocodyliformes. We also report that the elongate coronoid reported in some non-crocodyliform crocodylomorphs is present widely through the group as well as an apomorphy in thalattosuchians (Young & Andrade, 2009), but is absent in other Crocodyliformes. *Dibothrosuchus* is found to be closer to Solidocrania than other non-crocodyliform crocodylomorphs with the exception of *Hallopus*, though it lacks many of the synapomorphies. The position of *Hallopus* is based solely on postcranial characters and may belong within Solidocrania, but the lack of cranial material does not allow for this to be tested. We find that Hallopodidae is broken up in our analyses as *Almadasuchus* shares more features with Crocodyliformes than does *Macelognathus*, and *Hallopus* does not form a clade with either of them. The exception to this aforementioned topology is when homoplasy is most severely down weighted ($k = 6$) and Hallopodidae is found as a monophyletic clade including *Hallopus*, *Macelognathus* and *Almadasuchus*. We find limited support for (*Litargosuchus* + *Terrestrisuchus*) and (*Dibothosuchus* + *Sphenosuchus*). While we find a monophyletic Protosuchia in many of our analyses, the changes it makes to the tree and the relatively low support of the clade do not allow us to make a compelling case for the clade's monophyly. In addition, we find that the paraphyletic assemblage of protosuchians recovered when homoplasy is downweighted is better supported, and Crocodyliformes is better supported in this relationship (Table 5). We also found thalattosuchians most commonly nested in Crocodyliformes, and sister to neosuchians, a position that simplifies the evolution of the secondary palate, but requires reversals to plesiomorphic character states in the braincase and coronoid.

AUTHOR CONTRIBUTIONS

Alexander Ruebenstahl: Formal analysis (lead); investigation (lead); validation (supporting); writing – original draft (lead); writing – review and editing (equal). **Xing Xu:** Conceptualization (supporting); funding acquisition (supporting); resources (equal); writing – review and editing (supporting). **Michael Klein:** Investigation (supporting); writing – original draft (supporting). **Hongyu Yi:** Investigation (supporting); resources (supporting); writing – review and editing (supporting). **James Clark:** Conceptualization (lead); data curation (equal); funding acquisition (lead); project administration (lead); resources (lead); supervision (lead); validation (lead); writing – original draft (supporting); writing – review and editing (equal).

ACKNOWLEDGMENTS

The authors thank Catherine Forster, Andrew Moore, and especially Joseph Stiegler for their help in this project, and Juan Martin Leardi, Sterling Nesbitt and Wu Xiao-chun for extremely helpful reviews. The authors also thank the George Washington University, the Institute of Vertebrate Paleontology and Paleoanthropology, the University of California Museum of Paleontology, the Carnegie Museum of Natural History, the Evolutionary Studies Institute of the University of the Witwatersrand, the Yale Peabody Museum, and the American Museum of Natural History for access to specimens. Thanks to the Hennig Society for providing TNT. The skull of *Junggarsuchus* was prepared by Wang Hai-jun. Thanks to Jonah Choiniere and Christel Velasco for taking many of the photographs in our accessory data and in our text. Thanks to Bhart-Anjan Bhullar for access to VG studios.

DATA AVAILABILITY STATEMENT

The list of characters, character scorings, accessory figures, reduced resolution CT data and skull STLs are all available on Dryad at (link to be given after submission of MS).

ORCID

Alexander A. Ruebenstahl https://orcid.org/0000-0002-2852-0265

James M. Clark https://orcid.org/0000-0003-0980-4315

REFERENCES

Alcober, O. (2000). Redescription of the skull of *Saurosuchus galilei* (Archosauria: Rauisuchidae). *Journal of Vertebrate Paleontology*, *20*(2), 302–316.

Allen, D. (2003). When *Terrestrisuchus gracilis* reaches puberty, it becomes *Saltoposuchus connectens*! *Journal of Vertebrate Paleontology*, *23*, 29A.

Andrews, C. W. (1913). *A descriptive catalogue of the marine reptiles of the Oxford clay* (p. 206). British Museum (Natural History).

Benton, M. J., & Clark, J. M. (1988). Archosaur phylogeny and the relationships of the Crocodylia. In M. J. Benton (Ed.), *The phylogeny and classification of the tetrapods, volume 1: Amphibians, reptiles, birds*, Systematics Association Special (Vol. 35A, pp. 295–238). Clarendon Press.

Bonaparte, J. F. (1969). *Dos nuevas 'faunas' de reptiles Triasicos de Argentina* (Vol. 2, pp. 283–306). Gondwana Stratigraphy (IUGS Symposium, Buenos Aires).

Bonaparte, J. F. (1971). Los tetrapodos del sector superior de la Formacion Los Colorados, La Rioja, Argentina. *Opera Lilloana (Fund. Miguel Lillo)*, *22*, 1–183.

Bonaparte, J. F. (1984). Classification of the Thecodontia. *Geóbios, Mémoire Spéciale*, *6*, 99–112.

Boszczyk, B. M., Boszczyk, A. A., & Putz, R. (2001). Comparative and functional anatomy of the mammalian lumbar spine. *The Anatomical Record*, *264*, 157–168.

Bronzati, M., Benson, R. B., & Rauhut, O. W. (2017). Rapid transformation in the braincase of sauropod dinosaurs: Integrated evolution of the braincase and neck in early sauropods? *Palaeontology*, *61*, 289–302.

Bronzati, M., Montefeltro, F. C., & Langer, M. C. (2012). A species-level supertree of Crocodyliformes. *Historical Biology*, *24*(6), 598–606.

Brown, B. (1933). Ancestral crocodile. *American Museum Novitates*, *683*, 1–4.

Buhler, P. (1986). Das Vogelskelett-hochentwickelter Knochen-Leichtbau. *Arcus*, *5*, 221–228.

Butler, R. J., Sullivan, C., Ezcurra, M. N. D., Liu, J., Lecuona, A., & Sookias, R. B. (2014). New clade of enigmatic early archosaurs yields insights into early pseudosuchian phylogeny and the biogeography of the archosaur radiation. *BMC Evolutionary Biology*, *14*(1), 128.

Chatterjee, S. (1985). *Postosuchus*, a new thecodontian reptile from the Triassic of Texas and the origin of tyrannosaurs. *Philosophical Transactions of the Royal Society*, *309*, 395–460.

Choiniere, J. N., Clark, J. M., Norell, M. A., & Xu, X. (2014). Cranial osteology of *Haplocheirus sollers*. *American Museum Novitates*, *3816*, 1–44.

Clark, J.M. (1986). *Phylogenetic relationships of the crocodylomorph archosaurs*. Unpublished PhD Dissertation, The University of Chicago, Chicago.

Clark, J. M. (1994). Patterns of evolution in Mesozoic Crocodyliformes. In N. C. Fraser & H. D. Sues (Eds.), *In the shadow of the dinosaurs: Early Mesozoic tetrapods*. Cambridge University Press.

Clark, J. M. (2011). A new shartegosuchid crocodyliform from the upper Jurassic Morrison formation of western Colorado. *Zoological Journal of the Linnean Society*, *163*(s1), S152–S172.

Clark, J. M., Sues, H. D., & Berman, D. S. (2001). A new specimen of *Hesperosuchus agilis* from the upper Triassic of New Mexico and the interrelationships of basal crocodylomorph archosaurs. *Journal of Vertebrate Paleontology*, *20*, 683–704.

Clark, J. M., Xu, X., Eberth, D. E., Forster, C. A., Machlus, M., Hemming, S., Wang, Y., & Hernandez, R. (2006). The middle-to-late Jurassic terrestrial transition: New discoveries from the Shishugou formation, Xinjiang, China. In P. M. Barrett & S. E. Evans (Eds.), *9th international symposium, mesozoic terrestrial ecosystems and biota* (pp. 26–28).

Clark, J. M., Xu, X., Forster, C., & Eberth, D. (2004). New fossil vertebrates from the middle–late Jurassic Shishugou formation of Xinjiang, China. In *Proceedings of the XIXth international congress of zoology*. Zoological Society., Institute of Zoology, Chinese Academy of Sciences.

Clark, J. M., Xu, X., Forster, C. A., & Wang, Y. A. (2004). Middle Jurassic 'sphenosuchian' from China and the origin of the crocodilian skull. *Nature*, *430*, 1021–1024.

Clark, M., & Sues, H. D. (2002). Two new basal crocodylomorph archosaurs from the lower Jurassic and the monophyly of the Sphenosuchia. *Zoological Journal of the Linnean Society*, *136*, 77–95.

Colbert, E. H. (1952). A pseudosuchian reptile from Arizona. *Bulletin of the American Museum of Natural History*, *99*, 561–592.

Coombs, W. (1975). Theoretical aspects of cursorial adaptations in dinosaurs. *The Quarterly Review of Biology*, *53*(4), 393–418.

Crush, P. J. (1984). A late upper Triassic sphenosuchid crocodylian from Wales. *Palaeontology*, *27*, 131–157.

De Andrade, M. B., Edmonds, R., Benton, M. J., & Schouten, R. (2011). A new Berriasian species of *Goniopholis* (Mesoeucrocodylia, Neosuchia) from England, and a review of the genus. *Zoological Journal of the Linnean Society*, *163*, S66–S108.

Diogo, R. (2008). Comparative anatomy, homologies and evolution of mandibular, hyoid and hypobranchial muscles of bony fish and tetrapods: A new insight. *Animal Biology*, *58*, 123–172.

Drymala, S. M., & Zanno, L. E. (2016). Osteology of *Carnufex carolinensis* (Archosauria: Psuedosuchia) from the Pekin formation of North Carolina and its implications for early Crocodylomorph evolution. *PLoS One*, *11*(6), e0157528.

Dudley, R., & Yanoviak, S. P. (2011). Animal aloft: The origins of aerial behavior and flight. *Integrative and Comparative Biology*, *51*, 926–936.

Dufeau, D.L. (2011). The evolution of cranial pneumaticity in Archosauria: Patterns of paratympanic sinus development. Electronic Thesis or Dissertation, Ohio University.

Dufeau, D. L., & Witmer, L. M. (2015). Ontogeny of the middle-ear air-sinus system in *Alligator mississippiensis* (Archosauria: Crocodylia). *PLoS One*, *10*, e0137060.

Eberth, D. A., Brinkman, D. B., Chen, P. J., Yuan, F. T., Wu, S. Z., Li, G., & Cheng, X. S. (2001). Sequence stratigraphy, paleoclimate patterns and vertebrate fossil preservation in Jurassic–cretaceous strata of the Junggar Basin, Xinjiang autonomous region, People's Republic China. *Canadian Journal of Earth Sciences*, *38*, 1627–1644.

Fang, X. S., Pang, Q. Q., Lu, L. W., Zhang, Z. X., Pan, S. G., Wang, Y. M., Li, X. K., & Cheng, Z. W. (2000). Lower, Middle, and Upper Jurassic subdivision in the Lufeng region, Yunnan Province. In *Proceedings of the Third National Stratigraphical Conference of China, Beijing* (pp. 208–214). Geological Publishing House.

Fraas, O. (1877). Aetosaurus ferratus, die gepanzerte Vogelechse aus dem Stubensandstein bei Stuttgart. *Jahreshefte des Vereins für Vaterländische Naturkunde in Württemberg*, *33*, 1–21.

Gasc, J.-P. (1981). Axial musculature. In C. Gans & T. S. Parsons (Eds.), *Biology of the reptilia* (Vol. 11, pp. 355–435). Academic Press.

George, I. D., & Holliday, C. M. (2013). Trigeminal nerve morphology in *Alligator mississippiensis* and its significance for crocodyliform facial sensation and evolution. *Anatomical Record*, *296*, 670–680.

Göhlich, U. B., Chiappe, L. M., Clark, J. M., & Sues, H. D. (2005). The systematic positions of the late Jurassic alleged dinosaur *Macelognathus* (Crocodylomorpha: Sphenosuchia). *Canadian Journal of Earth Sciences*, *42*, 307–321.

Goloboff, P. A. (1993). Estimating character weights during tree search. *Cladistics*, *9*, 83–91.

Goloboff, P. A., & Catalano, S. A. (2016). TNT version 1.5, including a full implementation of phylogenetic morphometrics. *Cladistics*, *32*(3), 221–238. https://doi.org/10.1111/cla.12160

Goloboff, P. A., Farris, J. S., Källersjö, M., Oxelman, B., Ramírez, M. J., & Szumik, C. A. (2003). Improvements to resampling measures of group support. *Cladistics*, *19*, 324–332.

Goloboff, P. A., Torres, A., & Arias, J. S. (2017). Weighted parsimony outperforms other methods of phylogenetic inference under models appropriate for morphology. *Cladistics*, *34*, 1–31.

Goodrich, E. S. (1915). The chorda tympani and middle ear in reptiles birds and mammals. *Journal of Cell Science*, *242*, 137–160.

Gow, C. E. (2000). The skull of *Protosuchus haughtoni*, and early Jurassic crocodyliform form southern Africa. *Journal of Vertebrate Paleontology*, *20*, 49–56.

Gow, C. E., & Kitching, J. W. (1988). Early Jurassic crocodilomorphs from the Stormberg of South Africa. *Neues Jahrbuch fur Geologies und Palaontologie*, *1988*, 517–536.

Gradstein, F. M., Ogg, J. G., Schmitz, M. D., & Ogg, G. M. (Eds.) (2012). On the geologic time scale. In *The geological time scale 2012* (Vol. 2, p. 114). Elsevier.

Gradstein, F. M., Ogg, J. G., & Smith, A. G. (2004). *A geologic time scale 2004* (p. 589). University Press.

Harris, J. D., Lucas, S. G., Estep, J. W., & Jianjun, L. (2000). A new and unusual sphenosuchian (Archosauria: Crocodylomorpha) from the lower Jurassic Lufeng formation, People's Republic of China. *Neues Jahrbuch f Geolog Paläont, Abh*, *215*(1), 47–68.

Haughton, S. H. (1915). A new thecodont from the Stormberg beds. *Annals of the South African Museum*, *12*, 98–105.

Hay, O. P. (1930). *Second bibliography and catalogue of the fossil vertebrata of North America* (Vol. 2, p. 390). Carnegie Institute.

Herrera, Y., Leardi, J. M., & Fernandez, M. S. (2018). Braincase and endocranial anatomy of two thalattosuchian crocodylomorphs and their relevance in understanding their adaptations to the marine environments. *PeerJ*, *6*, e5686.

Hildebrand, M., & Goslow, G. (2001). *Analysis of vertebrate structure*. Wiley.

Holliday, C. M., Tsai, H. P., Skilijan, R. J., George, I. D., & Pathan, S. (2013). A 3D interactive model and atlas of the jaw Musculurature of *Alligator mississippiensis*. *PLoS One*, *8*(6), e62806.

Holliday, C. M., & Witmer, L. M. (2009). The epipterygoid of crocodyliforms and its significance for the evolution of the orbitotemporal region of eusuchians. *Journal of Vertebrate Paleontology*, *29*(3), 715–733.

Huene, F. V. (1921). Neue Pseudosuchier und Coelurosaurier aus dem württembergischen Keuper. *Acta Zoologica, Stockholm*, *2*, 329–403.

Hurum, J. H., & Currie, P. J. (2000). The crushing bite of tyrannosaurids. *Journal of Vertebrate Paleontology*, *20*(3), 619–621.

Irmis, R. B., Nesbitt, S. J., & Sues, H. D. (2013). Early Crocodylomorpha. *Geological Society, London, Special Publications*, *379*, 275–302.

Jouve, S. (2005). A new description of the skull of Dyrosaurus phosphaticus (Thomas 1893) (Mesoeucrocodylia: Dyrosauridae) from the lower Eocene of North Africa. *Canadian Journal of Earth Sciences*, *42*(3), 323–337.

Jouve, S. (2009). The skull of *Teleosaurus cadomensis* (Crocodylomorpha; Thalattosuchia), and phylogenetic analysis of Thalattosuchia. *Journal of Vertebrate Paleontology*, *29*, 88–102.

Jouve, S., Laroche, M., Bouya, B., & Amaghzaz, M. (2006). A new species of *Dyrosaurus* (Crocodylomorpha Dyrosauridae) from the early Eocene of Morocco: Phylogenetic implications. *Zoological Journal of the Linnean Society*, *148*, 606–656.

Kent, D. V., Santi-Malnis, P., Colombi, C., Alcober, O. A., & Martinez, R. N. (2014). Age constraints on the dispersal of dinosaurs in the late Triassic from magnetochronology of the Los Colorados formation (Argentina). *Proceedings of the National Academy of Sciences of the United States of America*, *111*, 7958–7963.

Kley, N. J., Sertich, J. J. W., Turner, A. H., Krause, D. W., O'Connor, P. M., & Georgi, J. A. (2010). Craniofacial morphology of *Simosuchus clarki* (Crocodyliformes: Notosuchia) from the late cretaceous of Madagascar. *Journal of Vertebrate Paleontology*, *30*, 13–98.

Kuzmin, I., Gombolevskiy, V., Boitsova, E. A., Mazur, E., Sennikov, A. G., Skutschas, P. P., & Sues, H. D. (2021). Braincase anatomy of extant Crocodylia, with new insights into the development and evolution of the neurocranium in crocodylomorphs. *Journal of Anatomy*, *00*, 1–56.

Langston, W. (1973). The crocodilian skull in historical perspective. In C. Gans (Ed.), *The biology of the reptilia* (4th ed., pp. 263–289). Academic Press.

Laurenti, J. N. (1768). *Specimen medicum, exhibens synopsin reptilium emendatam cum experimentis circa venena et antidota reptilium austriacorum*. J.T.N. de Trattnern.

Lautenschlager, S., Witmer, L. M., Altangerel, P., Zanno, L. E., & Rayfield, E. J. (2014). Cranial anatomy of *Erlikosaurus andrewsi* (Dinosauria, Therizinosauria): New insights based on digital reconstruction. *Journal of Vertebrate Paleontology*, *36*(6), 1263–1291.

Leardi, J. M., Pol, D., & Clark, J. M. (2017). Detailed anatomy of the braincase of *Macelognathus vagans* Marsh, 1884 (Archosauria, Crocodylomorpha) using high resolution tomography and new insights on basal crocodylomorph phylogeny. *PeerJ*, *5*, e2801.

Leardi, J. M., Pol, D., & Clark, J. M. (2020). Braincase anatomy of *Almadasuchus figarii* (Archosauria, Crocodylomorpha) and a

review of the cranial pneumaticity in the origins of Crocodylomorpha. *Journal of Anatomy*, *237*(1), 48–73.

Lecuona, A., Desojo, J. B., & Pol, D. (2017). New information on the postcranial skeleton of Gracilisuchus stipanicicorum (Archosauria: Suchia) and reappraisal of its phylogenetic position, *181*(3), 638–677.

Lecuona, A., Ezcurra, M. D., & Irmis, R. B. (2016). Revision of the early crocodylomorph *Trialestes romeri* (Archosauria, Suchia) from the lower upper Triassic Ischigualasto formation of Argentina: One of the oldest known crocodylomorphs. *PeerJ*, *4*(2), 585–622.

Lessner, E. J., & Holliday, C. (2020). A 3D Ontogenetic atlas of *Alligator mississippiensis* cranial nerves and their significance for comparative neurology of reptiles. *The Anatomical Record Special Issue*.

Li, J. L., Wu, X. C., & Li, X. M. (1994). New material of *Hsisosuchus chungkingensis* from Sichuan China. *Vertebrata Palasiatica*, *32*(2), 107–126.

Lipscomb, D. L. (1992). Parsimony, homology and the analysis of multistate characters. *Cladistics*, *8*, 45–65.

Luo, Z. X., & Wu, X. C. (1994). The small Tetrapods of the lower Lufeng formation, Yunnan, China. In N. C. Fraser & H. D. Sues (Eds.), *The shadow of the dinosaurs: Early Mesozoic tetrapods* (pp. 252–270). Cambridge University Press.

Maddison, W.P., & Maddison, D.R. (2005). Mesquite: A modular system for evolutionary analysis. Version 1.06, http://mesquiteproject.org

Maisch, M. W., Andreas, T. M., & Rathgeber, T. (2013). Re-evaluation of the enigmatic archosaur *Dyoplax arenaceus* O. Fraas, 1867 from the Schilfsandstein (Stuttgart formation, lower Carnian, upper Triassic) of Stuttgart, Germany. *Neues Jahrbuch für Geologie und Paläontologie – Abhandlungen*, *267*(3), 353–362.

Mansel-Pleydell, J. C. (1888). Fossil reptiles of Dorset. *Proceedings of the Dorset Natural History and Antiquarian Field Club.*, *9*, 1–40.

Marsh, O. C. (1877). Notice of some new vertebrate fossils. *American Journal of Science*, *14*(3), 249–256.

Marsh, O. C. (1884). A new order of extinct Jurassic reptiles (Macelognatha). *American Journal of Science*, *27*(3), 341.

Martínez, R. N., Alcober, O. A., & Pol, D. (2019). A new protosuchid crocodyliform (Pseudosuchia, Crocodylomorpha) from the Norian Los Colorados formation, northwestern Argentina. *Journal of Vertebrate Paleontology*, *38*, 1–12.

Meers, M. B. (2003). Crocodylian forelimb musculature and its relevance to Archosauria. *The Anatomical Record Part A*, *274*, 891–916.

Mehl, M. G. (1915). *Poposaurus gracilis*, a new reptile from the Triassic of Wyoming. *Journal of Geology*, *23*, 516–522.

Mimics Software. (n.d.). https://www.materialsise.com/en/medical/software/mimics

Montefeltro, F. C., Andrade, D. V., & Larsson, H. C. E. (2016). The evolution of the meatal chamber in crocodyliforms. *Journal of Anatomy*, *228*(5), 838–863.

Nascimento, P. M., & Zaher, H. (2010). A new species of Baurusuchus (Crocodyliformes, Mesoeucrocodylia) from the upper cretaceous of Brazil, with the first complete postcranial skeleton described from the family Baurusuchidae. *Papeis Avulsos de Zoologia*, *50*(21), 323–361.

Nash, D. S. (1975). The morphology and relationships of a crocodilian, *Orthosuchus Stormbergi*, from the upper Triassic of Lesotho. *Annals of the South African Museum*, *67*(1975), 227–329.

Nesbitt, S. (2007). The anatomy of *Effigia okeeffeae* (Archosauria, Suchia), theropod-like convergence, and the distribution of related taxa. *Bulletin of the American Museum of Natural History*, *302*, 84.

Nesbitt, S., Turner, A. H., & Weinbaum, J. (2013). A survey of skeletal elements in the orbit of Pseudosuchia and the origin of the crocodylian palpebral. *Earth and Environmental Science Transactions Royal Society of Edinburgh: Earth Sciences*, *103*(3–4), 365–381.

Nesbitt, S. J. (2011). The early evolution of archosaurs: Relationships and the origin of major clades. *Bulletin of the American Museum of Natural History*, *352*, 292.

Nesbitt, S. J., & Butler, R. J. (2012). Redescription of the archosaur *Parringtonia gracilis* from the middle Triassic Manda beds of Tanzania, and the antiquity of Erpetosuchidae. *Geological Magazine*, *1*, 1–14.

Nesbitt, S. J., Irmis, R. B., Lucas, S. G., & Hunt, A. P. (2005). A giant crocodylomorph from the upper Triassic of New Mexico. *Palaeontologische Zeitschrift*, *79*(4), 471–478.

Newton, E. T. (1894). Reptiles from the Elgin sandstone. Description of two new genera. *Philosophical Transactions of the Royal Society*, *B185*, 573–607.

Norell, M. A., Makovicky, P., & Clark, J. M. (2004). The braincase of *velociraptor*. In P. J. Currie, E. B. Koppelhus, M. A. Shuga, & J. L. Wright (Eds.), *Feathered dragons: Studies on the transition from dinosaurs to birds* (pp. 133–143). Indiana University Press.

Olsen, P. E., Sues, H. D., & Norell, M. A. (2000). First record of *Erpetosuchus* (Reptilia: Archosauria) from the late Triassic of North America. *Journal of Vertebrate Paleontology*, *20*, 633–636.

Osborn, H. F., & Brown, B. (1906). *Tyrannosaurus*, Upper Cretaceous carnivorous dinosaur. *Bulletin of the American Museum of Natural History*, *22*(16), 281–296.

Osmólska, H., Hua, S., & Buffetaut, E. (1997). *Gobiosuchus kielanae* (Protosuchia) from the late cretaceous of Mongolia: Anatomy and relationships. *Acta Palaeontologica Polonica*, *42*, 257–289.

Ostrom, J. H. (1969). Osteology of *Deinonychus antirrhopus*, an unusual theropod from the lower cretaceous of Montana. *Peabody Museum of Natural History Bulletin*, *30*, 1–165.

Owen, R. (1850). On the communications between the cavity of the tympanum and the palate in the crocodilian (*Gavialis*, *alligator* and crocodiles). *Philosophical Transactions of the Royal Society of London.*, *140*, 521–527.

Parrish, J. M. (1991). A new specimen of an early crocodylomorph (cf. *Sphenosuchus* sp.) from the upper Triassic Chinle formation of petrified Forest national park. *Journal of Vertebrate Paleontology*, *11*, 198–212.

Peyer, K., Carter, J. G., Sues, H. D., Novak, S. E., & Olsen, P. E. (2008). A new Suchian archosaur from the upper Triassic of North Carolina. *Journal of Vertebrate Paleontology*, *28*(2), 363–381.

Pierce, S. E., & Benton, M. J. (2006). *Pelagosaurus typus* Bronn, 1841 (Mesoeucrocodylia: Thalattosuchia) from the upper Lias (Toarcian, lower Jurassic) of Somerset, England. *Journal of Vertebrate Paleontology*, *26*(3), 621–635.

Pol, D., & Gasparini, Z. (2009). Skull anatomy of *Dakosaurus andiniensis* (Thalattosuchia: Crocodylomorpha) and the phylogenetic position of Thalattosuchia. *Journal of Systematic Palaeontology*, *7*, 163–197.

Pol, D., Ji, S., Clark, J. M., & Chiappe, L. M. (2004). Basal crocodyliforms from the lower cretaceous Tugulu group (Xinjiang, China), and the phylogenetic position of *Edentosuchus*. *Cretaceous Research*, *25*, 603–622.

Pol, D., & Norell, M. A. (2004a). A new crocodyliform from zos canyon, Mongolia. *American Museum Novitates*, *3445*, 1–36.

Pol, D., & Norell, M. A. (2004b). A new gobiosuchid crocodyliform taxon from the cretaceous of Mongolia. *American Museum Novitates*, *3458*, 1–31.

Pol, D., Rauhut, O. W., Lecuona, A., Leardi, J. M., Xu, X., & Clark, J. M. (2013). A new fossil from the Jurassic of Patagonia reveals the early basicranial evolution and the origins of Crocodyliformes. *Biological Reviews*, *88*(4), 862–872.

Porter, W. R., Sedlmayr, J. C., & Witmer, L. M. (2016). Vascular patterns in the heads of crocodilians: Blood vessels and sites of thermal exchange. *Journal of Anatomy*, *229*, 800–824.

Reig, O. A. (1963). La presencia de dinosaurios saurisquios en los "Estratos de Ischigualasto" (Mesotriasico Superior) de las provincias de San Juan y La Rioja (Republica Argentina). *Ameghiniana*, *3*, 3–20.

Romer, A. S. (1972). The Chañares (Argentina) Triassic reptile fauna. XIII. An early ornithosuchid pseudosuchian, *Gracilisuchus stipanicicorum*, gen. Et sp. nov. *Brevoria*, *389*, 1–24.

Sachs, S., Johnson, M. M., Young, M. T., & Abel, P. (2019). The mystery of *Mystriosaurus*: Redescribing the poorly known early Jurassic teleosauroid thalattosuchian *Mystriosaurus laurillardi* and *Steneosaurus brevior*. *Acta Palaeontologica Polonica.*, *64*(3), 565–579.

Sadleir, R. W., & Makovicky, P. J. (2008). Cranial shape and correlated characters in crocodilian evolution. *Journal of Evolutionary Biology*, *21*(6), 1578–1596.

Sampson, S. D & Witmer M. (2007). Craniofacial anatomy of Majungasaurus Crenatissimus (Theropoda: Abelisauridae) From The Late Cretaceous of Madagascar. *Journal of Vertebrate Paleontology. Society of Vertebrate Paleontology Memoir*. 8(27), 32–102.

Schwab, J. A., Young, M. T., Neenan, J. M., Walsh, S. A., Witmer, L. A., Herrera, Y., Allain, R., Brochu, C. A., Choiniere, J. N., Clark, J. M., Dollman, K. N., Etches, S., Fritsch, G., Gignac, P. M., Ruebenstahl, A., Sachs, S., Turner, A. H., Vignaud, P., Wilberg, E. W., … Brusatte, S. L. (2020). Inner ear sensory system changes as extinct crocodylomorphs transitioned from land to water. *Proceedings of the National Academy of Sciences of the United States of America*, *117*(19), 10422–10428.

Sedlmayr, J. C. (2002). Anatomy, evolution and functional significance of cephalic vasculature in Archosauria. Doctoral thesis, Ohio University

Sereno, P. C., Larson, H. C. E., Sidor, C. A., & Gado, B. (2001). The Giant Crocodyliform *Sarcosuchus* from the cretaceous of Africa. *Science*, *294*(5546), 1516–1519.

Sereno, P. C., & Wild, R. (1992). *Procompsognathus*: Theropod, 'thecodont', or both? *Journal of Vertebrate Paleontology*, *12*, 435–458.

Shute, C. C. D., & Ballairs, A. (1955). The external ear in Crocodylia. *Proceedings of the Zoological Society of London*, *124*(4), 741–749.

Sill, W. D. (1974). The anatomy of *Saurosuchus galilei* and the relationships of the rauisuchid thecodonts. *Bulletin of the Museum of Comparative Zoology at Harvard College*, *146*, 317–362.

Simmons, D. J. (1965). The non-therapsid reptiles of the Lufeng Basin, Yunnan, China, Fieldiana. *Geology*, *15*, 1–93.

Sookias, R. B., Dilkes, D., Sobral, G., Smith, R. M. H., Wolvaardt, F. P., Arcucci, A. B., Bhullar, B. A. S., & Werneburg, I. (2020). The craniomandibular anatomy of the early archosauriform *Euparkeria capensis* and the dawn of the archosaur skull. *Royal Society Open Science*, 7(7), 7200116200116.

Storrs, G. W., & Efimov, M. B. (2000). Mesozoic crocodyliforms of north-Central Eurasia. In M. J. Benton, M. A. Shishkin, D. M. Unwin, & E. N. Kurochkin (Eds.), *The age of dinosaurs in Russia and Mongolia* (pp. 402–419). Cambridge University Press.

Sues, H. D., Olsen, J. G., Carter, J. G., & Scott, D. M. (2003). A new crocodylomorph archosaur from the upper Triassic of North Carolina. *Journal of Vertebrate Paleontology*, *23*, 329–343.

Sumida, S. S. (1997). Locomotor features of taxa spanning the origin of amniotes. In S. S. Sumida & K. L. M. Martin (Eds.), *Amniote origins, completing the transition to land* (pp. 353–398). Academic Press.

Tennant, J. P., Mannion, P. D., & Upchurch, P. (2016). Evolutionary relationships and systematics of Atoposauridae (Crocodylomorpha: Neosuchia): Implications for the rise of Eusuchia. *Zoological Journal of the Linnean Society.*, *177*(4), 854–936.

Turner, A. H. (2015). A review of *Shamosuchus* and *Paralligator* (Crocodyliformes, Neosuchia) from the Cretaceous of Asia. *PLoS One*, *10*(2), e0118116.

Tykoski, R. S., Rowe, T. B., Ketcham, R. A., & Colbert, M. W. (2002). *Calsoyasuchus valliceps*, a new crocodyliform from the early Jurassic Kayenta formation of Arizona. *Journal of Vertebrate Paleontolog*, *22*(3), 593–611.

Vasilopoulou-Kampitsi, M., Goyens, J., Baeckens, S., Van Damme, R., & Aerts, P. (2019). Habitat use and vestibular system's dimensions in lacertid lizards. *Journal of Anatomy*, *235*, 1–14.

Verheyen, R. (1953). Contribution a l'etude de la structure pneumatique du crane chez les oiseaux. *Institut Royal des Sciences Naturelles de Belgique, Bulletin*, *29*, 1–24.

VGStudio MAX 3.5 (Volume Graphics). (2019). www.volumegraphics.com.

Huene, V. F. (1942). *Die Fossilen Reptilien des Südamerikanischen Gondwanalandes: Ergebnisse der Sauriergrabungen in Südbrasilien, 1928/1929*. C.H. Beck'sche Verlagsbuchhandlung.

Walker, A. D. (1970). A revision of the Jurassic reptile *Hallopus victor* (Marsh) with remarks on the classification of crocodiles. *Philosophical Transactions of the Royal Society B*, *257*, 323–372.

Walker, A. D. (1990). A revision of *Sphenosuchus acutus* Haughton, a crocodylomorph reptile from the Elliot formation (late Triassic or early Jurassic) of South Africa. *Philosophical Transactions of the Royal Society B*, *330*, 1–120.

Walker, D. (1961). Triassic reptiles from the Elgin area *Stagonelepis*, *Dasygnathus* and their allies. *Philosophical Transactions of the Royal Society B*, *244*, 103–204.

Weinbaum, J. C. (2013). Postcranial skeleton ofPostosuchus kirkpatricki (Archosauria: Paracrocodylomorpha), from the Upper Triassic of the United States. *Geological Society, London, Special Publications.*, *379*, 525–553.

Wilberg, E. W. (2015). What's in an outgroup? The impact of outgroup choice on the phylogenetic position of Thalattosuchia (Crocodylomorpha) and the origin of Crocodyliformes. *Systematic Biology*, *64*(4), 621–637.

Wilberg, E. W. (2017). Investigatign patterns of crocodyliform cranial disparity through the Mesozoic and Cenozoic. *Zoological Journal of the Linnean Society*, *181*(1), 189–208

Wilberg, E. W., Turner, A. H., & Brochu, C. A. (2019). Evolutionary structure and timing of major habitat shifts in Crocodylomorpha. *Scientific Reports*, *9*(1), 514.

Witmer, L., Ridgely, R., Dufeau, D., & Semones, M. (2008). *Anatomical imaging: Towards a new morphology*. Springer-Verlag.

Witmer, L. M. (1997). The evolution of the antorbital cavity of archosaurs: A study in soft-tissue reconstruction in the fossil record with an analysis of the function of Pneumaticity. *Journal of Vertebrate Paleontology*, *17*, 1–76.

Wu, X. C. (1986). A new species of *Dibothrosuchus* from Lufeng Basin. *Vertebrata Palasiatica*, *24*, 43–62.

Wu, X. C., & Chatterjee, S. (1993). *Dibothrosuchus elaphros*, a crocodylomorph from the lower Jurassic of China and the phylogeny of the Sphenosuchia. *Journal of Vertebrate Paleontology*, *13*, 58–89.

Wu, X. C., Donald, B. B., & Lu, J. C. (1994). A new species *Shantungosuchus* from the lower cretaceous of Inner Mongolia (China) with comments on S. chuhsiensis Young, 1961, and the phylogenetic position of the genus. *Journal of Vertebrate Paleontology*, *14*(2), 210–229.

Wu, X. C., Liu, J., & Li, J. L. (2001). The anatomy of the first archosauriform (Diapsida) from the terrestrial Upper Triassic of China. *Vertebrata Palasiatica*, *39*(4), 251–265.

Wu, X. C., & Russell, A. (2001). Redescription of *Turfanosuchus dabanensis* (Archosauriformes) and new information on its phylogenetic relationships. *Journal of Vertebrate Paleontology*, *21*(1), 40–50.

Wu, X. C., Sues, H. D., & Dong, Z. M. (1997). *Sichuanosuchus shuhanensis*: A new early cretaceous protosuchian (Archosauria: Crocodyliformes) from Sichuan (China), and the monophyly of Protosuchia. *Journal of Vertebrate Paleongology*, *17*, 89–103.

Young, C. C. (1973). On a new pseudosuchian from Turfan, Sinkiang. Reports of paleontological expedition to Sinkiang (I): Permo-Triassic vertebrate fossils of Turfan Basin. *Mem. Institute of Vertebrate Paleontology and Paleoanthropology Academy Sinica*, *10*, 15–37.

Young, M. T., & Andrade, M. B. (2009). What is Geosaurus? Redescription of *Geosaurus giganteus* (Thalattosuchia: Metriorhynchidae) from the upper Jurassic of Bayern, Germany. *Zoological Journal of the Linnean Society*, *157*(3), 551–585.

Young, M. T., Brusatte, S. L., De Andrade, M. B., Desojo, J. B., Beatty, B. L., Steel, L., Fernández, M. S., Sakamoto, M., Ruiz-Omeñaca, J. I., & Schoch, R. R. (2012). The cranial osteology and feeding ecology of the Metriorhynchid Crocodylomorph Genera *Dakosaurus* and *Plesiosuchus* from the Late Jurassic of Europe. *PLoS One*, *7*(9), e44985.

Zanno, L. E., Drymala, S., Nesbitt, S. J., & Schneider, V. P. (2015). Early crocodylomorph increases top tier predator diversity during rise of dinosaurs. *Science Reports*, *5*, 9276.

SUPPORTING INFORMATION

Additional supporting information may be found in the online version of the article at the publisher's website.

How to cite this article: Ruebenstahl, A. A., Klein, M. D., Yi, H., Xu, X., & Clark, J. M. (2022). Anatomy and relationships of the early diverging Crocodylomorphs *Junggarsuchus sloani* and *Dibothrosuchus elaphros*. *The Anatomical Record*, 1–94. https://doi.org/10.1002/ar.24949